



**BANGLADESH NETWORK
OFFICE FOR URBAN SAFETY**

BNUS ANNUAL REPORT-2013



BNUS ANNUAL REPORT-2013

BANGLADESH
NETWORK OFFICE
FOR



URBAN
SAFETY



BUET, DHAKA, BANGLADESH

Prepared By:

Mehedi Ahmed Ansary



CONTENTS

PART-I: THE BRAHMANBARIA TORNADO, 2013	1
PART-II: EARTHQUAKE VULNERABILITY ASSESSMENT IN SCHOOLS AND COLLEGES OF TANGAIL MUNICIPALITY	11
PART-III: NON-DESTRUCTIVE TESTING (NDT) IN A RESIDENTIAL BUILDING LOCATED AT GULSHAN	23
PART-IV: SAVAR BUILDING TRAGEDY IN BANGLADESH: WAY FORWARD	39
PART-V: SEISMIC RISK ASSESSMENT OF SOME HISTORICAL MOSQUE OF DHAKA USING NON-DESTRUCTIVE TESTING METHODS	49
PART-VI: APPLICABILITY OF PS SUSPENSION LOGGING DOWNHOLE SEISMIC METHOD FOR INVESTIGATION OF DYNAMIC SOIL PROPERTIES OF BANGLADESH	59
PART-VII: ENGINEERING CHARACTERISTICS OF GROUND MOTIONS RECORDED BY NORTHEAST INDIAN STRONG MOTION INSTRUMENTATION NETWORK FROM 2005 TO 2013	69
PART-VIII: STRUCTURAL QUALITY ASSESSMENT OF PADMA PICTURE LTD. MALIBAG, DHAKA	81
PART-IX: APPLICABILITY OF EXISTING CPT, SPT AND SOIL PARAMETER CORRELATIONS FOR BANGLADESH	91
PART-X: SLOPE STABILITY ANALYSIS OF AN EMBANKMENT AT JAMUNA RIVER	103
PART-XI: LIQUEFACTION ESTIMATION USING CPT	115
PART-XII: BURIED GAS PIPELINE DAMAGE ANALYSIS	133
PART-XIII: STRUCTURAL ASSESSMENT OF LIBRARY BUILDING, BUET, DHAKA	149
PART-XIV: NON-DESTRUCTIVE TESTING AT FACTORY BUILDING OF V GARMENTS LIMITED	155
PART-XV: MULTHAZARD VULNERABILITY ASSESSMENT OF WARD 29 IN DHAKA CITY	169
PART-XVI: STANDARD GARMENTS FIRE: AN INTRIGUE AGAINST RMG SECTOR OF BANGLADESH	207
PART-XVII: GROUND PENETRATING RADAR TESTING AT THE PROPOSED UNDERGROUND LPG STORAGE TANK AT SOUTHERN AUTOGAS STATION, TEJGAON	211



PART-I

THE BRAHMANBARIA TORNADO, 2013

**BANGLADESH NETWORK OFFICE FOR URBAN
SAFETY (BNUS), BUET, DHAKA**

Prepared By: KM Khaleduzzaman

Mehedi Ahmed Ansary

A deadly tornado occurred in March 22, 2013 at around 5:30 PM in the southeastern district of Brahmanbaria in Bangladesh. It travelled at a speed of 70 kilometer per hour and lasted for 15 minutes leaving an eight-kilometre trail of destruction in its path. It struck 20 villages with along an 8 kilometres (5.0 mi) of Ramrail, Basudeb, Chinair, Sultanpur union of Sadar Upazila, Bijohnagar Upazila and North Akhaura union of Akhaura upazila in Brahmanbaria district. The worst damage occurred in the Bijohnagar and Akhaura Upazila.



Figure 1: Affected srea of the tornado

Thousands of trees and utility poles were toppled and thousands of peoples were left homeless. The tornado disrupted both train and road communication, which interrupted rescue operations. Part of jail house of this district was collapsed, resulting in the death of seven jail keepers. Many crops,

mostly consisting of rice, were damaged as well. Both Prime minister Sheikh Hasina and opposition leader Khaleda Zia visited the impacted areas to meet the affected people and distribute relief.



Figure 2: Elephant trunk like tornado



Figure 3: Damaged house

Many tin- and mud-built houses and standing crops on a huge swathe of land were badly damaged by the tornado. The storm uprooted scores of trees and electric poles as it swept through Urshiura and its surrounding villages of the Sadar Upazila at around 5:30 PM. Local hospitals were crowded with injured villagers and it was difficult to move from one place to another as many of the roads were blocked by fallen trees. Thousands of people were rendered homeless, and power was out across a wide area. Crops, mostly rice, were damaged across a vast swath of land.



Figure 4: Affected people



Figure 5: Dead livestock



Figure 6: Affected trees



Figure 7: Damage structure



Figure 8: Dropped electric pole



Figure 9: Dropped trees on rail track

Prime Minister Sheikh Hasina went to Brahmanbaria on the 25 March 2013 to visit the areas hit hard by the tornado. Prime Minister Sheikh Hasina addresses a rally on Chinair Bangabandhu Degree College premises in Brahmanbaria Sadar upazila on Monday. Prime Minister Sheikh Hasina has assured the tornado affected people in Brahmanbaria of government support. She earlier visited three villages in the upazila.



Figure 10: Prime Minister met affected people



Figure 11: Opposition Party chief met affected people

BNP Chairperson Khaleda Zia visited Brahmanbaria on March 30, a week after the tornado. During the visit, she met the affected people and distributed relief to them. Some senior party leaders including Sadeque Hossain Khoka accompanied the BNP chief during her visit.

Damage

The tornado devastated a vast area of Brahmanbaria District. Total 3 upazilas are affected including 6 unions. Number of fully and partially affected families are 1326 and 402 respectively where as fully and partially affected people are 6630 and 1985 respectively. The tornado also destructed a number of houses where 2635 houses are affected fully and 752 are affected partially. Around 173 acres of agricultural crops are fully affected where as 1112 acres crops are partially affected.

Table 1: Damage statistics of the tornado

Affected Upazila (No.)	Affected Union (No.)	Affected Families (No.)		Affected People (No.)		Affected Households (No.)		Affected Crop (Acre)	
		Full	Partial	Full	Partial	Full	Partial	Full	Partial
3	6	1326	402	6630	1985	2635	752	173	1112

Number of death toll due to tornado is 32 where as 388 people are injured severely. Livestock and poultry are also affected greatly as 299 numbers of cows, cattle and goats died in this devastating disaster. About 910 numbers of cock, hen and duck died.

The tornado destroyed about 2.25 kilometer road. It also affected a school fully, 5 educational institution partially and 5 religious institution.

Table 2: Damage statistics of the tornado

Death (No.)	Injured (No.)	Livestock Death (No.)	Poultry Death (No.)	Affected Educational Institution (No.)		Affected Religious Institution (No.)	Affected Road (km)
				Full	Partial		
32	388	299	910	1	5	5	2.25

Others Damage

200ft boundary wall and 420ft security wall of district prison collapsed. Road communication disrupted due to tumbled trees. Electric lines and poles are affected. Women word kitchen, security wall and partition including main gate of prison collapsed.

Immediate Action Taken

- Rescue operation has been carried with the help of Police, BGB, Fire Service, Roads and Highway, PWD and local leaders.
- 10ft height CI sheet partition in district prison has been constructed.
- Electricity system is up now inside district prison by generator.
- Electric lines and poles repaired immediately.
- Two medical teams from Comilla cantonment are engaged for rendering medical services to the victims.
- Injured people are admitted in Brahmanbaria general hospital and other hospitals/clinics. Very seriously injured 15 persons are sent to Comilla Cantonment and some other persons are sent to Dhaka Medical College Hospital as well.
- Fire Service, BGB, Police, RHD have managed to restart road communication by removing fallen trees.
- Almost all affected families are getting cook food twice daily from the Government Administration.
- Dry food distribution among affected people is arranged by UP chairman, public representatives and other organizations.

Response

Government of Bangladesh

Department of Disaster Management (DDM) has sent 753 tents to build temporary shelter. Meanwhile, with the help of Bangladesh Army, 453 tents have been pegged. Remaining 300 tents are in the process. DDM has sent 1200 bundle of C.I Sheets (500 from DDM and 700 from Dutch Bangla Bank Ltd). District administration has also mobilized another 176 bundles of C.I sheets from its previous stock. So far, 673 bundles have been distributed. In addition, Tk.15,00,000 (fifteen lac) against 500 bundles has been allocated to distribute as Tk.3,000.00/bundle among CI sheet receivers to build their houses. DDM has allocated 200MT of GR Rice to distribute for affected families. DDM has allotted Tk.25,60,000 (Twenty Five Lac Sixty Thousand) to distribute at Tk. 20,000.00 for families of each dead people and Tk.5000.00 for each injured people. So far distributed amount is Tk.5,80,000 among family of 29 dead people and Tk.19,40,000.00 among 388 injured family. Also, 48.93MT out of 261.58MT allocated GR Rice is distributed among 1631 families at 30 kg for each family. DDM has deployed two officers along with other three officers (PIO) from adjacent Upazilas to make list of affected people and to help distribute relief materials. Besides, DDM has sent two emergency pick-up vans to DRRO to expedite the response activities. District Administration has engaged four Additional District Commissioners and two Upazila Nirbahi Officers (UNO) at Distribution Point to monitor post-disaster relief and rehabilitation activities.

Furthermore, the government is providing corrugated galvanised iron (CGI) sheets and cash grant BDT 6,000 (approximately CHF 73) to those with damaged house. Government has distributed 40 million tones (mts) of rice from its allocated 100 mts of rice from its gracious relief (GR) fund.

In addition, response from Dutch Bangla Bank Ltd (DBBL) -Tk. 1,050,000 and 700 tents has been reallocated among affected Upazilas.

Bangladesh Red Crescent Society (BDRCS)

Immediately after the tornado, BDRCS and the International Federation of Red Cross and Red Crescent Societies (IFRC) have been closely monitoring the situation. BDRCS Response department and its Unit Office have promptly assessed the situation in Brahmanbaria district. Volunteers of BDRCS Brahmanbaria district unit conducted search and rescue soon after the disaster struck. Within hours after the disaster, BDRCS deployed its National Disaster Response Team (NDRT) to assess the damages on people and their properties. Jointly, BDRCS national headquarters (NHQ) and IFRC jointly dispatched non-food items (NFIs) for 600 families for immediate distribution from its existing disaster preparedness (DP) stock. Each NFI included one tarpaulin, two water jerry cans and one family kit for each family.



Figure 12: BDRCS volunteers helping the affected people



Figure 13: NFIs distribution by BDRCS district unit to provide relief to the affected people

From BDRCS NHQ, a medical team has been deployed hours after the disaster to Brahmanbaria to help the injured, while 70 unit volunteers were providing first aid in the Brahmanbaria Sadar hospital. On 23 March, the medical team adapted its service to mobile unit and provided further medical assistance to the tornado affected villages: (1) Dubla, (2) Jarultala, (3) Bashudevpur, (4) Chandanpur and (5) Chinnai. A total of 62 patients were treated, largely for sharp cuts, laceration, bruises, scalp injury and fractured bones. The serious fracture cases were referred to B.Baria general hospital. Fortunately, most of the injuries of the patients were minor in nature.



Figure 14: BDRCS youth volunteers offering first aid to the affected people.



Figure 15: BDRCS mobile unit attending to the affected people in one of the villages

World Food Programme (WFP)

In order to complement Government efforts to support the victims of the Tornado, WFP has allocated 12.333 MT of fortified biscuits for distribution to 1631 affected households. WFP is

distributing 7.5 kilogrammes (kg) of high energy biscuits to each of the affected families to meet their nutritional need for at least five days. Provision of safe drinking water and household sanitation needs are yet to be sufficiently addressed. The Water, Sanitation and Hygiene (WASH) cluster is reviewing the situation and mobilizing resources to address these needs. All the development partners would continue to fill up the existing gaps with the resources that are available.

Other Supports

Concern worldwide has started psychosocial support to the affected people using their trained personnel; while Muslim Aid has a medical team in the affected area. Apart from these two organizations, CARE, Islamic Relief are conducting assessment. From the donor community, the European commission humanitarian aid (DG-ECHO) has dispatched a team to the affected area to assess the situation. The Humanitarian Country Task Team (HCTT) met on 25 March 2013 to take stock of the situation. The meeting concluded that no Joint Needs Assessment (JNA) will be launched. A total of 1,350 families have been provided with emergency shelter by Government and BDRCS. If there are more of shelter needs, the shelter cluster and relevant partners are to review and contribute towards meeting those needs. Government also reported that cooked food has been provided to the affected people. In order to meet the provision of cooked rice for families, more cooking pots need to be provided immediately.



PART-II

EARTHQUAKE VULNERABILITY ASSESSMENT IN SCHOOLS AND COLLEGES OF TANGAIL MUNICIPALITY

**BANGLADESH NETWORK OFFICE FOR URBAN
SAFETY (BNUS), BUET, DHAKA**

**Prepared By: Md. Rajib Hossain, Md. Sirajul Islam,
Mehedi Ahmed Ansary, Lutfun Naher Banna and
Tanmoy Roy Tusher**

Abstract

Assessing school and college vulnerability to earthquakes can be regarded as an ill-structured problem i.e. a problem for which there is no unique, identifiable and objectively optimal solution. The study was conducted to assess the earthquake vulnerability of the schools and colleges in Tangail municipality. The study investigated the present condition of the buildings or infrastructures of the schools and colleges where some buildings or infrastructures were highly vulnerable due to old age and the rest were vulnerable due to their plan or vertical irregularity. The study showed that 58.82% infrastructures made by concrete were non-engineered and the old concrete-frame buildings were vulnerable to earthquake. If they collapse due to any seismic event, they will be comparatively more lethal and will take higher percentage of lives than the masonry structures. The study demonstrated that 15.69% school buildings were older than 30 years, 21.57% was vertically irregular and 31.37% infrastructures showed plan irregularity. By analyzing the above circumstances, 64.71% school buildings/ infrastructures are needed to detailed evaluation as early as possible to save children and people from earthquake hazards.

Key words: Earthquake, Vulnerability, Plan irregularity, Vertical irregularity.

Introduction

Bangladesh is the most vulnerable to several natural disasters due to its geographical location, and every year natural calamities upset people's lives in some parts of the country. The destructive disasters concerned here are the occurrences of earthquake, flood, cyclone and storm surge, flash flood, drought, tornado, riverbank erosion and land slide (UNEP, 2001). Earthquake, the trembling or shaking movement of the earth is the most discussed topic among them. It is a form of energy of wave motion, which originates in a limited region and then spreads out in all directions from the source of disturbance (Banglapedia, 2008). The 1897 Great Indian earthquake with a magnitude of 8.7 affected almost whole of the Bangladesh. Damages were very severe particularly in Sylhet, Rangpur and Mymensingh. In the city of Dhaka, most of the brick masonry buildings either collapsed or were severely damaged (Oldham, 1899).

Bangladesh is surrounded by the regions of high seismicity which include the Himalayan Arc and Shillong Plateau the north, the Burmese Arc, Arakan Yoma anticlinorium's in the east and complex Naga-Disang-Jaflong thrust zones in the northeast. It is also the site of the Dauki Fault system along with numerous subsurface active faults and a flexure zone called Hinge Zone (SAARC, 2011). These weak regions are believed to provide the necessary zones for movements within the basin area. According to Sharfuddin (2001), both the seismic hazard analysis and the establishment of seismic maps were made difficult in Bangladesh due to the lack of homogenous, accurate and complete data.

The 1993 Bangladesh national building code has adopted a seismic zoning map consisting of three seismic zones, with zone coefficients of 0.25 (Zone 3 in the north and north-east), 0.15 (Zone 2 in the middle, north-west and south-east) and 0.075 (Zone 1 in the south west). This zoning map is based on peak ground accelerations estimated by Hattori (1979) for a return period of 200 years, where Modhupur fault is situated in Zone 2 which is not so far from the Tangail municipality (Ali and Choudhury, 1994). It is about only 40 km away from the fault, so it can be said that the infrastructure of Tangail municipality is highly vulnerable to earthquake.

There are three government colleges, seven non-government colleges, three government high school, thirty non-government high schools, one hundred and sixteen government primary schools, thirty five non-government primary schools, twelve madrasa in Tangail municipality but majority of them are very old (Banglapedia, 2008). Most of the existing schools and colleges' buildings are 2 or 3 storied reinforced concrete frame buildings with infill brick walls and 1 storied brick masonry building with reinforced concrete roofs and uses cement mortar in most of the cases. For this reason, a moderate level earthquake may create a huge damage to property and valuable lives. That is why this earthquake risk assessment was done to evaluate the existing condition of the schools and colleges in this region. School safety was given a major focus by the United Nations International Strategy on Disaster Reduction (UNISDR) when the 2006-2007 World Disaster Reduction Campaign was devoted to the theme Disaster Reduction Begins at School. This theme was chosen by United Nations International Strategy on Disaster Reduction (UNISDR) because (a) it is in line with the Priority 3 of the Hyogo Framework for Action 2005-2015: "Use knowledge, innovation and education to build a culture of safety and resilience at all levels, and (b) schools are the best venues for forging durable collective values; and therefore suitable for building a culture of prevention and disaster resilience (UNISDR, 2009).

From Bangladesh's perspective, school infrastructures are the most vulnerable during disasters due to poor construction, lack of proper maintenance and many other issues related to the schools and colleges. Moreover, as a result of the rapid urbanization and over population in urban areas, schools and colleges are growing in an unplanned way to accommodate students in the education system. As a result, vulnerability is increasing in education sector and safety of the students is becoming questionable day by day. Considering all these, school safety has become an issue of major priorities to make schools safer for the well being of our next generation. In the study, the earthquake vulnerability of schools and colleges in this region was identified to evaluate the existing condition of the schools and colleges.

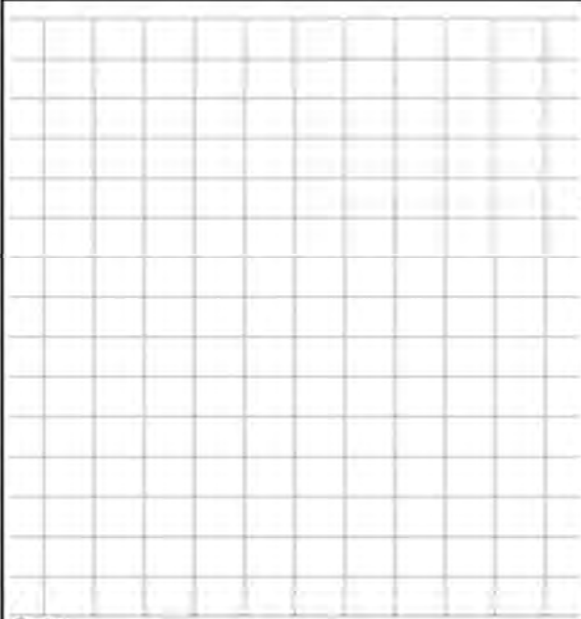
Materials and Methods

The study was conducted to know the earthquake vulnerability assessment of schools and colleges at Tangail municipality in Tangail district, Bangladesh. Tangail municipality is the central part and the most crowded area of Tangail district. For completing the study, 51 educational institutions including 20 primary schools, 17 high schools, 2 madrasa and 12 colleges in Tangail municipality was selected because most of the schools and colleges are situated in urban areas where population density is so high. These infrastructures are vulnerable to earthquake due to rapid urbanization and also as the educational institutions are not following the building code and many of them are more than 100 years old. Moreover, the institutions are just 40 km away from the Modhupur fault which is an active fault.

The research work was done on the basis of Rapid Visual Screening (RVS) of Buildings for Potential Seismic Hazards (PSH) method. To perform with this method, at first a data collection form was selected which known as FEMA-154 data collection form (Fig. 1). The data collection form was completed for each building screened through execution of the following steps: a) verifying and updating the building identification information, b) walking around the building to identify its size and shape, and sketching a plan and elevation view on the data collection form, c) determining and documenting occupancy, d) determining soil type, e) identifying the seismic lateral-load resisting system (entering the building, if possible, to facilitate this process) and circling the related Basic Structural Hazard Score on the data collection form, f) Seismic Performance Attribute Score Modifiers (e.g., number of storeys, design date, and soil type on the data collection form), g) determining the final score, S (by adjusting the basic structural hazard score with the score modifiers identified in step g) and deciding if a detailed evaluation is required, and h) photographing the building and attaching the photo to, or indicating a photo reference number on, the form. The masonry building structures have more than seven storeys, and those schools that have no permanent educational building were excluded from the present assessment.

Rapid Visual Screening of Buildings for Potential Seismic Hazards
FEMA-154 Data Collection Form

HIGH Seismicity

	<p>Address: _____ Zip: _____</p> <p>Other Identifiers: _____</p> <p>No. Stories: _____ Year Built: _____</p> <p>Screener: _____ Date: _____</p> <p>Total Floor Area (sq. ft.): _____</p> <p>Building Name: _____</p> <p>Use: _____</p>
	<p>PHOTOGRAPH</p>

Scale: _____

OCCUPANCY			SOIL		TYPE						FALLING HAZARDS			
Assembly	Govt	Office	Number of Persons 0 - 10 11 - 100 101-1000 1000+		A	B	C	D	E	F	<input type="checkbox"/>	<input type="checkbox"/>	<input type="checkbox"/>	<input type="checkbox"/>
Commercial	Historic	Residential			Hard	Avg	Dense	Stiff	Soft	Poor	Unreinforced	Parapets	Cladding	Other
Emer. Services	Industrial	School			Rock	Rock	Soil	Soil	Soil	Soil	Chimneys			

BASIC SCORE, MODIFIERS, AND FINAL SCORE, S															
BUILDING TYPE	W1	W2	S1 (MRF)	S2 (BR)	S3 (LM)	S4 (RC SW)	S5 (URM INF)	C1 (MRF)	C2 (SW)	C3 (URM INF)	PC1 (TU)	PC2	RM1 (FD)	RM2 (RD)	URM
Basic Score	4.4	3.8	2.8	3.0	3.2	2.8	2.0	2.5	2.8	1.6	2.6	2.4	2.8	2.8	1.8
Mid Rise (4 to 7 stories)	N/A	N/A	+0.2	+0.4	N/A	+0.4	+0.4	+0.4	+0.4	+0.2	N/A	+0.2	+0.4	+0.4	0.0
High Rise (> 7 stories)	N/A	N/A	+0.6	+0.8	N/A	+0.8	+0.8	+0.6	+0.8	+0.3	N/A	+0.4	N/A	+0.6	N/A
Vertical Irregularity	-2.5	-2.0	-1.0	-1.5	N/A	-1.0	-1.0	-1.5	-1.0	-1.0	N/A	-1.0	-1.0	-1.0	-1.0
Plan Irregularity	-0.5	-0.5	-0.5	-0.5	-0.5	-0.5	-0.5	-0.5	-0.5	-0.5	-0.5	-0.5	-0.5	-0.5	-0.5
Pro-Code	0.0	-1.0	-1.0	-0.8	-0.6	-0.8	-0.2	-1.2	-1.0	-0.2	-0.8	-0.8	-1.0	-0.8	-0.2
Post-Benchmark	+2.4	+2.4	+1.4	+1.4	N/A	+1.6	N/A	+1.4	+2.4	N/A	+2.4	N/A	+2.8	+2.6	N/A
Soil Type C	0.0	-0.4	-0.4	-0.4	-0.4	-0.4	-0.4	-0.4	-0.4	-0.4	-0.4	-0.4	-0.4	-0.4	-0.4
Soil Type D	0.0	-0.6	-0.6	-0.6	-0.6	-0.6	-0.4	-0.6	-0.6	-0.4	-0.6	-0.6	-0.6	-0.6	-0.6
Soil Type E	0.0	-0.8	-1.2	-1.2	-1.0	-1.2	-0.8	-1.2	-0.8	-0.8	-0.4	-1.2	-0.4	-0.6	-0.8

FINAL SCORE, S	
COMMENTS	<p>Detailed Evaluation Required</p> <p>YES NO</p>

* = Estimated, subjective, or unreliable data
DNK = Do Not Know

BR = Braced frame MRF = Moment-resisting frame SW = Shear wall
FD = Flexible diaphragm RC = Reinforced concrete TU = Tilt up
LM = Light metal RD = Rigid diaphragm URM INF = Unreinforced masonry infill

Fig. 1. FEMA-154 data collection form used in the study (FEMA, 2002).

Results and Discussions

Types of Infrastructures

In the study, three types of infrastructures were found: wooden, concrete and masonry. Among them 23.52, 58.82 and 17.65% were wooden, concrete and masonry, respectively. The percentages goes higher towards the concrete building because people thought that it is more reliable against various types of disasters and has a sustainable utilization, but it is also found that low quality or old construction may also be great deadly for school student (Fig. 2). According to OECD (2004), a primary school in San Giuliano, Italy, collapsed during Earthquake, killing 29 children and one teacher in 2002. It is observed from the study that numbers of wooden buildings are not modest

amount in this area which is comparatively safer than old concrete and masonry construction. Thus, strong infrastructure plays important role as an earthquake resistor and reduce damage during earthquake.

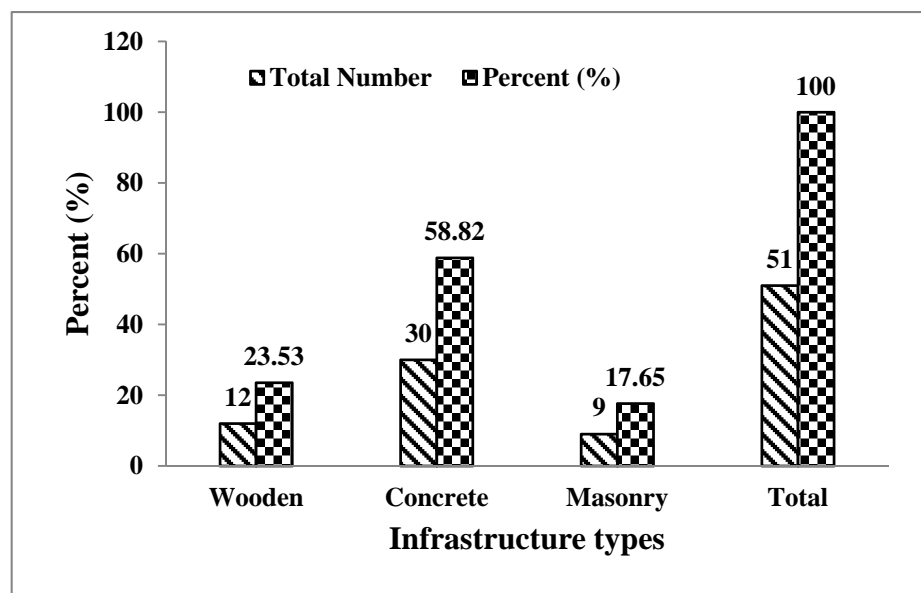


Fig. 2. Types of infrastructures of schools and colleges in Tangail municipality.

Epoch (age) of Infrastructures

Most of the school buildings of the study area were very old. Many of them, e.g. Santosh Zambhi High School, were built in British Period. From the study, 7 (13.73%) buildings were less than 10 years old, 19 (37.25%) buildings were less than 20 years old, 17 (33.33%) buildings were less than 30 years old and 8 (15.69) buildings were found more than 30 years old. Hays et al. (1998) found that with the passage of time buildings loss their lateral resistance and turn into more vulnerable to an earthquake. It is revealed from the study that 15.69% visited educational institutions were built about more than 30 years ago that have followed low construction standards (Fig. 3). They are vulnerable to earthquake and age related decay compel then to fall a victim to seismic vibration. Many of older buildings also showed vertical and plan irregularity whereas some of the new buildings and infrastructures have also not been sited, designed, and constructed with adequate enforcement of modern, state-of-the-art building regulations, lifeline standards, and land use ordinances.

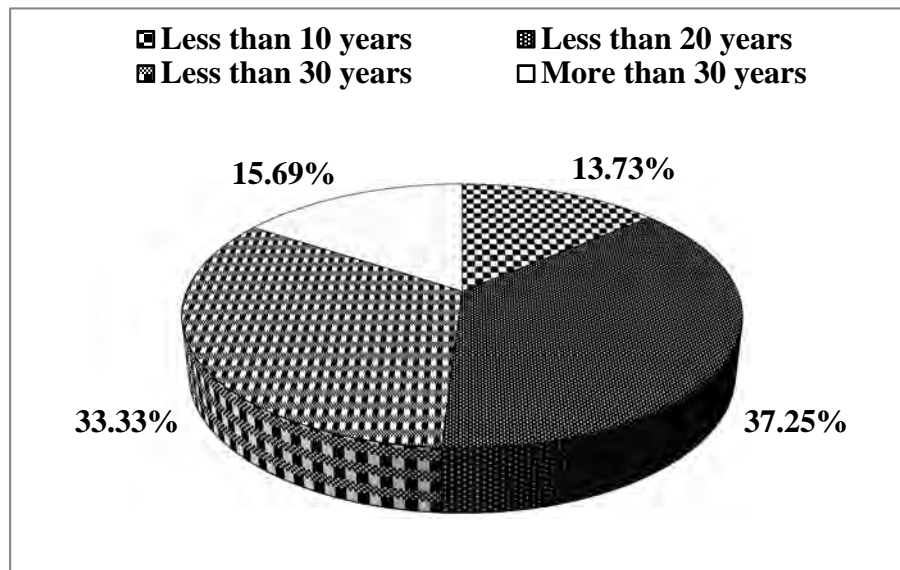


Fig. 3. Epoch (age) of the infrastructures of schools and colleges in Tangail municipality.

Number of Storeys of the Infrastructures

Height of the building is important as it is directly related to the weight of the structures and their response to ground motion. The natural frequency of building is low for tall buildings and high for short buildings. From the study it is revealed that 37.25, 23.53, 21.57 and 11.76% infrastructures were 1, 2, 3 and 4 and above 4 stored, respectively (Fig. 4). Short buildings tend to collapse or experience damage when amplification is higher in high frequency domain and tall buildings experience damage when amplification is higher in low frequency domain that means the safety of building depends on its resonance. According to BIS (2002), one and two storeys buildings have physical frequency of 10 and 5, respectively, whereas 3 to 5 storeys buildings have frequency of 2.

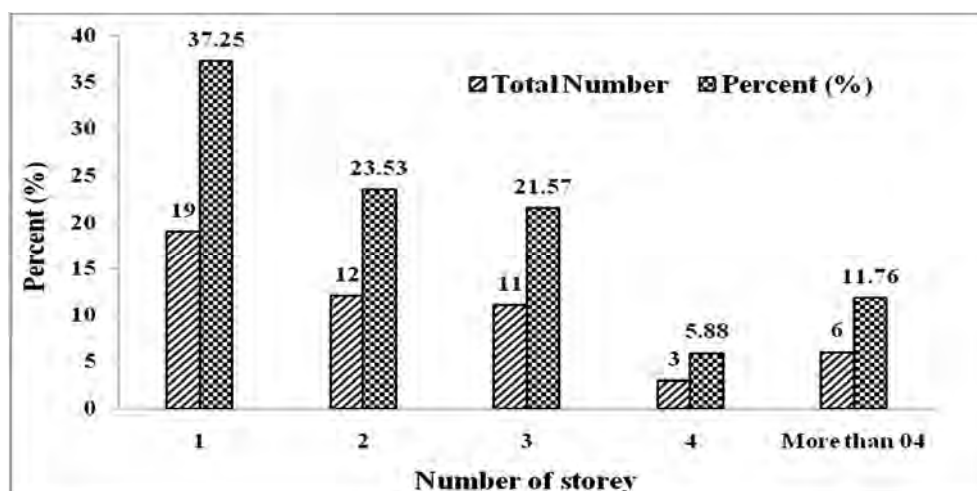


Fig. 4. Storeys of the infrastructures of schools and colleges in Tangail municipality.

Plan Irregularity

The buildings appearing to be E, L, T, U, or + shaped show plan irregularity, whereas square shaped building has no plan irregularity for what they are more strong in structure. From the study it was found that 31.37% of the infrastructures had plan irregularity which may fall in as victim to earthquake and other 68.63% had no plan irregularity (Fig. 5). Plan irregularity often results in shape irregularity. It is an unfavorable feature of buildings. The shapes determine the probability of damage in specific parts or storeys of a building which may even cause collapse. According to Herrera and Soberón (2008), it is observed from seismic events during 1980 to 2008 that the building damaged causes due to plan irregularities. McCrum (2012) found that the effect of strength eccentricity on the seismic response of plan irregular structures needs further investigation and increasing the strength of a lateral force resisting element in the infrastructure.

Vertical Irregularity

Structures having significant physical discontinuities in vertical configuration or in their lateral force resisting systems are termed as vertically irregular structure. Vertical irregularity plays an important role in the earthquake vulnerability detection of the buildings. FEMA (2012) showed that vertical irregularity includes buildings with setbacks, hillside buildings, and buildings with soft storeys. The observed 21.57% infrastructures have vertical irregularity that results from the uneven distribution of mass, strength or stiffness along the elevation of a building structure and other 78.43% infrastructures have no vertical irregularity (Fig. 6). Mass irregularity results from a sudden change in mass between adjacent floors, such as mechanical plant on the roof of a structure, where stiffness irregularity results from a sudden change in stiffness between adjacent floors, such as setbacks in the elevation of a building. SAARC report (2011) explained that vertical irregularity particularly is considered a serious weakness and the corresponding score modifier is negative for all building types with a recommendation for detailed evaluation.

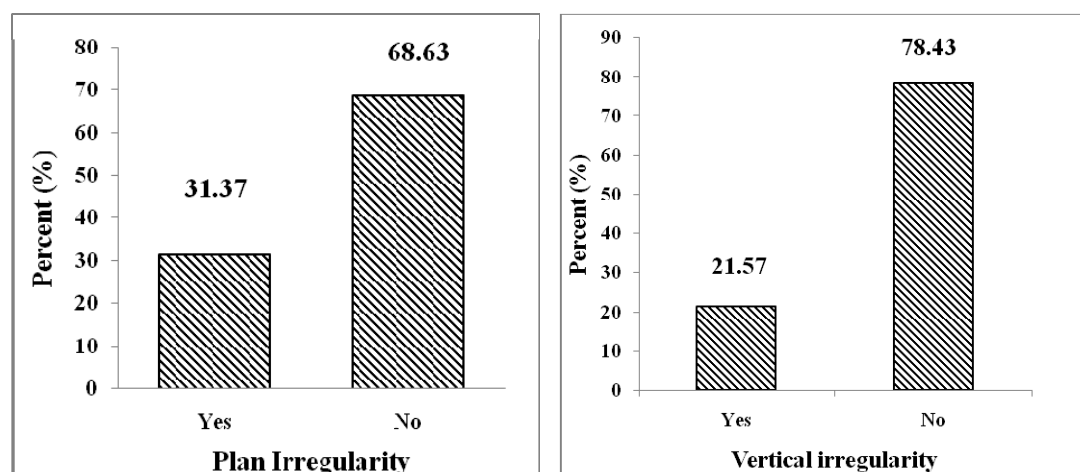


Fig. 5. Plan irregularity of the infrastructures of schools and colleges (left) and the vertical irregularity of the studied infrastructures (right).

Detailed Evaluation

On the basis of the final score, S , it is measured that detailed evaluation of the infrastructure is needed or not. If the value is 2 or more than 2 then no need to detailed evaluation. But if the value is less than 2, then the infrastructure should be detailed evaluated (the value vary from country to country). According to Wang and Goettel (2007), a final score, S , of 2.0 means that the calculated probability of building collapsed at the maximum considered earthquake is 10^{-2} or 0.01 i.e., 1% chance of collapse, where a building with a final score of 3.0 has a factor of 10 times lower probability of collapse than does a building with a final score of 2.0. Similarly, a building with a final score of 1.0 is 10 times more likely to collapse than a building with a final score of 2.0. From the study, 33 out of 51 infrastructures (64.71%) were needed detailed evaluation due to low final score of S and vertical irregularity with plan irregularity, and others 18 (35.29%) infrastructures didn't need detailed evaluation (Fig. 6). According to SAARC report (2011), if any of these irregularities (plan and vertical irregularity) are noticed, the building may undergo much more severe damage even up to Grade 4 or 5 and should be recommended for detailed.

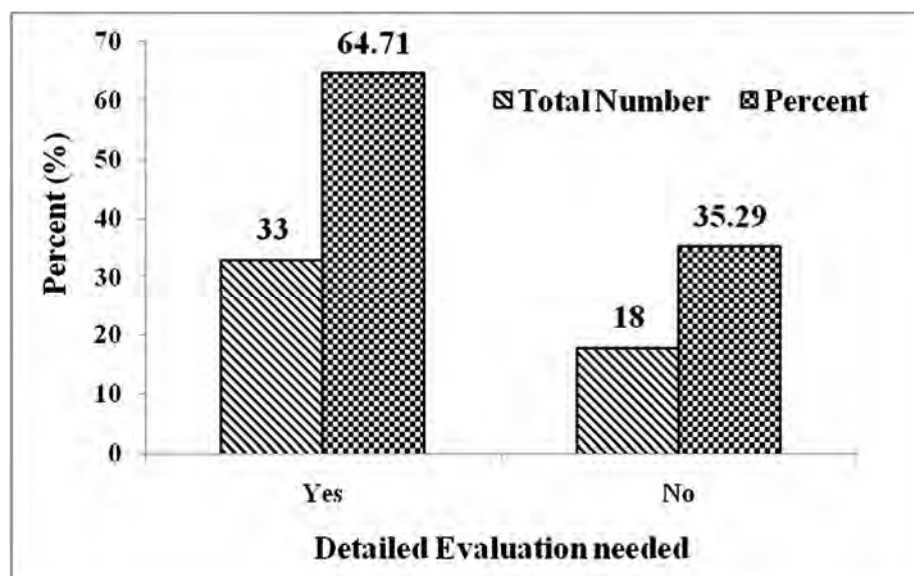


Fig. 6. Detailed evaluations of the infrastructures is needed or not to needed.

Conclusion

Some of the schools and colleges in Tangail municipality were new and earthquake resistant. In contrast more than half of the buildings were made of concrete, but most of the buildings were ancient and visually they need further evaluation, some of them were built in British Period. Modern

engineering concrete-framed buildings were generally safer than non engineering infrastructures because old buildings are devoid of modern engineering technology for what their architectural longevity is vulnerable as they sometimes collapse due to earthquake or other natural forces. The ultimate result of the fault line in architectural activity is considerably more lethal which kills higher percentage of people than masonry structures. The worst victims will be the school and college students. The observation found that the majority of the buildings were more than 20 years old and were not appropriately followed plan irregularity and vertical irregularity. Seismic Performance Attributes Score Modifiers showed that most of the infrastructures were needed detailed evaluation to reduce the vulnerability of earthquake and vulnerable buildings or infrastructures should be replaced by new earthquake resisting buildings; and occupancy load would be maintained in every building.

Acknowledgements

The author is grateful to engineer K.M. Khaleduzzaman, member of Bangladesh Earthquake Society and Bangladesh Society for Geo-technical Engineering. Sincere gratitude to the District Education Officer (DEO), Tangail, and all the Headmasters and the Principals of the schools and colleges, respectively in Tangail municipality for their kind cooperation during the study period.

References

- Ali, M. H. and J. R. Choudhury. 1994. Seismic Zoning of Bangladesh. In: the International Seminar on Recent Developments in Earthquake Disaster Mitigation, Institution of Engineers, Dhaka.
- Banglapedia. 2008. National Encyclopedia of Bangladesh. Asiatic Society of Bangladesh.
- BIS (Bureau of Indian Standards). 2002. Indian standard criteria for earthquake resistant design of structures, Part 1: general provisions and buildings. Engineering, 1893: 41.
- FEMA (Federal Emergency Management Agency). 2002. Rapid Visual Screening of Buildings for Potential Seismic Hazards- FEMA 154. Federal Emergency Management Agency, Washington DC, USA.
- Hays, W., B. Mohammadioun and J. Mohammadioun. 1998. Seismic Zonation: A Framework for Linking Earthquake Risk Assessment and Earthquake Risk Management (Monograph), Quest Editions Presses Academiques.
- Herrera, R. G. and C. G. Soberón. 2008. Papers on Influencing of Plan Irregularity of Building. The 14th World Conference on Earthquake Engineering, October 12-17, 2008, Beijing, China
- McCrum, D. P. 2012. Seismic Analysis of Braced Plan Irregular Structures Using Hybrid Testing and Numerical Modeling. Department of Civil, Structural and Environmental Engineering, University of Dublin, Trinity College.

- OECD (Organization for Economic Cooperation and Development). 2004. Keeping Schools Safe in Earthquakes School Safety and Security. OECD Programme on Educational Building. Paris.
- Oldham, T. 1899. Report on the great Indian earthquake of 12th June, 1897, Memoir of Geological Survey of India, 29: 1-349.
- SAARC (South Asian Association of Regional Cooperation). 2011. Rapid Visual Screening of School and Hospital Buildings in SAARC Countries. SAARC Disaster Management Centre New Delhi.
- Sharfuddin, M. 2001. Earthquake Hazard Analysis for Bangladesh. M. Sc. Engineering Thesis, Department of Civil Engineering, BUET, Dhaka, Bangladesh.
- UNEP (United Nations Environmental Program). 2001. United Nations Environmental Program. Annual Evaluation Report.
- UNISDR (United Nations International Strategy on Disaster Reduction). 2009. Terminology on Disaster Risk Reduction and Response. Geneva, Switzerland: United Nations International Strategy for Disaster Risk Reduction.
- Wang, Y. and K. A. Goettel. 2007. Enhanced Rapid Visual Screening (ERVS) Method for Prioritization of Seismic Retrofits in Oregon. Oregon Department of Geology and Mineral Industries, California.



PART-III

Non-destructive Testing (NDT) in a residential building located at Gulshan

**BANGLADESH NETWORK OFFICE FOR URBAN
SAFETY (BNUS), BUET, DHAKA**

Prepared By: KM Khaleduzzaman

Mehedi Ahmed Ansary

1.0 Introduction

Mr. Ahmed, a house owner of Gulshan, Dhaka approached BUET for technical assistance to find out as built status of different structural members of the existing residential building located at Gulshan. It has been agreed that the terms of reference of the work would be limited to concrete strength determination using two core tests and Schmidt Hammer test, identification of structural detailing at selected locations through non-destructive testing (Ferrosan), excavating and physical checking of two foundations.

2.0 Determination of Concrete Strength by Using Schmidt Hammer and Core Test

Figure 1 shows the layout plan (showing the location of in-situ tests) of the area at which locations Schmidt Hammer test have been carried out. Figure 2 shows the use of Schmidt Hammer and Table 1 shows the results of the Schmidt Hammer test. The concrete (cylinder) strength varies from 4050 to 48300 psi. Also concrete cores have been collected from four locations of the building (three from the footing and one from the roof column) and concrete strength of core has been measured at the BUET Concrete laboratory. The concrete strength of core collected from the foundation varies between 3530 to 5670 psi and the concrete strength of the core collected from the roof column is 4070 psi.

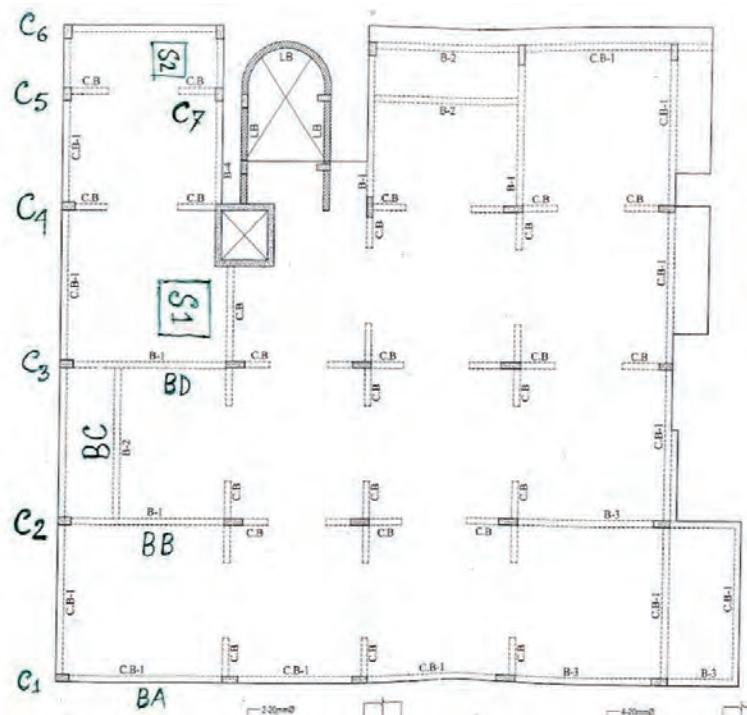


Fig. 1 Locations of Schmidt Hammer Test



Fig. 2 Use of Schmidt Hammer to estimate concrete strength

Table 1. Results of Schmidt Hammer Test (Beams and Columns)

Location	Direction	Impact Values	Avg. Impact Values $M \pm \sigma$	Compressive Strength (Cylinder), psi
BD	Horizontal	39, 48, 32, 31, 42, 40, 40, 38, 39, 40	39 ± 4.8	4050
BD	Vertical (Upward)	43, 42, 42, 43, 43, 41	$42 \pm .82$	4350
BB	Horizontal	43, 33, 40, 43, 40, 39, 41, 42, 43	40 ± 3.2	4170
BC	Horizontal	42, 39, 40, 41, 36, 38, 41, 40, 39	40 ± 1.8	4170
C3	Horizontal	49, 40, 42, 42, 49, 41, 42, 42, 42, 44	43 ± 3.2	4830
C4	Horizontal	40, 32, 39, 40, 40, 39, 41, 40	39 ± 2.8	4050
C7	Horizontal	41, 50, 40, 42, 43, 41, 43, 42, 41	43 ± 2.9	4830
S2	Vertical (Upward)	49, 49, 42, 30, 51, 43, 41, 43	43 ± 6.6	4590

3.0 Checking of Footing Sizes

Excavations have been made at the north-east corner of the building to expose two footings (FC2 and F6). It should be mentioned here that the owner of the building allowed the BUET consultants to excavate only these two locations. After excavation, the thickness and smaller width of the foundation have been measured. Figure 2 shows the location of the footings and Table 2 compares the as built dimension with design values.

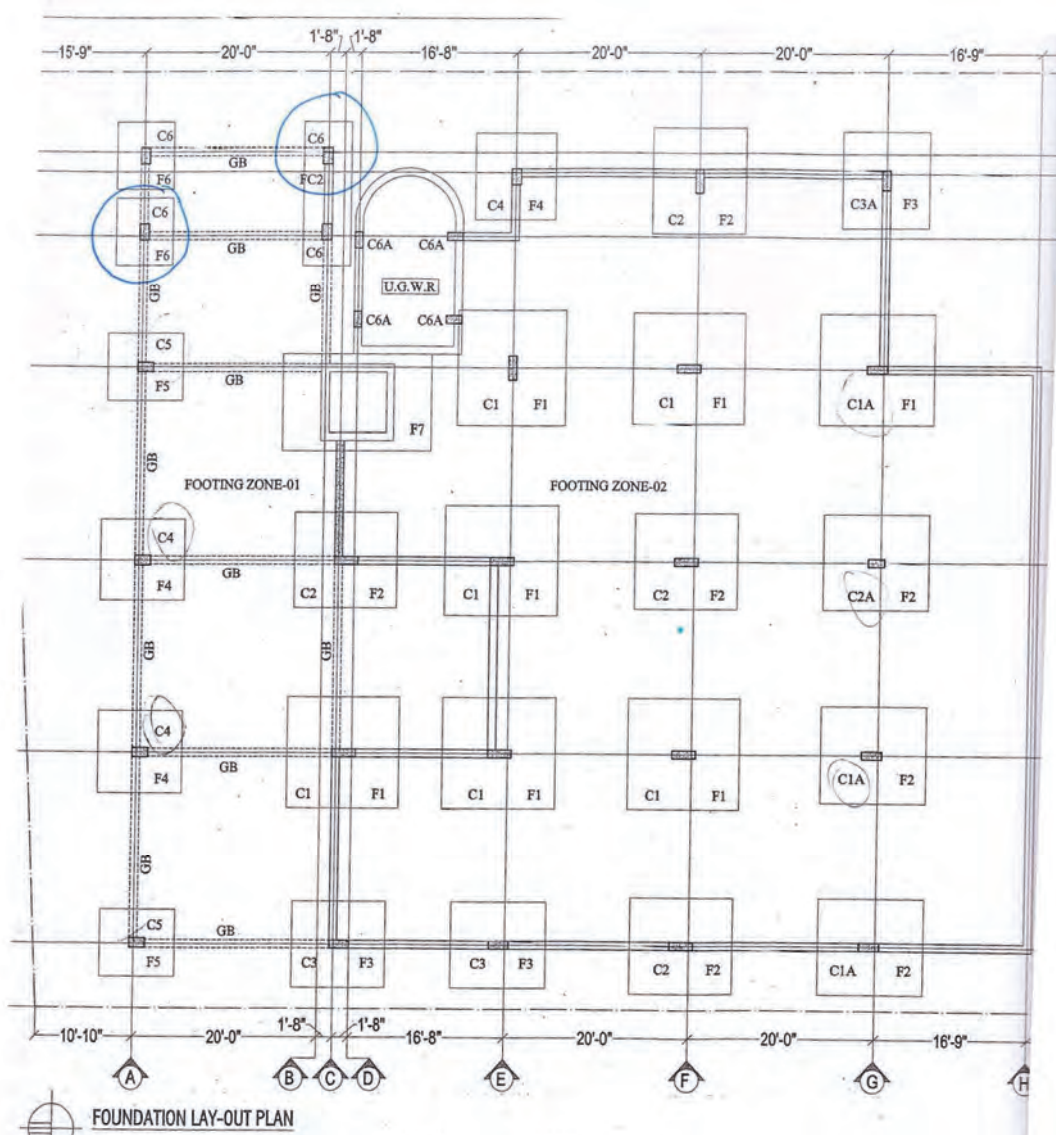


Fig. 2 Locations of columns and footings

Table 2 Verification of physical dimensions of footings

Footing Designation	As-built size (ft)	As-built thickness (inch)	Remarks
FC2	5 ft	24	ok
F6	7 ft	18	ok

4.0 Non-Destructive Testing (NDT) Using Ferrosan

The four storied building at Gulshan, Dhaka has been assessed with a view to check the as-built condition of the structural design of different structural members (i.e, column, beam, and slab) of the building. It is important to note that several cracks have been observed at the bottom side of the hanging cantilever verandah. Several ties (suspenders) have been provided in the design to support the bottom part of the cantilever verandah. Cracks are also observed at the false ceiling of two bathrooms. Initially, few columns and some parts of slab (including RCC false ceiling of two bathroom) of ground floor and 2nd floor have been scanned with ferrosan machine to check the number and diameter of the steel used in these structural members. Figure 3 shows the position of scanned columns and roof slabs of second floor.

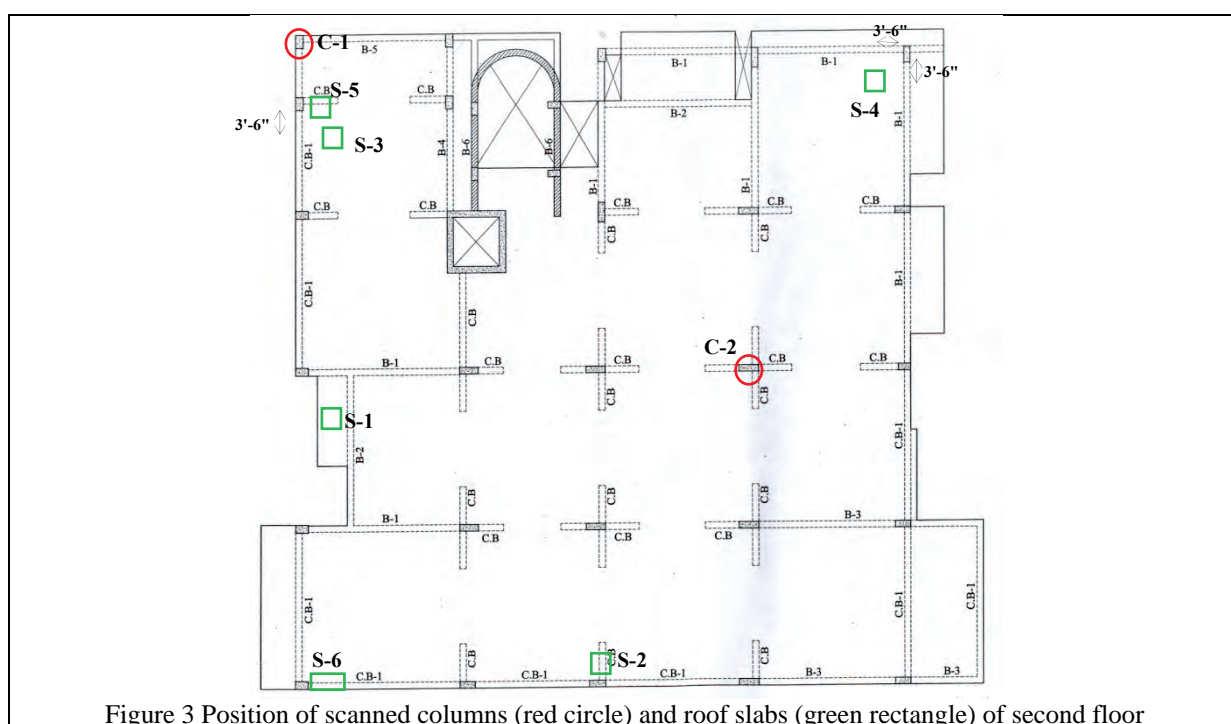
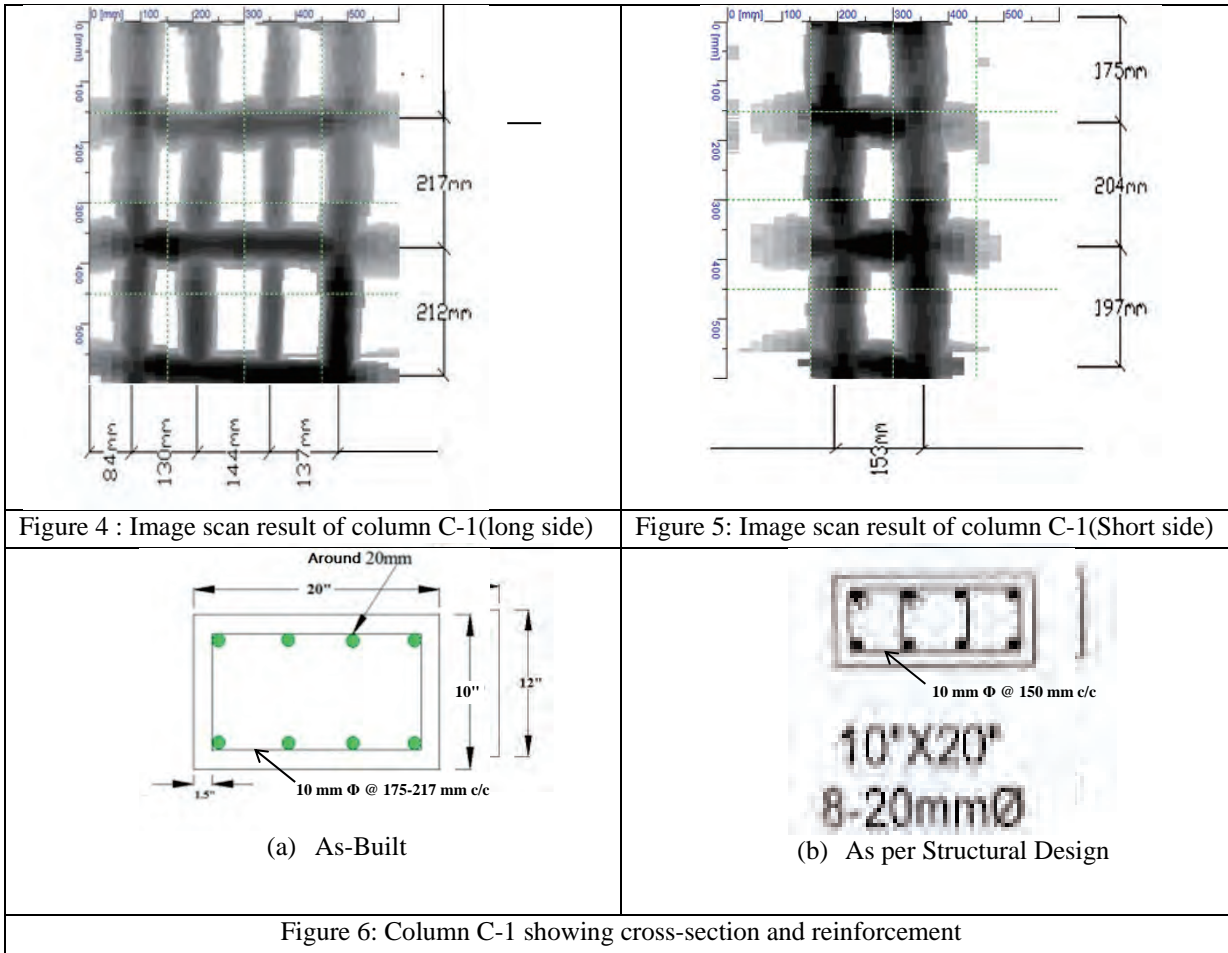


Figure 3 Position of scanned columns (red circle) and roof slabs (green rectangle) of second floor

4.1 Scanning of Columns of Second Floor

Figures 4 and 5 are showing the Image scan result of column C-1 (long side and short side respectively) at a height of 2'-8" from the ground. Figure 6 shows the cross section and reinforcement in column after scanning. The spacing of column ties (as per structural design) is 150 mm c/c. However, from the As-Built drawing, it shows that the spacing varies from 175 to 217 mm c/c.



Similarly Figures 7 and 8 show the Image scan result of column C-2 (long side and short side respectively) at a height of 2'-0" from the ground. Figure 9 shows the cross section the column reinforcement. The spacing of column ties (as per structural design) is 100 mm c/c. However, from the As-Built drawing, it shows the spacing varies from 101 to of 110 mm c/c.

4.2 Scanning of Ceiling of Second Floor

Due to problems with accessibility, only bottom layer reinforcements of floor slab have been ferroscored. Figures 10 and 11 indicate the image scan result of six different positions of ceiling of second floor. S-1 position is at the slab of veranda which is just near the position where some cracks are found. In this location according to design 12 mm Φ @ 300 mm c/c has been provided with 1-12 mm Φ extra bottom (both directions). S-2 position is at the slab inside a middle room. In this location according to design 12 mm Φ @ 87.5 mm c/c has been provided (both directions). S-3 position is at the slab inside a middle room. In this location according to design 12 mm Φ @ of 150 mm c/c has been provided (both directions).

In S-4 location according to structural design, 12 mm Φ @ of 87.5 mm c/c has been provided in both directions. In S-5 location according to design 12 mm Φ @ 75mm and 87.5 mm c/c have been provided in two directions. S-6 position is situated at edge of the room where integral (so called concealed) beam, CB-1 has been provided. In this location according to structural design,

12 mm Φ @ 75mm and 87.5 mm c/c have been provided in two directions. In integral beam CB-1, 4-20 mm Φ rebars has been provided for both top and bottom of the slab.

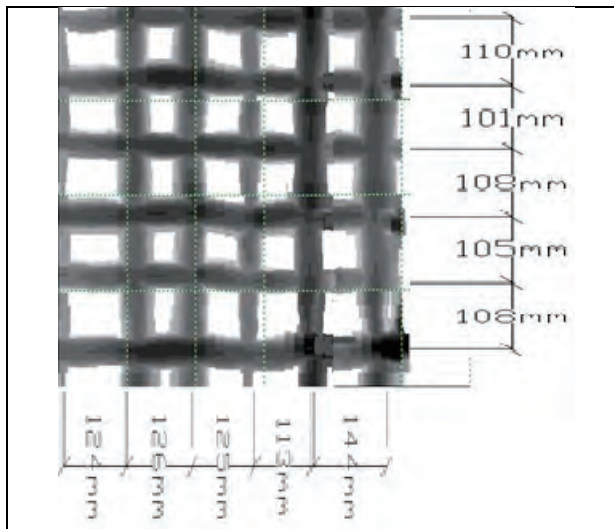


Figure 7: Image scan result of column C-2 (long side)

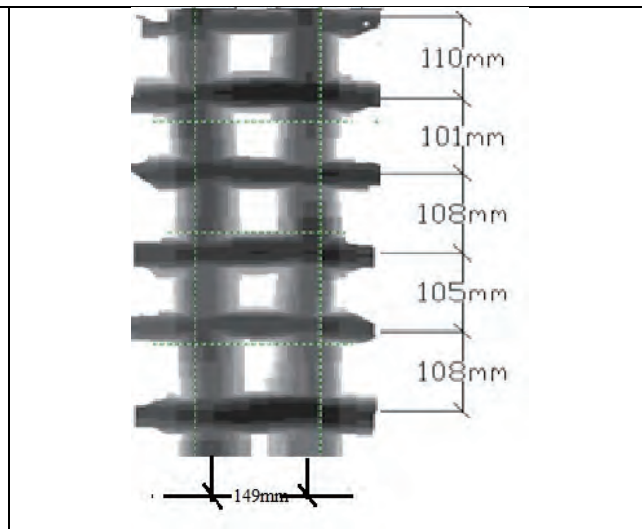


Figure 8: Image scan result of column C-2 (Short side)

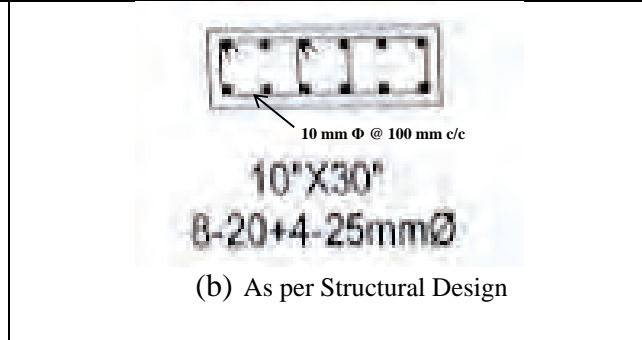
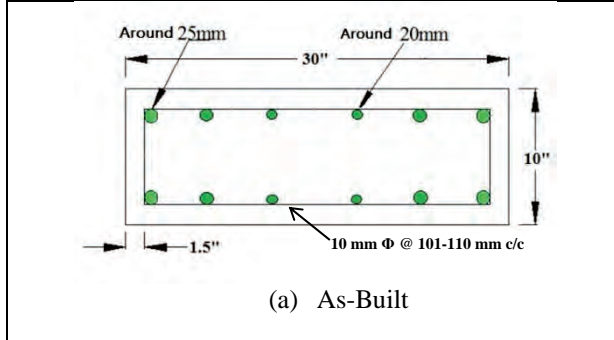


Figure 9: Column C-2 showing cross-section and reinforcement

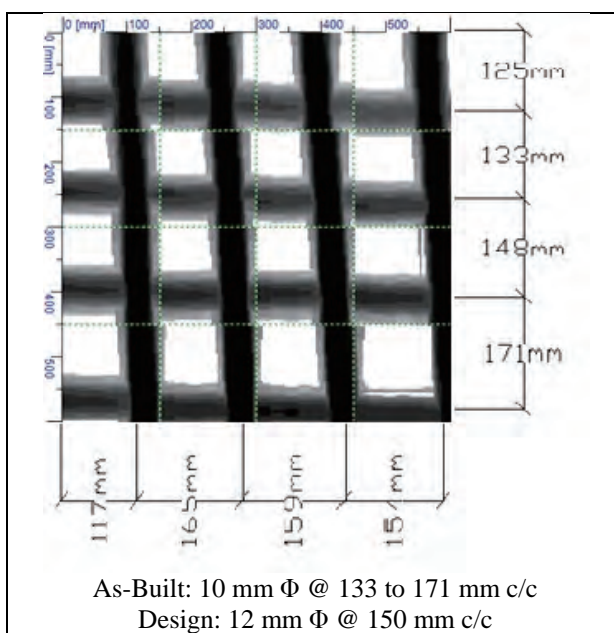


Figure 10: Block image of slab at S-1 position

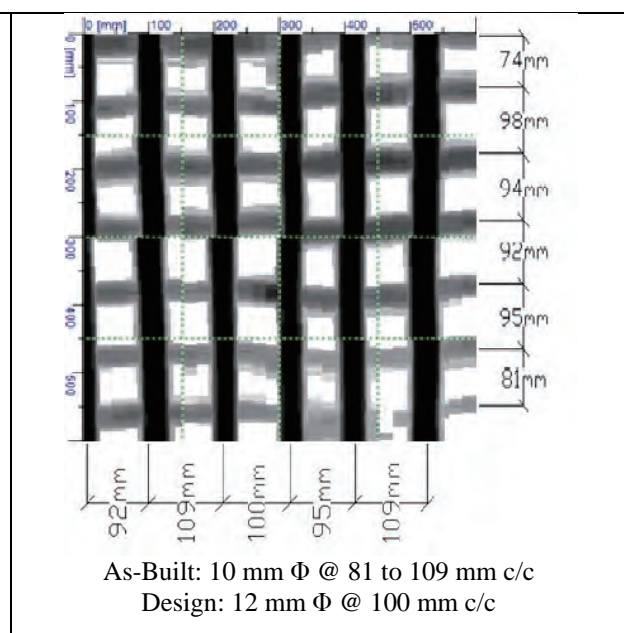


Figure 11: Block image of slab at S-2 position

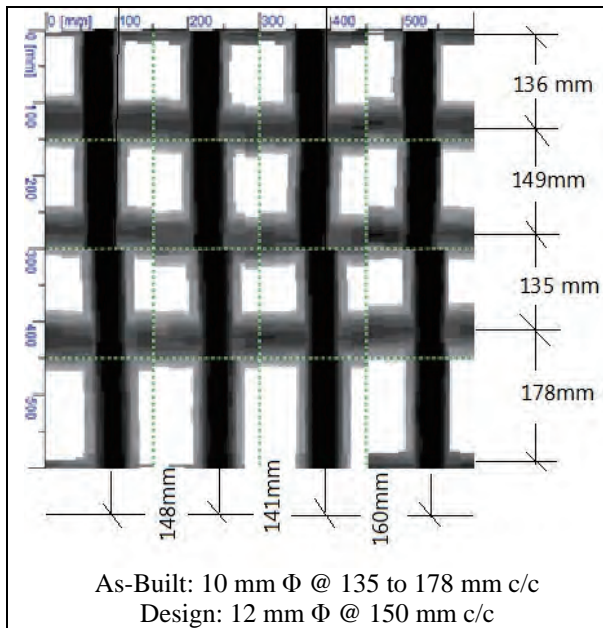


Figure 12: Block image of slab at S-3 position

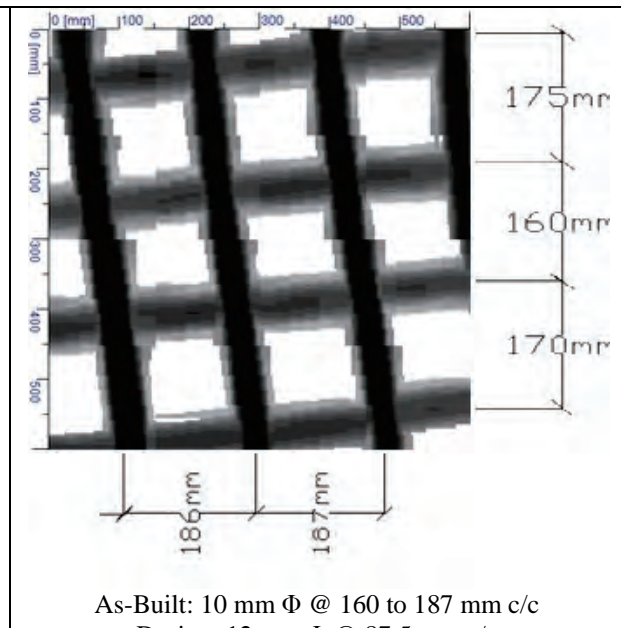
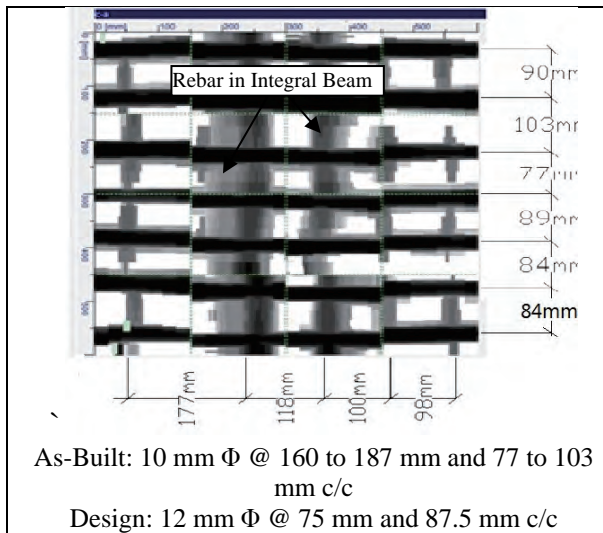


Figure 13: Block image of slab at S-4 position



Integral Beam: 2-20 mm Φ (bottom) after scanning; 4-20 mm Φ (bottom) according to Design

Figure 14: Image scan of Concealed beam at S-5 position (middle steel Diameter around 20mm found)

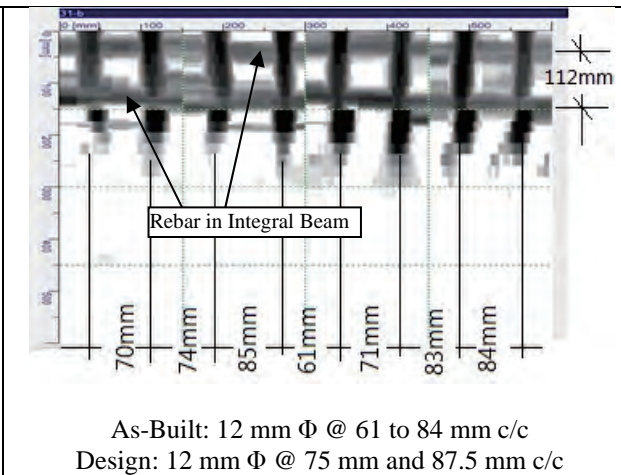
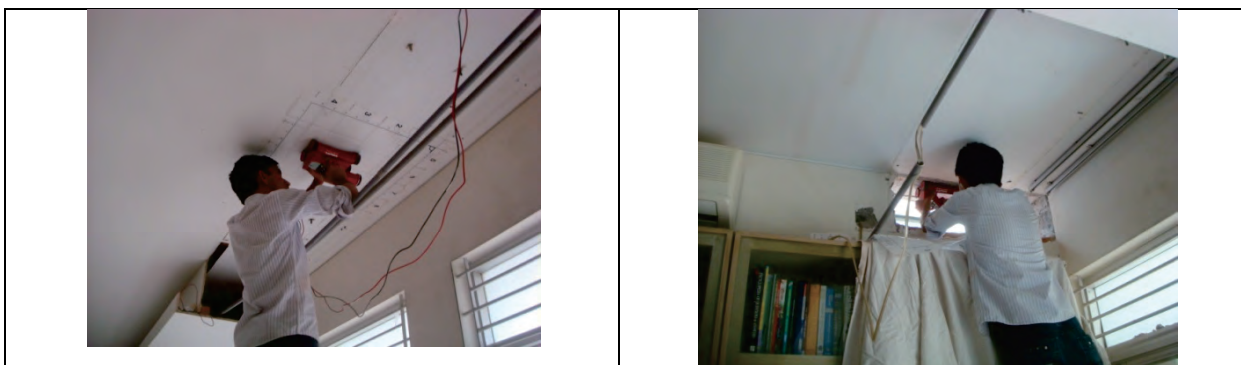


Figure 15: Image scan of Concealed beam at S-6 Position (middle steel Diameter around 20mm found)



4.3 Scanning of Cantilever Verandah with Suspended Bottom Slab of Second Floor

A suspended bottom slab of the cantilever verandah of the second floor has been scanned. Location of the suspender or tie rod has been identified as shown in Figure 16. In structural design, the number of suspenders is more than the number provided in the construction.

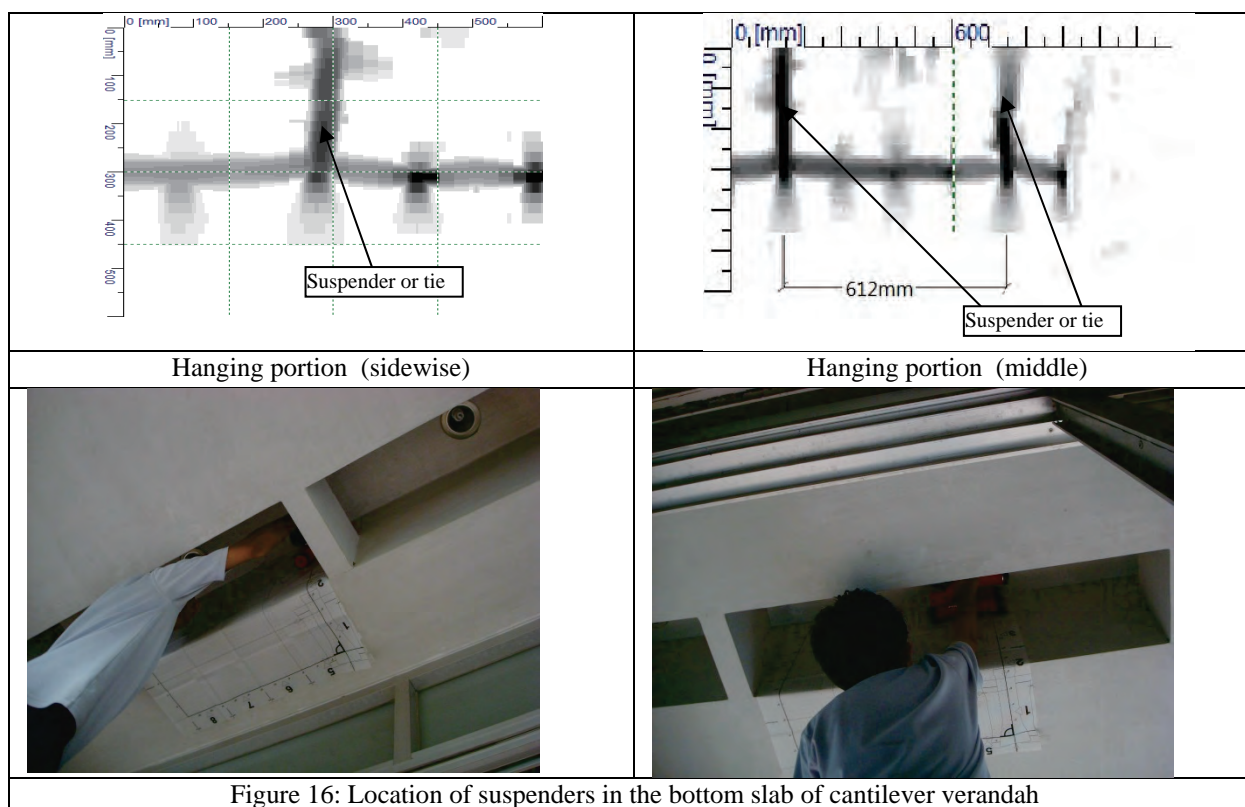


Figure 16: Location of suspenders in the bottom slab of cantilever verandah

4.4 Scanning of Columns of Ground Floor

Figure 17 shows the position of scanned columns and roof slabs of ground floor. Figures 18 and 19 show the Image scan result of column C-1 (long side and short side respectively) at a height of 2'-8'' from the ground. Figure 20 shows the cross section of the column and reinforcement. The spacing of the tie bar from the design shows 100 mm c/c. From the As-Built drawing, it shows the spacing varies from 180 to of 280 mm c/c. Similarly, Figures 21 and 22 shows the Image scan result of column C-2 (long side and short side respectively). Figure 23 shows the cross section of the column and reinforcement. The spacing of the tie bar from the design shows 100 mm c/c. From the As-Built drawing, it shows the spacing varies from 120 to of 230 mm c/c.

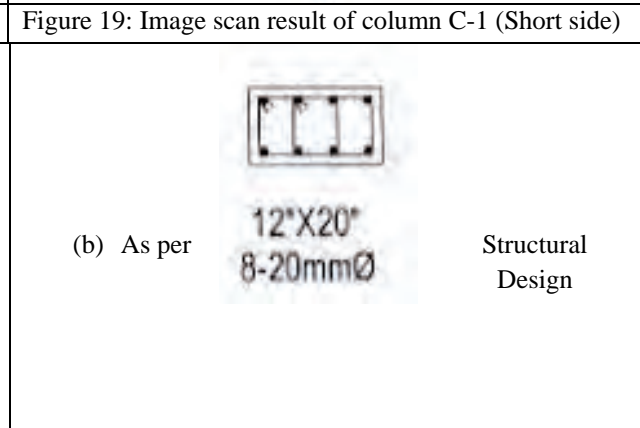
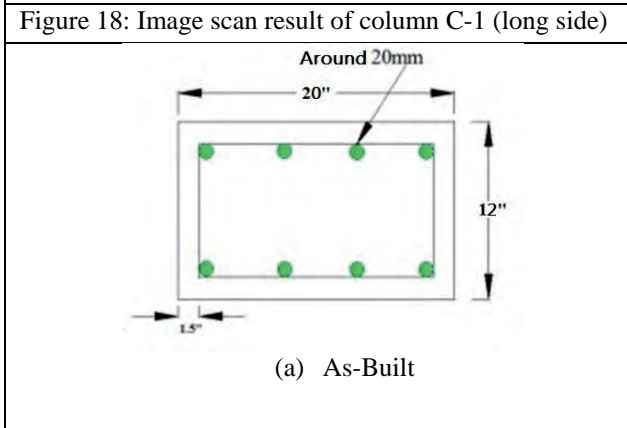
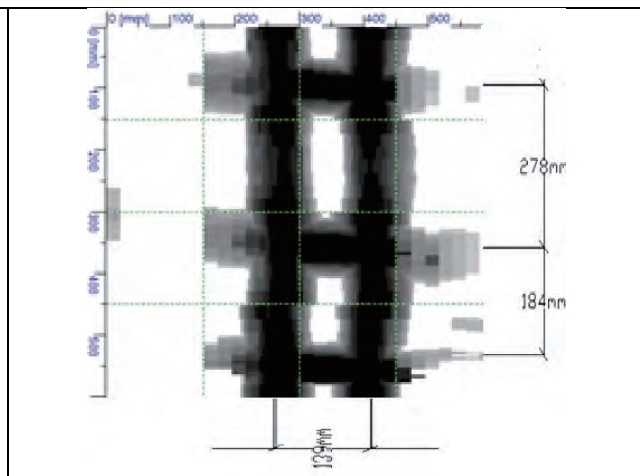
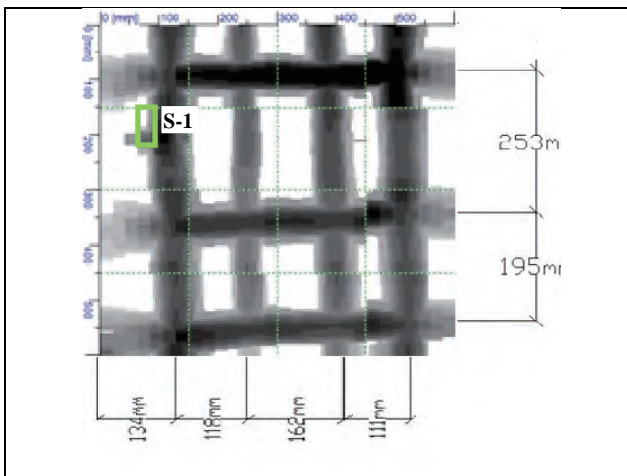
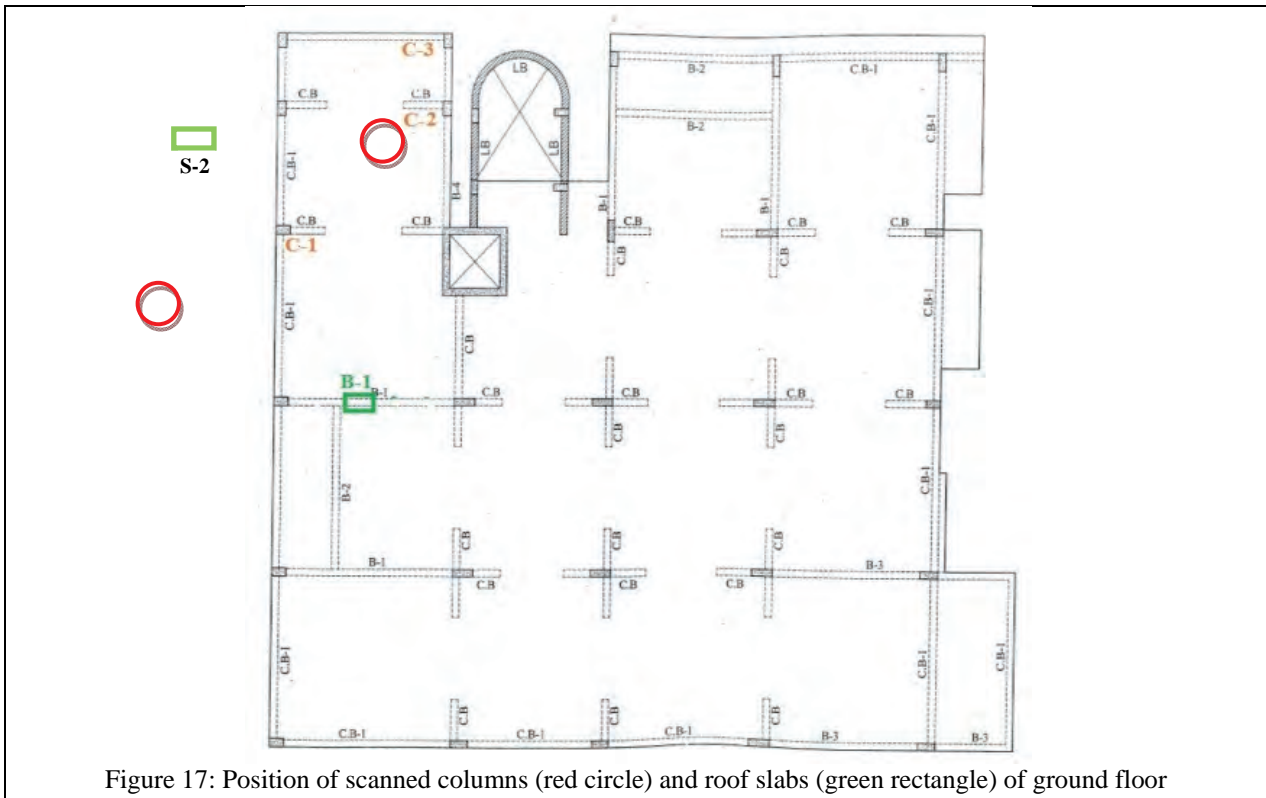


Figure 20: Column C-1 showing dimension and reinforcement

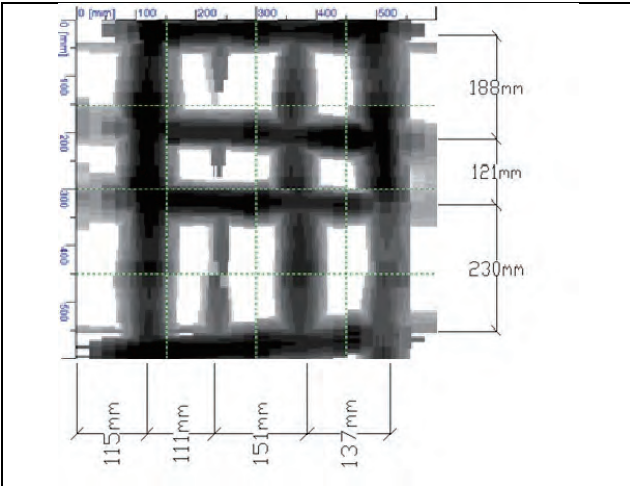


Figure 21: Image scan result of column C-2 (long side)

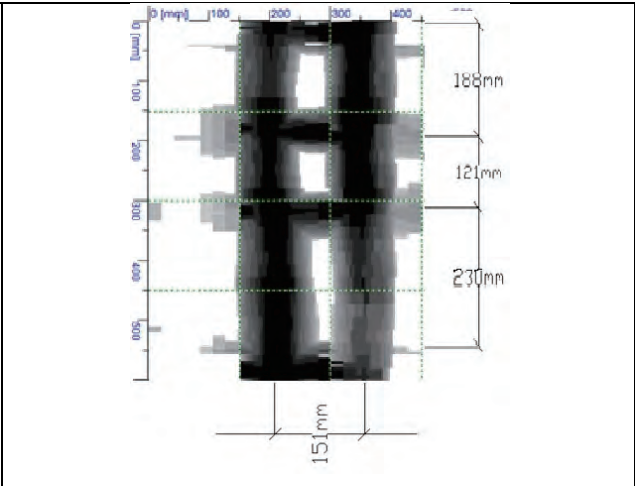
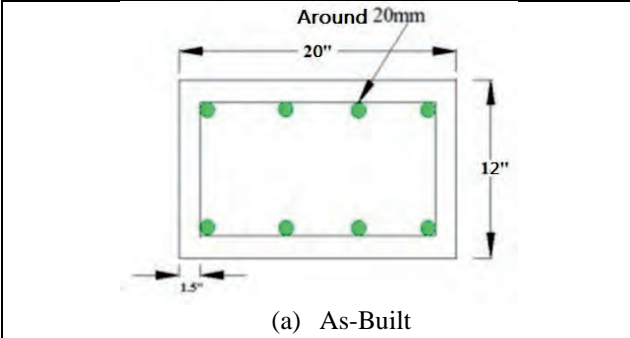
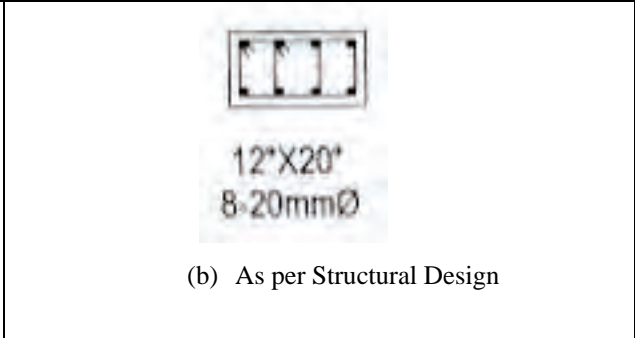


Figure 22: Image scan result of column C-2 (Short side)



(a) As-Built



(b) As per Structural Design

Figure 23: Column C-2 showing dimension and reinforcement



4.5 Scanning of Beams of Ground Floor

Ferros scanning has also been performed to know the as built status of floor beams. Beam B1 has been selected in this case due of its accessibility to the scanner. For beam B1, the spacing of the stirrup from the design shows 100 mm c/c. From the As-Built drawing, it shows the spacing varies from 88 to of 113 mm c/c. Therefore, it is apparent from scanning that the spacing of stirrup complies with the structural design.

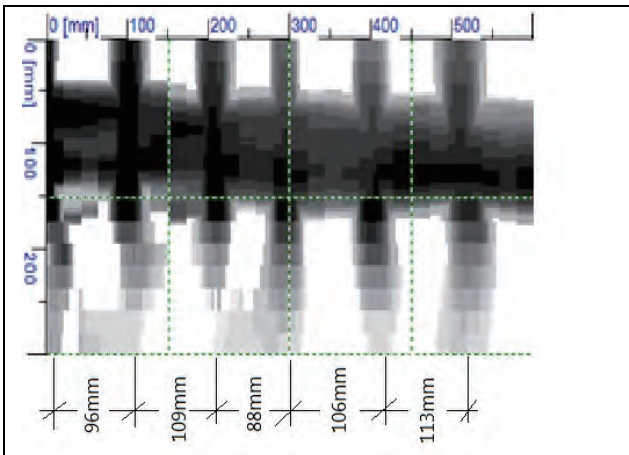


Figure 24: Long section of beam after scanning showing spacing of stirrup

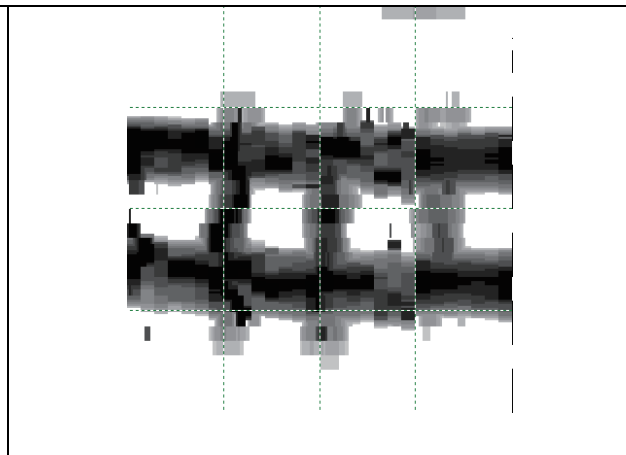
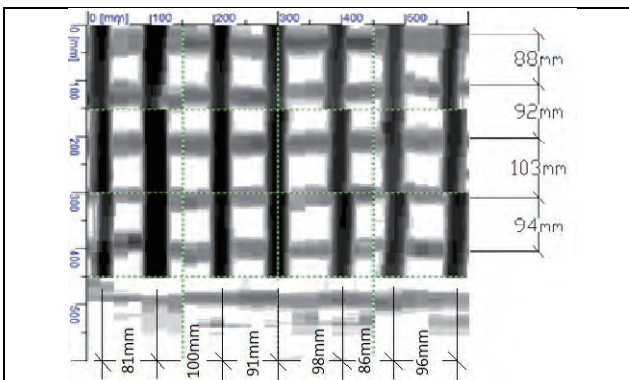


Figure 25: Beam soffit after scanning showing two rebars widthwise



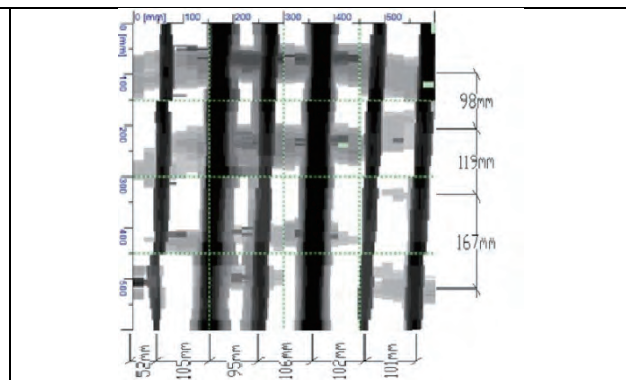
4.6 Scanning of Ceilings of Ground Floor

In S-1 location just below the integral beam CB1, according to design 12 mm Φ @ of 87.5 mm c/c has been provided. In S-2 location just below the integral beam CB, according to design 12 mm Φ @ of 150 mm c/c has been provided in one direction and 87.5 mm c/c in another direction.



As-Built: 10 mm Φ @ 81 to 103 mm c/c

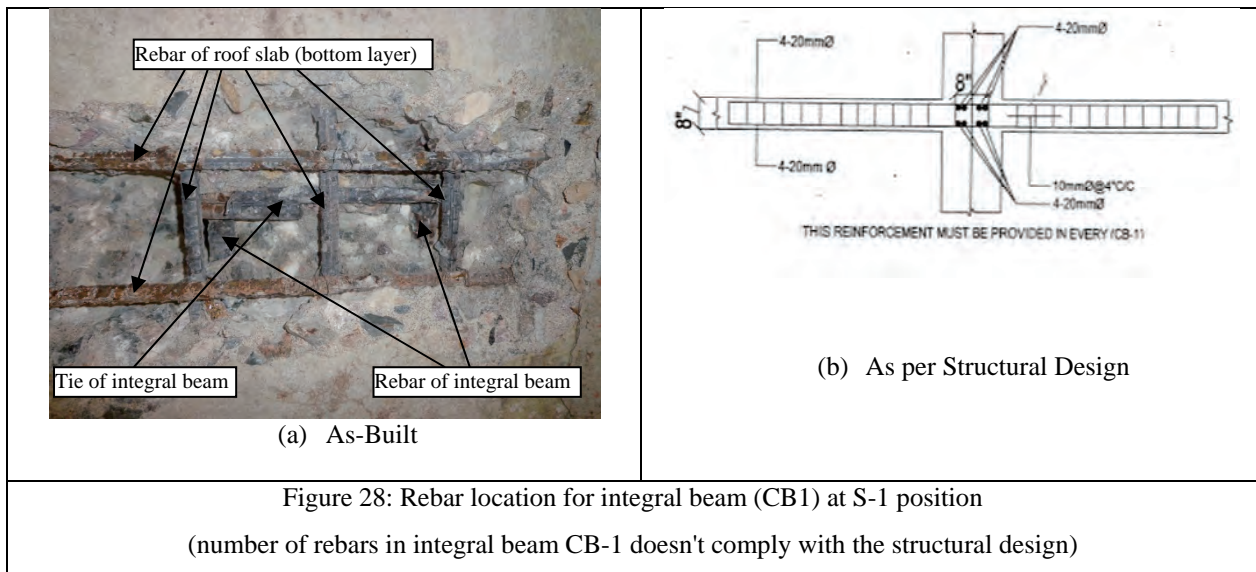
Figure 26: Block image of slab at S-1 position



As-Built: 10 mm Φ @ 95 to 119 mm c/c

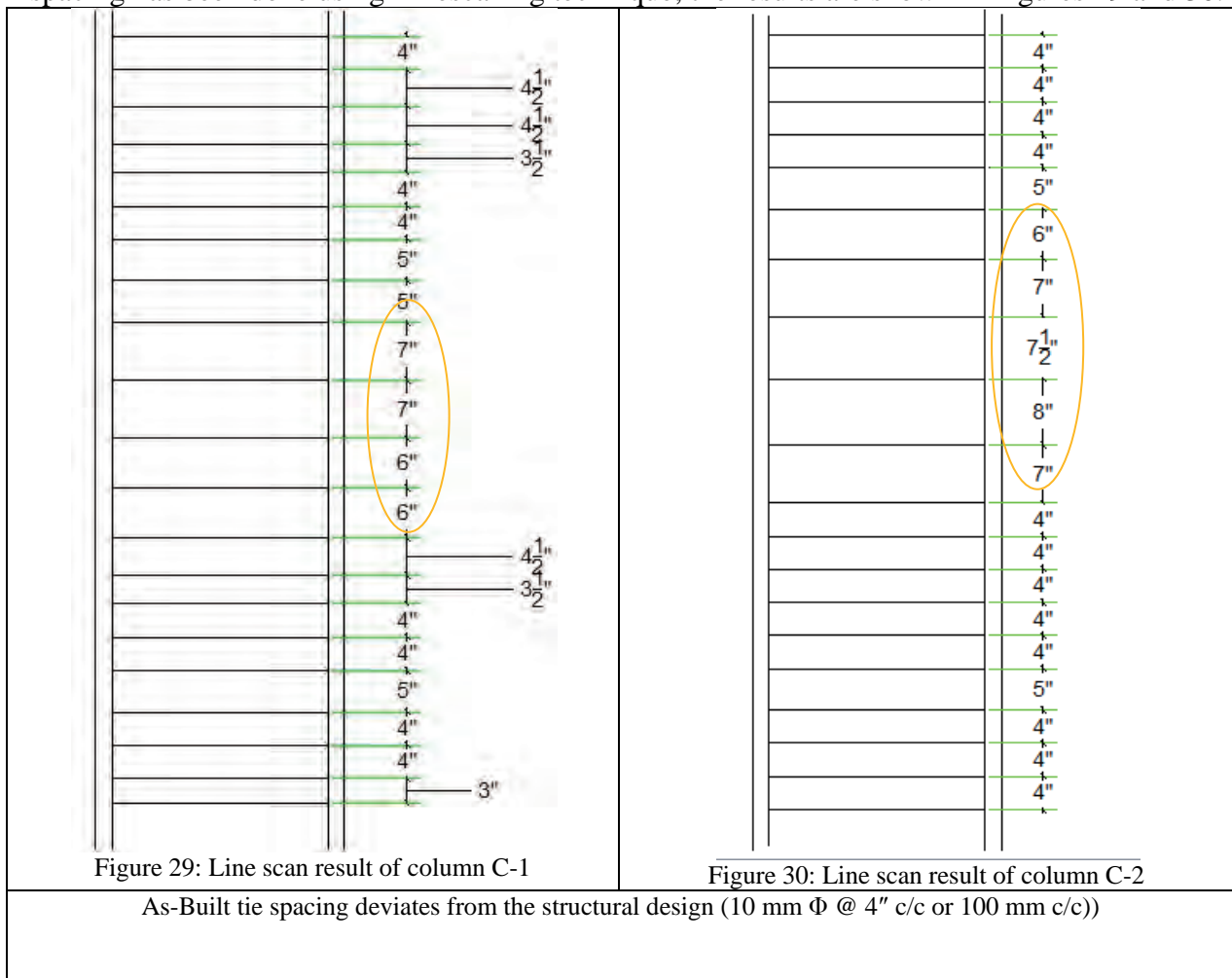
Figure 27: Block image of slab at S-2 position





4.7 Verification of Tie Spacing of Column of Ground Floor by Using Linescanning Technique

From Imagescan results of columns of ground floor, it has been observed that As-Built tie bar spacing does not match with the structural design spacing in a few locations. A verification of the spacing has been done using Linescanning technique; the results are shown in Figures 29 and 30.



5.0 Concluding Remarks

Scanning results show that

1. There is compliance of main rebar in columns with the structural design
2. In general, the as built concrete strength of different structural members (Footings, Columns, Beams and floor slab) complies with the structural design.
3. Spacing of column ties has found to vary from the spacing provided in the design
4. In general, steel rebars in floor slabs (bottom layer) has found to comply with the design
5. The provision of integral beams along column lines (CB) has been confirmed by the scanning. However, the number of rebars in CB1 location doesn't comply with the structural design. Therefore, the integral beam CB1 may not be adequate to transfer unbalanced moment to the columns. Some of the column-integral beam joints may need to be strengthened to ensure the transfer of this unbalanced moment.
6. The spacing of the suspenders (to support the bottom slab of the cantilever verandah) does not comply with the structural design. This may affect the stability of these structural members.
7. Long section of the beam shows the location of the stirrups



PART-IV

SAVAR BUILDING TRAGEDY IN BANGLADESH: WAY FORWARD

**BANGLADESH NETWORK OFFICE FOR URBAN
SAFETY (BNUS), BUET, DHAKA**

Prepared By: Naima Rahman

Mehedi Ahmed Ansary

As garments industries have become the main source of foreign income of Bangladesh, many new factories have been established in Dhaka City. But due to lack of concern from authorities, this industry has become one of the highly risk working sector for workers. Garment industry has been experienced many fire accidents in the last decades taking life of many workers. But the recent accident of building collapse in Savar is the worst of all. This incident took lives of 1132 people and left many disabled. About 332 people are still missing according to their families. Six garments factories, one bank and many shops are going into debris within a few minutes without any shake from outside. In this study, the authors discuss the reason behind the accident, the role of authorities in search and rescue, overall co-ordination, rehabilitation and legal activities. The authors also recommend some measures to avoid this type of disaster in Bangladesh.

1. INTRODUCTION

1.1 Background

On 24 April at 9am, a nine-storey building collapsed in Savar, 25 kilometers north of the Bangladesh capital, Dhaka (see Figure 1). As of August, 1132 people died (CPD, 2013), 2438 people were rescued and were provided with immediate basic first aid or transferred to nearby hospitals for medical attention. The building housed several garment factories, a bank and several shops. The factories manufactured apparel for brands including Benetton, Bonmarché, Cato Fashions, the Children's Place, El Corte Ingles, Joe Fresh, Mango, Matalan, Primark and Wal-Mart. According to BGMEA (Bangladesh Garments Manufacturers and Exporters Association) 2800 workers of the 6 garment factories were in the building during the accident. But the actual number is around 3900 (CPD, 2013). Day before the incident, some cracks developed on some pillars and a few floors of the building following a jolt, causing panic among the people working there. They rushed out of the building and some even got injured in the process, said a number of garment workers and locals. The industrial police visited the building that day and asked the building authorities not to open the building. But the warnings and instructions were ignored. The shops and the bank on the lower floors immediately closed after cracks were discovered in the building. But workers of at least two garment factories at Rana Plaza were forced to join their workplaces following a false assurance on the building's safety from a local engineer, relatives of the victims alleged. As a result the deadliest garment-factory accident in the history of Bangladesh occurred which is also considered as the deadliest accidental structural failure in the modern world.

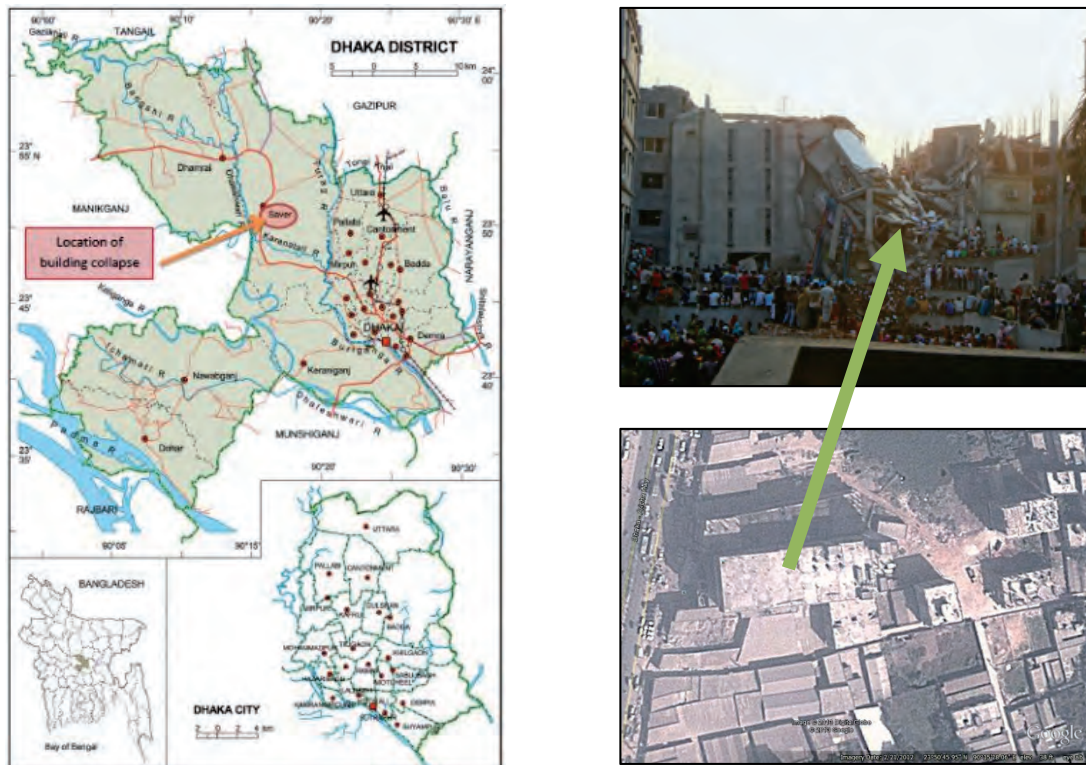


Figure 1. Location of the collapsed building

1.2 Purpose of the Study

The purpose of the study is to focus on overall scenario of the Savar tragedy. This article presents the search and rescue effort undertaken by different agencies in Bangladesh to rescue people from underneath the collapsed building and tries to explain the reasons behind the building collapse. Figure 2 shows the collapsed building.



Figure 2. The collapsed building

2. REASONS BEHIND THE BUILDING COLLAPSE

Rana Plaza was a 9-storied industrial building with a single basement. The local municipality gave the owner permission to construct a 5 storey commercial building with one basement in 2005 and later allowed the owner to extend it up to 9-storey, without considering the consequence of such action. The width of the building was around 25 m and length around 80 m. A typical grid of the building is 5.2 m by 8.2 m. The column sizes vary from 35 cm by 35 cm to 45 cm by 45 cm. The building was supported by pile foundation having 450 mm diameter and length of 18.3 m. Three main reasons can be attributed to the collapse of the structure: (i) Addition of four extra floors; (ii) Conversion of the building from commercial to industrial use and (iii) Placement of Power

Generators at the higher floors. The steel grade used was 60 grade deformed bar and concrete strength was found around 3000 psi [see Figure 3].



Figure 3. (a) Broken samples collected from the building site and (b) Concrete cores collected from beams, columns and slabs of the collapsed building

2. SEARCH AND RESCUE OPERATIONS

2.1 Search and Rescue

Local Volunteers, volunteers of Bangladesh Red Crescent Society, personnel from Bangladesh Fire Service and Civil Defense, Bangladesh Armed Forces personnel, Border Guard Bangladesh and local police were involved in search, rescue and evacuation operation of trapped garment workers at Savar Building collapse site. On the day of incident, these organizations rescued 1762 people alive.



Figure 4. Search and rescue operation

The local people started rescue operation immediately after the incident. Then Bangladesh Army, Navy, Fire Service, BGB, Police and different volunteer teams joined in the rescue activities. Police and RAB are engaged to maintain law and order situation at the site. Rescue operation is continuing. 1200 volunteer from Dhaka, Keraniganj and Narayanganj area (trained by Comprehensive disaster management Programme (CDMP) under Ministry of Disaster Management and Relief) are working in Rescue operation. To purchase rescue equipment instantly, MoDMR has given BDT 5,00,000 to Fire Service and Civil Defense. Figure 4 and 5 shows the activity of people during Search and rescue operation



Figure 5. Search and rescue operation

More than 200 volunteers under the Department of Fire Service and Civil Defense (FSCD) who have received training under the previous DIPECHO VI Project implemented under the NARRI Consortium were immediately deployed after the incident and are working on location.

2.2 Overall Coordination

Armed Forces Division (AFD) of Bangladesh coordinated the search and rescue operation. Eman medical hospital played an important role for the injured victims by providing medical support. Fifteen Medical teams from Bangladesh Army, two from Navy, one from Air Force, one from BGB and ten teams from health department, the doctors and medical workers of local hospital and clinic are engaged for treatment of injured people.

2.3 Contribution of local volunteer

Some local people involved in search and rescue operation among them some died unexpectedly. Figure 6 shows the number of death and rescued alive from the day of accident to the day of last dead body found.

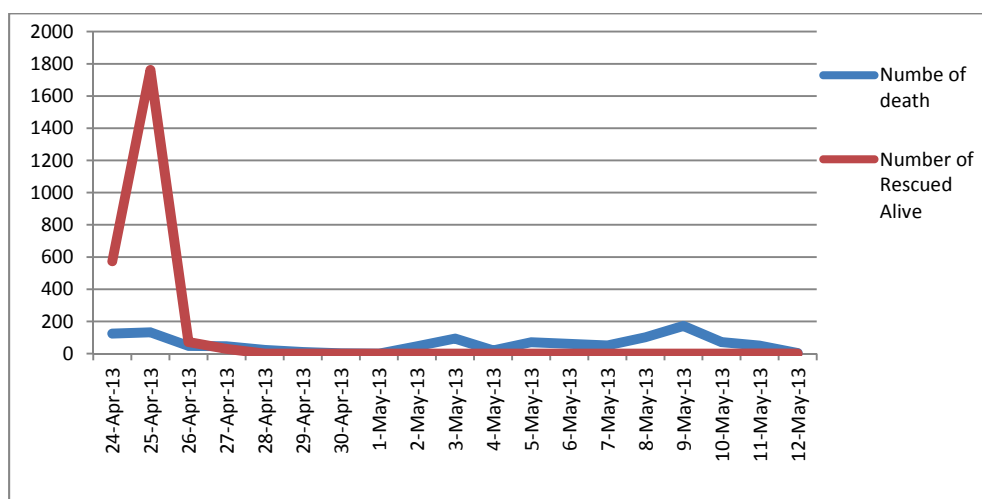


Figure 6. Number of death and rescued alive

From the day of accident, 574 people were rescued alive whereas 124 people were found dead. On the second day the highest number of people (1762) was saved alive. Alive people were found up to 4 days of the accident. But a woman named Reshma was found and rescued alive and almost unhurt

under the rubble 17 days after the accident on 10 May. Dead bodies were found almost every day from 24 April to 12 May.

The Bangladesh Red Crescent Society was among the first responders on the scene. 100 trained volunteers are on the ground on a rotation providing search and rescue, basic first aid and safe drinking water. The organization also established a mobile medical team assisting the wounded. The Red Crescent Society ambulance service transported wounded people to various hospitals, and the organization also helped with the management of dead bodies. Restoration of Family Link (RFL) volunteers provided mobile phone services for the injured (see Figure 8) to connect with their families and relatives, and also compiled a list of the missing, injured and dead.

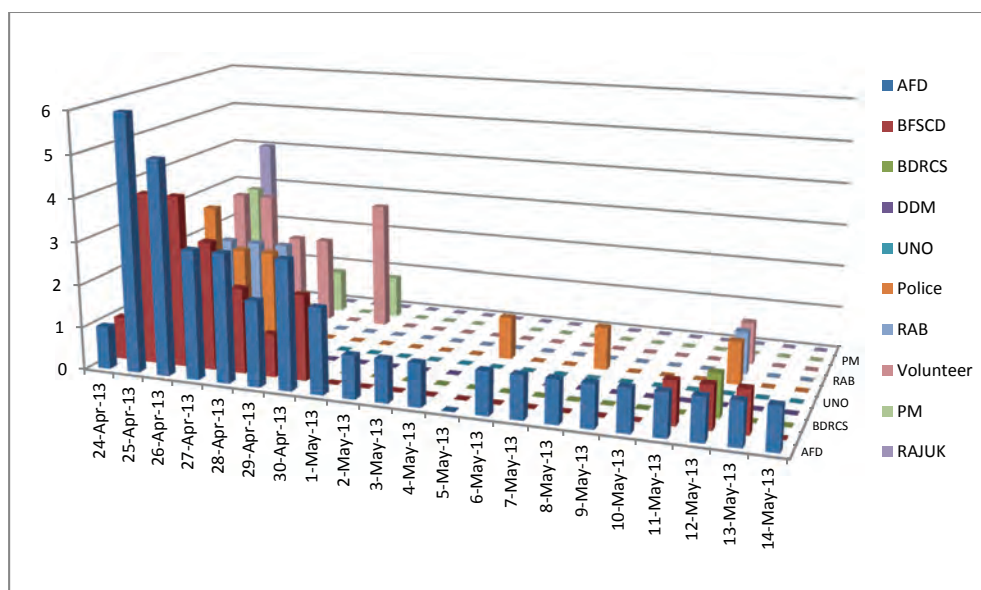


Figure 7. Number of key words in newspaper articles

Armed Forces Division (AFD) of Bangladesh engaged in the disaster management of the accident most as their name came in newspaper articles for 37 times. They appeared every day in newspaper from the day of accident to 14 May. Then come Bangladesh Fire Service and Civil Defence (BFSCD) with 20 times. Local volunteers contributed significantly with 15 times appearance in newspaper. The Department of Disaster Management (DDM) which is responsible for disaster management in the whole country appeared only 3 times in newspaper articles. The figure 7 shows the number of key words in newspaper articles from 24 April to 14 May.



Figure 8. Some of the critically injured garments workers

3. MENTAL TRAUMA AND REHABILITATION

After the Savar tragedy, many victims and volunteers have been suffering from mental trauma of accident. One volunteer named Rubel committed suicide from the shock. Many of those who survived have lost their limbs, many have become paralyzed. Ironically, all those people are in their productive age and most of them are the only earning member of their family. With disability and deformity, it has become extremely difficult for them to get back to work again. But with long term rehabilitation support, they can lead a better life with acquiring productivity and mobility. After such traumatic experiences, nearly everyone will have the symptoms of stress and grief for the first month which is a natural grieving process. Some will still experience those symptoms and they cannot come to terms with what has happened and suffer Post Traumatic Stress Disorder (PTSD). Mental trauma can be solved by rehabilitation for a long time

4. NATIONAL VS. INTERNATIONAL RESPONSE

The Savar tragedy took limelight of both national and international media after the day of incident. Many international leaders including Pope, Secretary General of United Nations, ILO and international NGOs showed their deepest concern for the victims. The European Union (EU) has raised strong concern over labor conditions and declared appropriate action to encourage improvements in working conditions in Bangladeshi factories. Major western clothing retailers are squeezing Asian suppliers and a flawed approach to ensuring even basic working standards are fuelling conditions for tragedies like the Savar disaster.

United States of America suspended the Generalized System of Preferences (GSP) facilities on the entrance of Bangladeshi product into the US market after Savar tragedy considering the accident of Savar Rana Plaza, Tazrin Fashion, and unsolved case of murder of a trade union leader. They have also concerned about the safety, development of the standards of the laborers in Bangladesh as the biggest labor union of the USA, AFL-CIO has been convincing the government of USA to stop the GSP facilities for Bangladesh since 2007.

World Health Organization is going to provide more emergency drugs as per government request and has already provided blood transfusions sets, dressing and first aid materials along with emergency medicines to Savar Upazila Health Complex and Enam Medical College Hospital for the injured persons.

Islamic Relief, Bangladesh provided various equipments to support search and rescue to Fire Service and Civil Defense (FSCD). Action Aid, Bangladesh has provided emergency rescue equipment worth BDT 2,00,000 for FSCD's rescue team and food worth BDT 50,000,00 for Urban Community Volunteers. Emergency medicine of BDT 10,000.00 is also supplied for injured people.

BDT 20000.00 has been provided to each deceased family. Total BDT 86,60,000 has been distributed to 433 families. Each injured person will get BDT 5000. BDT 47,15,000 has been distributed among 943 injured. BDT 4,00,00,000 has been allocated from MoDMR to DDM. DDM has allotted BDT 3,00,00,000 to District Administration for distribution.

The following graph shows the number of national and international articles on Savar tragedy in the Daily Star Bangladesh.

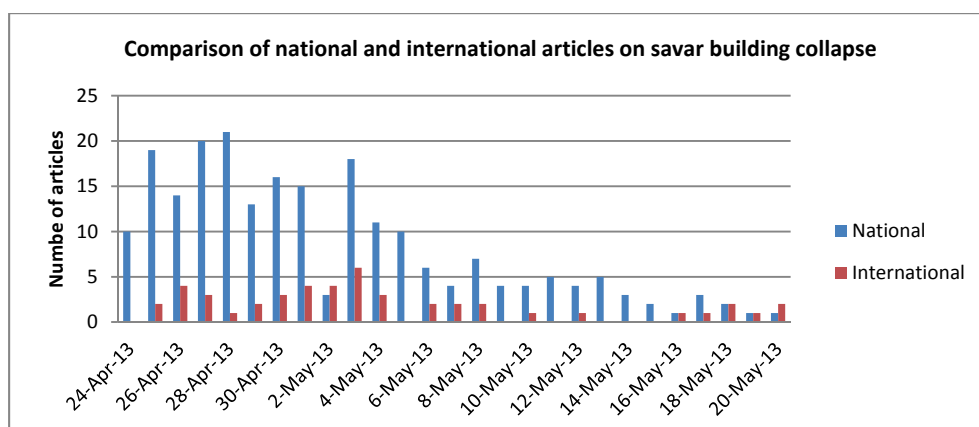


Figure 9. Comparison of national and international articles on savor building collapse

After the disaster, government of Bangladesh promised to give about \$1,250 in cash and \$19,000 in savings certificates to the families or relatives of died workers, but yet has provided about \$1,250 to \$5,000 to some 777 families. Nearly 300 bodies were not identified and claimed by families or relatives.

5. RECOMMENDATION

Bangladesh faced its worst human tragedy through Rana Plaza building collapse at Savar, Dhaka. In 1996 at Kalabagan, in 1997 at Khilgaon, in 2004 at Sakaribazar, in 2005 in Savar, in 2006 at Mahakhali, in 2010 at Hatirjheel and at Kathalbagan similar incidence occurred where altogether several hundred people were killed. Enforcement of Bangladesh National Building Code (BNBC) has become the top priority.

Immediately, we need to set up a Building Regulatory Authority (BRA) as prescribed in BNBC. BRA will aim to deliver: Better safeguards for consumers; Building industry transformation and Legislative reform. The Building Authority will work closely with four statutory bodies to provide industry leadership and will regulate building quality. The associated bodies will be the Building Advisory Council, Building Appeals Board, Building Practitioners Board and the Building Regulations Advisory Committee. The Authority and four bodies will

- Regulate Bangladesh's building industry
- Administer the registration of a country's building practitioners and monitor their conduct
- Advise the relevant Minister and the Government on building regulatory development
- Administer building legislation, the Building Act 1952 and Building Regulations 2008
- Resolve disputes and appeals arising from the Building Act
- Inform consumers about building and renovating
- Communicate changes that occur in building legislation
- Promote improved building standards nationally and internationally
- Provide comprehensive information on building activity
- Inform industry decision making through data and analysis
- Facilitate industry research
- Support the uptake of information technology and e-commerce
- Encourage sustainable and accessible building design, construction and use

The BRA will carry out these functions in consultation with a wide variety of stakeholders.

6. CONCLUSIONS

Many questions have already been raised about the future of the garments industry in Bangladesh after a number of accidents like Spectrum Garment Accident, Tazreen Fashion Disaster and the latest Savar Building Collapse. A large number of foreign buyers including Disney have decided not to buy clothes from Bangladesh because of the poor working condition in the garments industry. It may severely damage the social and economic future of Bangladesh in long term. The government, the leaders of the garments industry, the NGOs, and the civil society have to come forward in unity to increase the quality of working conditions and livelihood of the workers of this sector. The foreign buyers need assurance from the government that they will never again face this kind of disaster in Bangladesh.



PART-V

SEISMIC RISK ASSESSMENT OF SOME HISTORICAL MOSQUE OF DHAKA USING NON-DESTRUCTIVE TESTING METHODS

**BANGLADESH NETWORK OFFICE FOR URBAN
SAFETY (BNUS), BUET, DHAKA**

Prepared By: KM Khaleduzzaman

Mehedi Ahmed Ansary

Dhaka city, the capital of Bangladesh is one of the most densely populated cities of the world. Old Dhaka, the oldest part of Dhaka city, is considered as a highly earthquake vulnerable zone due to its very high density of population living in a very compact land area with close proximity of buildings including vulnerable structures along narrow local streets. In proportion to the population density, the availability of critical facilities is not sufficient in this area. In this paper, the findings of seismic vulnerability assessment of five mosques, four educational institutes and one community centre of ward number-65 of Dhaka city have been presented. Initially Rapid Visual Screening (RVS) survey and Modified Turkish Method have been used to evaluate the vulnerability of these critical structures; later Ferroskan and Microtremor have been used to assess their existing condition.

1. INTRODUCTION

In earthquake prone areas there is a need for the assessment of the capacities of large numbers of existing buildings. The results of such assessment are essential for rational planning of retrofit programs for existing buildings before the occurrence of a strong earthquake, for the allocation of rescue forces and equipment to optimally deal with the forecasted damage. Dhaka city is one of the megacities of the world which has recently experienced earthquakes at regular intervals that have not caused immense damage but makes us aware about the future risk. As the older part of Dhaka city, popularly known as old Dhaka, is one of the most densely populated area with a huge number of older constructed buildings. Ward 65 of Dhaka City Corporation South is one of these kinds of older part of Dhaka city. There are around 20 critical facility structures (educational institutions, religious prayer place, community centre etc.) in this ward. Earthquake vulnerability assessment of 10 structures of these critical structures has been carried out and the findings are presented in this paper.

2. STUDY AREA

All the assessed structures are located in ward number-65 of Dhaka city Corporation South. This area is situated at around 23°42'55.88" N latitude and 90°43'45.40"E longitude. Figure:-1 is showing the locations of the evaluated structures.

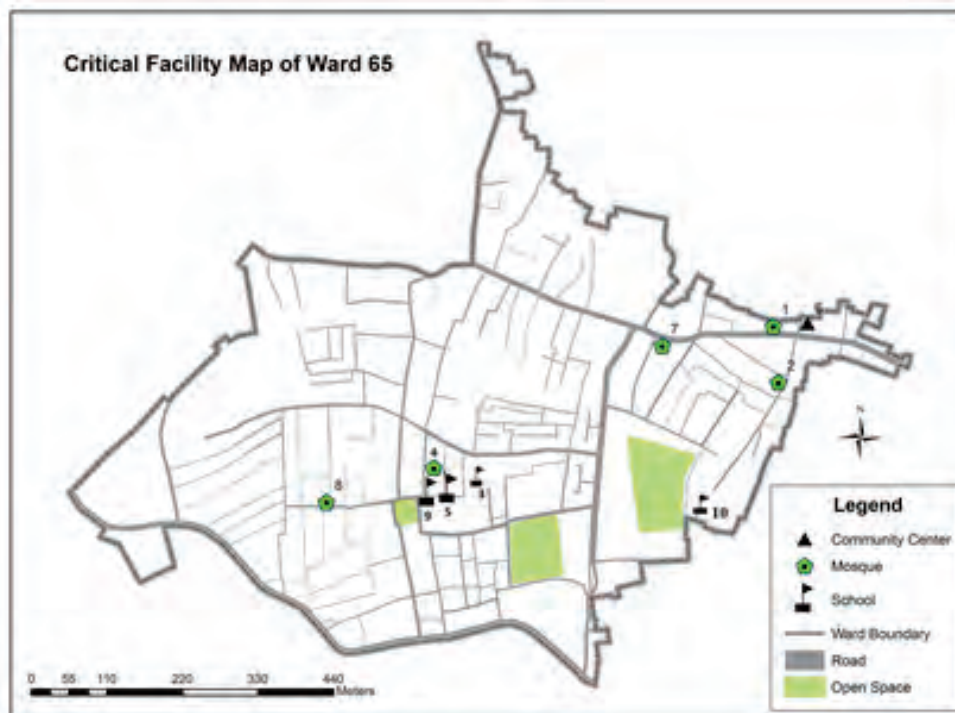


Figure 1: Location of the assessed buildings

1. Hazi Abdul Latif Mosque, 2. Mosjid-A-Noor, 3. Islambag Jamia Islamia Madrasah, 4. Islambag Jamia Islamia Mosque, 5. Haji Ibrahim Govt. Primary School, 6. Jamal Sordar Community Center, 7. Rahamotganj Chhata Minar Mosque, 8. Baitul Aman Mosque, 9. Islambag Ashraf Ali High School and 10. Metropolis Degree College.

3. RVS RESULTS

Modified Turkish method tier-1 (RVS) has been carried out for the ten selected structures. The result of RVS of these structures is presented in Table 1. RVS scores of all the structures are greater than 50, which indicates that none of the structures are seismically vulnerable.

Table: 1: Modified Tarkish Method tier-1 (RVS) results

Name of the structure	No. of Stories	Base Scores (BS)	Vulnerability Scores (VS)						RVS Score
		Zone II	Soft Story	Heavy Overhang	Apparent Quality	Short Column	Pounding Effect	Topo. Effect	
Metropolis Degree College	5	85	0	0	0	-5	-3	0	77
Islambag Ashraf Ali High School	4	100	-20	0	-10	-5	-3	0	62
Haji Ibrahim Govt. Primary School	4	100	-20	0	-10	-5	-3	0	62
Hazi Abdul Latif Mosque	3	120	-15	0	0	-5	-2	0	98
Mosjid-A-Noor	2	130	0	0	-5	-5	0	0	120
Islambag Jamia Islamia Madrasah	5	85	0	-15	-15	0	-3	0	52
Islambag Jamia Islamia Mosque	2	130	0	0	0	-5	0	0	125
Rahamotganj Chhata Minar Mosque	3	120	-15	0	0	-5	-2	0	98
Jamal Sordar Community Center	5	85	-25	0	-15	-5	-3	0	37
Baitul Aman Mosque	3	120	-15	0	0	-5	-2	0	98

4. MICROTREMOR OBSERVATION

Soil characteristics can be assessed by Microtremor measurement. Hard soil gives high frequency and soft soil gives low frequency. A structure may experience a vibration period at which it oscillates in the earthquake vibration motion and will tend to response to that. Natural frequency of

structure is obtained based on the spectral ratio of horizontal component of the structure to that of ground. Wave propagation mechanism of Microtremor and its relation with ground vibration characteristics were studied from the beginning of Microtremor studies (Aki, 1957; Kanai and Tanaka, 1961).

Basically there are two types of Microtremor observations to the number of observation points. These are point and array observations of microtremors (Ansary et al., 1996). From the array observation of Microtremor of period greater than 1 sec, Rayleigh-wave and Love-wave originating from natural sources, such as sea wave, variation of air and wind pressure can be recognized. On the other hand, short-period Microtremor of period less than 1 sec is thought to be generated by artificial noises such as traffic vehicles, industrial plants, household appliances, etc. Some researches (Sato et al., 1991; Tokimatsu and Miyadera, 1992; Tokimatsu et al., 1994) have showed that microtremors are mainly composed of Rayleigh-wave and some (Nakamura, 1989; Wakamatsu and Yasui, 1995) have showed that short-period Microtremor bears resemblance to shear-wave characteristics. On the other hand, Microtremor can also be dominated by Love-wave (Tamura et al., 1993). Recently, Suzuki et al. (1995) have applied Microtremor measurements to the estimation of earthquake ground motions based on a hypothesis that the amplitude ratio defined by Nakamura can be regarded identical with half of the amplification factor from bedrock to the ground surface. However, the real generation and nature of microtremors have not yet been established.

In general, the approaches to the identification the dynamic properties of structure can be categorized into three main approaches: (1) empirical, (2) numerical analysis, and (3) direct measurement approaches. The empirical approach provides simplified formulas for estimating the fundamental periods of structures in terms of geometric dimensions of the structures. The second approach, the numerical analysis, is normally used during the design process. A finite model of the structure is first formulated. Dynamic properties such as natural frequencies and vibration mode shapes are obtained by the Eigen analysis. The third approach is the direct measurement approach, which first measures dynamic responses of existing structures, and then identifies their dynamic properties from the measured responses.

4.1. DATA COLLECTION AND PROCESSING

For Microtremor observation at the selected buildings, initially the sensors are deployed. One sensor is fixed on the roof of the buildings and another one on the free field near the structure. After taking the observation with the help of microtremor, the time domain velocity data is converted to frequency domain data and the natural period of the structures have been estimated. Around the investigated structure three 3-dimensional accelerometers are assembled to measure the ground response of the ambient excitation.

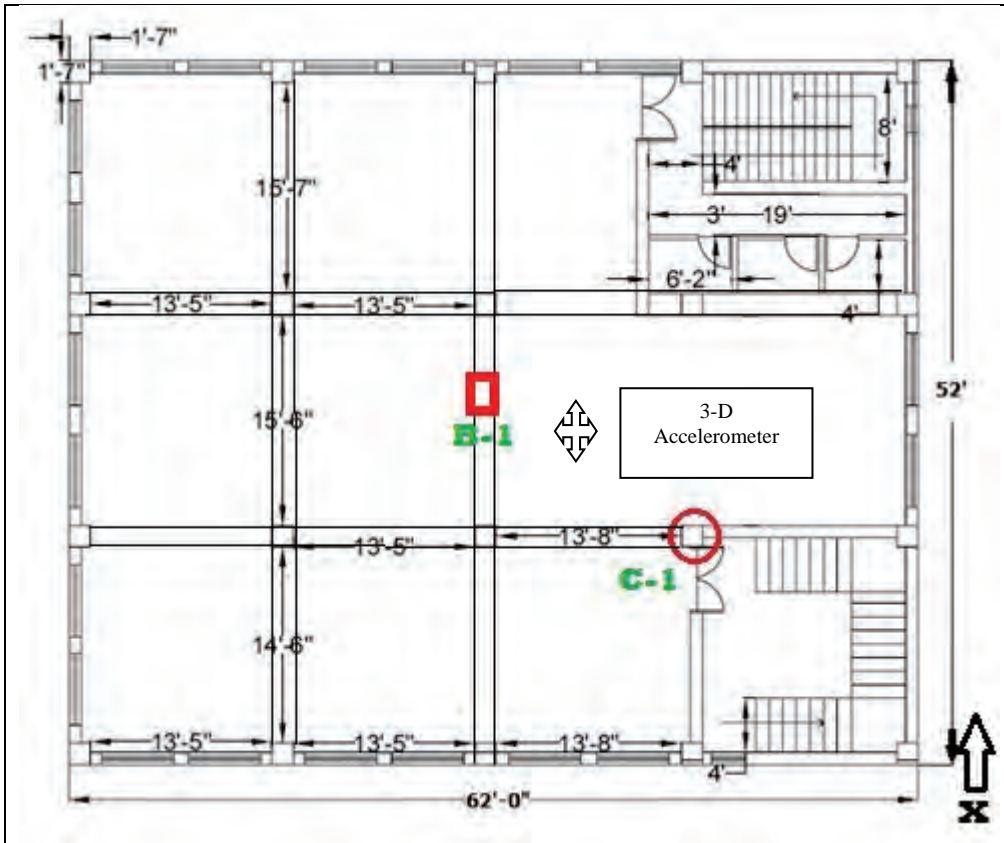


Figure 2: Typical floor plan of Jamal Sardar Community Centre

The computation steps of the spectrum analysis is shown in Figure 4 and described as follows:

- Pre-Processing:
 - 3-dimensional input (the accelerometer in northward direction to get North-South, East-West and vertical components)
 - Windowing of the signal (in our case only the ambient parts are of interest, observe, in case of transient excitation only the transient parts of the time response are of interest)
- Main Data-Processing:

Hence the three different components of the signal were considered separately. The main data processing is repeated for every input-signal (n-Steps according to the numbers of preliminary separated windows).

 - FFT is applied to obtain the several spectral amplitudes of the three components
 - Smoothing of the three spectral amplitudes with a bandwidth factor of 10 to 15
 - Afterwards the resulting horizontal component and vertical component are plotted to obtain the amplitude in frequency domain.



Figure 3: Data collection by Microtremor

4.2. MICROTREMOR ANALYSIS RESULTS

Figure 4 shows individual time histories for X, Y and Z components for a building. Figure 5 shows FFT of those time histories. Table 2 presents the predominant frequency of the buildings in both directions.

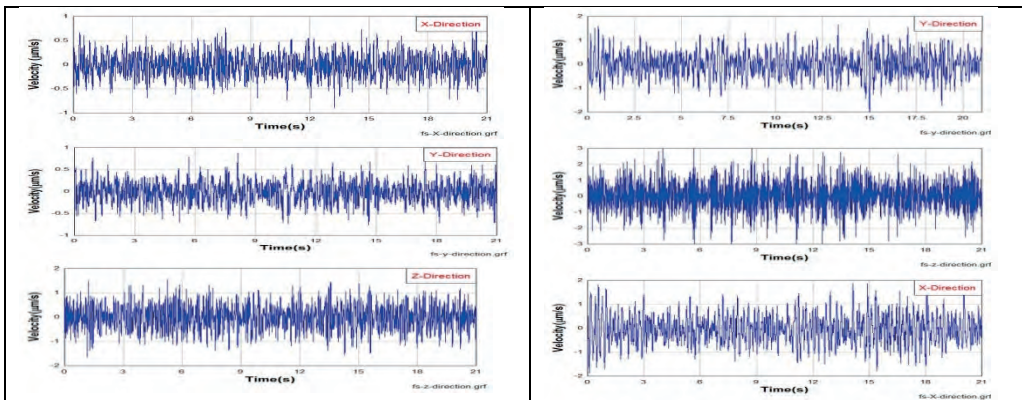


Figure 4: Time history data on the soil and top of the building of Jamal Sardar Community Centre

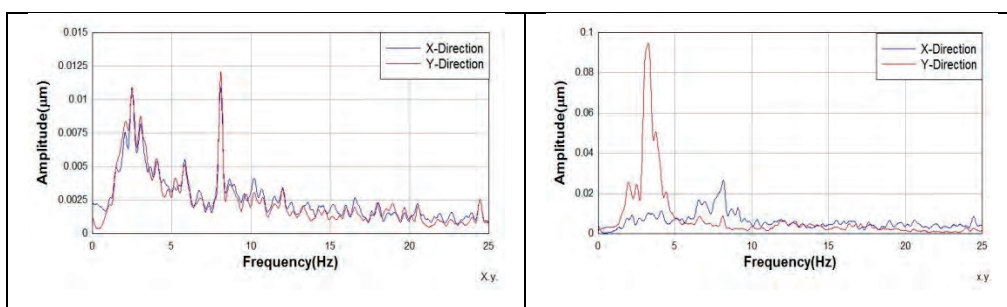


Figure 5: Smoothed data of horizontal Fourier spectra of microtremors at soil and top of the building of Jamal Sardar Community Centre

Table 2: Predominant frequency of the buildings

Name of the Structure	First Mode (X Direction)		Second Mode (Y Direction)	
	Frequency (Hz)	Period (s)	Frequency (Hz)	Period (s)
Metropolis Degree College	2.58	0.39	2.96	0.34
Islambag Ashraf Ali High School	2.51	0.40	2.48	0.40
Haji Ibrahim Govt. Primary School	4.01	0.25	20.01	0.05

Hazi Abdul Latif Mosque	7.79	0.13	14.85	0.07
Mosjid-A-Noor	5.42	0.18	14.9	0.07
Islambag Jamia Islamia Madrashah	5.69	0.18	5.69	0.18
Islambag Jamia Islamia Mosque	6.70	0.15	9.49	0.11
Rahamotganj Chhata Minar Mosque	10.15	0.10	6.32	0.16
Jamal Sordar Community Center	8.2	0.12	3.12	0.32
Baitul Aman Mosque	5.5	0.18	4.73	0.21

5. FERROSCAN RESULTS

Imagescan and linescan results of beam, column and slab have been carried out for a beam, column and slab of the buildings in the first floor. Figure 6 shows the observation by using Ferroscan. Figure 7 presents the findings of Ferroscan measurement for column C1 (marked at figure 1) and figure 8 represents the findings for beam B-1(marked at figure 1). Table 3 presents linescan analysis of column C1.



Figure 6 : Ferroscan observations of Column and beam

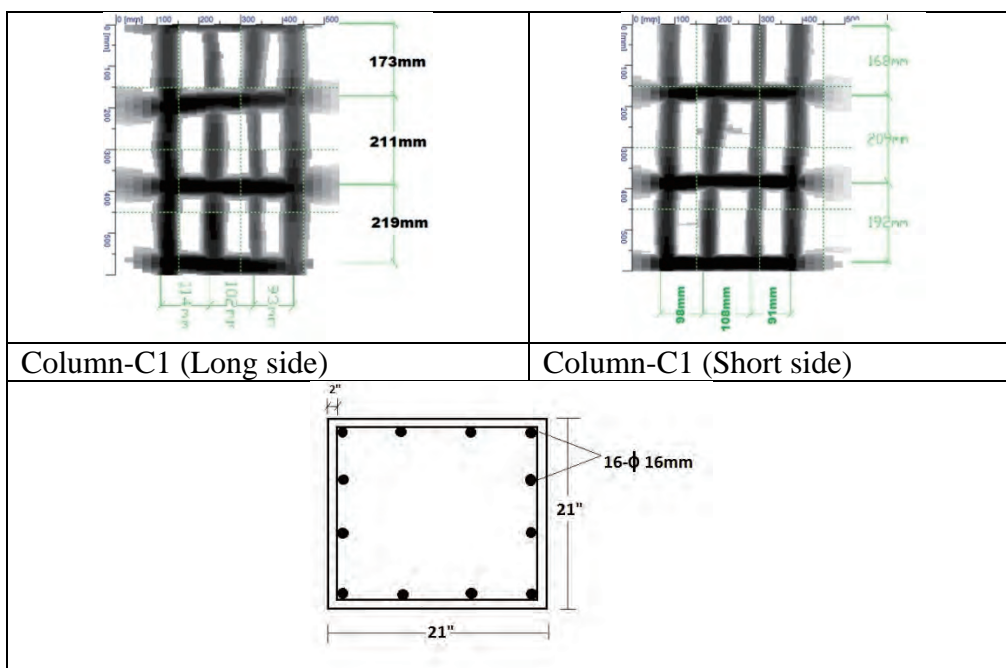


Figure 7: Cross section (in built) of column C1 (marked at figure 2)

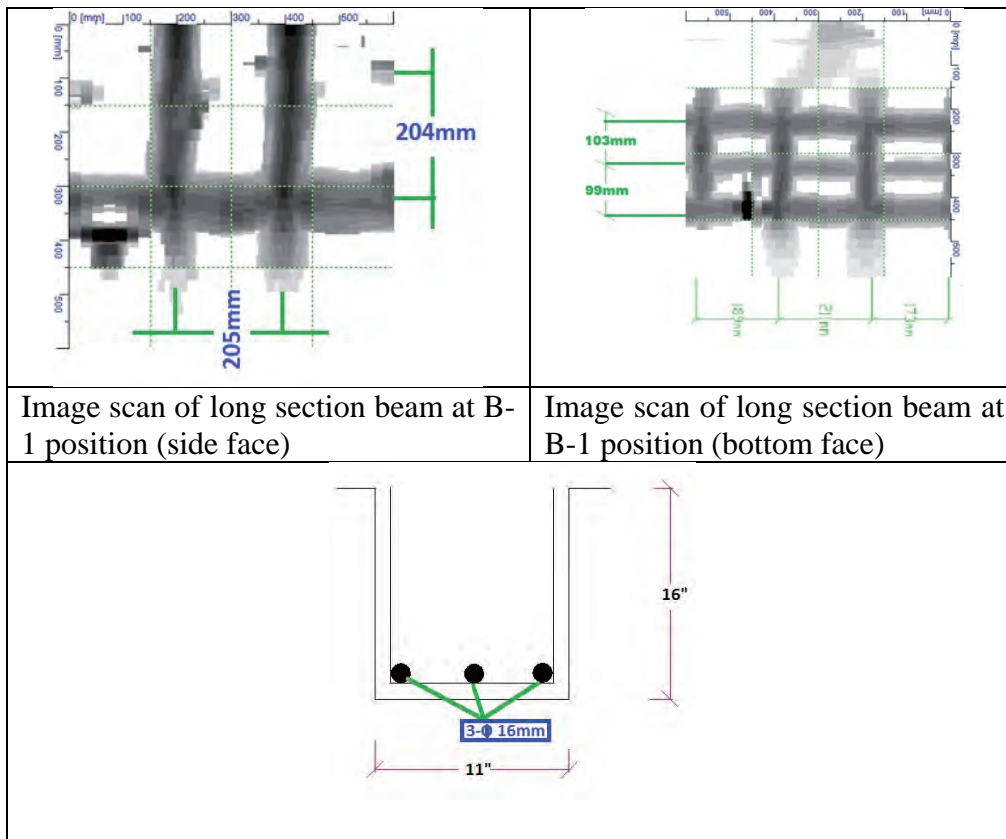


Figure 8: Cross section (in built) of beam at B-1 position (marked in figure - 1) at ground floor

Table 3: Line Scan, hoop position check (Ref: American Concrete Institute, 2002)

Transverse Reinforcement Requirements - Rectangular hoop reinforcement for Column (C1-1F)				
Column Dimension	x	y	$L_0 \geq$	
	12	12	Larger of C1 or C2	12in
Column Height (Clear Span)	9.75	ft	Clear Span/6	19in
	117	in	18"	18in

Longitudinal Bar Used	16	mm
Diameter , D	0.62	in
Max. Value between tie (in a plane), h_x	7	in
End Strip Length	19	in
Middle Strip length	76	in

Spacing Recommended for End Strip :			$S \leq$	
S	3	in	0.25 X Smaller of C1 or C2	3in
	5	in	6 X Longitudinal Bar Diameter, D	3 in
Remark	Not Satisfied		$S_x = 4 + [(14 h_x)/3]$	6in

Spacing Recommended for Middle Strip				
S	3.75	in	$S \leq$	
Existing Spacing	8	in	6"	6in

Remark	Not Satisfied	6 X Longitudinal Bar Diameter, D	3.75in
--------	---------------	-------------------------------------	--------

Clear Cover		
Cover depth \geq	38.1	mm
Existing min Depth	44	mm
Remark	Satisfied	

6. CONCLUSION

This paper presents the findings of seismic vulnerability assessment of five mosques, four educational institutes and one community centre of ward number-65 of Dhaka city. Initially Rapid Visual Screening (RVS) survey and Modified Turkish Method have been used to evaluate the vulnerability of these critical structures; later Ferrosan and Microtremor have been used to assess their existing condition. According to the Turkish Tier-1 survey, none of the buildings are seismically vulnerable. The building heights vary from 1 to 5 stories and their periods vary from 0.1 to 0.5 seconds. None of the critical facilities in this ward have any as-built drawings. Using Ferrosan and other NDTs, BNUS have helped the local community people to develop the as-built drawings of those structures.

REFERENCES

- Aki, K. (1957). Space and time spectra of stationary stochastic waves, with special reference to microtremors, Bull. Of earthquake research institute, 35, 415-456
- Ansary, M.A., Yamazaki, F. and Katayama, T. (1996). Application of Microtremor Measurements to the estimation of site amplification characteristics, Bulletin of ERS, Vol 29, PP: 96-113.
- Kanai, K. and Tanaka T. (1961). On Microtremor VIII, Bull. Earthq. Res. Inst. Tokyo University, Vol.39, pp.97-114.
- Nakamura, Y. (1989). A method for dynamic characteristics estimation of subsurface using microtremor on the ground surface, QR of RTRI, 30, 25-33
- Sato, T. H. Kawase, M. Matsui, and S. Kataoka (1991). Array measurement of high frequency microtremors for underground structure estimation, proc. 4th int. conf. on seismic zonation, 11, 409-416
- Tamura, T., O. Nagai, H. Kikubo, and H. Sumita (1993). Characteristics of wave group microtremors obtained by array measurement, J. Struct. Consr. Eng. AIJ 449, 83-91 (in Japanese).
- Toshinawa, T., Inoue M., Yoneyama N., Hoshino Y., Mimura K., and Yokoi Y. (2003). Geologic-profile estimates of Kofu Basin, Japan, by making use of microtremor observations, Geophysical Research Abstracts, Vol. 5, 02079.
- Tokimatsu, K. and Y. Miyadera (1992), "Characteristics of Rayleigh waves in microtremors and their relation to underground structures, J. structure. consr. Eng. AIJ 439, 81-87



PART-VI

APPLICABILITY OF PS SUSPENSION LOGGING DOWNHOLE SEISMIC METHOD FOR INVESTIGATION OF DYNAMIC SOIL PROPERTIES OF BANGLADESH

**BANGLADESH NETWORK OFFICE FOR URBAN
SAFETY (BNUS), BUET, DHAKA**

Prepared By: Fahad Hossain

Mehedi Ahmed Ansary

Abstract:

With the increased use of machines on super structures along with frequently occurring natural hazards like earthquakes, liquefactions, slope failures; requires analysis for foundation vibrations which subsequently leads us to characterize and investigate soils for its dynamic properties. The paper deals with the methodology and the use of PS suspension logging down-hole seismic testing system for measurement of shear wave velocities. It also covers the relationships of wave velocities with the dynamic parameters. It's basically a review paper which will provide detailed application process and analysis method to the researchers requiring the use of PS Suspension Logging down-hole seismic testing method to determine earthquake waves and dynamic properties.

Introduction:

Few of the major earthquakes over the years, alike the Sumatran Earthquake [1] or the Great Indian Earthquake [2] along the coast of bordering countries of Bangladesh has augmented the demand for earthquake resistant designs for the vibration induced parameters of soil. For this reason accurate and proper soil investigation has become an essential concern to grasp precise knowledge about the underground soil condition.

The PS suspension logging method (Kitsunezaki, 1980) directly measures and provides accurate and high-resolution Shear (S) wave velocity profiles. The primary (P) or the compression wave velocity profiles can also be created accurately by using PS Suspension Logging.

During an earthquake, the subsurface soil column acts like a filter with strain-dependent properties that can increase the duration and amplitude of shaking in a narrow frequency band related to the soil thickness, physical properties (P and S -wave velocities, densities), shape of the surface and subsurface boundaries [3]. The spectral content (amplitude, period, and phase) and duration of earthquake recordings can therefore be significantly affected by local site conditions, especially at unconsolidated soil and sediment sites with a near-surface impedance contrast with underlying bedrock. The resonant period of the ground is therefore of great importance for earthquake engineering. Also the response of soils to cyclic loading is controlled mostly by the mechanical properties of the soil [4].

The most common types of dynamic loadings are, machine vibrations, seismic loading, liquefactions and cyclic transient loading, etc. The dynamic properties associated with these dynamic loadings are shear wave velocity (V_s), shear modulus (G), damping ratio (D), and Poisson's ratio (ν), Young's Modulus (E) of soil. [5]

History of PS Suspension Logging:

P-S suspension velocity logging was first developed in the mid-1970s to measure seismic shear-wave velocities in deep, uncased boreholes; it was originally used by researchers at the OYO Corporation of Japan (Kaneko et al, 1990). It gained acceptance in Japan in the mid-1980s and was used for other velocity measurement methods to characterize earthquake site response. Public Works Research Institute (PWRI) has measured S-wave velocities in boreholes using the PS suspension logging tool since 1980. Since the early 1990s it has gained acceptance in the U.S., especially among earthquake engineering researchers. [6]

Worldwide Use of PS Suspension logging:

PS Logging techniques are using worldwide and some example of some research works includes, Tomio Inazaki [7] investigations; where shear wave velocities of surficial unconsolidated sediments was used to correlate with geotechnical properties determined by laboratory testing. The S-wave velocity data, all of them were accurately measured in boreholes using the PS suspension logging tool. N-values obtained by in situ Standard Penetration Test (SPT), bulk densities, solidities, and mean grain sizes measured by the standard soil test, and elastic constants determined by tri-axial dynamic loading tests were correlated with the S-wave velocities at the same horizons in the same boreholes. However the dynamic range and measurement accuracy of SPT was too low to compare with S-wave velocity data obtained using the suspension logging tool. So it was possible to estimate N-values from S-wave velocity data using his empirically synthesized equation.

Ming-Hung Chen et al. [8] showed that 175 strong-motion station sites were investigated by National Center for Research on Earthquake Engineering (NCREE) and Central Weather Bureau (CWB) to characterize the subsurface conditions that affect measured ground motions measuring in soil, gravel and rock layers throughout Taiwan. The suspension P-S Logging method was applied at most sites because of its high accuracy and resolution. He showed that that the frequencies and wave lengths of receiving signals varied with different subsoil materials. The investigated shear wave velocity profiles of an alluvial deposit in southwestern Taiwan were introduced. Based on the abundant and reliable shear wave velocities, an empirical formula for alluvial deposits was developed. Depth and corrected SPT-N value were chosen to be two major parameters of the empirical formula. For some specific sites, surface wave, seismic refraction, or down-hole velocity measurements were also executed. The results of various tests are generally very close and increase the reliability of the measurements.

Emre Biringen and John Davie [9] made correlations between the values of P-wave velocity and dynamic elastic modulus through in-situ dynamic testing (suspension P-S logging) and the values of uniaxial compressive strength (UCS) and static elastic modulus through laboratory static testing

(uniaxial compressive) of sound rock from two sites located in South Carolina and Virginia. For both sites, the bedrock, which classified as good to excellent, is hard fresh to slightly discolored metamorphic rock, or igneous rock with numerous metamorphic inclusions. Suspension P-S logging tests were performed in 12 uncased fluid-filled boreholes, to rock depths of over 120 m.

Ming-Hung Chen and Bing-Ru Wu [10] showed in another paper, the site investigation at 175 TSMIP stations was completed by National Center for Research on Earthquake Engineering (NCREE) cooperating with Central Weather Bureau (CWB) in Taiwan. By sampling soils in the borehole and using the Suspension P-S Logger Technique, specific geological and geotechnical data are obtained including the soil profile, the physical properties of soils, and the wave velocities of the stratum. This database is helpful to the site effect analysis and the earthquake-resistant design.

Michael W. Asten and David M. Boore [11] showed that measurement or estimation of the shear-velocity (V_s) profile of sediments overlying geological basement is a vital part of site zonation studies for earthquake hazard prediction, and more generally for geotechnical studies. A series of boreholes drilled in the Santa Clara Valley Water District provide opportunity for the comparison of geophysical methods (Ps Logging, SASW, MASW) with known geological data. The author compared the shear-wave velocity profiles obtain from fourteen invasive and non-invasive methodologies obtained in and near a single 300 m borehole.

Itzair Perez et al. [12] compared SASW and PS-logging (in-hole) seismic techniques with the relatively new ReMi (Refraction Micro tremor) method at a common site with a well-known soil profile: a recently constructed high-speed railway embankment. The author showed that the PS-logging is the most accurate technique in identifying the soil profile of the embankment followed by Re-Mi and SASW. Mean shear wave velocity estimations are also higher for PS-logging, followed by SASW and ReMi, while mean deviation is similar in each technique.

Methodology for Downhole Seismic Test:

The down hole seismic test requires only 1 borehole (preferably a 3 inch diameter hole with PVC pipe installed upto the depth in which competent soil or rock is reached) to be used for the geophone receiver. Usually PVC pipes are used to permanently stabilize the hole. The standard for the test technique is set forth in the ASTM D4428/D4428M. A installed cased borehole is shown in figure 1. For the test, a wooden plank source shown in is used. A 6 in x 30 in area approximately 3 m (10 ft) from the borehole is cleared off. 6 in x 6 in x 30 in (or similar) wooden plank in the cleared off area is positioned and pinned down by driving a vehicle onto the plank (as shown in Figure 2) so that one of the drive wheels is centered on the plank as shown below. The plank should extend farther beyond the outside diameter of the tire. Then the accelerometer should be mounted on to the wooden plank using grease/ epoxy glue.

The plank is hit separately on both ends to generate shear wave energy in two different directions.

The plank is also hit vertically in the downward vertical direction to generate vertically polarized compressional wave energy. The shear wave energy is polarized in the direction parallel to the plank as is the transverse component (marked T on the geophone shell). The transverse component is used to measure the shear wave energy. The vertical component marked V on the geophone shell is used to measure the vertically polarized compressional wave energy. Typically 3-5 records are taken for each type of wave – shear east going, shear west going and compressional vertical. Using the test plans that come with the Freedom Data PC Downhole Seismic / Cross Hole Seismic – 2 system, 8 records are taken for each wave type. In all, 3 different tests are performed at each depth for the 3 different wave polarizations collected; all depths are recorded together in one file. [13]



Figure 1: PVC pipe cased borehole.



Figure 2: Wooden Plank Source Used In Downhole Seismic Test

The set up of the equipment may be shown below as flow chart:

Some data found from a PS Logging test in Down-hole Seismic method are shown in Figure 4 for calculating compression wave and shear wave. In figure we can see the data of compression wave. For computing the arrival time of the compression wave, take the first point of the time domain data of the vertical component when the response starts for both geophones.

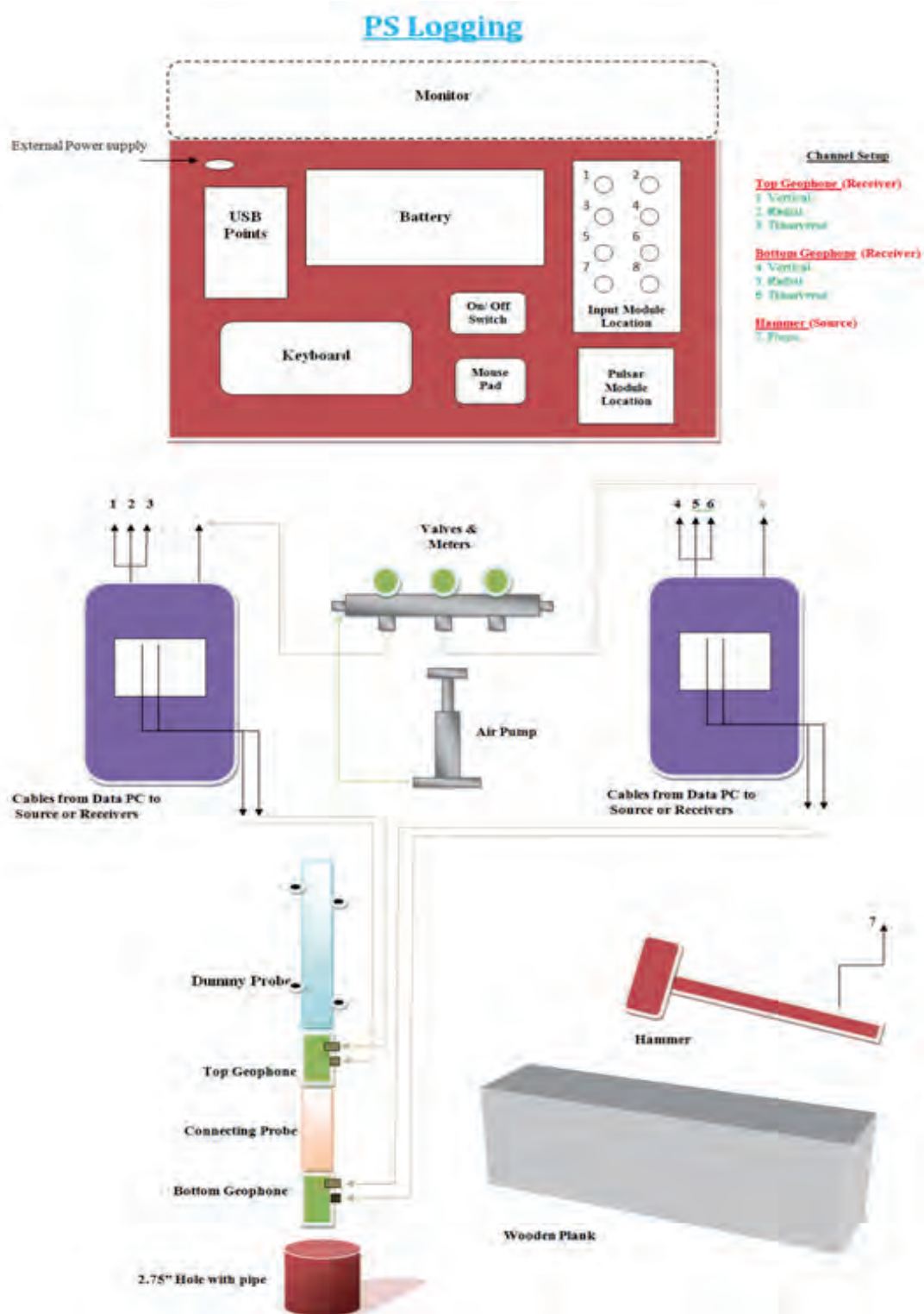


Figure 3: Installation of PS Logging test (Downhole seismic method)

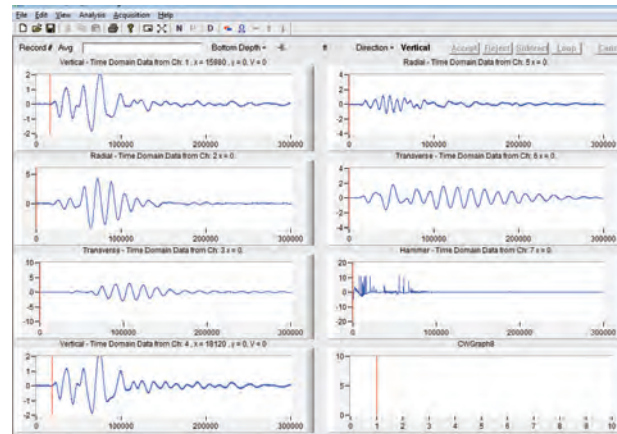


Figure 4: Time Domain data for compression wave.

In figure 5 we can see the data of shear wave generated by giving blow with hammer in both horizontal directions. For computing the arrival time of the shear wave, take the first point of the time domain data of the radial and transverse component when both wave generated from both horizontal direction just overlap each other.

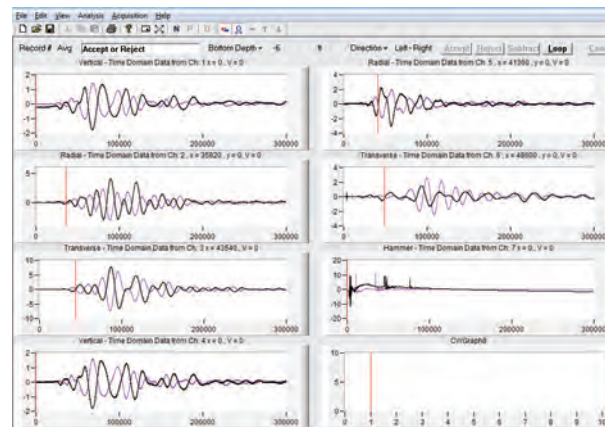
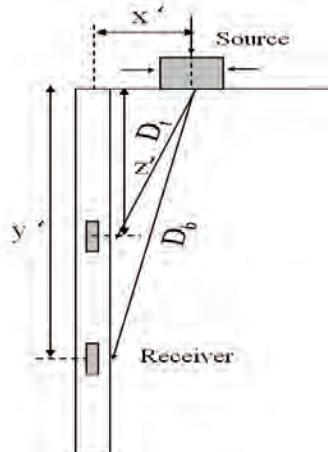


Figure 5: Time Domain data for shear wave.

From the calculated travel time of the compression and shear wave, the velocity can be determined by dividing the distance of the source to receiver by the travel time. Both compression wave and shear wave velocity are determined in this method. The calculation is shown below with figure 6 and equations.



$$D_t = \sqrt{(z^2 + x^2)}$$

$$D_b = \sqrt{(y^2 + x^2)}$$

$$V_p = \frac{D_b - D_t}{t_b - t_t}$$

Here,

D_t = Distance between top receiver to source

D_b = Distance between bottom receiver to source

T_t = Travel time of wave to top geophone

T_b = Travel time of wave to bottom geophone

Figure 6: PS Logging test in Seismic Downhole method.

The data sheet for the calculation of compression and shear wave is shown in Appendix-1, Table 1 and Table 2.

Determination of Different Dynamic Soil Properties of Soil:

As stated above, some dynamic properties of soil such Shear Modulus, Constrain Modulus, Poisson's Ratio and Young Modulus can be determined from the shear wave velocity. The equations for determining the dynamic properties are given below. The data sheet for computing the dynamic properties is given in Appendix 1, Table 3.

$G = \rho V_s^2$	G = Shear Modulus
$M = \rho V_p^2$	M = Constrained Modulus
$\nu = [0.5(\frac{V_p}{V_s})^2 - 1] / [(\frac{V_p}{V_s})^2 - 1]$	ρ = Density
	V_s = Shear Wave Velocity
	V_p = Compressional Wave Velocity
$E = 2G(1 + \nu)$	ν = Poisson's Ratio
	E = Young's Modulus

Conclusion:

PS Logging test is a precise and accurate testing method among the available geophysical methods for seismic wave velocity determination. Using this test compression and shear wave velocity can be measured quite easily rather than the other methods. For this reason, it is getting its importance day by day among the researchers. But its demerits are, it is costly, its installations and set-ups requires expertise and skilled manpower, it also takes much time, data acquisition should be done very carefully. That may be the cause that it is not widely used in Bangladesh for research work. But considering its accuracy its use should be increased in Bangladesh.

References:

- [1] Ali, M.H and Choudhury, J.R (1992) "Tectonics and Earthquake Occurrence in Bangladesh", 36th Annual Convention, IEB, Dhaka.
- [2] U.S Geological Survey, National Seismic Hazard Maps (2012).
- [3] Molnar, S., Cassidy, J.F., Monahan, P. A. and Dosso1, S. E., "Comparison Of Geophysical Shear-Wave Velocity Methods" in Ninth Canadian Conference on Earthquake Engineering Ottawa, Ontario, Canada, 26-29 June, 2007, pp. 390-391.
- [4,5] Luna, R. and H. Jadi, "Determination of Dynamic Soil Properties Using Geophysical Methods," Proceedings of the First International Conference on the Application of Geophysical and NDT Methodologies to Transportation Facilities and Infrastructure, St. Louis, MO, December 2000.
- [6] "SUSPENSION P-S VELOCITY LOGGING METHOD"-GEO Vision.
- [7] Inazaki, T., "Relationship between S-Wave Velocities And Geotechnical Properties Of Alluvial Sediments" in 19th EEGS Symposium on the Application of Geophysics to Engineering and

Environmental Problems, Apr. 2006.

[8] Chen, M.H., Wen, K. L., Loh, C. H. and Nigbor, R. L., “Experience of Suspension P-S Logging Method and Empirical Formula of Shear Wave Velocities in Taiwan” presented at - U.S.-Taiwan Workshop on Soil Liquefaction, Mar 2, 2012.

[9] Biringen, E. and Davie, J., “Assessment of dynamic and static characteristics of igneous bedrock by means of suspension P-S logging and uniaxial compressive strength tests” in “2011 Pan-Am CGS Geotechnical Conference” October 2-6, 2011.

[10] Chen, M.H., Wu, B. R., “The Engineering Geological Database for Strong Motion Stations In Taiwan”

[11] Asten, M. W. and Boore, D. M., “Comparison of Shear-Velocity Profiles of Unconsolidated Sediments near the Coyote Borehole (CCOC) Measured With Fourteen Invasive and Non-Invasive Methods”, U.S. Geological Survey Open-File Report 2005-1169.

[12] Perez-Santisteban, I., Garcia-Mayordomo, J., Martin, A. M., Carbo, A., “Comparison among SASW, ReMi and PS-Logging techniques: Application to a railway embankment” in journal of applied geophysics, Vol 1; pp. 59-64, 2011.

[13] System Reference Manual 2007 Crosshole and Downhole Seismic Test by Olson Instruments, Inc. Revised (May 2007).

Appendix 1

Table 1: Determination of P wave Velocity:

Depth ft	P Wave						
	Geophone-1			Geophone-2			Compression wave Velocity ft/s $V_p = \frac{D_b - D_t}{t_b - t_t}$
	Arrival time (Vertical) T_t μs	Arrival time, T_t sec	Distance, D_t ft	Arrival time (Vertical) T_b μs	Arrival time, T_b sec	Distance, D_b ft	

Table 2: Determination of S wave Velocity:

Depth ft	S Wave									
	Geophone-1					Geophone-2				
	Arrival time (Radial) μs	Arrival time (Transverse) μs	Average Arrival time μs	Arrival time, T_t sec	Distance D_t ft	Arrival time (Radial) μs	Arrival time (Transverse) μs	Average Arrival time μs	Arrival time, T_b sec	Distance D_b ft

Table 3: Determination of Dynamic Properties:

Depth D ft	Compression Wave Velocity (Vp)	Shear Wave Velocity (Vs)	Shear Modulus (G)	Young Modulus (E)	Bulk Modulus (K)	Poisson's Ratio (v)



PART-VII

ENGINEERING CHARACTERISTICS OF GROUND MOTIONS RECORDED BY NORTHEAST INDIAN STRONG MOTION INSTRUMENTATION NETWORK FROM 2005 TO 2013

**BANGLADESH NETWORK OFFICE FOR URBAN
SAFETY (BNUS), BUET, DHAKA**

Prepared By: Mehedi Ahmed Ansary

ABSTRACT

Indian Institute of Technology, Roorkee (IITR) is operating a nationwide network of instruments for recording strong ground motion. Total 298 instruments are installed in seismic zone III, IV and V along Himalayan belt. Primary goal of this project is to acquire strong ground-motion (SGM) data for various studies in the field of earthquake engineering and seismology in general and in particular to understand propagation and site response characteristics of the sediments that underlie and are thought to produce large site amplification and seismic hazard. This network has so far recorded around 150 earthquake events having magnitude from 3 to 7 starting from 2005 to 2013. Ground-motion prediction equations (GMPEs) based on Peak Ground Motions and Spectral Values are presented for the first time using local SGM data. This paper also presents an engineering analysis of 13 ground motion records of 2011 Sikkim Earthquake. H/V ratio is estimated for 9 soil and 4 rock sites. H/V ratios indicate that soil sites show predominant site frequencies of about 0.6 to 2.5 Hz and Rock sites show predominant site frequencies between 3 to 5 Hz.

Introduction

More than half of the area of India is susceptible to strong ground motions from earthquakes; therefore it is essential to know about the probable characteristics of strong ground motion of future earthquakes in this region. For earthquake engineering purposes, a number of different parameters are typically used to characterize strong motion records. These parameters include peak acceleration, peak velocity, peak displacement, duration of strong shaking, and response spectra. A rational assessment of the expected seismic hazard in different regions of the country will lead to substantial monetary savings in the design of structures and reduce potential losses from earthquakes. Indian Institute of Technology, Roorkee (IITR) is operating a nationwide network of instruments for recording strong ground motion. Total 298 instruments are installed in seismic zone III, IV and V along Himalayan belt [1-2]. Primary goal of this project is to acquire strong ground-motion (SGM) data for various studies in the field of earthquake engineering and seismology in general and in particular to understand propagation and site response characteristics of the sediments that underlie and are thought to produce large site amplification and seismic hazard.

Ground-motion prediction equations (GMPEs) describe the scaling of ground-motion amplitudes with magnitude, style-of-faulting and site class, and the decay (attenuation) of the amplitudes at increasing distances from the source. GMPEs based on Peak Ground Motions and Spectral Values are presented for the first time using local SGM data recorded from 2005 to 2013. For this purpose two attenuation models proposed by Joyner and Boore [3] and Bommer and Akkar [4] are used in this study to fit the SGM data.

The amplification of ground motions due to the local site condition plays an important role in seismic damage [5-7]. Idriss [5] found that the PGA values recorded at soft-soil sites during the 1989 Loma Prieta earthquake were significantly greater than those recorded at other sites at distances of about 45 to 100 km. The use of the site soil stiffness represented by the shear wave velocity in the upper 30 m of soil deposits was then initiated in the early 1990s [8] by assigning a range of V_{S30} to different site categories (e.g., NEHRP categories). However, prior to Sikkim earthquake, there has not been one single large earthquake that recorded 9 strong ground motions at soft-soil sites in Indian sub-continent. Such a limitation makes the strong motion records at soft-soil sites from this earthquake very valuable for studying the effect of soft soil on site responses.

In addition, the horizontal-to-vertical (H/V) ratio technique proposed by Nakamura [9] was used to estimate predominant site periods of soft-soil sites with V_{S30} between 200 and 375 m/s and rock sites

with V_{S30} between 700 and 1620 m/s, which is an important parameter for assessing building damage and in evaluating local site amplification.

Strong Motion Network

The main objective of the seismic instrumentation is to record the ground motion arising due to natural and manmade disturbances and, in particular, to monitor the seismicity of a given region. This Strong Motion Network is also a first step toward developing a “Rapid Response and Damage Prediction System” for India where near real-time strong ground-motion records can be used to compute ground- shaking maps showing the area most strongly affected by earthquakes [2].

The Strong motion instrumentation network of IITR covers the Indian Himalayan range from Jammu and Kashmir to Meghalaya. In total, 298 strong motion stations have been installed in the states of Himachal Pradesh, Punjab, Haryana, Rajasthan, Uttarakhand, Uttar Pradesh, Bihar, Sikkim, West Bengal, Andaman and Nicobar, Meghalaya, Arunachal Pradesh, Mizoram and Assam. 20 instruments out of 298 are installed in Delhi, the national capital of India. Figure 1 shows location of stations of this network along the Himalayan belt while Figure 2 shows location of stations installed in Delhi.

Site Characterization

The local site conditions play an important role in the recorded time history of earthquake ground motions. Different site conditions can induce amplifications of different period ranges in the response spectra [10-11]. Therefore, the local site conditions become important in ground motion analysis and in earthquake resistant designs. This network has recorded large numbers of ground motion histories. These data are invaluable for strong-motion studies and site effect analyses, as well as for the study of a practical site classification system. The objective of site classification is to classify a group of strong motion station sites into several classes so that the conditions within the same site class are similar and design engineers may understand the general site condition by the class that it belongs to.

Because quantitative subsurface soil properties are not commonly available for every site, the use of surface geology becomes important in understanding the subsurface geologic conditions. Most site effect studies of earthquake ground motion are based on the soil properties in the upper 30 meters. Some researchers had combined the use of surface geology and shear-wave velocity for site classification [8].

Site characterization is a must for strong ground motion studies. Ideally, detailed geotechnical investigation using bore hole of 20 to 30 meter depth should be carried out at each site. Such data base is available for large number of strong motion stations of Japan. However, such tests are costly and therefore other simple approaches for site characterization are being employed at several places [2].

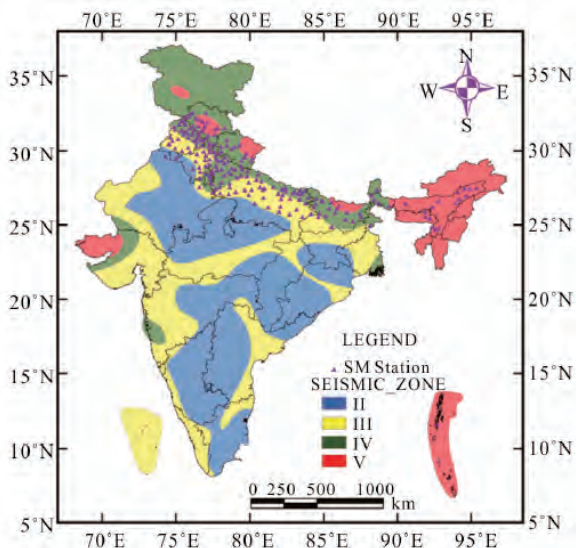


Figure 1. Map showing the location of instruments along the Himalayan belt

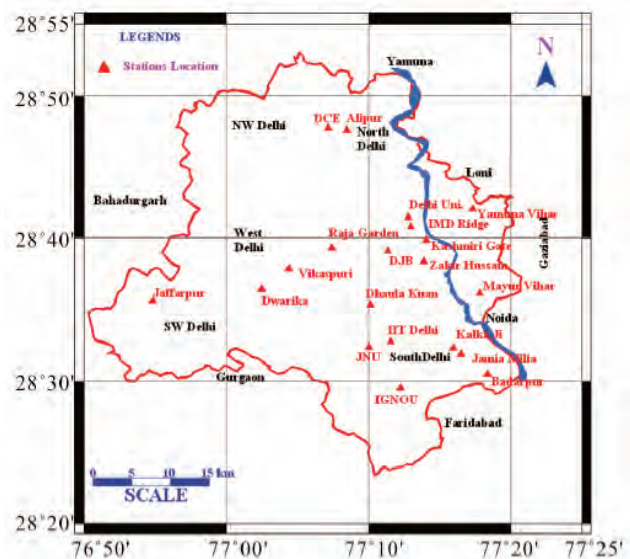
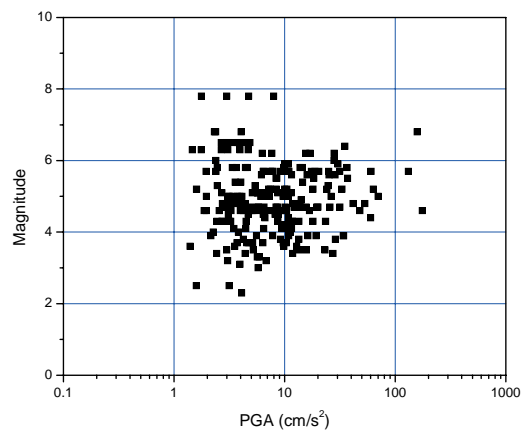
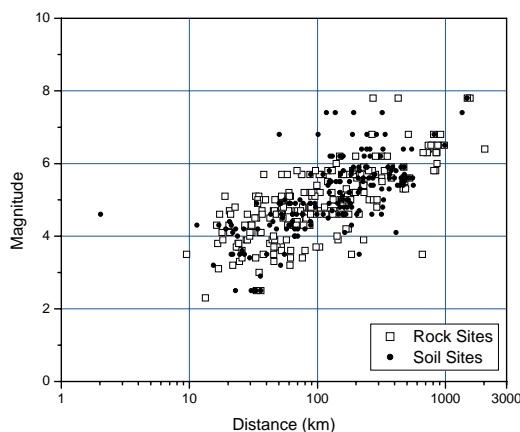


Figure 2. Map showing the location of instruments in Delhi

Recorded Database

This state-of-the-art instrumentation has partially filled the long-felt need for monitoring ground motion generated by earthquakes in the Himalayas using modern strong motion instruments. Since its installation, the instrumentation has been working in a satisfactory manner and has captured about 300 strong ground motion records from 150 earthquakes between 2005 and 2013. This database contains PGA values within 1000 km of the fault from earthquakes having magnitudes (M) in the range of 2.5 to 7.8. The distribution of PGA, PGV, PGD, ARS (Acceleration Response Spectrum) and VRS (Velocity Response Spectrum) for 0.3s, 1.0s and 2.0s values against M and hypocentral distance (r) is shown in Figure 3.



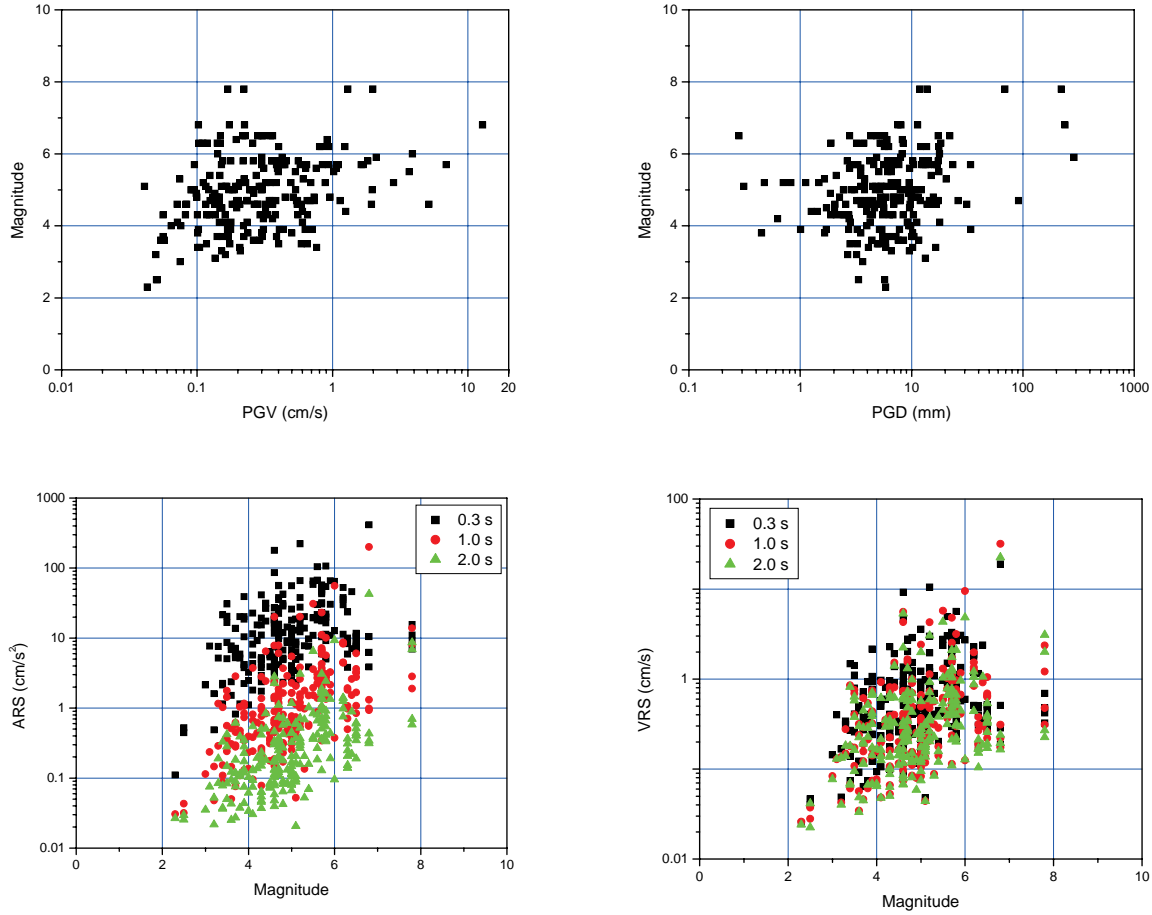


Figure 3. Distribution of different SGM parameters with respect to distance and magnitude

Ground Motion Prediction Equations

GMPEs based on Peak Ground Motions and Spectral Values are presented for the first time using local SGM data recorded from 2005 to 2013. For this purpose two attenuation models proposed by Joyner and Boore (Eq. 1) [3] and Bommer and Akkar (Eq. 2) [4] are used in this study to fit the SGM data. These models predict PGA, PGV, PGD, ARS and VRS spectral ordinates at response periods of up to 2 seconds as a function of magnitude (M), hypocentral distance (r) and site class.

$$\log Y = b_1 + b_2 r + b_3 M + b_4 \log r \quad (1)$$

$$\log Y = b_1 + b_2 M + b_3 M^2 + (b_4 + b_5 M) \log r \quad (2)$$

where b_i are coefficients. Tables 1 and 2 show coefficients determined by multistage regression analysis for rock and soil sites for Joyner and Boore GMPE. Tables 3 and 4 show coefficients determined by multistage regression analysis for rock and soil sites for Bommer and Akkar GMPE.

Table 1. Regression coefficients for Peak Ground Motions and Spectral Values using Joyner and Boore GMPE for rock sites

Y	b ₁	b ₂	b ₃	b ₄	σ	R ²
Acceleration: All (n=229)	0.57259	-5.77618E-4	0.16954	-0.20404	0.36013	0.1768
Acceleration: Depth < 70 km (n=201)	0.58663	-4.85358E-4	0.17325	-0.22588	0.36984	0.12567
Acceleration: M > 4 and h < 70 km (n=160)	0.43375	-5.97479E-4	0.2742	-0.40632	0.35759	0.21903
Velocity	-1.61154	-6.0865E-4	0.2871	-0.11565	0.36277	0.24078
Displacement	0.0276	-4.00625E-4	0.162	0.01906	0.39369	0.08931
ARS (0.3s)	-0.52966	-7.94703E-4	0.33601	0.02032	0.43034	0.25796
ARS (1.0s)	-2.13378	-5.71718E-4	0.53349	-0.19762	0.43887	0.45259
ARS (2.0s)	-2.57562	-5.87236E-4	0.50984	-0.21742	0.38974	0.47817
VRS (0.3s)	-1.53457	-7.53946E-4	0.27602	0.02851	0.40357	0.2113
VRS (1.0s)	-1.89432	-5.43274E-4	0.36211	-0.12884	0.39917	0.30122
VRS (2.0s)	-1.87658	-6.4472E-4	0.33797	-0.10632	0.37425	0.29547

Table 2. Regression coefficients for Peak Ground Motions and Spectral Values using Joyner and Boore GMPE for soil sites

Y	b ₁	b ₂	b ₃	b ₄	σ	R ²
Acceleration: All (n=187)	0.80932	-5.09526E-4	0.2297	-0.46683	0.3755	0.23661
Acceleration: Depth < 70 km (n=163)	1.11211	-2.89605E-4	0.27169	-0.74158	0.38073	0.2925
Acceleration: M > 4 and h < 70 km (n=147)	1.53895	-1.19581E-4	0.21482	-0.80811	0.38551	0.27896
Velocity	-1.57759	-6.49273E-4	0.35968	-0.27458	0.34227	0.38619
Displacement	0.23063	4.12536E-5	0.19717	-0.16678	0.44828	0.12407
ARS (0.3s)	-0.93043	-0.00124	0.3956	0.1109	0.40639	0.41102
ARS (1.0s)	-2.58486	-0.00105	0.58422	0.01915	0.38519	0.63044
ARS (2.0s)	-2.87772	-7.2129E-4	0.64174	-0.28807	0.34534	0.69558
VRS (0.3s)	-1.83674	-0.00112	0.34558	0.03888	0.3925	0.35311
VRS (1.0s)	-2.08334	-7.631E-4	0.45142	-0.194	0.36564	0.48627
VRS (2.0s)	-1.94739	-5.44397E-4	0.4944	-0.42454	0.33371	0.55687

Table 3. Regression coefficients for Peak Ground Motions and Spectral Values using Bommer and Akkar GMPE for rock sites

Y	b ₁	b ₂	b ₃	b ₄	b ₅	σ	R ²
Acceleration: All (n=229)	-1.29562	0.33231	0.05844	1.38054	-0.36172	0.34269	0.25789
Acceleration: Depth < 70 km (n=201)	-1.32206	0.30076	0.06902	1.5027	-0.3951	0.35074	0.21764
Acceleration: M > 4 and h < 70 km (n=160)	-2.71702	1.14476	-0.03585	0.52328	-0.22012	0.3476	0.2668
Velocity	-3.05898	0.20369	0.09203	1.64876	-0.40306	0.3459	0.3128
Displacement	0.8236	-0.69163	0.15131	1.36491	-0.31162	0.37426	0.18066
ARS (0.3s)	-3.33127	1.05512	-0.01043	1.26107	-0.30505	0.40898	0.33278
ARS (1.0s)	-3.78211	0.58329	0.07222	1.438	-0.37273	0.4259	0.48677
ARS (2.0s)	-3.48421	0.09253	0.13718	1.80411	-0.45637	0.36826	0.53617
VRS (0.3s)	-3.99831	0.83772	0.00662	1.3009	-0.30979	0.38627	0.28066
VRS (1.0s)	-3.39839	0.35642	0.07683	1.4897	-0.3676	0.38551	0.35111
VRS (2.0s)	-3.36514	0.25431	0.09473	1.70841	-0.41611	0.35732	0.36064

Table 4. Regression coefficients for Peak Ground Motions and Spectral Values using Bommer and Akkar GMPE for soil sites

Y	b ₁	b ₂	b ₃	b ₄	b ₅	σ	R ²
Acceleration: All (n=187)	0.53083	1.0689	-0.13013	-2.0099	0.24215	0.35542	0.31984
Velocity	-2.37111	1.01273	-0.07409	-0.84805	0.04971	0.33944	0.39958
Displacement	1.37341	-0.12068	0.01496	-0.54034	0.0786	0.44554	0.13948
ARS (0.3s)	-3.48393	1.93489	-0.15661	-0.66353	0.02995	0.36863	0.51802
ARS (1.0s)	-4.4399	1.77184	-0.12272	-0.66217	0.03155	0.36735	0.66573
ARS (2.0s)	-3.53819	0.96448	-0.01719	-0.20032	-0.0769	0.35488	0.68029
VRS (0.3s)	-3.95773	1.73599	-0.14831	-0.84031	0.06138	0.36153	0.45415
VRS (1.0s)	-3.18244	1.44493	-0.12206	-1.23378	0.12478	0.34789	0.53746
VRS (2.0s)	-2.5624	1.11056	-0.07643	-1.11373	0.08031	0.32884	0.57205

Figure 4 shows comparison of predicted PGA values for magnitude 6 earthquake using Joyner and Boore and Bommer and Akkar GMPEs at various distances for rock as well as soil sites. The data of three earthquakes having magnitude 6 or a little more have been also plotted for comparison. From the figures, it can be said that rock site data fits relatively well with Bommer and Akkar GMPE and on the other hand soil site data fits well with Joyner and Boore GMPE.

Figure 5 compares Bommer and Akkar GMPE for rock site data for different datasets. The three datasets show almost similar prediction values. Since the dataset where $M > 4$ and $h < 70$ km has a slightly higher correlation coefficient, this prediction values are plotted with $\pm\sigma$. Figure 5 also compares Joyner and Boore GMPE for soil site data for different datasets. The three datasets also show almost similar prediction values. Since the dataset where $h < 70$ km has a slightly higher correlation coefficient, this prediction values are also plotted with $\pm\sigma$.

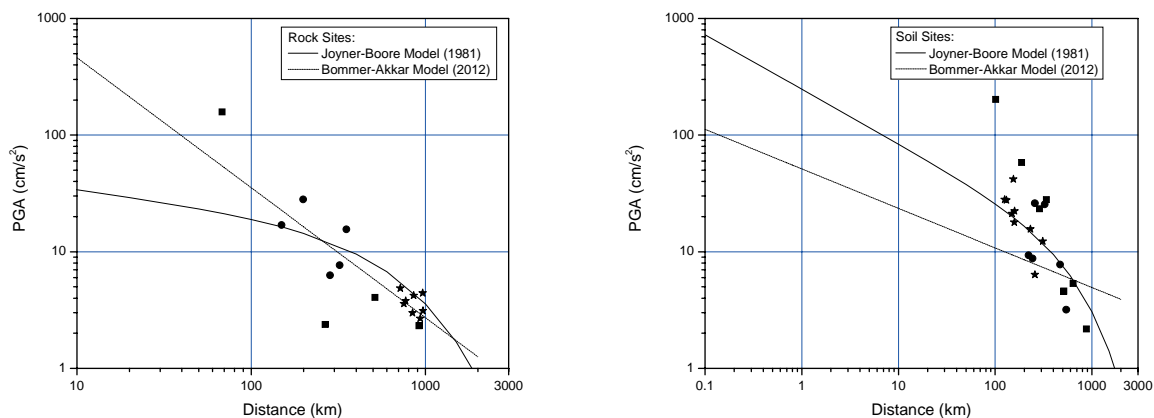


Figure 4. Predicted PGA values for a $M = 6.0$ earthquake at various distances, using two GMPEs

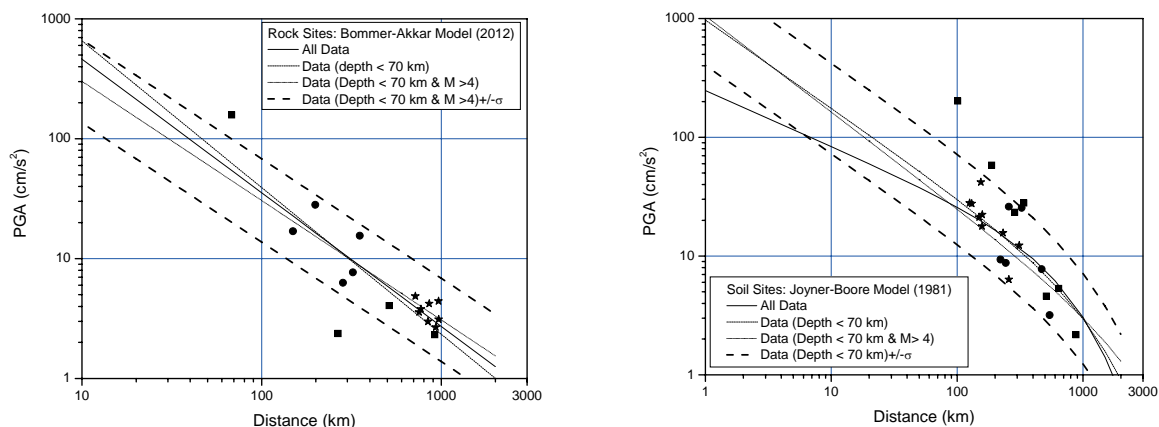


Figure 5. Predicted PGA values for a $M = 6.0$ earthquake at various distances, for different datasets for a fixed GMPE

Site Response Characteristics

Nakamura (1989) proposed a methodology of using the H/V ratio of Fourier amplitude spectra to estimate local site response characteristics. Although the absolute level of the H/V ratio depends on the wave field and source mechanism, extensive studies [12-15] have demonstrated that the H/V ratio shape shows good stability and is insensitive to source location and mechanism. If a clear impedance contrast exists at the site, the H/V ratio has been shown to provide an adequate estimate of the predominant period of a site, which is an important parameter for assessing building damage [16-17] and in evaluating local site amplification. In this study, the H/V ratio technique was used to investigate the site response characteristics.

The main shock of the 18 September 2011 Sikkim Earthquake generated a total of 9 ground motion records from stations located on soft-soil sites (V_{S30} ranging from about 200 to 375 m/s) with r ranging from about 100 to 900 km. On the other hand, a total of 4 ground motions were recorded on rock sites (V_{S30} ranging from about 700 to 1620 m/s) with r ranging from about 50 to 800 km. The H/V ratio is calculated as the Fourier amplitude spectral ratio between the geometric mean of the two horizontal components and the vertical component. These Fourier amplitude spectra were smoothed by a Parzen window of 0.4 Hz bandwidth.

Figure 6b shows plots of H/V ratios of Fourier amplitude spectra of 9 ground motions on the soft-soil sites along with the geometric mean. Overall, these soft-soil sites appear to show broadband predominant site frequencies ranging from around 0.6 to 2.5 Hz corresponding to the peak of the geometric mean H/V ratio curve. In general, a typical predominant site frequency of about 1.6 to 3 Hz should be anticipated for a similar soft-soil site with V_{S30} of between 200 and 375 m/s. The observed lengthening in the predominant site period for some of the soft-soil sites is likely caused by the nonlinear behavior of soil deposits under a relatively high level of excitation. The predominant site period has been observed to be lengthened when the soil deposit behaves more nonlinearly during a strong shaking. Figure 6a plots H/V ratios of Fourier amplitude spectra of 4 ground motions on rock sites along with the geometric mean. In general, these rock sites showed a predominant site frequency between 3 to 5 Hz, which is typical for a rock site. For ease of comparison, the geometric mean H/V ratios for soft-soil sites and for rock sites are plotted in Figure 6c.

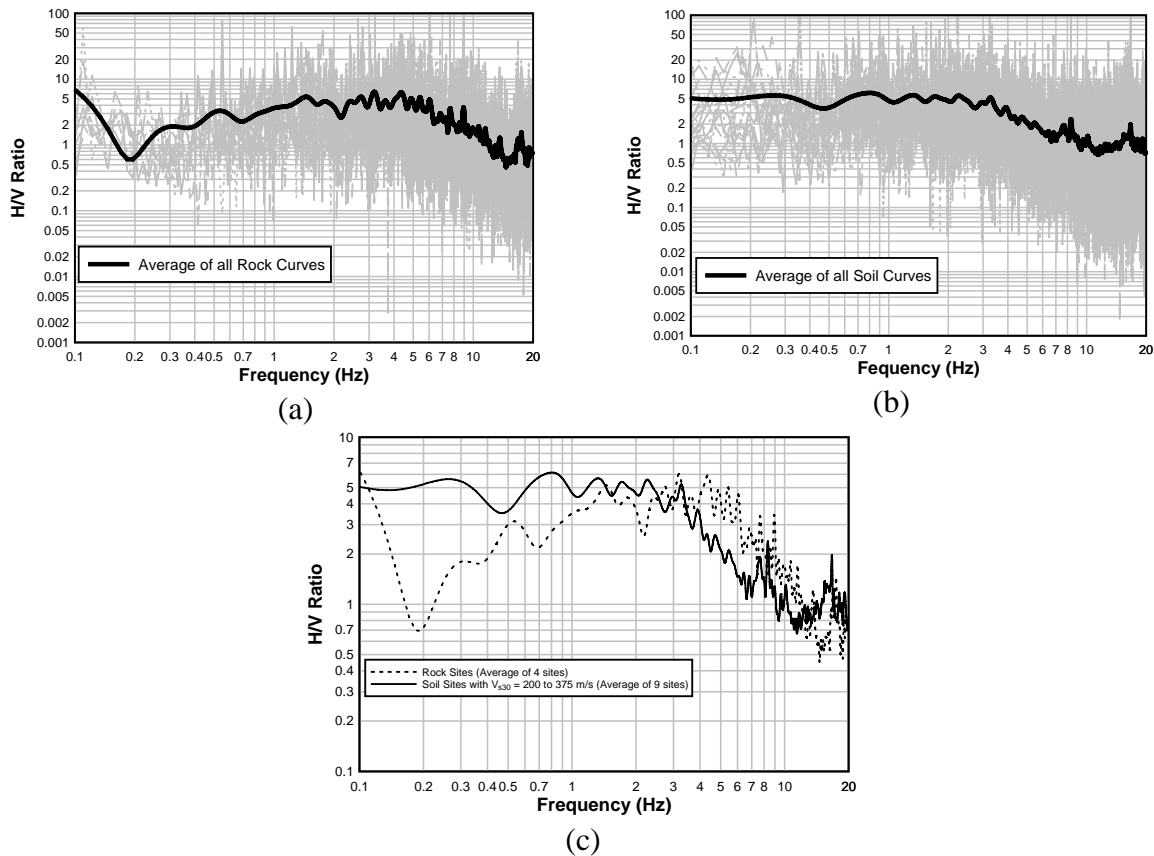


Figure 7. H/V ratios of Fourier amplitude spectra of the 2011 Sikkim earthquake: (a) all rock sites; (b) all soil sites; thick lines represent the geometric mean H/V ratios and, (c) geometric mean H/V ratios for the soft-soil sites and for the rock sites.

It is noted that the predominant site frequencies, amplitudes, and shapes of the H/V ratios are remarkably different between the two site classes, which revalidates the capability of the H/V ratio to estimate the predominant frequency of soil deposits. To clarify the issue further, H/V ratios of Fourier amplitude spectra of Gangtok (rock) [around 50 km from the epicentre] and Siliguri (soil) [around 100 km from the epicentre] site during the 2011 Sikkim earthquake has been compared and showed in Fig 7. The Siliguri site shows a predominant peak at 2 Hz and the Gangtok site shows a predominant peak at 9 Hz.

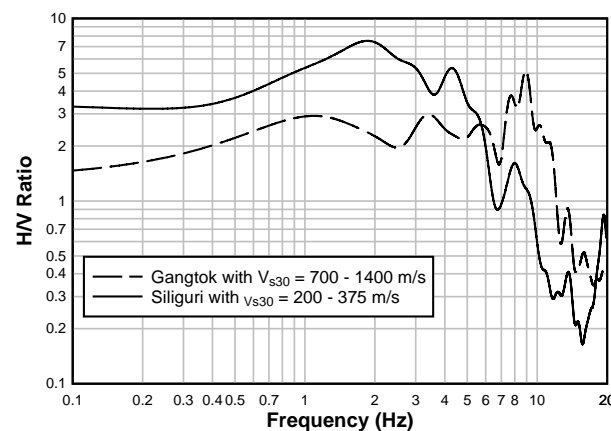


Figure 7. H/V ratios of Fourier amplitude spectra of Gangtok (rock) and Siliguri (soil) site during the 2011 Sikkim earthquake

Conclusions

In this study, two GMPE proposed by Joyner and Boore and Bommer and Akkar were used to fit the SGM data. The recorded peak ground accelerations from three earthquakes having magnitude greater than six were also compared with those GMPEs for soil and rock sites. The study found that for soil sites, Joyner and Boore GMPE may be used to predict peak ground acceleration values and on the other hand for the rock sites Bommer and Akkar proposed GMPE may be used.

Results of H/V ratios reveal that some soft-soil sites with V_{S30} between 200 and 375 m/s show a predominant site frequency around 0.6 to 2.5 Hz. The lengthened predominant site periods are likely results from the nonlinear behavior of soil deposits under a high level of excitation. The rock sites show a predominant site frequency around 3 to 5 Hz. The remarkably different predominant site frequencies, amplitudes, and shapes of the H/V spectral ratios between the two sites revalidate the capability of the H/V spectral ratio method for estimating predominant site periods, which is an important parameter for assessing building damage.

Acknowledgments

The author would like to acknowledge the support provided by PESMOS, India regarding strong motion data usage.

References

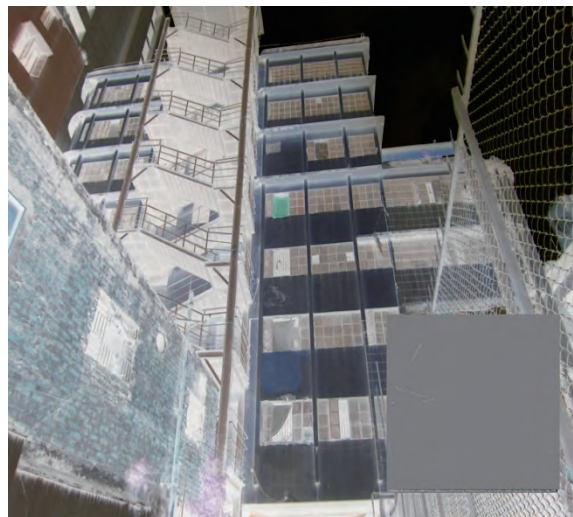
1. Kumar A, Mittal H, Sachdeva R, Kumar A. Indian Strong Motion Instrumentation Network, *Seismological Research Letters* 2012; **83** (1): 59-66.
2. Mittal H., Kumar A, Ramhmachhuani, R. Indian National Strong Motion Instrumentation Network and Site Characterization of Its Stations, *International Journal of Geosciences* 2012; **3**: 1151-1167.
3. Joyner WB, Boore DM. Peak Horizontal Acceleration and Velocity from Strong Motion Records Including Records from the 1979 Imperial Valley, California, Earthquake, *Bull. Seism. Soc. Am.* 1981; **71** (6): 2011-2038.
4. Bommer JJ, Akkar S. Consistent Source-to-Site Distance Metrics in Ground-Motion Prediction Equations and Seismic Source Models for PSHA, *Earthquake Spectra* 2012; **28** (1): 1-15.
5. Idriss IM. Earthquake ground motions at soft soil sites, *Proceedings of the 2nd International Conference on Recent Advances in Geotechnical Earthquake engineering and Soil Dynamics*, St. Louis, MO, 1991; 2265–2272.
6. Singh JP. Site specific ground motions for high-tech seismic design, *ATC/JSCA 8th U.S.-Japan Workshop on the Improvement of Structural Design and Construction Practices*, Honolulu, HI, 1998.
7. Liao Y, Meneses J. Engineering Characteristics of Ground Motion Records from the 2010 Mw 7.2 El Mayor–Cucapah Earthquake in Mexico, *Earthquake Spectra* 2013; **29** (1): 177-205.
8. Borchardt RD. Estimates of site-dependent response spectra for design (methodology and justification), *Earthquake Spectra* 1994; **10**: 617–653.
9. Nakamura T. A method for dynamic characteristics estimation of subsurface using microtremor on the ground surface, *Quarterly Report of Railway Technical Research Institute* 1989; **30**: 25–33.
10. Seed HB, Ugas C, Lysmer J. Site-Dependent Spectra for Earthquake-Resistant Design, *Bulletin of the Seismological Society of America* 1976; **66** (1): 221-243.

11. Mohraz B. A Study of Earthquake Response Spectra for Different Geological Conditions, *Bulletin of the Seis-mological Society of America* 1976; **66** (3): 915-935.
12. Field EH. Spectral amplification in a sediment-filled valley exhibiting clear basin-edge induced waves, *Bulletin of Seismological Society of America* 1996; **86**: 991–1005.
13. Yamazaki F, Ansary MA. Stability of H/V spectrum ratio of earthquake ground motion, *Transactions of the 14th International Conference on Structural Mechanics in Reactor Technology (SMiRT 14)*; Lyon, France, August 17–22, 1997.
14. Rodríguez VHS, Midorikawa S. Comparison of spectra ratio techniques for estimation of site effects using microtremor data and earthquake motions recorded at the surface and in boreholes, *Earthquake Engineering and Structural Dynamics* 2003; **32**: 1691–1714.
15. Ansary MA, Rahman MS. Site amplification investigation in Dhaka, Bangladesh, using H/V ratio of microtremor, *Environ. Earth Science* 2013; 70: 559-574.
16. Fellahi A, Alaghebandian R, Miyajima M. Microtremor measurements and building damage during the Changureh-Avaj, Iran, earthquake of June 2002, *Journal of Natural Disaster Science* 2003; **25**: 37–46.
17. Gosar A. Microtremor HVSR study for assessing site effects in the Bovec Basin (NW Slovenia) related to 1998 Mw 5.6 Earthquakes, *Engineering Geology* 2007; **91**: 178–193.



PART-VIII

STRUCTURAL QUALITY ASSESSMENT OF PADMA PICTURE LTD. MALIBAG, DHAKA



**BANGLADESH NETWORK OFFICE FOR URBAN
SAFETY (BNUS), BUET, DHAKA**

Prepared By: Pushpendu Biswas

Mehedi Ahmed Ansary

Image Scan of Column's:-

Figure 2 and Figure 3 are showing the Image scan result of column S-1(long side and short side respectively) at a height of 2'-8'' from the ground. And figure 4 is the cross section of that column.

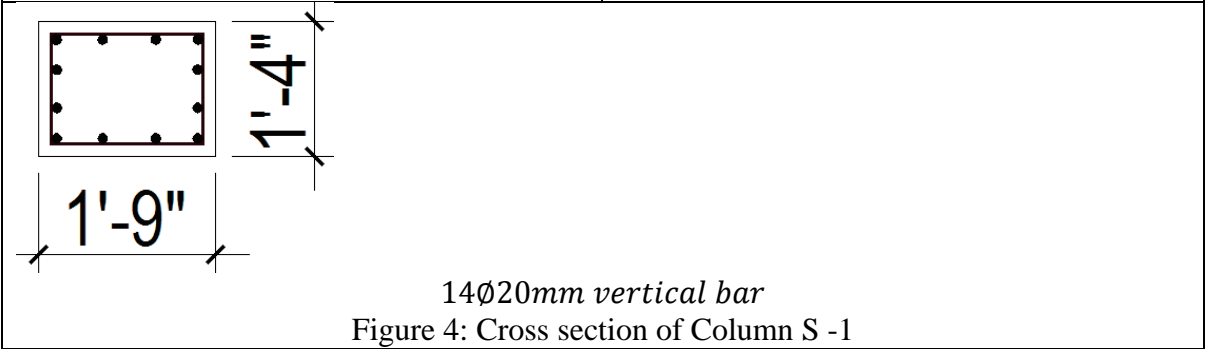
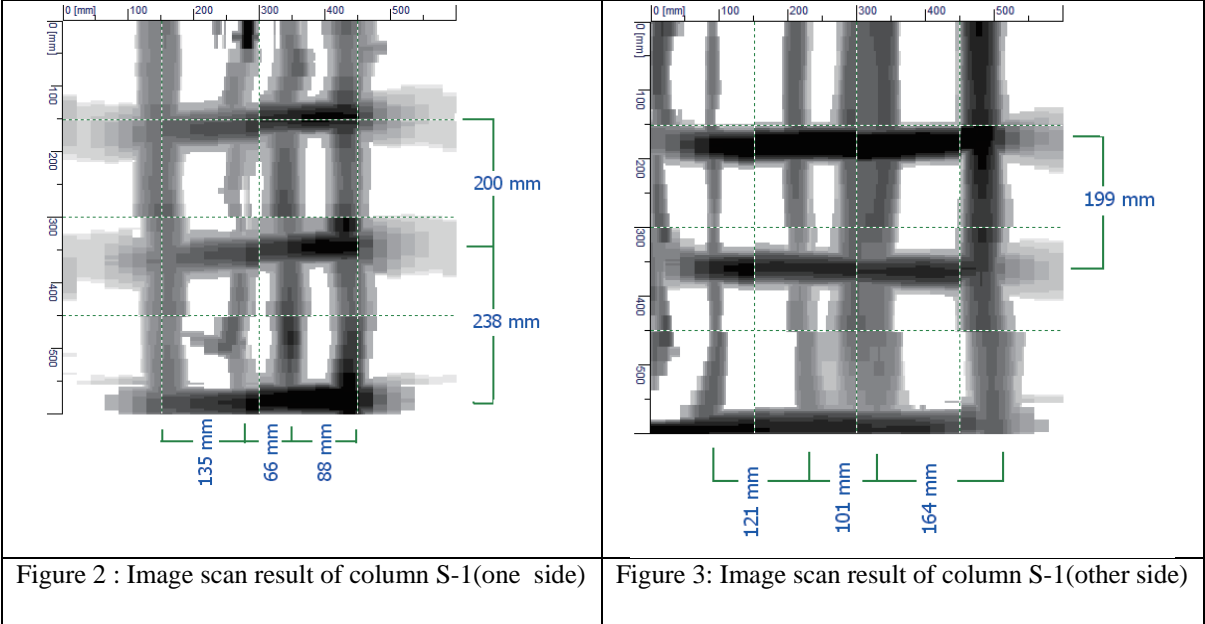
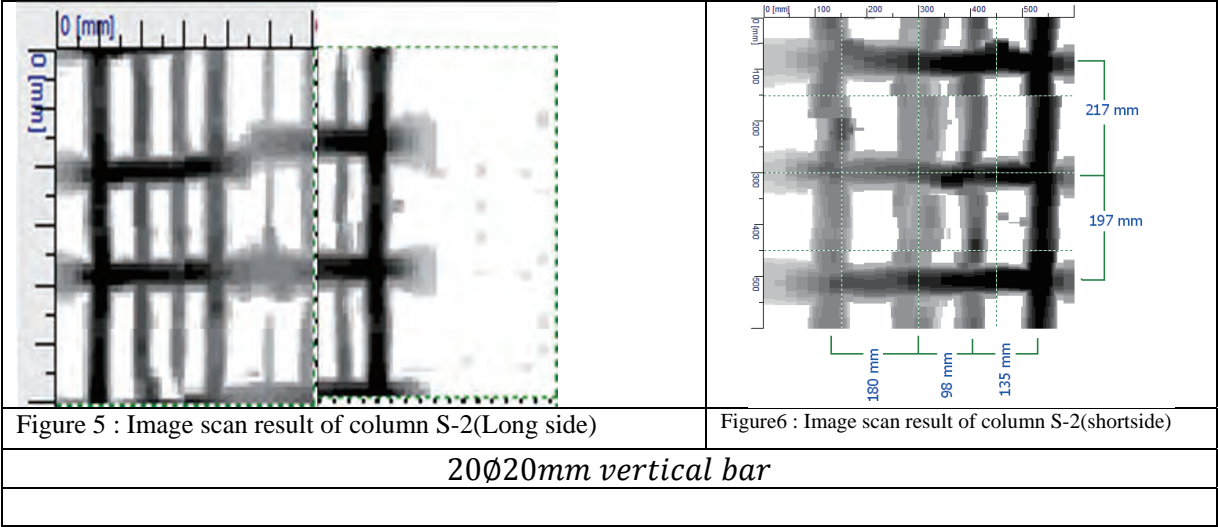


Figure5 and Figure6 are showing the Image scan result of column S-1(long side and short side respectively) at a height of 2'-8'' from the ground. And figure 7 is the cross section of that column.



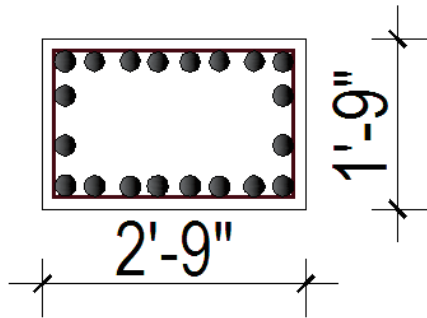


Figure 7:- Cross section of Column S -2

Figure 8 and Figure 9 are showing the Image scan result of column S-3(long side and short side respectively) at a height of 2'-8'' from the ground. And figure 10 is the cross section of that column.

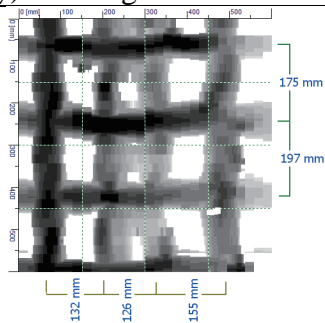


Figure 8: Image scan result of column S-3(Long side)

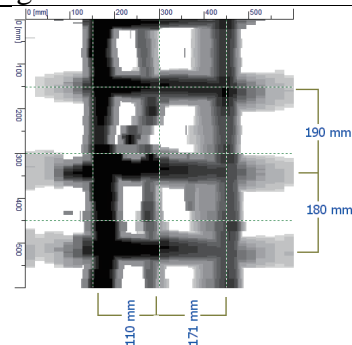


Figure 9: Image scan result of column S-3(other side)

14Ø20mm vertical bar

Figure 10 : Cross section of Column S -3

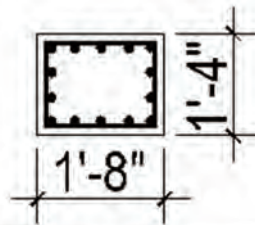


Figure 11 and Figure 12 are showing the Image scan result of column S-4(long side and short side respectively) at a height of 2'-8'' from the ground. And figure 13 is the cross section of that column.

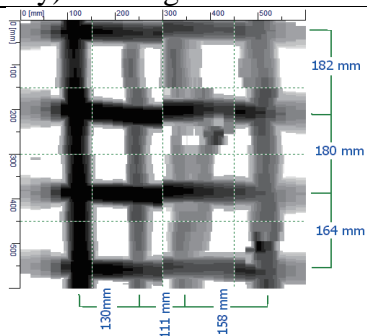


Figure 11 : Image scan result of column S-1(Long side)

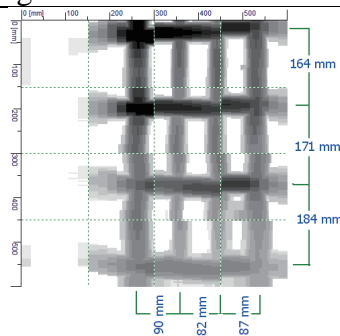


Figure 12: Image scan result of column S-1(short side)

14Ø20mm vertical bar

Figure 13 : Cross section of Column S -4

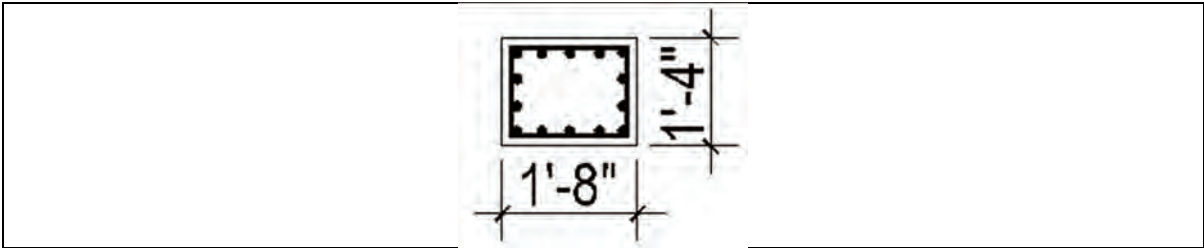
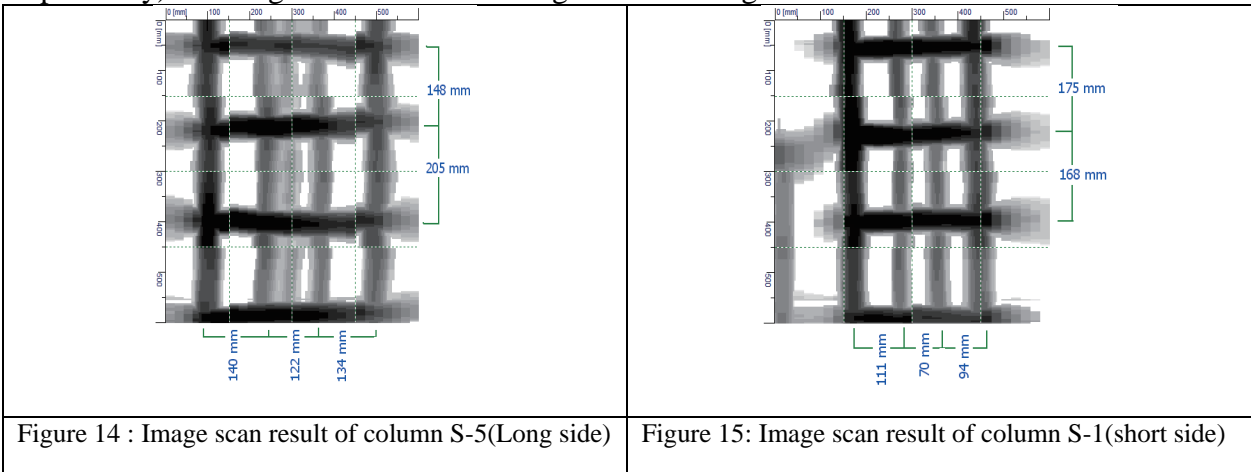


Figure 14 and Figure 15 are showing the Image scan result of column S-5(long side and short side respectively) at a height of 2’-8’’ from the ground. And figure-16 is the cross section of that column.



14Ø20mm vertical bar
Figure 16 : Cross section of Column S -5

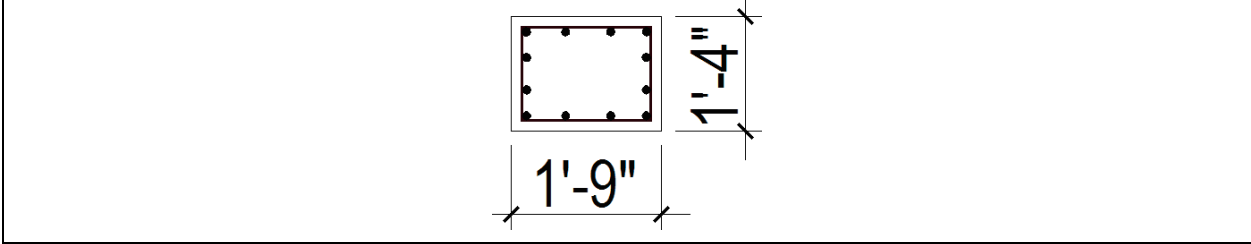
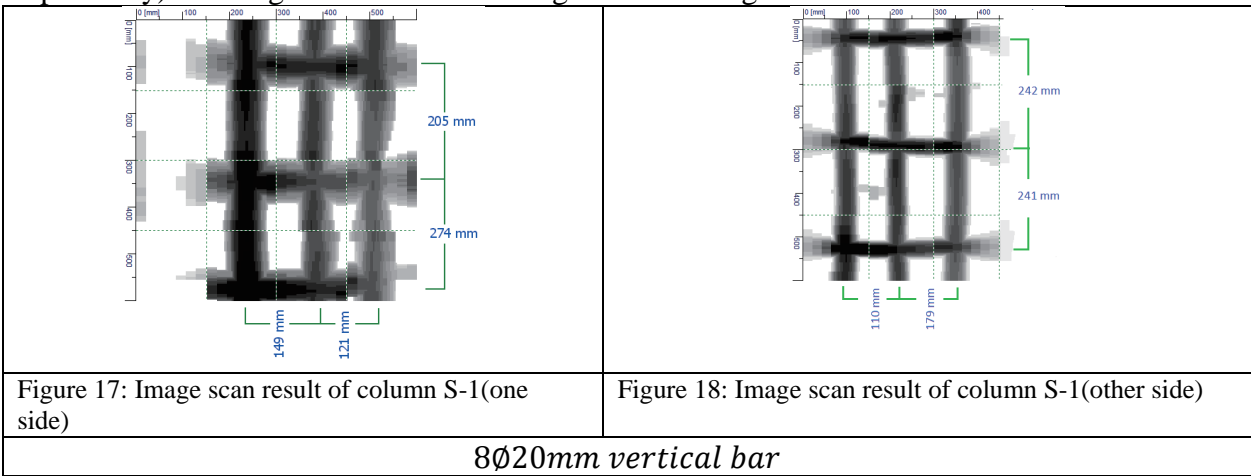


Figure 17 and Figure 18 are showing the Image scan result of column S-8(long side and short side respectively) at a height of 2’-8’’ from the ground. And figure 19 is the cross section of that column.



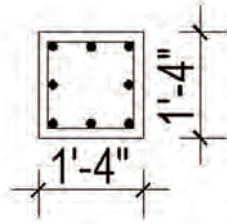


Figure 19 : Cross section of Column S -8

The Image scan result of column S-9(both side respectively) at a height of 2'-8'' from the ground.

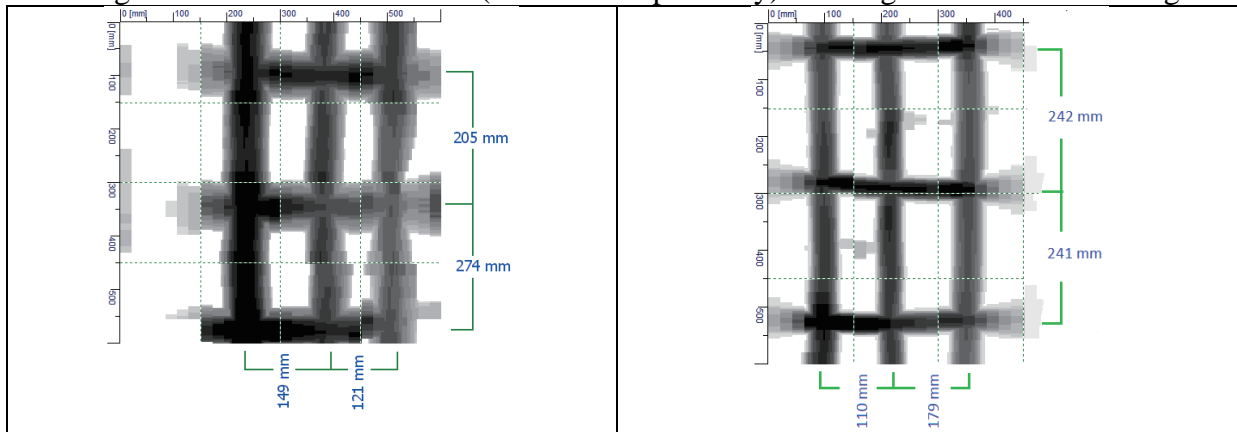
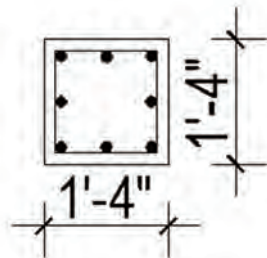


Figure 20 : Image scan result of column S-1(one side)

Figure21: Image scan result of column S-1(other side)



8Ø20mm vertical bar

Figure 22 : Cross section of Column S -9

The Image scan result of column S-10(both side respectively) at a height of 2'-8'' from the ground.

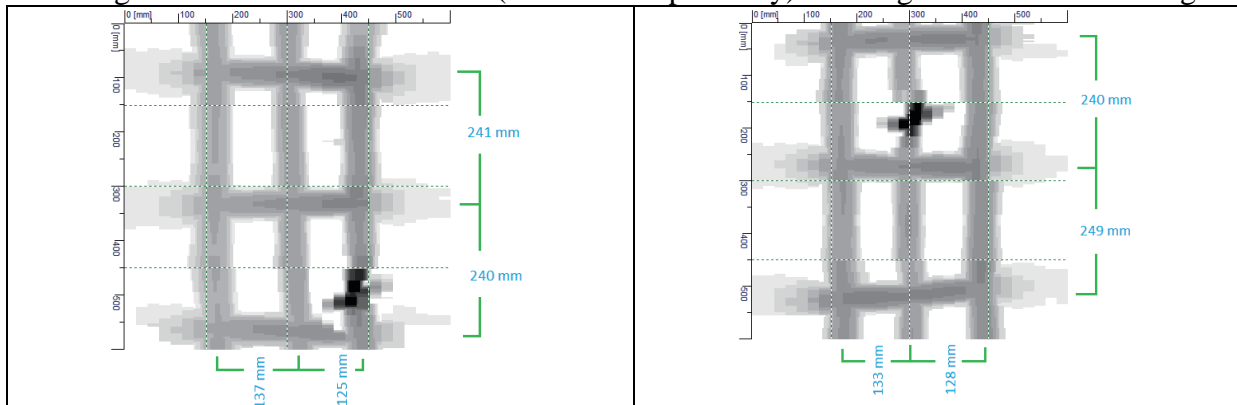


Figure 23 : Image scan result of column S-1(one side)

Figure24: Image scan result of column S-1(other side)

8Ø20mm vertical bar

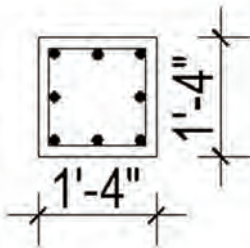


Figure 25 : Cross section of Column S -10

Scan of Beams:-

Figure 26, Figure 27 and Figure 28 are showing the Image scan result of Beam B-1(depth, Bottom and top respectively) at . And figure 29 is the cross section of that beam.

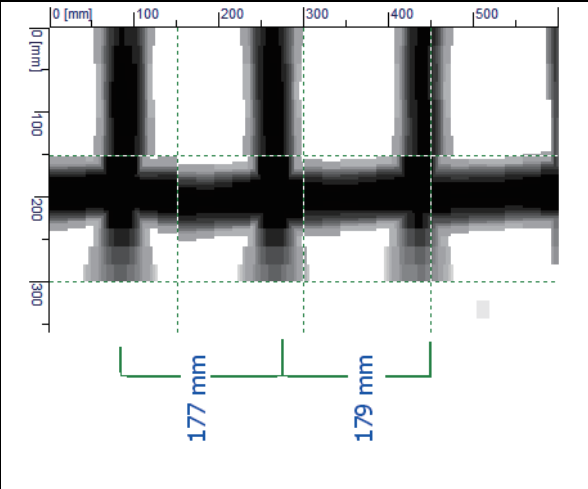


Figure 26 : Image scan result of beamB-1(Side)

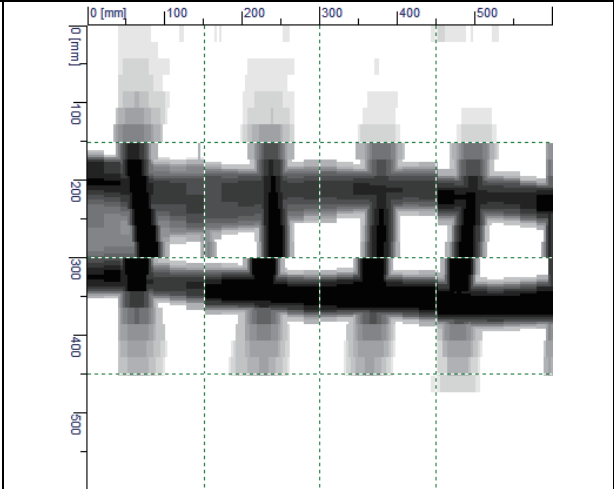


Figure 27: Image scan result of beam B-1(Bottom)

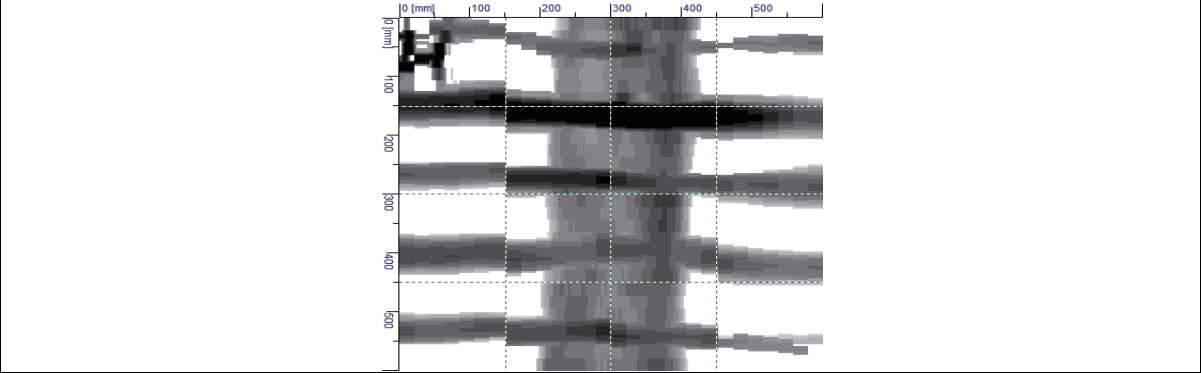


Figure 28:-Image scan result of beamB-1(Top slab)

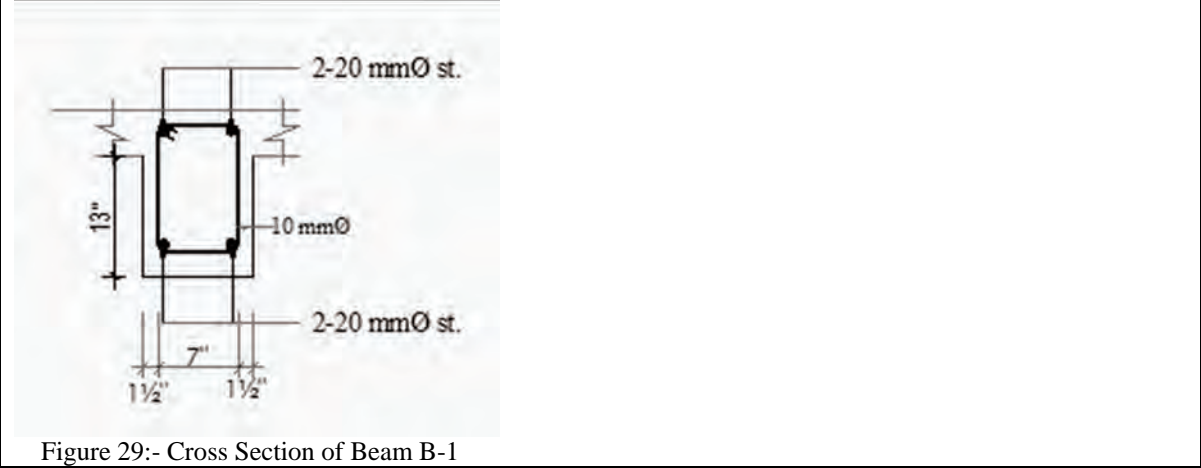


Figure 29:- Cross Section of Beam B-1

Figure 30 and Figure 31 are showing the Image scan result of Beam B-2(depth and Bottom respectively) at . And figure 32 is the cross section of that column.

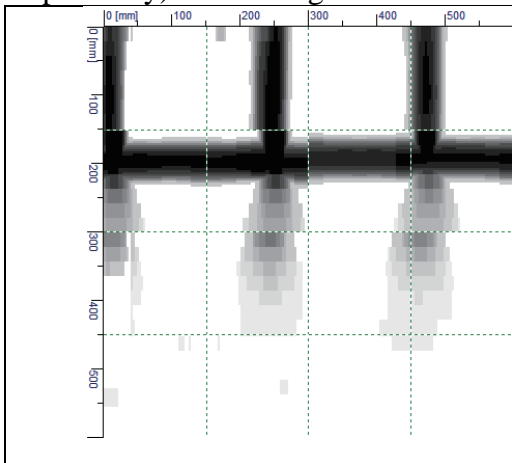


Figure 30 : Image scan result of beamB-2(Side)

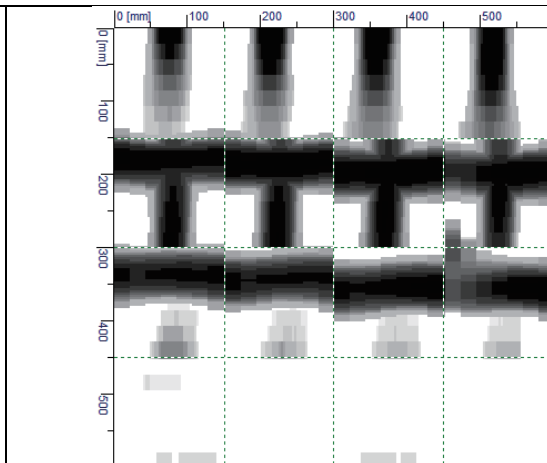


Figure 31: Image scan result of beam B-2(Bottom)

2Ø20mmbar at bottom

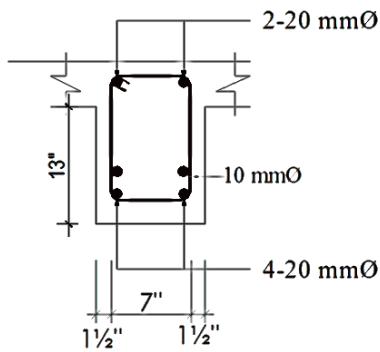


Figure 32:- Cross Section of Beam B-2

Figure 33 and Figure 34 are showing the Image scan result of BeamB-4(depth and top respectively) at . And figure 35 is the cross section of that Beam.

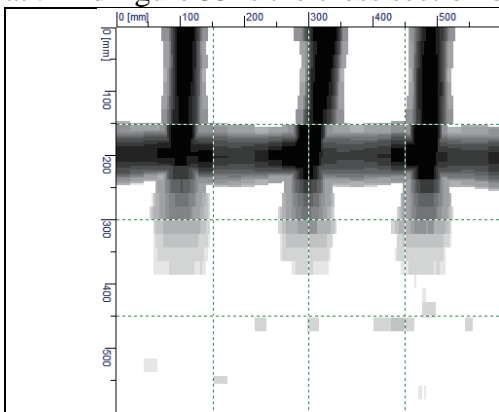


Figure 33 : Image scan result of beamB-4(Side)

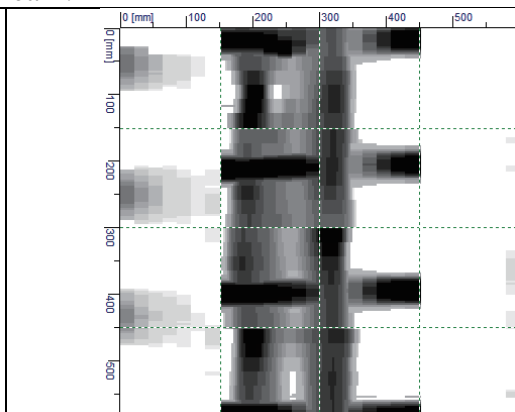


Figure 34: Image scan result of beamB-4(top)

2Ø20mm bar at bottom& top

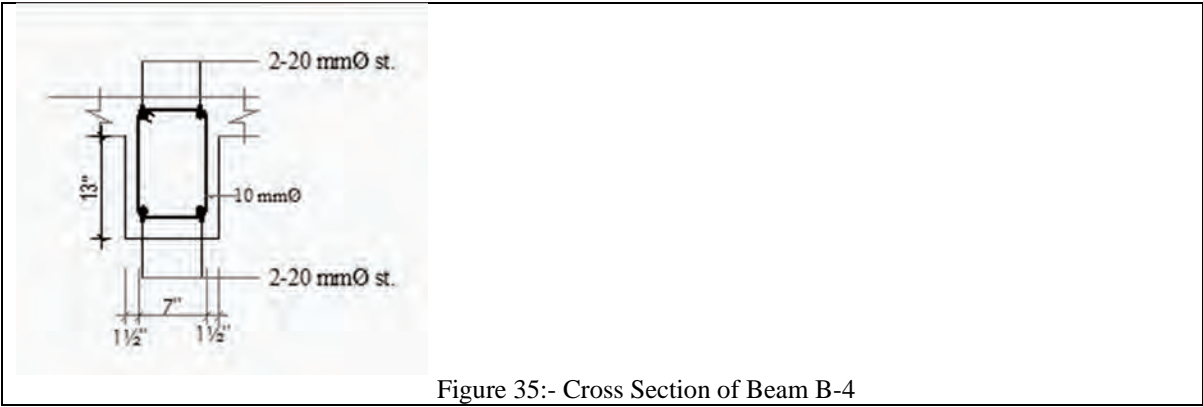
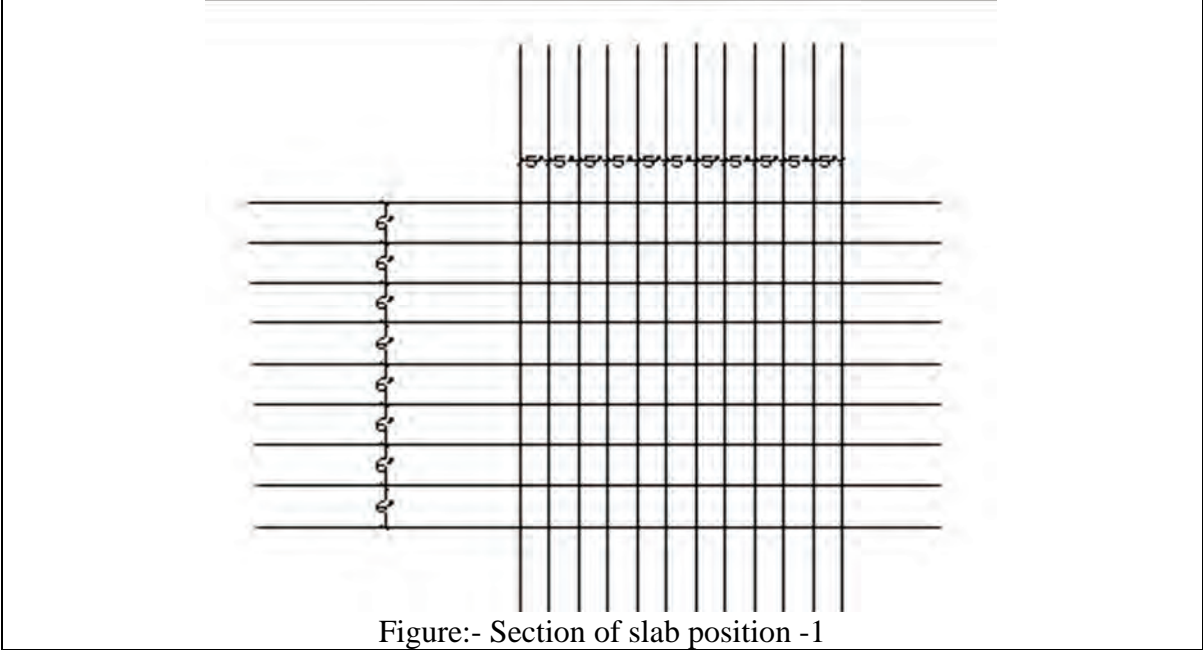
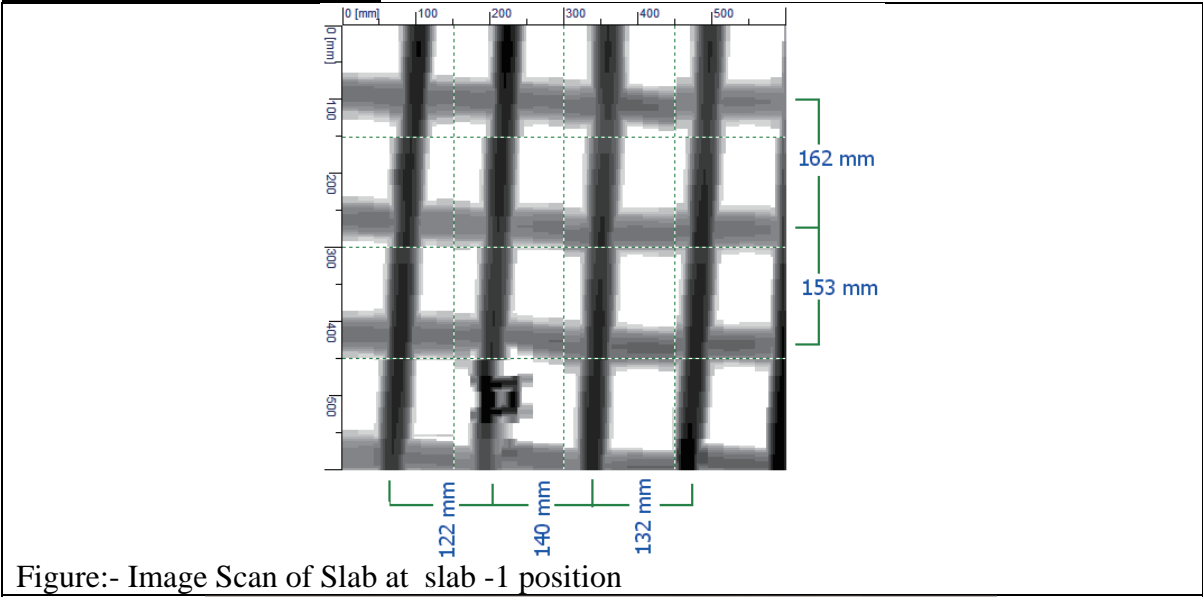
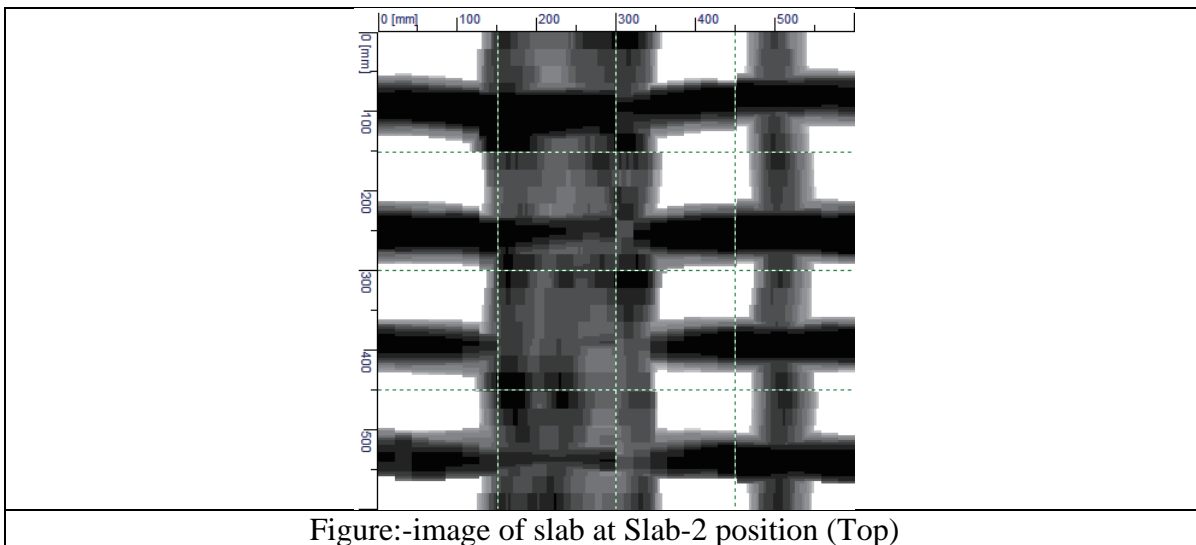


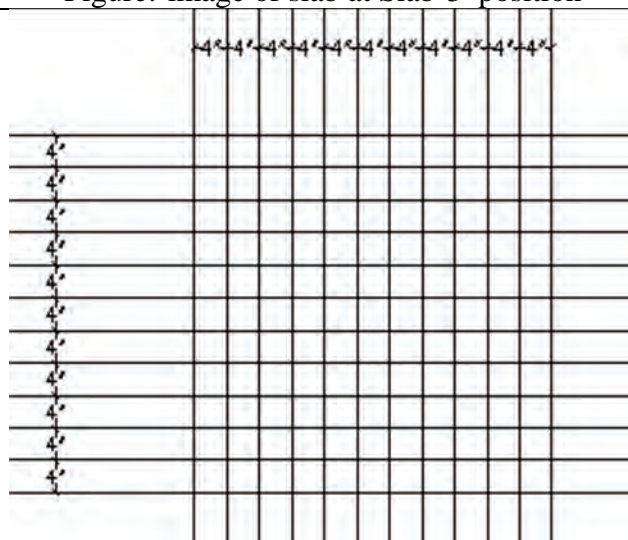
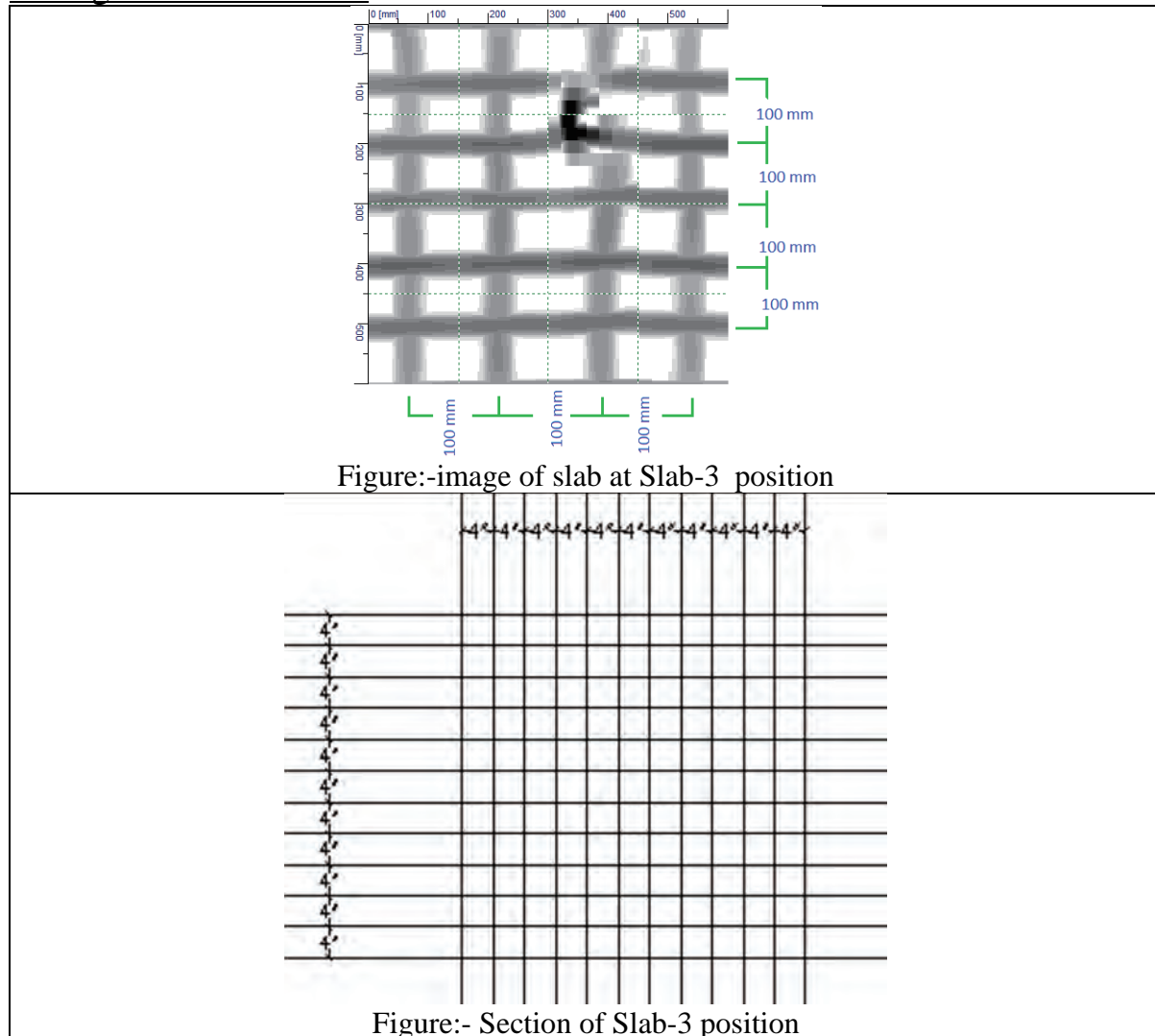
Image Scan of Slab:-



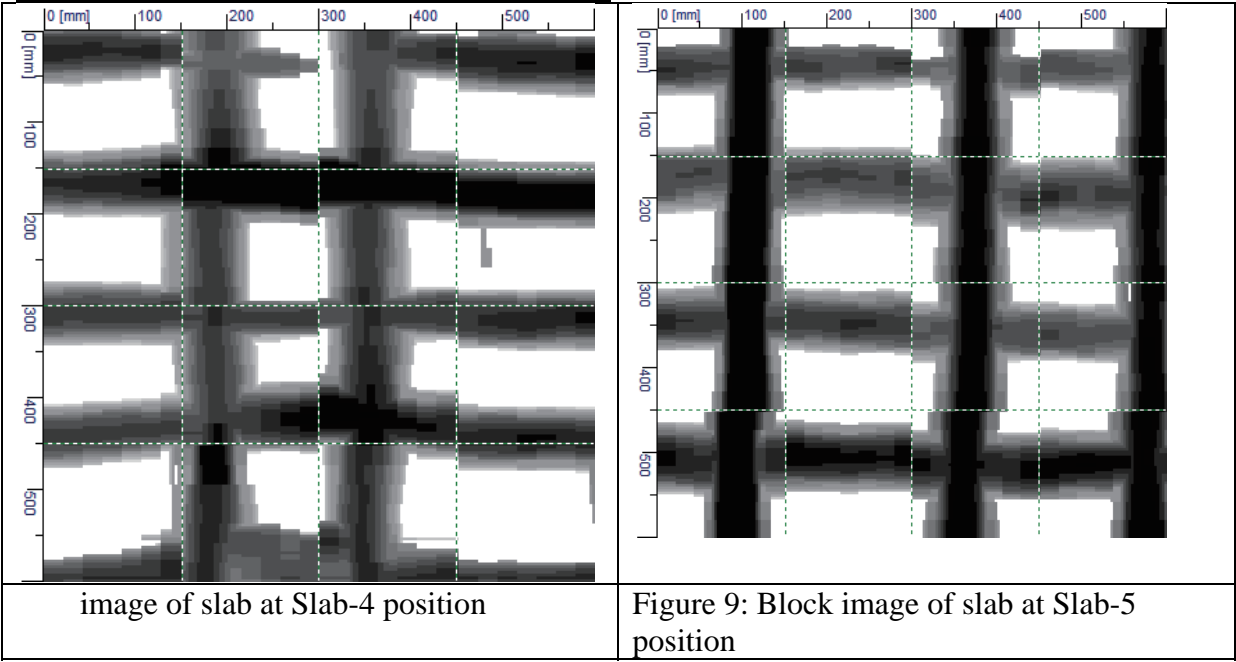
2. Image Scan of Slab Position :-



3. Image Scan of Slab-3:-



4. Image of Top Slab position -4:





PART-IX

APPLICABILITY OF EXISTING CPT, SPT AND SOIL PARAMETER CORRELATIONS FOR BANGLADESH

**BANGLADESH NETWORK OFFICE FOR URBAN
SAFETY (BNUS), BUET, DHAKA**

Prepared By: Mominul Haque

Mehedi Ahmed Ansary

ABSTRACT: Many correlations have been established between CPT, SPT and other soil parameters that relate to direct applications in engineering practice. In this research, four pairs of CPT and SPT tests were performed in order to examine the applicability of various existing CPT-SPT correlations to the studied soils. The recovered samples from SPT tests contain appreciable amount of fines (f_c) ranging from 3.5 to 39.2 percent and mean grain size (D_{50}) ranging from 0.09 to 0.23 mm. Study results indicated that q_c/N ratio as a function of D_{50} and f_c based correlations are poorly applicable to the local soils. This paper suggests that $q_{t1}/(N_1)_{60}$ ratio as a function of multiplying constant can be better correlated in local soils instead of laboratory based D_{50} or f_c correlations. An effort has also been made to perform a comparative analysis for the effective angle of internal friction obtained from CPT, SPT, direct shear and triaxial tests

1 INTRODUCTION

At the present time, the cone penetration test (CPT) is becoming increasingly popular in subsoil investigation for its rapid and convenient way to measure continuous soil stratigraphy. On the other hand, the standard penetration test (SPT) is one of the most commonly used in-situ test procedure for subsoil investigation in many places around the world. However, application of the CPT has started in Bangladesh since last decade for soil exploration and engineering design purpose, but SPT is still the most widespread and economic mean for subsoil investigation than any other test.

Due to the lack of soil sampling during CPT, in many engineering projects it is most common to use both CPT and SPT together for subsoil investigation and a combination of obtained soil parameters from these tests are being used for design purpose. From that point of view, many empirical correlations have been established between CPT cone tip resistance (q_c), SPT N-value and other engineering soil properties that relate to direct applications in engineering practice. Most of the currently available correlations apply only to ideal soils. Sometimes where the soils are not ideal the usual correlations are inadequate or lead to inconsistent conclusions. Although designers use these correlations in practice, it is necessary to examine the applicability of various existing correlations prior to direct application in local soils.

The primary objective of this research is to examine the applicability of various existing CPT-SPT correlations for local soils and to propose possible new correlations. The study included field explorations, laboratory testing, comparative analyses of resulting data. For this study purpose, four pairs of high quality CPT and SPT tests were carried out up to 25 m at the bank of the Jamuna River, Bangladesh. Although, this is a small-scale research work, it is hoped that this work will provide useful contribution for further improvement of region specific CPT-SPT correlations.

2 LITERATURE REVIEW

Since last few decades, much research have taken place to properly utilize abundant experiences and available database on SPT to more reliable CPT. As a result, a considerable number of correlations have been proposed by several researcher between CPT cone tip resistance (q_c), SPT N-values and other engineering soil properties. These correlations can be considered in three major groups. Most of the primary correlations considered q_c/N as a function of grain characteristics, such as mean grain size (D_{50}) and/or fines content (f_c). Some other researchers proposed a constant value of q_c/N for different soil types in a chart of corrected cone tip resistance (q_t) versus friction ratio (R_f).

Compiling a number of studies, Robertson et.al (1983) accumulated several research outputs and presented a relationship of q_c/N_{60} as a function of mean grain size (D_{50}). Similar effort has been made by Kasim et al. (1986) and, Kulhawy and Mayne (1990), where they have presented more updated databases to correlate q_c/N as a function of mean grain size (D_{50}) compared to the proposed relationship by Robertson et.al (1983). These correlations

provide a very useful guideline to convert the CPT tip resistance to the equivalent SPT N-value for soils with D_{50} varying between 0.001 mm to 10 mm. From these correlations it is observed that the q_c/N ratio increases with increasing mean grain size. They have also noted that the scatter in q_c/N ratio appears to increase with increasing mean grain size. Unfortunately, correction factors for q_c or N-value have not been applied to most of their original data. It should be noted that, energy measurements on SPT data indicate that the average energy ratio of about 55 to 60 % may represent the average energy level associated with the q_c/N correlation (Robertson et.al 1983). Robertson and Campanella (1985) suggested a representative value of q_c/N_{60} ratio of 4.5-5.0 and 4.0 for medium and silty soils, respectively.

In other studies, Chin et al. (1988) have presented correlation between q_c/N as a function of percentage fines (smaller than 0.074 mm). In their study measured N-values were corrected corresponding to 55 % of the maximum energy. They showed that, for sands q_c/N decreases significantly with increasing fine content. In addition to these data, Kulhawy and Mayne (1990) summarized several research results (Muromachi 1981, Jamiolkowski et al. 1985, Kasim et al. 1985, Chin et al. 1988) which display a similar trend between q_c/N and fines content as proposed by Chin et al. (1988). McNulty and Harney (2010) have compared effective angle of internal friction (ϕ) estimated from the CPT with those determined from SPT N-values and laboratory triaxial tests. Their study revealed that effective angle of internal friction (ϕ) obtained from triaxial tests correlated well with those obtained from the CPT and SPT below the water table, but above the ground water obtained ϕ values from the CPT and SPT were significantly high compared to laboratory measurement.

Research by Elbanna et al. (2011) suggested that, in the absence of site specific CPT-SPT correlations, it is suitable to use the general correlation proposed by Robertson, et al (1983). In the absence of grain size data, they have also proposed a new correlation using the $q_{t1}/(N_1)_{60}$ ratio of 0.45. However, some of the existing correlations provide best estimated relationship between q_c and N-value, but region specific study result presented by Elkateb and Ali (2010) represents quite inapplicability of existing correlations. Therefore, direct application of the average relationship presented in several correlations may lead to significant deviation from exact result.

3 FIELD INVESTIGATIONS

Field investigations were carried out mainly through the application of cone penetration testing (CPT) and standard penetration testing (SPT). A total of four pairs of CPT and SPT were performed in different locations within the study area and each pair of CPT and SPT were carried out as close as possible, maximum horizontal distance was not greater than 10 m. In this research, field investigations were carried out along the riverbank of the Jamuna River, Bangladesh. The geologic formations of the research site are mainly consisting of alluvial sand and silt deposits of Holocene age. The alluvial sands are light to brown-grey colored, coarse to fine silty sand of subrounded in shape. The sand contains mostly quartz, feldspar, mica and significant amount of heavy minerals. The alluvial silts have the same color as the sands, but are fine sandy to clayey silt and are poorly stratified (Alam et al. 1990).

3.1 Cone Penetration Test (CPT)

CPT soundings were advanced using a Hogentoglar type piezocone penetrometer with a cross sectional area of 10 cm² and which can measure the pore water pressure (u_2), as well as the cone tip resistance (q_c) and sleeve friction (f_s). To perform the test, the cone was pushed vertically into the ground at a constant rate of approximately 20 mm/sec. During the advancement, measurements of dynamic pore water pressure, tip resistance and sleeve

friction were recorded continuously at 10 mm depth increments. The typical penetration depth for this study was approximately 25 m below from ground surface.

3.2 Standard Penetration Test (SPT)

SPT were conducted according to ASTM D1586. Boreholes for the SPT were advanced by percussion (chopping) method with Bentonite clay. The split spoon sampling method was used to obtain soil samples from boreholes and disturbed representative samples were collected. Samples recovered from boreholes were stored in plastic bags that were used for laboratory testing. An automatic type SPT hammer-release was used for the SPT. Potential source of uncertainty that may affect SPT N-values have been carefully taken into account. Borehole drilling, soil sampling and SPT N-value recording procedures were observed by experienced geologist during the entire test program and this individual provided visual descriptions of the collected samples. The SPT N-value and samples were collected every 1.52 m intervals. The corrected cone tip resistance (q_t) in MPa (top scale), measured SPT N, N_{60} and $(N_1)_{60}$ values (bottom scale) are presented in Figure 1.

boreholes.

Based on the results of the subsurface explorations, the subsoil profile at the study area can be divided into two strata. The soil within the test area is primarily comprised of clay, silt, fine and medium sand particles. As such, the combination of fines and sand are generally non-plastic and the combination of fines and clay are low-plastic. The top layer consists of silt and clay mixture with a total thickness approximately varied from 3 m to 7.3 m. Immediately below this layer a combination of fine to medium sand and with some silt layer extended to a depth of 25 m. Soil layers are moist from ground surface to ground water table and ground water table is located at 3 m below from ground surface. Note that, there was considerable variability in the measured SPT N-value in different boreholes at different depths ranging from 1 to 52 and maximum cone tip resistance (q_c) was close to 20 MPa. Consistency of the soils at different depth varies from stiff to loose.

4 LABORATORY INVESTIGATIONS

Laboratory investigations included sieve analysis, direct shear tests and triaxial tests. The main objectives of the laboratory investigations are to classify the soil samples recovered from SPT tests and to estimate effective angle of internal friction. Details of the laboratory investigations are described in the following sections.

4.1 Sieve analysis

Soil samples recovered from various depths were individually assessed and classified based on dry sieve analysis. Sieve analysis was performed on each soil sample according to ASTM C136. Among the 64 recovered samples only 51 of the sandy samples were used both for sieve analysis (excluding silty clay samples) and to examine existing correlations. Note that these soils are containing appreciable amount of fines ranging from 3.5 to 39.2 percent, fineness modulus (defined as cumulative percent retained on standard sieve divided by 100) ranging from 0.18 to 1.11 and mean grain size (D_{50}) ranging from 0.09 to 0.23 mm. Based on the sieve analysis results, the soils are generally classified into two groups; either well graded sands with little silt or poorly graded sands with silt. According to the unified soil classification system, the soils can be symbolized as SW and SP-SM respectively. The mean grain size (D_{50}), percent finer than 0.074 mm (f_c) and fineness modulus (F.M.) for each borehole are presented in Table 1.

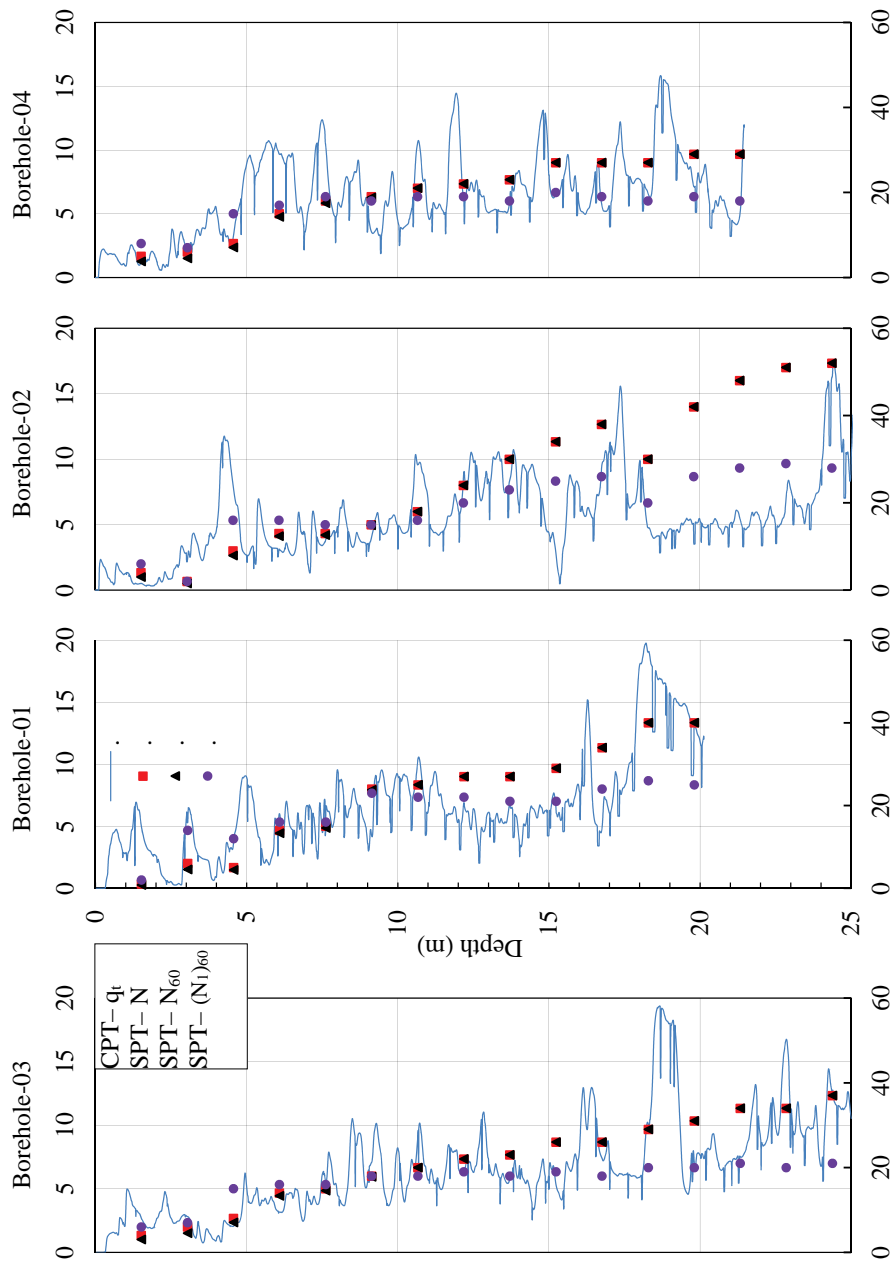


Figure 1. Depth versus corrected cone tip resistance (q_t), SPT N , N_{60} and $(N_1)_{60}$ values for all

Table 1. Sieve analysis results.

Depth	Borehole-01			Borehole-02			Borehole-03			Borehole-04		
m	D ₅₀	f _c	F.M.	D ₅₀	f _c	F.M.	D ₅₀	f _c	F.M.	D ₅₀	f _c	F.M.
3.05	0.1	26.8	0.21	ND*	ND*	ND*	0.16	17.96	0.51	ND*	ND*	ND*
4.57	0.09	32.5	0.16	0.16	32.44	0.64	0.15	16.89	0.51	ND*	ND*	ND*
6.10	0.095	32.5	0.16	0.175	26.39	0.62	0.175	19.8	0.55	ND*	ND*	ND*
7.62	0.09	38.4	0.39	0.095	36.35	0.28	0.16	20.7	0.51	0.185	5.85	0.66
9.14	0.23	11.3	1.11	0.1	39.2	0.33	0.195	16.95	0.83	0.18	6.25	0.67
10.67	0.2	12.4	0.87	0.095	38.1	0.3	0.17	17.8	0.57	0.18	5.5	0.68
12.19	0.2	8	0.92	0.095	38	0.31	0.2	7.44	0.9	0.18	5.5	0.68
13.72	0.18	17.3	0.71	0.09	22	0.48	0.2	5.5	0.92	0.185	5.39	0.71
15.24	0.2	12.5	0.88	0.14	24.4	0.44	0.2	4.15	0.94	0.185	5.4	0.71
16.76	0.2	7.68	0.96	0.195	5.85	0.81	0.2	5.05	0.93	0.185	5.15	0.71
18.29	0.09	32.03	0.18	0.195	7.5	0.79	0.2	4.95	0.93	0.18	6.75	0.67
19.81	0.1	22.7	0.23	0.195	6.85	0.78	0.2	3.7	0.95	0.18	6	0.67
21.33	ND*	ND*	ND*	0.195	6.95	0.77	0.2	3.5	0.95	0.18	4.7	0.7
22.86	ND*	ND*	ND*	0.195	6.8	0.77	0.2	5.2	0.95	ND*	ND*	ND*
24.38	ND*	ND*	ND*	0.18	8.55	0.73	0.2	7	0.94	ND*	ND*	ND*

* Not determined and D₅₀ in mm

4.2 Preparation of reconstituted laboratory sample

To acquire sufficient amount of soils for direct shear and triaxial tests, samples with similar grain size distribution curve, mean grain size (D₅₀) and fines content (f_c) were selected to be mixed together to prepare reconstituted samples for direct shear and triaxial tests. Mixing was carried out by carefully stirring small portions of the selected samples together until all soil was mixed homogeneously. After mixing the sample was stored in an air-tight plastic box and handled carefully to avoid any significant loss of sample.

4.3 Direct shear test

A total of 36 direct shear (DS) tests, with three tests at each stress level, were carried out on reconstituted specimens at different relative densities varying from 42% to 70% and different effective stresses varying from 25 kPa to 200 kPa. The selected test stresses and relative densities were considered equivalent to field conditions at depths of 6 m, 12 m and 18 m. Specimen relative densities were back calculated from SPT N-values in different boreholes at that depth by using N-value versus relative density relationship proposed by Meyerhof (1956). First, the amount of dry samples required to prepare the specimens at desired density were calculated. After taking required amount of dry sample in a container, a measured amount of de-aired water was added to the soil to bring the soil moisture content of approximately 10 percent. Specimens were prepared in a shear mold with inside diameter of 63.5 mm and height of 25.4 mm by hand tamping method. All tests were performed on saturated samples. During the test, vertical displacement gage, shear load gage and horizontal displacement gage reading were recorded until the horizontal shear load peaks and then falls. Angle of internal friction was calculated in a plot of maximum shear stress versus corresponding normal stress.

4.4 Triaxial test

A total of 36 consolidated undrained triaxial tests (TX), with three tests at each stress level, were carried out on reconstituted specimens. The effective stresses and relative densities for triaxial tests were the same as the direct shear tests. Cylindrical soil specimens of 142 mm height and 71 mm diameter were used and prepared using wet tamping technique. The specimens were first saturated with back-pressure saturation until the pore pressure parameter reaches a value equal to 0.90. Following saturation, the specimens were then isotropically consolidated at the desired effective stress. To cause shear failure in the specimen, deviator

stress was applied to the specimen until the maximum axial deformation reaches to a value of 15%. The deviator stress was applied at a rate of 0.08 percent/min. During the test, deviator stress, shear stress, normal stress and pore water pressure was recorded at every 10 sec interval. Angle of internal friction was calculated by plotting effective-stress Mohr's circles for various tests (three tests at each depth) and drawing a common tangent to these Mohr's circles passing through the origin. The effective angle of internal friction obtained from direct shear and triaxial tests are given in Table 2.

Table 2. Effective angle of internal friction calculated from direct shear and triaxial tests.

Depth	Direct shear tests				Triaxial tests			
	Borehole-01	Borehole-02	Borehole-03	Borehole-04	Borehole-01	Borehole-02	Borehole-03	Borehole-04
m	ϕ	ϕ	ϕ	ϕ	ϕ	ϕ	ϕ	ϕ
6	31.8	28.81	28.81	31.38	32.5	31.8	31.5	33.5
12	33.82	32.21	34.22	33.02	37	35	35.5	35
18	40.03	34.21	36.87	35	38.5	37	36.5	36

5 RESULTS AND DISCUSSIONS

Based on the most commonly used CPT, SPT and soil parameter relationships, several calculated and correlated soil parameters were determined as part of the data interpretation and to check the applicability of existing correlations to the local soils. A total of 51 data points for the sand deposits from the 4 boreholes presented in Table 1 were selected for this study to perform comparative analysis with mean grain size (D_{50}) and percent finer (fc) based CPT-SPT correlations. Calibrations were performed on recorded cone tip resistance data to eliminate pore pressure effect on tip resistance by a calibration factor of 0.32, as provided by the cone manufacturer. Furthermore, the normalized cone tip resistance (q_{t1}) was calculated foreffective overburden stress level as proposed byJamiołkowski et al. (2001) and Kulhawy and Mayne (1990). The SPT energy corrections and overburden pressure corrections were applied to the recorded field N-values to calculate $(N_1)_{60}$. The assumed energy level was 60 % for energy correction and soil unit weight was calculated from the SPTN-value versus soil unit weight correlation proposed by Bowles (1982)to normalize N-value. Both the CPT and SPT data presented in this study are normalized for overburden stress. If overburden corrections on cone tip resistance (q_c) and N-values would not have been made, the ratio of q_c/N is more deviated from the average line presented in correlations. It should be noted that, in this study the same CPT equipment and SPT rig were used in all tests to minimize inherent test variability.

Mean grain size (D_{50}) based correlations illustrated by Robertson et al. (1983) and Kulhawy and Mayne (1990) are presented in

Figure 2. The data sets selected for this study are than plotted on the same figure to evaluate the applicability of these correlations to the local soils. A significant scatter in the data can be seen around the average correlation curves of these two correlations. It can also be observed that with a small change in D_{50} can cause significant change in $q_{t1}/(N_1)_{60}$ ratio and most of the cases $q_{t1}/(N_1)_{60}$ ratio decreases with increasing D_{50} ,whichis somewhat contradictory to the existing correlations. Furthermore, no general trend can be observed in the plotted data with the change in D_{50} suggesting poor applicability of these correlations to the local soils.

The fines content correlation proposed by Chin et al. (1988) and Kulhawy and Mayne (1990) are presented in Figure 3 along with collected data sets of this study. The collected data sets showed a poor fit to the fines content based correlations and cannot substantiate a general trend between fines content and $q_{t1}/(N_1)_{60}$ ratio. From the plotted data it can also be noted that the $q_{t1}/(N_1)_{60}$ ratio increased with increasing fines content, which is quite contradictory to the existing correlations. In a similar fashion, fines content based correlations also indicate poor applicability to the study soils.

The data scatter in compared results may be due to the inherent variability of the two penetration tests and inaccuracy of overburden calculation during N-value correction. Besides soil structure, site geology or changes in subsurface conditions some of the inconsistency may be due to the somewhat large distance between the SPT and CPT locations. Figure 4 compares the measured data from Jamuna with the single value of $q_{t1}/(N_1)_{60}$ ratio of 0.45 suggested by Elbanna et al. (2011) for sands. The data set from this study shows good agreement and clusters together around the average relationship. However, the plotted data shows a slightly higher value than the average value of 0.45, but it is surprising that this relationship shows a general trend and less scatter plot relative to previous comparisons. It is believed that the correlation between normalized cone tip resistance (q_{t1}) and normalized SPT $(N_1)_{60}$ can serve as a better relationship for these sandy soils. The main advantage of this relationship is that it can be used in the absence gradation results. Therefore, it is a need to collect additional high quality CPT and SPT data to develop a better relationship.

The fundamental shear strength parameter of sands is the effective angle of internal friction. Therefore, an effort has been made to perform a comparative analysis between the angle of internal friction estimated from CPT, SPT, and those measured in direct shear (DS) and triaxial (TX) tests. In-situ effective angle of internal friction were calculated from established correlations given by Robertson and Campanella (1983) and Meyerhof (1956) for CPT and SPT tests. Laboratory friction angles were estimated from consolidated undrained triaxial and direct shear tests on reconstituted soil specimens at the estimated in-situ relative densities. The effective angle of internal friction values estimated from CPT and SPT tests and those obtained from laboratory triaxial and direct shear tests are presented in Figure 5. From Figure 5 it can be seen that ϕ value obtained from laboratory triaxial and direct shear test place within a narrow range and compared well with each other and increased with increasing depth. The ϕ value calculated from CPT and SPT data shows no general trend and represents higher value at smaller depth and lower value at greater depth than those obtained from direct shear and triaxial tests.

6 SUMMARY AND CONCLUSIONS

This paper presents the applicability of various existing correlations between CPT and SPT for local soils. It was observed that the CPT and SPT data used for this study better suit with $(q_{t1}/N_1)_{60}$ ratio of 0.45. Except that, results of this study considerably vary from existing laboratory dependent CPT-SPT correlations and indicating that most of these existing correlations are poorly applicable to the local soils. Therefore, it would be significant value to established reliable correlations based on locally available soils. General speaking, available established correlations provide a good framework to start with, but the direct application of the average curve in engineering practice may lead to significant deviation. Unfortunately it is true that, only selected data sets were used which place relatively narrow range to develop most of the prominent correlations. Thus, it is need to further investigation by accumulating large amount of high quality data from various soils types, ranging from clay to gravelly sand.

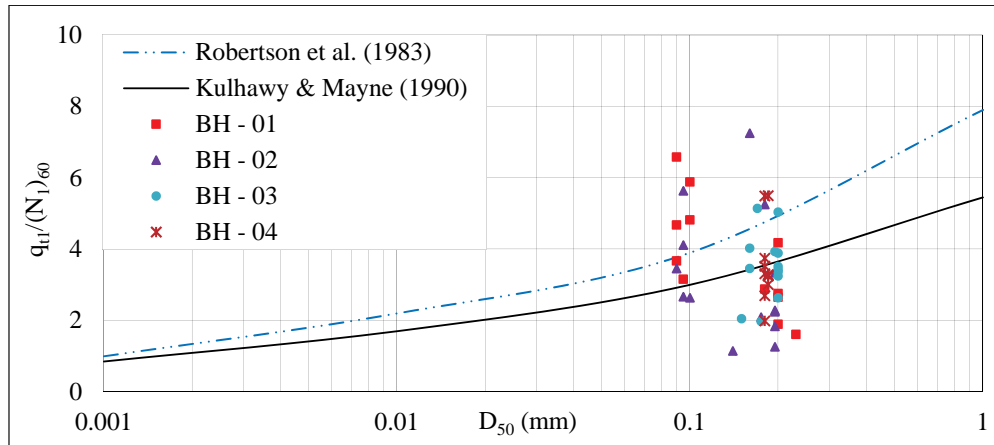


Figure 2. Variation of the ratio $q_{t1}/(N_1)_{60}$ with mean grain size (D_{50}) comparison.

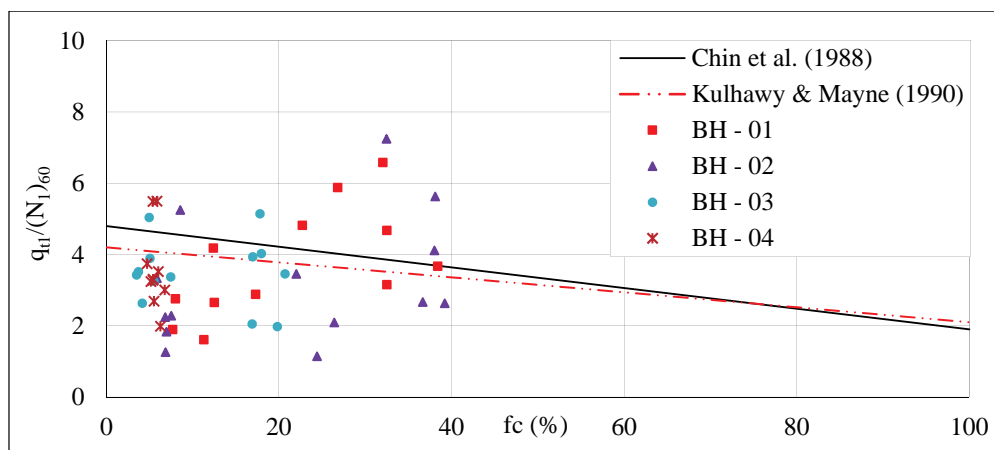


Figure 3. Variation of the ratio $q_{t1}/(N_1)_{60}$ with fines content (f_c) comparison.

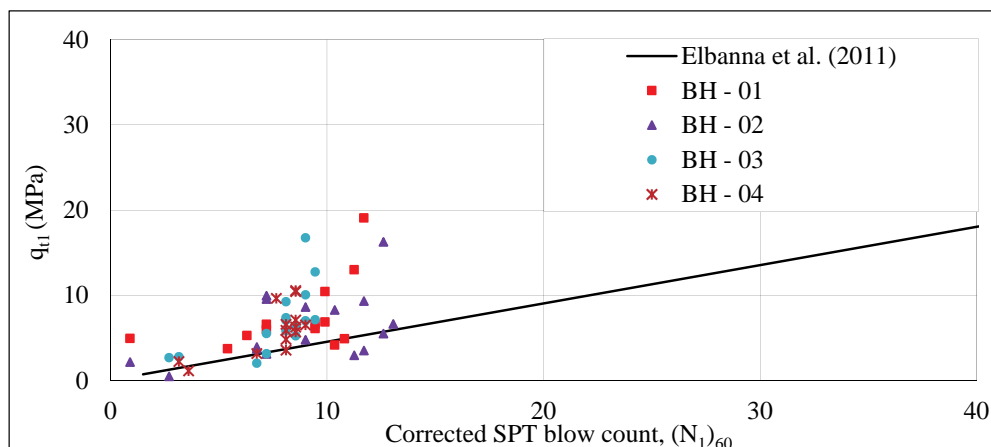


Figure 4. Variation of normalized cone tip resistance (q_{t1}) with normalized SPT blow count $(N_1)_{60}$ comparison.

7 SUMMARY AND CONCLUSIONS

This paper presents the applicability of various existing correlations between CPT and SPT for local soils. It was observed that the CPT and SPT data used for this study better suit with $(q_{t1}/N_1)_{60}$ ratio of 0.45. Except that, results of this study considerably vary from existing laboratory dependent CPT-SPT correlations and indicating that most of these existing correlations are poorly applicable to the local soils. Therefore, it would be significant value to established reliable correlations based on locally available soils. General speaking, available established correlations provide a good framework to start with, but the direct application of the average curve in engineering practice may lead to significant deviation. Unfortunately it is true that, only selected data sets were used which place relatively narrow range to develop most of the prominent correlations. Thus, it is need to further investigation by accumulating large amount of high quality data from various soils types, ranging from clay to gravelly sand.

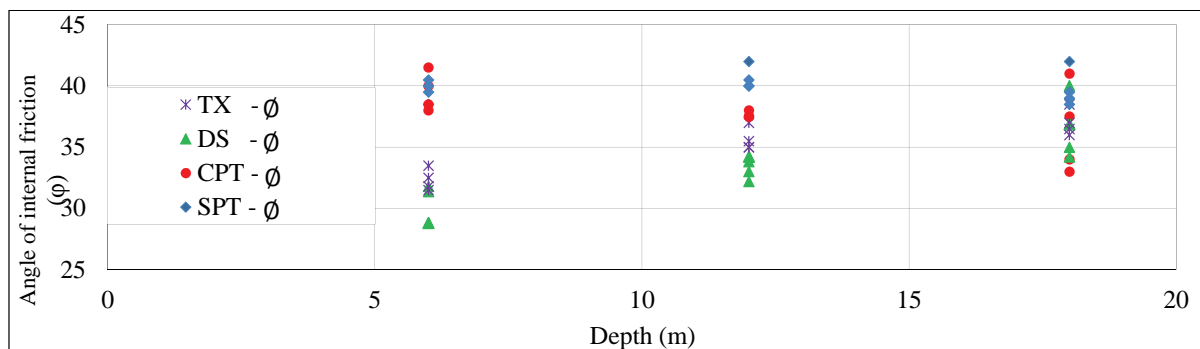


Figure 5. Comparative analysis of effective friction angle calculated from SPT, CPT, DS and TX tests.

8 REFERENCES

- Alam, M.K. Hasan, S.A.K.M. Khan, M.R. and Whitney, J.W. 1990. Geological Map of Bangladesh. Dhaka: Geological Survey of Bangladesh.
- Bowles, J.E. (3rd ed.) 1982. Foundation Analysis and Design. New York: McGraw-Hill.
- Chin, C.T. Duann, S.W. & Kao, T.C. 1988. SPT-CPT correlations for granular soils. *Proc. 1st international symposium on cone penetration testing*. Orlando, USA. (1): 335-339.
- Elbanna, M. Quinn, J. & Martens, S. 2011. SPT-CPT correlations for oil sand tailings sand. *Proc. Tailings and Mine Waste*, Vancouver, BC, 6-9 November 2011.
- Elkateb, T.M. & Ali H.E. 2010. CPT-SPT correlations for calcareous sand in the Persian Gulf Area. *2nd international symposium on cone penetration testing*, CPT'10, California, USA, Paper N0. 2-13.
- Jamiolkowski, M. Baldi, G. Bellotti, R. Ghionna, V. & Pasqualini, E. 1985. Penetration resistance and liquefaction of sands. *Proc. 11th international conference on soil mechanics and foundation engineering*, San Francisco, (4): 1891-1896.
- Jamiolkowski, M., Lo Presti, D.C.F. & Manassero, M. 2001. Evaluation of Relative Density and Shear Strength of Sands from Cone Penetration Test and Flat Dilatometer Test. *Soil Behavior and Soft Ground Construction (GSP119)*, ASCE, Reston, Virginia, pp. 201-238.
- Kasim, A. Chu, M. & Jensen, C. 1986. Field Correlation of Cone and Standard Penetration Tests. *J. Geotech. Engrg.*, 112(3): 368-372.
- Kulhawy, F.H. & Mayne, P.W. 1990. Manual on estimating soil properties for foundation design. New York: Electric Power Research Inst., Geotechnical Engineering Group, (EPRI-EL-6800): 2-28 to 2-36.
- McNulty, G. & Harney, M. D. 2010. Comparison of CPT and DMT-correlated effective friction angle in clayey and silty sands. *2nd international symposium on cone penetration testing*, CPT'10, California, USA, Paper ID 2-53.
- Meyerhof, G.G. 1956. Penetration tests and bearing capacity of cohesionless soils. *Proc. SM1*, (82): 1-19.
- Muromachi, T. 1981. Cone penetration testing in Japan, cone penetration testing and experience: In G.M. Norris and R.D. Holtz (eds), *ASCE*, New York, 49-75.

- Robertson, P.K. Campanella, R.G. & Wightman, A. 1983.SPT-CPT Correlations. *J. Geotech. Engrg.*, 109(11): 1449-1459.
- Robertson, P.K.&Campanella, R.G.1985.Liquefaction Potential of Sands Using the CPT. *J. Geotech.Engrg.*, 111(3): 384-403.
- Robertson, P.K.&Campanella, R. G. 1983.Interpretation of cone penetration tests. Part I: Sand. *Canadian Geotechnical Journal*. 20(4): 718-733.
- Schmertmann,J.H. 1975. Measurement of in-situ shear strength. In ASCE Specialty Conference on In-Situ Measurement of Soil Properties. (2): 57-138.



PART-X

SLOPE STABILITY ANALYSIS OF AN EMBANKMENT AT JAMUNA RIVER

**BANGLADESH NETWORK OFFICE FOR
URBAN SAFETY (BNUS), BUET, DHAKA**

Prepared By: Nuzhat Fatema

Mehedi Ahmed Ansary

ABSTRACT

A study on Slope Stability Analysis of an embankment has been carried out considering different slopes at different conditions. For this purpose embankment soil has been collected from Basuria in Sirajganj near the bank of Jamuna River. Grain size analysis of the sample reveals that it contains 63% sand, 35% silt and 2% clay. The cohesion and angle of internal friction are found to be 7 kPa and 21° respectively from shear test. For the parametric study, shear strength parameters have been modified to be 10 kPa; 14° and 20 kPa; 12°. Based on the results of soil investigations, stability analysis using STB2010 at some conditions (dry, high flood level, low flood level and rapid drawdown with slope 1:1, 1:1.5 and 1:2) of the embankment has been performed. It has been found that the safety factor decreases with steep slope while increasing with flatter one. The maximum safety factor has been found 2.255 for soil at dry condition with a slope 1:2 while the minimum factor is 0.66 at rapid drawdown condition with 1:1 slope. The soil having minimum factor possesses very bad condition which needs to be protected with a conventional design solution, Revetment Design.

Keywords: *Embankment, shear strength, Slope Stability*

1. Introduction

Over the last few decades, nearly 13000 km of flood and river embankments have been repaired in Bangladesh (Hossain, M.Z. and Sakai, T., 2011). But, earthen embankments in Bangladesh are facing problems like erosion, breaching in every year. The major causes of failure identified were breach of the embankment cutting by the public, overflow, erosion, seepage and sliding. Furthermore, insufficient supervision during construction results in poor-quality earthworks with the use of inappropriate soil materials, insufficient or no clod breaking, inadequate compaction and or insufficient laying of topsoil layers, the use of inferior materials, inadequate maintenance, river migration and cutting by the public (Hoque and Siddique, 1995). The stability of earthen embankments is influenced by seepage occurred during the increase and decrease of the adjacent water level in the river or reservoir (Morii and Kunio, 1993). In Bangladesh, nearly 4,600 km of embankments along the bank of big rivers are flowing across the country. JAMUNA, one of the big rivers is flowing alongside of Sirajganj district of Bangladesh (Figure 1). At 41 locations of its bank, the length of failure occurring is about 160.62km.

The concept of stability is one of the most important issues in Civil Engineering field. Stability concept comprises some of the important factors in Civil Engineering namely: force, moment and equilibrium. The factors contributing to the slope stability include: the type of soil, geometry of the cross-section of the slope, weight, loads and load distribution, gravity, increase in moisture content of the soil material, decrease in shear strength of soil, vibrations and earthquakes, due to human action like excavation, undercutting and overloading. Revetment Design is the most conventional and gratifying solution for river bank protection (<http://www.kennisbank-waterbouw.nl/DesignCodes/rockmanual/chapter%208.pdf>). Revetments are used to protect banks and shorelines from erosion caused by waves and currents. It is assumed to be easily accessible for Bangladesh. Revetment design using concrete block is considered to be economical rather than using other materials. Articulating concrete blocks (ACBs) are designed to provide stability and erosion control in a wide variety of hydraulic applications. Made on dry cast block machines, the individual units are engineered to capitalize on the weight of concrete, friction between units, and the interconnection of units into flexible mattresses. Flexibility between units is provided to allow the mat to conform to minor deformations in the sub grade. Classes of individual units can be produced at varying thicknesses, providing the designer flexibility in selecting appropriate levels of protection. The range of block classes allows selection of the proper combination of unit weight, surface roughness, and open area for hydraulic stability. For example, an Armor Flex armor unit, shown in Figure 2, is substantially rectangular, having a flat bottom to distribute the weight evenly over the sub grade.

As Slope stability is influenced by physical features of the embankment, for different types of embankment and embankment geometry many comprehensive studies have been conducted in the developed countries and reported in their research reports (Flate and Preber, 1974; Mesri et al, 1994; Olson 1998). This paper is aimed to determine the stability and settlement characteristics of Jamuna embankment at selected conditions. It presents a study on the investigation of physical and mechanical properties of Jamuna river embankment materials located at Basuria in Sirajganj district of Bangladesh. Attempt has also been made to evaluate the existing design methodology for embankment stability analysis through a case study.

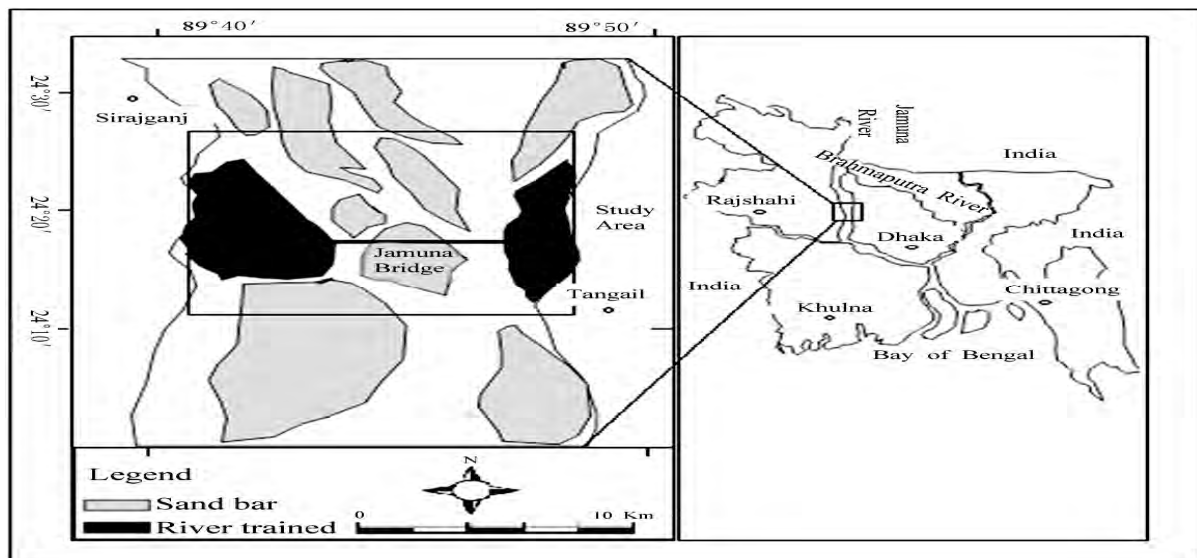


Figure 1: Location map of the study area.

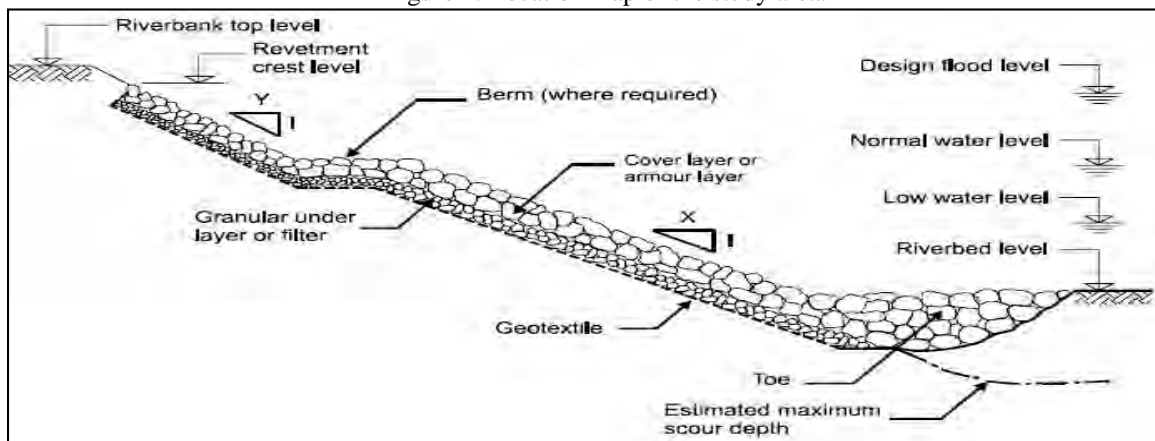


Figure 2: Components of typical armor stone revetment.

2. GEOLOGY OF THE STUDY AREA

The study Jamuna River in 1787 a tectonic movement followed by an abnormal flood led changes in the course of the Brahmaputra and started its flow through a new course known as the Jamuna (Bhuiyan, M.A.H., Rakib, M.A., Takashi, Rahman, M.J.J. and Suzuki, Shigeyuki, 2010). It is the main channel of the Brahmaputra River when it flows out of India into Bangladesh. Jamuna enters in Bangladesh from the North West side of Kurigram district and flows to south, ending its independent existence as it joins the Padma River near Goalundo Ghat. Bounding coordinates of the river area is W: 89.532, E: 89.871, N: 25.228, S: 23.869. The climate of the study area is tropical monsoon. Jamuna Bridge site is located between Tangail and Sirajganj town. It lies within latitude 24022'50"–24026'30"N and longitude 89055'30"–89058'45"E. The river reach is characterized by well defined braiding nature, meta-stable islands, nodes, sandbars, shifting ana-branches and rigorous bank erosion. Geomorphologically, the eastern bank is bounded with the lateral extension of Madhupur Tract and the west bank is the Barind Tract, which is composed of silty clay. During monsoon, the average annual discharge of Jamuna River (JR) at Ba-hadurabad point is about 50000 m³/s. However, the discharge increased to 100000 m³/s during the 1988 and 1998 flood events. The average water surface slope is approximately 6.5 cm/km for the lower reach.

The soil deposits mainly consist of the following types of soils: (after Geological Map of Bangladesh, GSB, 1990)

ASL – Alluvial Silt – Light to medium – grey, fine sandy to clayey silt. Commonly poorly stratified; average grain size decreases away from main channels. Chiefly deposited in flood basins and inter stream areas. Unit includes small back swamp deposits and varying amounts of thin, inter stratified sand, deposited during episodic or unusually large floods. Illite is the most abundant clay minerals.

Most areas are flooded annually. Included in this unit are thin veneers of sand spread by episodic large floods over flood – plain silts. Historic pottery, artifacts and charcoal (radiocarbon dated 500 – 6000 years B.P.) found in upper 4m.

3. SAMPLE COLLECTION AND LABORATORY TESTS

The soil samples were collected directly from the broken part of the right bank embankment of Jamuna River at Basuria in Sirajganj district. The field investigations consisted of drilling of boreholes, identification of subsoil layer, assessment of density and consistency of subsoil layers by carrying out Standard Penetration Test, collection of disturbed and undisturbed tube samples. One borehole was drilled at Basuria site on the bank of Jamuna River. Geologic profile of the subsoil is made from the bore log data at Basuria site. The soil overall the whole depth possesses non – plastic behavior. Silt with little clay, brown in color, having very loose density exists near the top of the ground surface extending to about 8 feet depth. The SPT – N value of this type of soil at the given depth is 1. Very fine sand with little silt trace mica is encountered just below the top clay layer having grey in color and non-plasticity behavior. It extends up to the final depth of boring 102 feet (30m) and possibly beyond. The density varies with depth such as loose density up to 28 feet depth, medium density up to 63 feet depth and dense density for the rest. At the layer up to 28 feet depth, the average SPT – N value is 3 while the range of SPT – N value is 15 – 25 up to 63 feet depth. Again SPT – N value up to 73 feet depth is 26 and up to 102 feet the range is 28 – 32 feet. Polythene bags have been used for the storage of sample for laboratory tests. The laboratory tests have been conducted in the Laboratory of Bangladesh University of Engineering And Technology. The testing procedures are in accordance with American Society for Testing and Materials (ASTM). The following tests were conducted in the laboratory in order to access the collected sample: Grain size analysis, Compaction test, Consolidated – Undrained Direct Shear test (CU test).

4. LABORATORY TEST RESULTS AND DISCUSSION

Figure 3 and 4 shows grain size distribution of sandy soil and moisture content vs.dry density relationship of sandy soil for Standard Proctor Compaction test respectively. Figure 5 and 6 show Shear stress vs. displacement curve and Shear stress vs. normal stress graph of soil ($c = 7$ kPa, $\phi = 21^\circ$) for Consolidated undrained direct shear test.

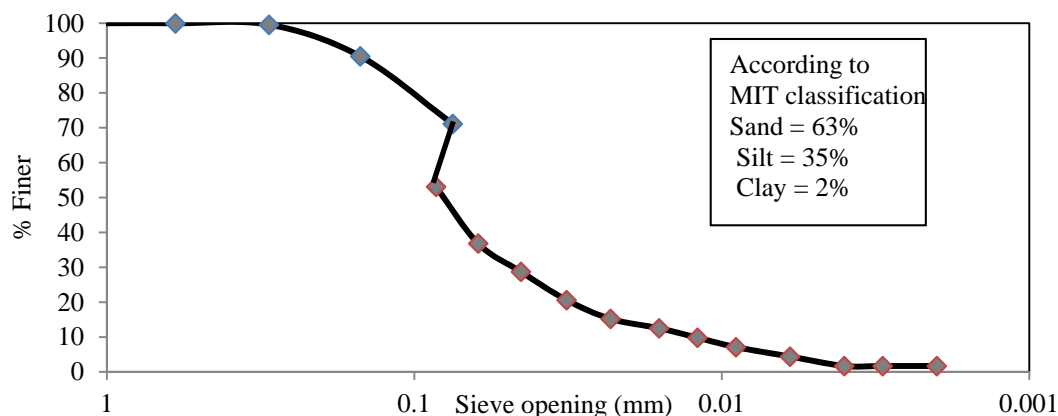


Figure 3: Grain size distribution of sandy soil.

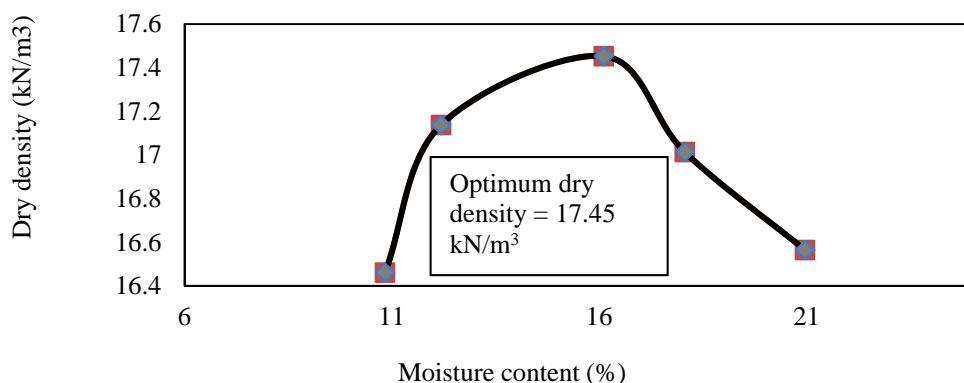


Figure 4: Moisture content vs.dry density relationship of sandy soil for Standard Proctor Compaction test.

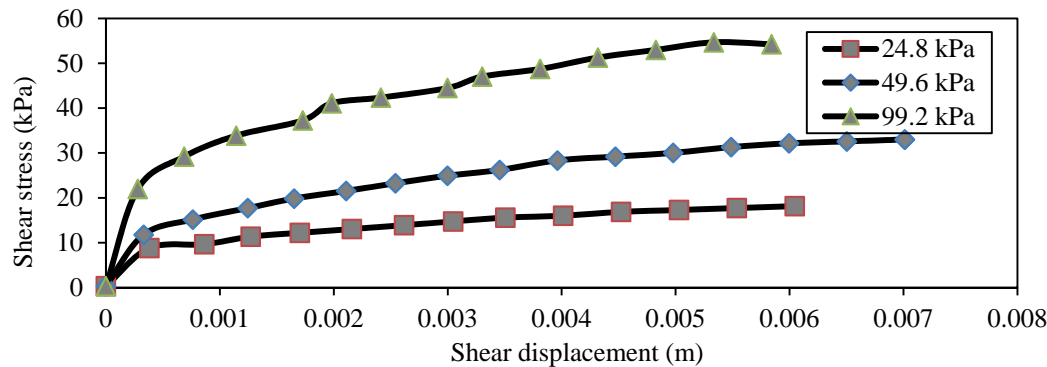


Figure 5: Shear stress vs. displacement curve for Consolidated undrained direct shear test of soil ($c = 7$ kPa, $\phi = 21^\circ$).

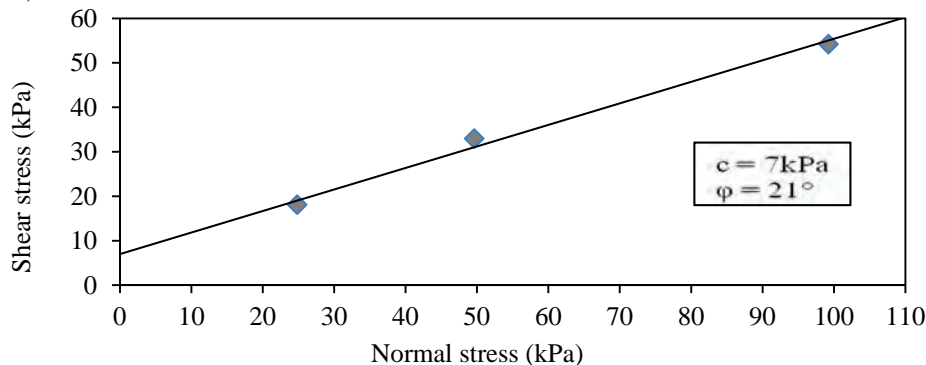


Figure 6: Shear stress vs. normal stress graph of soil ($c = 7$ kPa, $\phi = 21^\circ$)

According to MIT classification the percentage of sand, silt and clay at our soil sample have been found 63%, 35% and 2% respectively. Hence it can realize that the sample is not the pure sand. According To Unified Soil Classification system (USCS) the soil sample is SW-SM. It has a portion of silt and clay. From the shear test the values of cohesion and angle of internal friction have been obtained for sand. For further parametric study, shear strength parameters have been modified. Table 1 shows the values of cohesion and angle of internal friction of three types of soil obtained from Consolidated Undrained direct Shear Test.

Table 1
Results from Consolidated Undrained direct Shear Test

Soil sample	Cohesion, c (kN/m ²)	Angle of internal friction, ϕ (degree)
Type 1	7	21
Type 2	10	14
Type 3	20	12

From the table 1 we can analyze that cohesion is increasing with the increase of clay while angle of internal friction is decreasing along with it. The more the cohesion the more would be the presence of clay while the reverse case happens for angle of internal friction. The values of cohesion and angle of internal friction have been used in the stability analysis. The shear strength parameters of the underlying soils have been obtained using the existing correlation with SPT-N value shown in the bore logs.

5. SLOPE STABILITY ANALYSIS

Civil engineers are often expected to make calculations to check the safety of natural slopes, slopes of excavations, and compacted embankments. This check involves determining the shear stress developed along the most likely rupture surface and comparing it with shear strength of the soil. This process is called slope stability analysis. The most likely rupture surface is the critical surface that has the minimum factor of safety.

THE PROGRAM STB2010

This is a program for the analysis of the stability of slope (Verruijt, A., Delft University, 2010). The program uses Bishop's simplified method with some modifications introduced at GeoDelft and the Delft University for the calculation of the facto of safety of circular slip surface, with Koppejan's correction for very deep circles, and a modification to account for the strength reduction of a double sliding model. The program also allows for a possible horizontal body force, to simulate the effect of an earthquake. The soil properties used in the program are:

- W_d : Dry unit weight (kN/m³).
- W_s : Saturated unit weight (kN/m³).
- K_o : coefficient of neutral horizontal stress (-).
- c : Cohesion (kN/m²).
- ϕ : angle of internal friction (degrees).
- P/F: switch for the groundwater condition (-).
- $p = 0$: Zero level of the pore water pressure (m).
- cap: Thickness of capillary zone, above groundwater table (m).
- The unit weight of water is 10 kN/m³.

6. RESULTS OF STABILITY ANALYSIS USING STB2010

STB2010 is used for the analysis of stability of slope, using Bishop's method with some conditions. Figure 7 shows the results of Stability Analysis of soil ($c = 7$ kPa, $\phi = 21^\circ$) at one of the four conditions (dry condition) with slope 1:1.5.

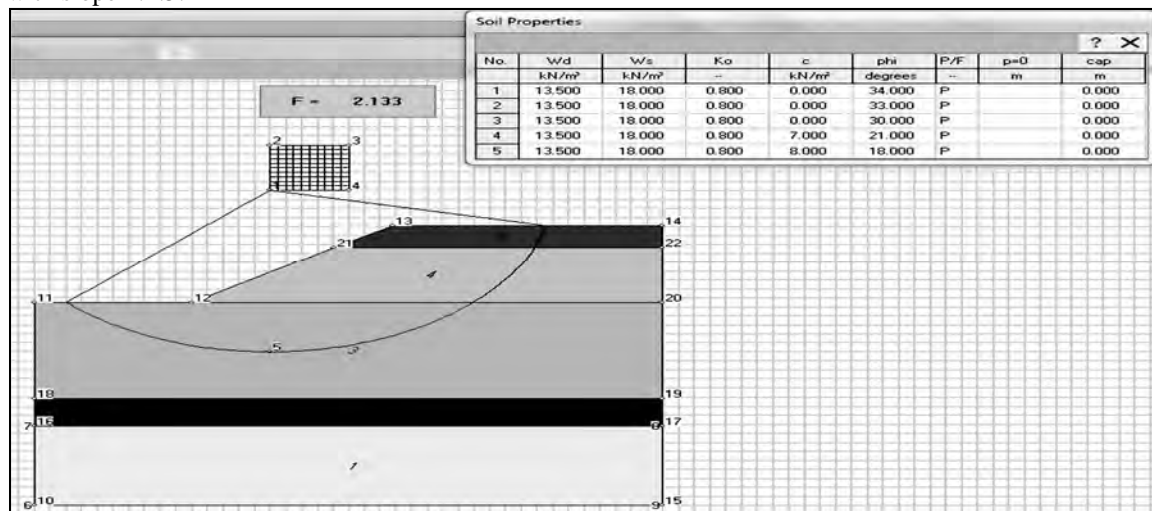


Figure 7: Result of stability analysis of soil ($c = 7$ kPa, $\phi = 21^\circ$) at dry condition for slope 1:1.5

The results obtained from the analysis using STB2010 are shown in Table 2 to 4. The fluctuation of the safety factor along with four conditions and three slopes for the soils having different parametric characteristics has been shown in Figure 8 to 10. From the figures for all kinds of soil, it has been realized that the safety factor increases with the increase of water due to seepage into the soil. But at rapid drawdown condition the safety factors have been found to be least among all conditions. It causes due to rapid reduction of external water level. Figure 11 and 12 show the variation of safety factors at high flood level and rapid drawdown condition for different soil condition respectively.

Table 2
Results of Stability Analysis of Soil Sample Type 1 ($c = 7$ kPa, $\phi = 21^\circ$)

Slope	Dry Condition	Low flood Level Condition	High flood Level Condition	Rapid drawdown
1:1	1.536	1.244	0.904	0.66
1:1.5	2.133	1.634	1.508	0.963
1:2	2.255	1.669	1.478	0.986

Table 3
Results of Stability Analysis of Soil Sample Type 2 ($c = 10$ kPa, $\phi = 14^\circ$)

Slope	Dry Condition	Low flood Level Condition	High flood Level Condition	Rapid drawdown
1:1	1.477	1.206	0.916	0.672
1:1.5	2.092	1.594	1.485	0.953
1:2	2.213	1.626	1.461	0.984

Table 4
Results of Stability Analysis of Soil Sample Type 3 ($c = 20$ kPa, $\phi = 12^\circ$)

Slope	Dry Condition	Low flood Level Condition	High flood Level Condition	Rapid drawdown
1:1	1.581	1.305	0.841	0.6
1:1.5	2.162	1.66	1.576	1.02
1:2	2.284	1.692	1.554	1.054

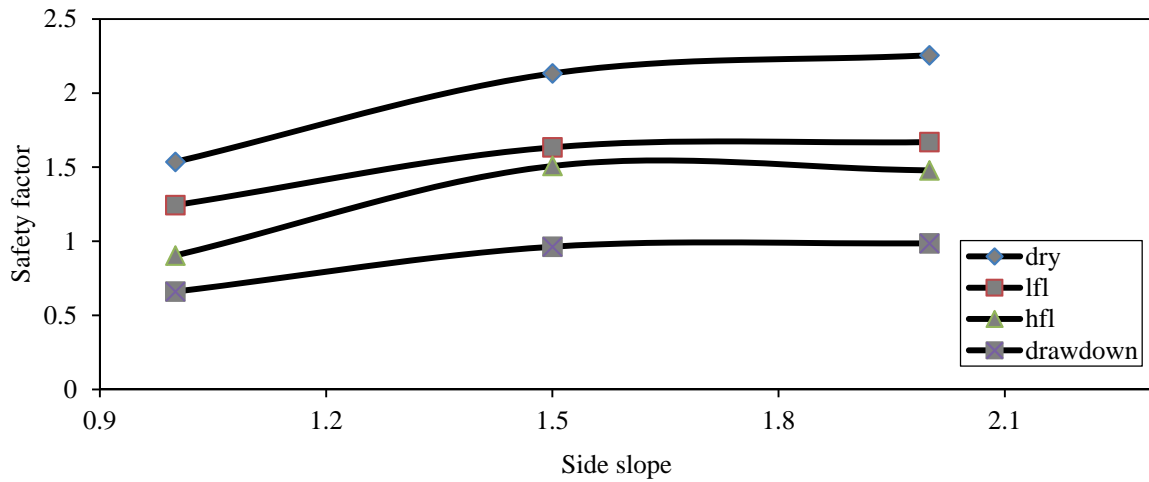


Figure 8: Comparison on three conditions with three slopes for soil sample Type 1 ($c = 7$ kPa, $\phi = 21^\circ$)

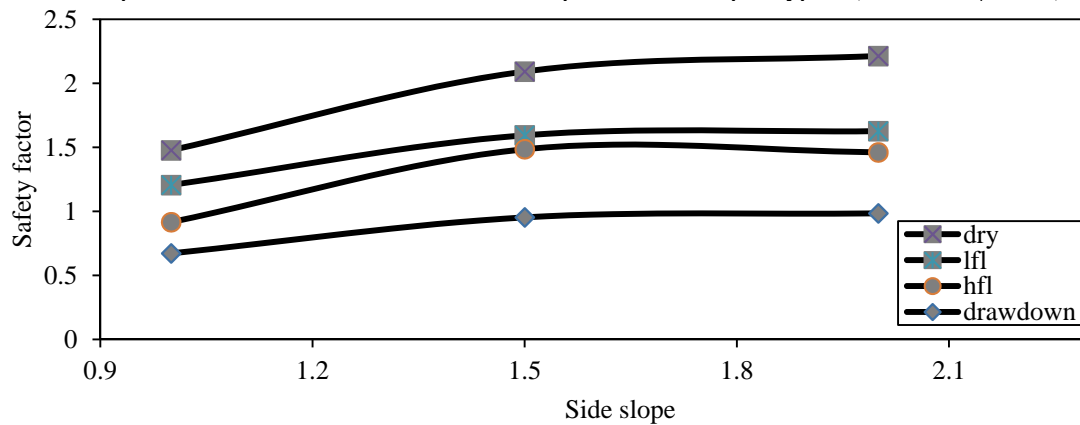


Figure 9: Comparison on three conditions with three slopes for soil sample type 2 ($c = 10$ kPa, $\phi = 14^\circ$)

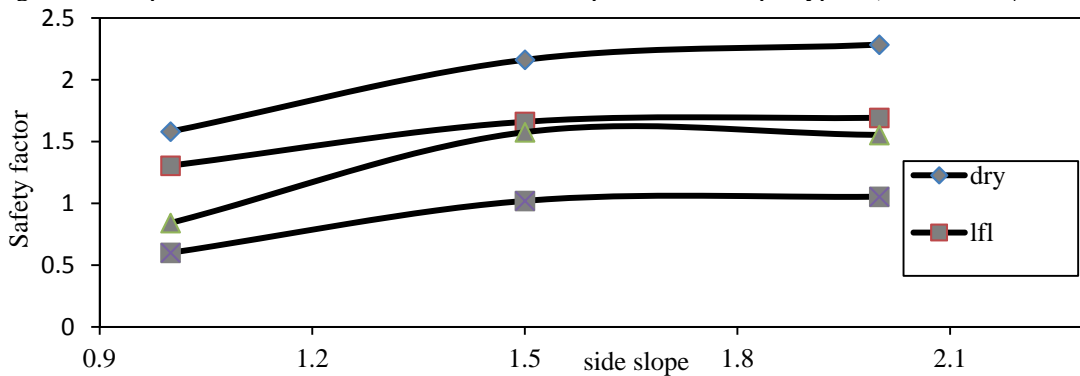


Figure 10: Comparison on three conditions with three slopes for soil sample Type 3 ($c = 20$ kPa, $\phi = 12^\circ$)

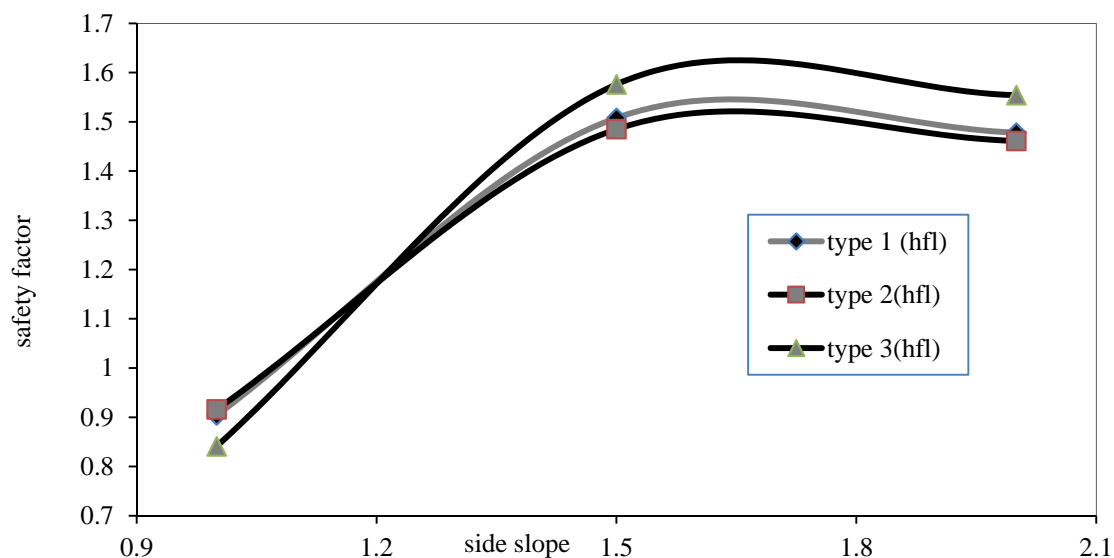


Figure 11: Variation of safety factor for different soil condition at high flood level condition.

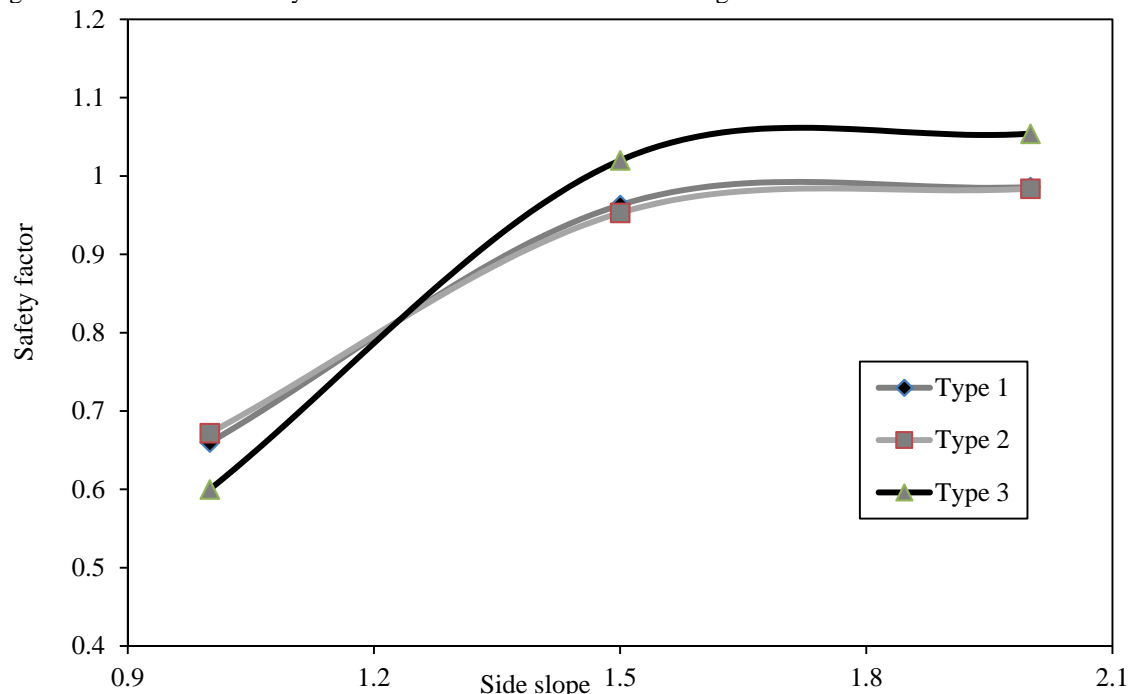


Figure 12: Variation of safety factor for different soil condition at rapid drawdown condition.

After analysis the safety factors for all types of soil at high flood level condition with slope 1:1 and at rapid drawdown for all three slopes have been found to be lower than the minimum recommended factor 1.2. So a typical design is needed to ensure the strength of soil. Revetment design is the most beneficial and affordable solution for Bangladesh. Using concrete block is considered to be efficient for Revetment design.

In the revetment design, concrete blocks are given in one or two layers, sometimes it extends to three, four or five layers either along with or without geotextile layer. It depends on the range of safety factor that is to be increased. From Stability analysis using STB2010, the safety factors for high flood level condition at slope 1:1 and rapid drawdown with three slopes for all categories of soil have been found to be below the minimum recommended value 1.2. So the revetment design has been performed here to raise the strength of soil. For the design, first a thin layer of geotextile has been given of 15 cm thickness. Then a layer is given with 45 cm * 45 cm concrete block. For the total layer including concrete block and geotextile, the unit weight would be the sum of $\gamma * h$ of both two materials. If the unit weight of concrete and geotextiles are 23.57 kN/m³ (150 pcf) and 16 kN/m³ (102 pcf) respectively then the total unit weight 13 kN/m² ($\gamma * h$) for 1 m strip would be counted for one layer in the design. When it is of two layers then the unit weight would be 23.5 kN/m³ by adding extra unit weight of 2nd layer concrete block. The value of unit weight increases with the increase of concrete block layer adding 10.5 for each layer. Again it causes huge cost while increasing block layer one by one. As it costs much to layer the embankment overall with uniform concrete block, we can differ in placing the block layer

depending on the satisfaction of safety factor. For sandy soil, four layers of concrete block have been placed at the bottom through toe up to the middle of the slope while two layers have been placed from middle up to the top of the embankment due to make the design economical. Table 5 shows the safety factor for different soil conditions at high flood level. For type 1 ($c = 7 \text{ kPa}$, $\phi = 21^\circ$), four layers for high flood level condition have been placed at the bottom through toe up to the middle of the slope while two layers have been placed from middle up to the top of the embankment. For type 2 ($c = 10 \text{ kPa}$, $\phi = 14^\circ$) four layers have been placed uniformly across the embankment for high flood level condition. For type 3 ($c = 20 \text{ kPa}$, $\phi = 12^\circ$), four layers have been placed at the bottom through toe up to the middle of the slope while one layer has been placed from middle up to the top of the embankment for high flood level condition. Again for rapid drawdown condition, the distribution of block layers along with obtained safety factors have been given in table 6. The distribution of block layers is on the basis of making the design economical. Figure 13 shows the slope of an embankment indicating bottom and top. Table 7 shows the variation of safety factor for Type 1 ($c = 7 \text{ kPa}$, $\phi = 21^\circ$) depending on the distribution of concrete block layers. Safety factor has been found to be 1.198 for placing 4 layers at the bottom through toe up to the middle of the slope and 1 layer from the middle up to the top of the embankment. But it doesn't satisfy the condition. So 2 layers have been placed instead of 1 layer from the middle up to the top and the safety factor has been found to be 1.208. Table 8 shows the variation of safety factor for Type 2 ($c = 10 \text{ kPa}$, $\phi = 14^\circ$) depending on the distribution of concrete block layers. Safety factor has been found to be 1.204 for placing 4 layers uniformly across the embankment.

Table 9 shows the variation of safety factor for Type 3 ($c = 20 \text{ kPa}$, $\phi = 12^\circ$) depending on the distribution of concrete block layers. Safety factor has been found to be 1.288 for placing 4 layers at the bottom through toe up to the middle of the slope and 1 layer from the middle up to the top of the embankment which satisfies the condition. The variation of safety factor for different parametric soil at high flood level condition has been shown in figure 14 to 16.

Table 5
Results of Revetment Design at high flood Level condition.

Embankment Soil Properties	Factor of safety
$c = 7 \text{ kPa}$, $\phi = 21^\circ$	1.208
$c = 10 \text{ kPa}$, $\phi = 14^\circ$	1.204
$c = 20 \text{ kPa}$, $\phi = 12^\circ$	1.288

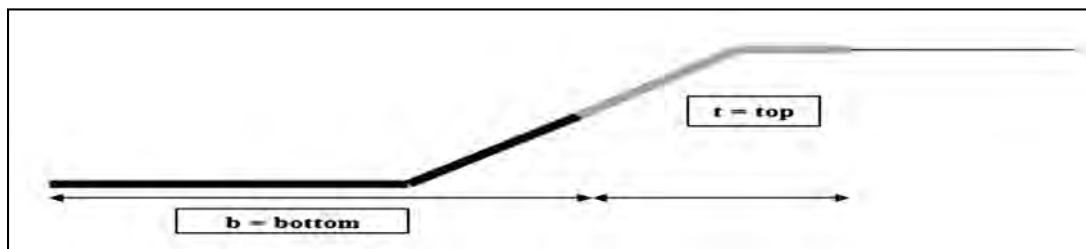


Figure 13: Slope of an embankment

Table 6
Results of Revetment Design at Rapid drawdown condition.

slope	$c = 7 \text{ kPa}$, $\phi = 21^\circ$	$c = 10 \text{ kPa}$, $\phi = 14^\circ$	$c = 20 \text{ kPa}$, $\phi = 12^\circ$
1:1	1.201 (7b+1top)	1.200(7b+2top)	1.213 (6b+1top)
1:1.5	1.214 (3b+1top)	1.208 (3b+1top)	1.273(3b+1top)
1:2	1.276 (3b+1top)	1.268 (3b+1top)	1.213(1b+1top)

Table 7
Variation of safety factor of Type1($c = 7 \text{ kPa}$, $\phi = 21^\circ$) soil

Layer 1	safety factor	Layer 2	safety factor	Layer 3	safety factor	Layer 4	safety factor
1b + 1t	0.968	2b + 1t	1.043	3b + 1t	1.12	4b + 1t	1.198
1b + 2t	0.981	2b + 2t	1.055	3b + 2t	1.131	4b + 2t	1.208
1b + 3t	0.994	2b + 3t	1.067	3b + 3t	1.141	4b + 3t	1.218
1b + 4t	1.006	2b + 4t	1.078	3b + 4t	1.151	4b + 4t	1.227

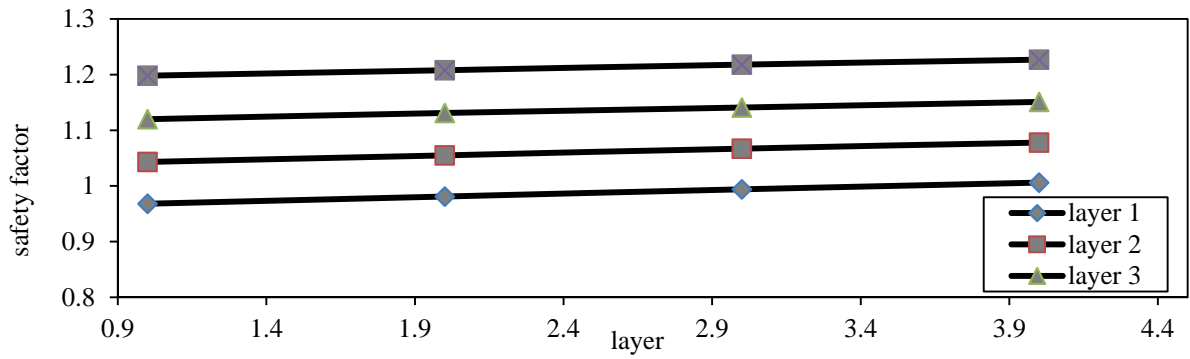
Figure 14: Safety factor vs. layer graph for Type1($c = 7$ kPa, $\phi = 21^\circ$) soil.

Table 8

Variation of safety factor of Type2($c = 10$ kPa, $\phi = 14^\circ$) soil

Layer 1	safety factor	Layer 2	safety factor	Layer 3	safety factor	Layer 4	safety factor
1b + 1t	0.951	2b + 1t	1.024	3b + 1t	1.098	4b + 1t	1.175
1b + 2t	0.964	2b + 2t	1.036	3b + 2t	1.109	4b + 2t	1.185
1b + 3t	0.976	2b + 3t	1.0477	3b + 3t	1.12	4b + 3t	1.195
1b + 4t	0.988	2b + 4t	1.058	3b + 4t	1.131	4b + 4t	1.204

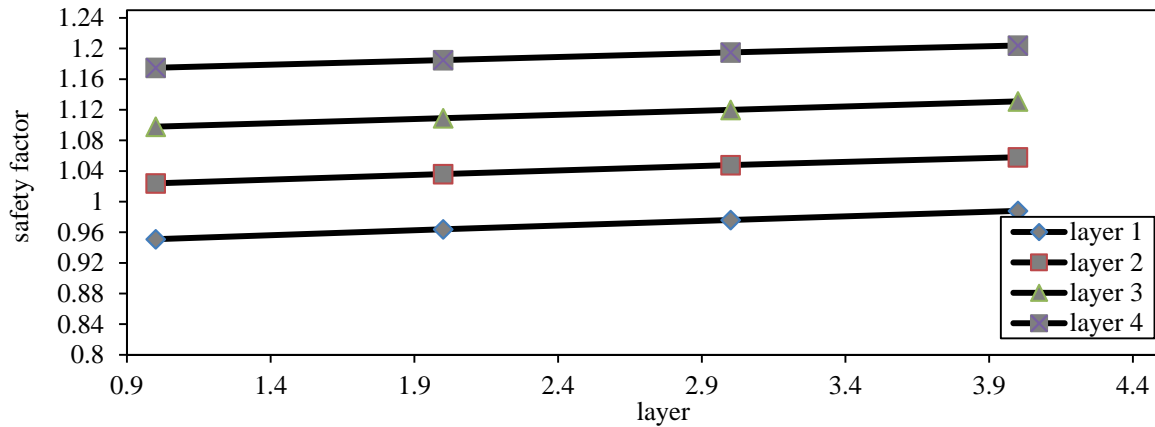
Figure 15: Safety factor vs. layer graph for Type2 ($c = 10$ kPa, $\phi = 14^\circ$) soil.

Table 9

Variation of safety factor of Type3($c = 20$ kPa, $\phi = 12^\circ$) soil

Layer 1	safety factor	Layer 2	safety factor	Layer 3	safety factor	Layer 4	safety factor
1b + 1t	1.059	2b + 1t	1.134	3b + 1t	1.21	4b + 1t	1.288
1b + 2t	1.071	2b + 2t	1.144	3b + 2t	1.219	4b + 2t	1.296
1b + 3t	1.082	2b + 3t	1.154	3b + 3t	1.228	4b + 3t	1.304
1b + 4t	1.092	2b + 4t	1.164	3b + 4t	1.237	4b + 4t	1.312

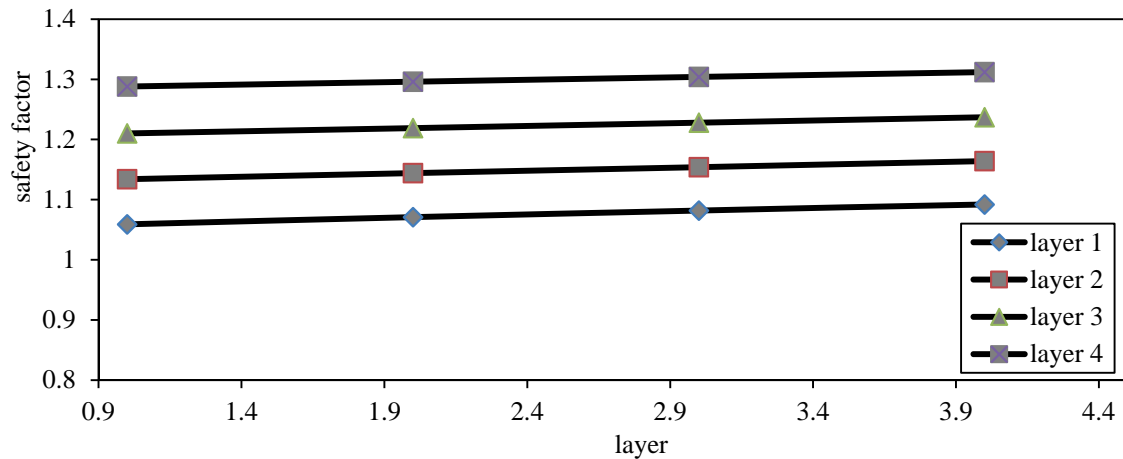


Figure 16: Safety factor vs. layer graph for Type 3 ($c = 20$ kPa, $\phi = 12^\circ$) soil.

After Revetment Design the conditions are satisfied for the soil samples at high flood level and rapid drawdown conditions. For all cases, the safety factors are above the recommended value (1.2). These values have ensured the shear strength of soil along with the protection of river embankment. The soil having better safety factors are assumed to be more protective from erosion. After the design, the number of layers at rapid drawdown has been found to be greater in quantity than high flood level condition. But in practice, rarely rapid drawdown condition is considered, so the number of layers used is minimum.

7. CONCLUSION

This research has been carried out to investigate the geotechnical characteristics of the embankment and presented results of more recent soil investigation along the embankment alignment. For this purpose embankment soil has been collected from Basuria in Sirajganj near the bank of Jamuna River. Also field bore logs has been done up to a depth of 30 m. Direct from the broken part of the embankment, the soil samples are collected by which the following laboratory tests: Grain Size Analysis, Compaction Test, Shear Test have been performed.

The collected sample contains 63% sand, 35 % silt and 2% clay. According to the Unified Soil Classification System (USCS), the soil sample is SW – SM.

With a view to making a remolded sample to obtain the shear strength parameters of the collected disturbed sample of the embankment, a Standard Proctor Compaction test has been conducted in the laboratory. The remolded sample has been made with the corresponding water content of 95% peak value of the dry density at wet side. The optimum dry density has been found to be 17.45 kN/m^3 .

Due to obtain the shear strength parameters, Consolidated Undrained Shear test has been performed in the laboratory. The cohesion and angle of internal friction has been found to be 7 kPa and 21° respectively. For further parametric study, Shear strength parameters has been modified to be 10 kPa; 14° and 20 kPa; 12° . The parameters of the soil sample of the embankment have been found directly from the laboratory tests, while for the underlying soils the shear strength parameters have been obtained from the correlation with SPT – N value shown in the bore logs.

Based on the data of the present investigation, stability analysis of some critical sections of the embankment has been carried out. The stability analysis has been conducted using STB2010. The analysis depends on the soil parameters obtained during the construction of embankment. The analysis has been performed for soils at three conditions; dry, low flood level, high flood level and rapid drawdown with three different slopes; 1:1, 1:1.5 and 1:2. The values of cohesion and angle of internal friction obtained from the shear test have been used in STB2010. The maximum safety factor has been obtained 2.255 for soil at dry condition with a slope 1:2 while the minimum factor is 0.66 at rapid drawdown condition with 1:1 slope. As long as water increases, the soil becomes weakened for steepening slope. But at rapid drawdown condition safety factor has been found to be the least because of rapid reduction of external water level. So the soil would fail at any time as having lower shear strength to protest against erosion. It has been realized that, soil at dry condition has better strength to protect embankment from failure. Again the strength increases with flatter slope rather than steep slope. The main reason of the failure at high water level is considered to be water seepage into the soil while the reason is rapid reduction of external water level for rapid drawdown condition. For this type of soil, a design named Revetment Design with a thin geotextile layer and concrete block layer has been conducted to protect river embankment.

This design is affordable and suitable for Bangladesh. After Revetment Design a reasonable safety factor has been achieved for the soils at critical condition which ensures the protective strength of soil against failure.

ACKNOWLEDGEMENTS

Special thanks to Professor Dr. Mehedi Ahmed Ansary, Department of Civil Engineering, BUET (undergraduate thesis supervisor). I also like to thank my father Md. Nurul Islam and my mother Yasmin Jahan for inspiring me all time.

REFERENCES

- Alam, M.K., Hasan, A.K.M.S., Khan, M.R. "Geological Map of Bangladesh: Geological survey of Bangladesh", Whitney, John W., 1990, United States Geological Survey.
- Bhuiyan, M.A.H., Rakib, M.A., Takashi, Rahman, M.J.J. and Suzuki, Shigeyuki "Regulation of Brahmaputra-Jamuna River around Jamuna Bridge Site, Bangladesh: Geoenvironmental Impacts". *J. Water Resource and Protection*, 2010, 2, 123-130 Doi:10.4236/jwarp.2010.22014 Published Online February 2010 (<http://www.SciRP.org/journal/jwarp/>).
- Das, B.M. (Fifth Edition). "Principles of Geotechnical Engineering"
- Flaate, K. and Preber, T. (1974). "Stability of Road Embankments", Canadian Geotechnical Journal, Vol. 11, No. 1, pp. 72 – 78.
- Hoque, M.M. and M.A.B Siddique, 1995. Flood control projects in Bangladesh: Reasons for failure and Recommendations for improvement. *Disasters*, 19: 260-263. DOI: 10.1111/j.1467- 7717.1995.tb00344.x
- Hossain, M.Z. and Sakai, T. "River Embankment and Bank Failure: A Study on Geotechnical Characteristics and Stability Analysis", *American Journal of Environmental Sciences* 7 (2): 102-107, 2011
- <http://www.kennisbank-waterbouw.nl/DesignCodes/rockmanual/chapter%208.pdf>
- Morii, T. and H. Kunio, 1993. Finite element analysis of stress and stability of earth dams during reservoir filling. *J. Fac. Agric., Tottori Univ.*, 29: 45-53.
- M. Z. Hossain and T. Sakai. "Severity of Flood Embankments in Bangladesh and Its Remedial Approach". *Agricultural Engineering International: the CIGR Ejournal*. Manuscript LW 08 004. Vol. X. May, 2008.
- Thornton, Christopher I. and Kane, Richard (October 2007). "Revetment Design Considerations in Sheltered Water Wave Conditions". Professional Development Series.
- Verruijt, A., Delft University, 2010, a.verruijt@verruijt.net



PART-XI

LIQUEFGACTION ESTIMATION USING CPT

**BANGLADESH NETWORK OFFICE FOR
URBAN SAFETY (BNUS), BUET, DHAKA**

Prepared By: Ripon Hore

Mehedi Ahmed Ansary

1.1 General

The objective of this chapter is to describe the different parts of the cone penetration test machine. It also describes the variation of the different parameters like friction, cone resistance, friction ratio and SPT value (N value) with depth. Here the locations of the tests for the research have been described.

1.2 General Specifications of CPT

Pushes down the CPT cone at a nominal rate of 2 cm per second. Pull up rate is 5 cm per second. Handled by two men, the complete equipment can be transported on a pick-up van. After that the soil anchors have been installed, the machine has been positioned on the test site, the wheels have been removed and the reaction beams installed and secured. The anchors can give between 8 and 16 tons reaction force. The Machine can also be used as a separate stand alone unit with the wheels arrangement removed. Figure 3.1 shows a typical CPT machine.



Fig 3.1 : CPT

Machine (Ref: Envi 200 kN CPT Pusher / Puller
Operating Manual)

In the following articles different preparatory steps of CPT have been described. Figure 3.2 shows these steps.

3.2.1

Soil Anchors

Start to install the 4 SOIL ANCHORS in a square configuration with the size 1.3 x 1.6 m. Install the MANUAL CROSS HEAD or the MOTOR DRIVE on top of the SOIL ANCHOR

using two 12 mm BOLTS. Use 2 or 3 CPT RODS to turn the SOIL ANCHOR into the ground. Screw down the auger until the top of the rod is 0.6 m above the ground. If the soil is hard, it can be enough with the soil anchor rod, but if the upper soil is soft, use the extension rods. Use wood pieces to support the pusher and erect it horizontally. The SUPPORTS shall be high enough so that the wheels are free from the ground. Remove the bolts that are locking the wheel and pull out the wheels. Insert the two SHORT BEAMS inside the machine like the picture shows.

3.2.2 Hydraulic pump

Before connecting the **HYDRAULIC HOSES**, clean the quick coupling with a rag. Before starting the engine, the **PUMP VALVE** shall be in **OPEN** position. Check the **OIL LEVEL** in the engine.

3.2.3 Start Engine

Turn the FUEL VALVE to OPEN. To apply CHOKE on a cold engine, turn the choke lever to the left. Put the IGNITION SWITCH to ON. Start the engine by pulling the starter line.

3.2.4 Operation

Firstly Close the PUMP VALVE . Then run the CYLINDERS UP. With no load or light load on the machine, Both VALVES can be used to increase the speed going upwards. This does not function going down. Pull the right lever for push down. The speed has been regulated by changing the engine r.p.m. For CPT, the standard RATE OF PENETRATION shall be 1.2 meter/minute + / - 25 %.

3.2.5 Prepare for CPT

Before the penetration can be started, the Memocone must have been prepared. This includes filling the filter point and connecting to the Datalogger for start up and zero readings. Ref. to PC-mon manual. When the MEMOCONE has been prepared and started up together with the datalogger, put it inside the machine. Adjust the DEPTH SENSOR WHEEL. Turn the

LEVER to the right. Adjust if necessary on the screw so that the wheel is turning when the memocone is moving up and down. Do not press the wheel too hard against the memocone, only so much that it turns the wheel safely. Depth sensor. Connect the depth sensor cable with the datalogger. Insert the PUSHING HEAD or MICROPHONE into the ANVIL It will stay in position by the means of magnets. Move the head down and guide the Memocone into the center. When the head makes contact with the Memocone, press the + button on the datalogger and start the penetration. When the resistance is getting higher, check that the automatic locks are gripping OK. PUSH about 0.5 meter.

3.2.6 PRESSURE READING

It is possible to know the pushing force by checking the hydraulic pressure.

50 Bar = 6 ton

100 Bar = 12 ton

150 Bar = 18 ton

200 Bar = 24 ton

3.2.7 Maintenance:

Every 1 year should be executed the following scheme:

1. Change engine oil.
2. Lubricate the depth sensor wheel with oil.

Every 2 year:

1. Change the hydraulic oil.



Use wood pieces to support the pusher and erect it horizontally.



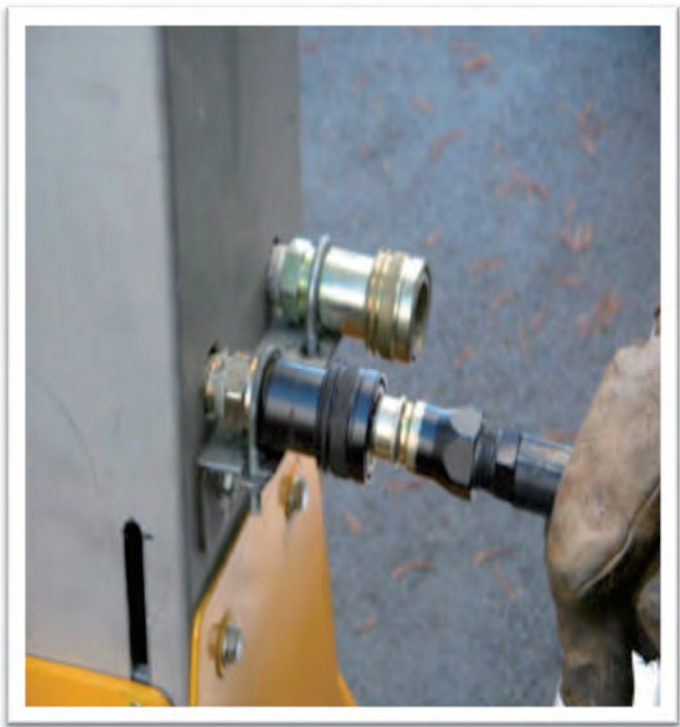
Insert the two SHORT BEAMS inside the machine



Place the two LONG BEAMS on top of the short ones.



AUTOMATIC LOCKS on the auger rods.



Hydraulic pump



Close the PUMP VALVE



DEPTH SENSOR WHEEL



LEVER to the right



Insert the PUSHING HEAD



Start the pull up.

Fig 3.2: Cone Penetration Test Procedure.

3.2.8 PC-Mon.

PC-mon stands for PC Interface monitor. This unit is the link between the CPTU probes Memocone type II and type III and a portable PC. The portable PC is NOT INCLUDED in the delivery. The software PC-mon v 1.0 or later has to be installed in the portable PC. The handling of the PC-Mon is totally menu operated. All possibilities at upstart, operation, registration of data and collection of data is clearly described on the screen. All input has been done by the keyboard and arrow-up and arrow-down buttons.

Technical specification:

Size: 420 x 300 x 55 mm

Weight: 5 Kg

Cabinet: Machined Aluminium

Power requirement: 12 V DC (Car battery)

Consumption: 1 A , FUSE : 6 A

Inputs: 12 Volts power, CPT Probe, Depth transducer encoder, Microphone,

Pressure sensor (Bosch type)

Outputs: 12 Volts for PC, USB port

3.3 Selected areas for the Research

Total ten areas of the Dhaka city have been selected for this research. The main targeted areas have been reclaimed lands since some of these lands found susceptible to liquefaction (Ahmed, 2005). Total ten areas have been selected which almost surrounding the Dhaka city. The reclaimed areas are **Bramangaon, Ashian City, Badda, Banasree, Gabtoli, Kawran Bazar, Purbachal, United City, Uttara** and **Kamrangirchar**. Figure 3.3 shows the selected study area.



Fig 3.3: Map Showing the selected areas of Dhaka City for the Research

3.4 Standard Penetration Test (SPT)

It has been conducted at all ten areas. SPT has been used for the determination of liquefaction potential. To utilize SPT results in measuring liquefaction potential, SPT have been conducted according to ASTM D1586 (ASTM,2000). The main objective of SPT are as follows:

- (a) Boring and recording of soil stratification.
- (b) Sampling (both disturbed and undisturbed)
- (c) Recording of SPT N value
- (d) Recording of ground water table.

3.5 Cone Penetration Test (CPT)

It has been conducted at all ten areas. CPT is being used for the determination of liquefaction potential. Tip resistance (q), sleeve friction (f) have been found from this test.

3.6 Laboratory Tests

Disturb and undisturb samples have been collected during SPT. Collected samples have been tested at geotechnical laboratory of BUET. Grain size analysis have been performed according to the procedure specified by ASTM D 422. These test results have used in the correlation between CPT and SPT.

3.7 Sub-Soil characteristics

Total ten locations have been selected for investigating liquefaction potential in Dhaka city in this research. SPT has been conducted and disturbed as well as undisturbed samples collected from all these locations. Sub-soil characteristics ,SPT and laboratory test results of these samples have been presented in this section. Besides this CPT test results have also been described.

3.7.1 Sub- Soil characteristics of BRAMANGAON

This site has been situated in southeast part of Dhaka city. It is a private land development project where main filling has been done by dredged river sand. The depth of filling of fine sand is 5.0 m from existing ground level. The clayey silt layer exists from 5.0 m to 6.5 m from EGL. After that 1.5 m is sandy silt layer. Then 12.0 m is clayey silt. The uncorrected SPT N value of filling fine sand varies from 4 to 5. The SPT N value of clayey silt layers varies from 5 to 8. The maximum value of SPT N is 8. The minimum value of SPT N is 4.

From the CPT test, the cone resistance varies from 0.51 to 16.78 MPa. The average value of cone resistance is 3.88 MPa. Friction varies from 0 to 120.2 kPa. The average value of Friction is 30.79 kPa. Friction ratio varies from 0 to 4.13 kPa. The average value of Friction ratio is 1.11 kPa. Figure 3.4 shows a) Depth (m) vs N b) Depth (m) vs Cone Resistance (MPa) c) Depth (m) vs Friction (kPa) d) Depth (m) vs Friction Ratio at BRAMANGAON.

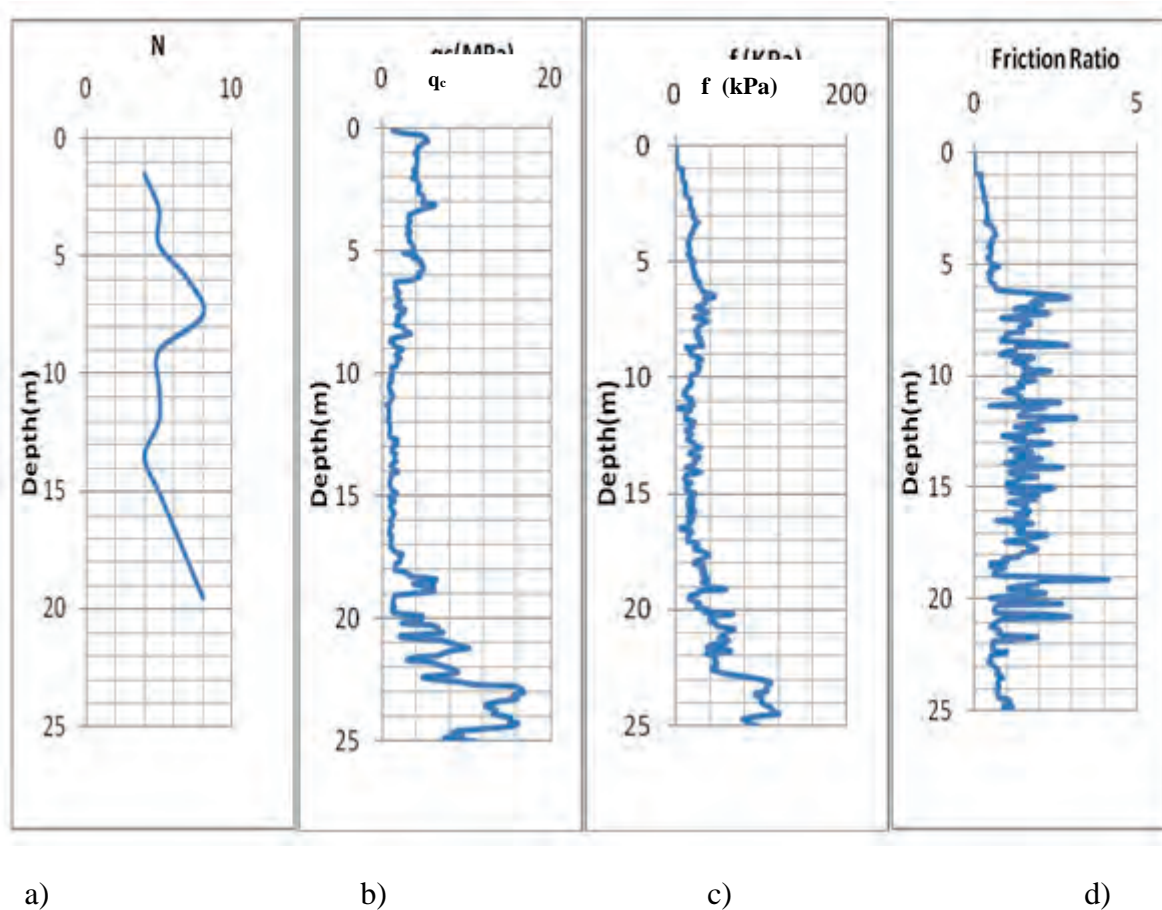


Fig 3.4: a) Depth (m) vs N b) Depth (m) vs Cone Resistance (MPa) c) Depth (m) vs Friction (kPa) d) Depth (m) vs Friction Ratio at BRAMANGAON

SPT Results:

SPT has been conducted in the area following procedure described in ASTM D1586. The SPT N values of the boreholes have been shown in the Table 3.1(a). The graph between depth vs N value has been shown in Fig 3.4 (a).

CPT results:

The graph between depth vs friction and cone resistance have been shown in Fig 3.4(c) and 3.4(b). From the CPT test, the cone resistance varies from 0.51 to 16.78 MPa. The maximum

value of cone resistance is 16.78 MPa. The minimum value of cone resistance is 0.51 MPa. The average value of cone resistance is 3.88 MPa. Friction varies from 0 to 120.2 kPa. The maximum value of Friction is 120.2 kPa. The minimum value of Friction is 0 kPa. The average value of Friction is 30.79 kPa. Friction ratio varies from 0 to 4.13 kPa. The maximum value of Friction ratio is 4.13 kPa. The minimum value of Friction ratio is 0 kPa. The average value of Friction ratio is 1.11 kPa.

Grain size analysis results:

Results from grain size analysis of the soil samples have been presented in Table 3.1(a). The mean grain size (d_{50}), fine content (F_c) of filling sand varies 0.16 to 0.17 mm, 20 to 21% respectively. The mean grain size (d_{50}), fine content (F_c) of silt are 0.046 mm, 71% respectively. Table 3.1 b shows Probable soil classification using CPT data (Robertson, 1990) at BRAMANGAON.

Table 3.1(a) : Grain size analysis at BRAMANGAON

Depth(m)	Description of Soil	SPT N Value	$F_c(\%)$	$d_{50}(\text{mm})$
1.5	Filling Sand	4	20	0.16
3	Filling Sand	5	21	0.17
4.5	Filling Sand	5	20	0.17
6	Clayey Silt	7	71	0.046
7.5	Sandy silt	8	51	0.076
9	Clayey Silt	5	71	0.046
10.5	Clayey Silt	5	71	0.046
12	Clayey Silt	5	72	0.046
13.5	Clayey Silt	4	71	0.046
15	Clayey Silt	5	71	0.046
16.5	Clayey Silt	6	71	0.046
18	Clayey Silt	7	71	0.046
19.5	Clayey Silt	8	71	0.046

Table 3.1(b): Probable soil classification using CPT data (Robertson, 1990) at BRAMANGAON

Depth Range(m)	I _c Range	Probable Soil Classification
0-3	0.82-1.52	Sand
3-6	1.22-1.92	Sand
6-9	1.77-2.82	Sand/Silt
9-12	2.34-3.24	Silty Sand/Siltly Clay
12-15	2.48-3.1	Silty Sand/Siltly Clay
15-18	2.51-3.11	Silty Sand/Siltly Clay
18-21	1.99-3.15	Silty Sand/Siltly Clay
21-24	1.66-2.67	Sand

3.7.2 Sub-Soil Characteristics of ASHIANCITY

This site has been situated in Northern part of Dhaka city. The depth of filling of fine sand is 3.5 m from existing ground level. The silty clay layer exists from 3.5 m to 12.5 m from EGL. After that 4.5 m is fine sand layer. Then 3.0 m is silty clay. The uncorrected SPT N value of filling fine sand varies from 4 to 5. The SPT N value of silty clay layers varies from 3 to 7. The maximum value of SPT N is 42. The minimum value of SPT N is 3. From the CPT test, the cone resistance varies from 0.195 to 7.805 MPa. The average value of cone resistance is 1.78 MPa. Friction varies from 0 to 233.9 kPa. The average value of Friction is 31.21 kPa. Friction ratio varies from 0 to 6.35 kPa. The average value of Friction ratio is 1.29 kPa. Figure 3.5 shows a) Depth (m) vs N b) Depth (m) vs Cone Resistance (MPa) c) Depth (m) vs Friction (kPa) d) Depth (m) vs Friction Ratio at ASHIANCITY.

SPT has been conducted in the area following procedure described in ASTM D1586. The SPT N values of the boreholes have been shown in the Table 3.2(a). The graph between depth vs N value has been shown in Fig 3.5 (a).

CPT results:

The graph between depth vs friction and cone resistance have been shown in Fig 3.5(c) and 3.5(b). From the CPT test, the cone resistance varies from 0.195 to 7.805 MPa. The maximum value of cone resistance is 7.805 MPa. The minimum value of cone resistance is 0.195 MPa. The average value of cone resistance is 1.78 MPa. Friction varies from 0 to 233.9 kPa. The maximum value of Friction is 233.9 kPa. The minimum value of Friction is 0 kPa. The average value of Friction is 31.21 kPa. Friction ratio varies from 0 to 6.35 kPa. The

maximum value of Friction ratio is 6.35 kPa. The minimum value of Friction ratio is 0 kPa. The average value of Friction ratio is 1.29 kPa.

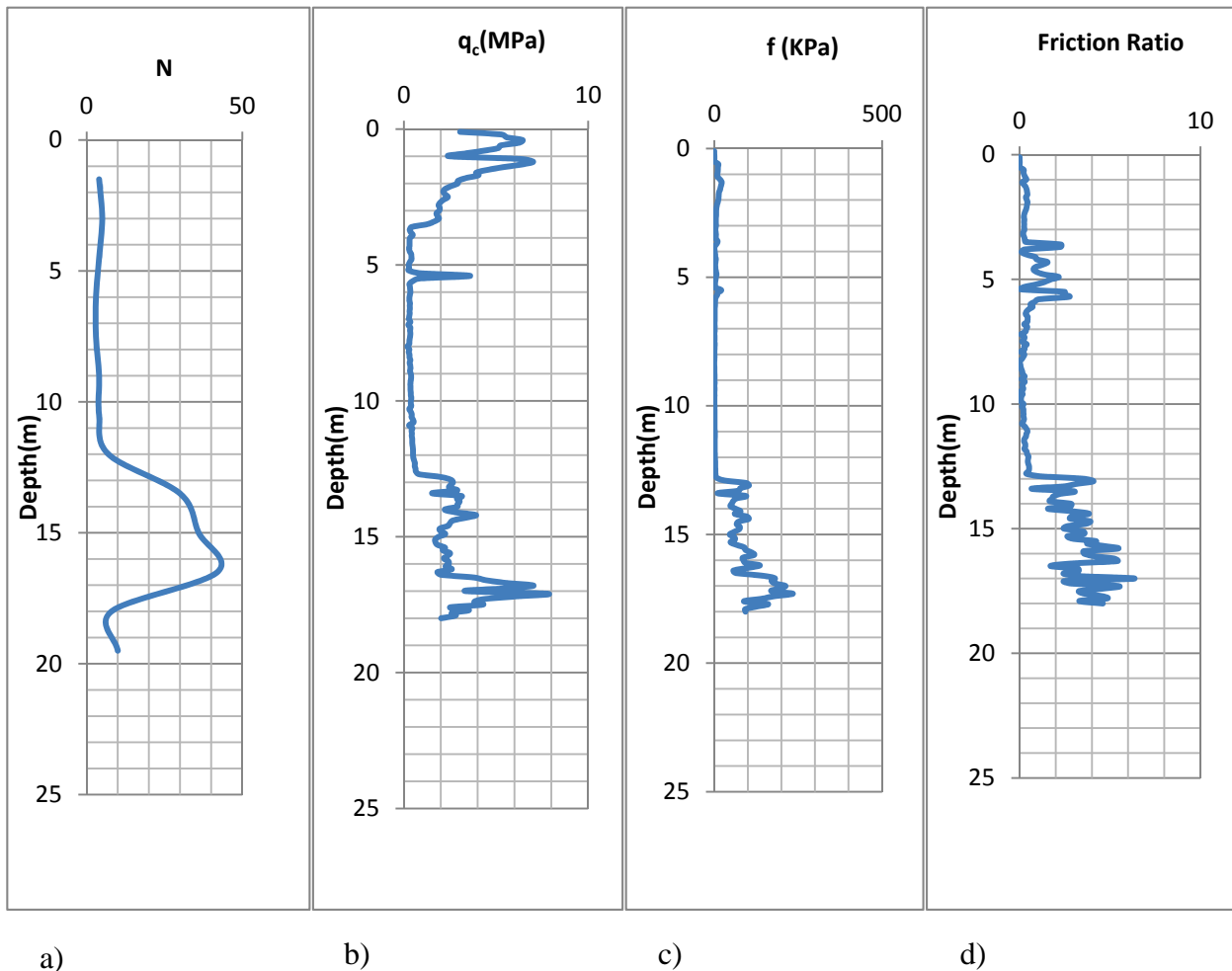


Fig 3.5: a) Depth (m) vs N b) Depth (m) vs Cone Resistance (MPa) c) Depth (m) vs Friction (kPa) d) Depth (m) vs Friction Ratio at ASHIANCITY.

SPT Results:

Grain size analysis results:

Results from grain size analysis of the soil samples have been presented in Table 3.2(a). The mean grain size (d_{50}), fine content (F_c) of filling sand varies 0.16 to 0.17 mm, 20 to 21% respectively. The mean grain size (d_{50}), fine content (F_c) of clay varies 0.002 to 0.003 mm, 94 to 96% respectively. The mean grain size (d_{50}), fine content (F_c) of sand are 0.16 mm, 21% respectively. Table 3.2(b) shows the probable soil classification using CPT data (Robertson, 1990) at ASHIANCITY.

Table 3.2(a) : Grain size data at ASHIANCITY

Depth(m)	Description of Soil	SPT N Value	F _c (%)	d ₅₀ (mm)
1.5	Filling Sand	4	20	0.16
3	Filling Sand	5	21	0.17
4.5	Silty Clay	4	94	0.002
6	Silty Clay	3	95	0.0025
7.5	Silty Clay	3	96	0.003
9	Silty Clay	4	96	0.003
10.5	Silty Clay	4	96	0.003
12	Silty Clay	7	96	0.003
13.5	Sand	30	21	0.16
15	Sand	36	21	0.16
16.5	Sand	42	21	0.16
18	Silty Clay	8	95	0.0025
19.5	Silty Clay	10	95	0.0025

Table 3.2 (b): Probable soil classification using CPT data (Robertson, 1990) at ASHIANCITY

Depth Range(m)	I _c Range	Probable Soil Classification
0-3	0.64-1.61	Sand
3-6	1.44-3.25	Sand/Silty clay
6-9	2.84-3.51	Silty Clay
9-12	2.81-3.45	Sandy silt/Silty Clay
12-15	2.28-3.05	Silty sand/Silty Clay
15-18	2.29-3.04	Silty sand/Silty Clay

LIQUEFACTION POTENTIAL ANALYSIS BASED ON SPT AND CPT

1.1 General

The main objective of this chapter is to present the liquefaction potential of the selected reclaimed areas. Soil characteristics of the selected reclaimed areas have been determined by field and laboratory tests. Test results have been presented in Chapter Three. Liquefaction potential have been estimated using two methods based on CPT (Robertson and Wride, 1998) and SPT (Seed et al; 1983) data. The results of these estimations have been presented in this chapter. Results obtained from different methods have been compared and suitable methods for estimating liquefaction potential has been presented.

1.2 Liquefaction Potential

In this research liquefaction potential has been estimated by procedures based on both SPT and CPT test results. Detail procedures have been discussed in chapter Three. Parameter of analysis and details results of estimations based on these procedures has been discussed below.

Parameters for analysis

Liquefaction analysis based on SPT and CPT need ground motion characteristics and moment magnitude due to earthquake and depth of analysis. In this study, following values of these parameters have been considered.

1) Ground motion and Moment Magnitude:

In this research, the value of a_{max} has been taken as 0.15g as Dhaka city exist in the zone 2 of seismic zonation map of Bangladesh (BNBC, 1993). Other researchers (Ansary and Rashid, 2000) also used similar values of a_{max} for the similar purpose. Though at present the value of a_{max} is being update by various researchers and agencies from 0.15 to 0.2. But it has not been taken to the consideration for this study since it has not been incorporated to BNBC yet. Earthquake ground motion has been influenced by a number of factors. Most important factors are moment magnitude, epicenter distances, local soil conditions, earthquake sources, etc. In seed-Idriss simplified procedure moment magnitude (M_w) input parameter is also important correction factor. From Table 2.1, it is seen that ranges of M_w at nearby faults from Dhaka varies 7.5~8.5. However, this value can not be considered directly for Dhaka since those faults are at quite distant places from Dhaka. Due to non-availability of attenuation law and suitable correlations between distance and ground motion characteristics for Dhaka, the design moment magnitude has been taken 7.0 for this study, which is the lowest value in Table 2.1.

2) Sources of Damaging Earthquake near Dhaka city:

Bangladesh covers one of the largest deltas and one of the thickest sedimentary basins in the world. According to the report on time predictable fault modeling (2009), earthquake and tsunami preparedness component of CDMP have identified five tectonic fault zones which may produce damaging earthquakes in Bangladesh. These are Madhupur fault zone, dauki fault zone, plate boundary fault zone -1, plate boundary fault zone -2, and plate boundary fault zone -3. Among these, Madhupur fault zone has been considered as a source of damaging earthquake near Dhaka in this study.

1.2.1 Liquefaction Potential of BRAMANGAON

On the basis of soil characteristics of this locations that have been presented in chapter 3. Liquefaction potential based on CPT (Robertson and Wride, 1998) and SPT (Seed et al;1983) data have been estimated. A typical liquefaction potential analysis has been shown in Fig 4.1. Liquefiable zone is where $F_1 < 1$, on the other hand Non liquefiable zone is where $F_1 > 1$. The liquefaction analyses results by different procedures have been presented below:

- Liquefaction susceptibility has been estimated based on the method proposed by Seed et al;1983 at different depths. The liquefaction zones vary between 1.5~4.5 m. (Fig 4.1).
- Liquefaction susceptibility has been estimated based on the method proposed by Robertson and Wride, 1998. From the Fig 4.1, liquefaction zones vary between 1.5 ~10 m and from 18~22.5m.

From the above discussion, it has been seen that liquefaction potential result slightly varies in the two methods. It may be concluded that the soil may liquefy from 1.5~10 m and from 18~22.5 m depth if an earthquake of sufficient energy occurs. CPT is more reliable than SPT as it is performed at each 0.1m depth.

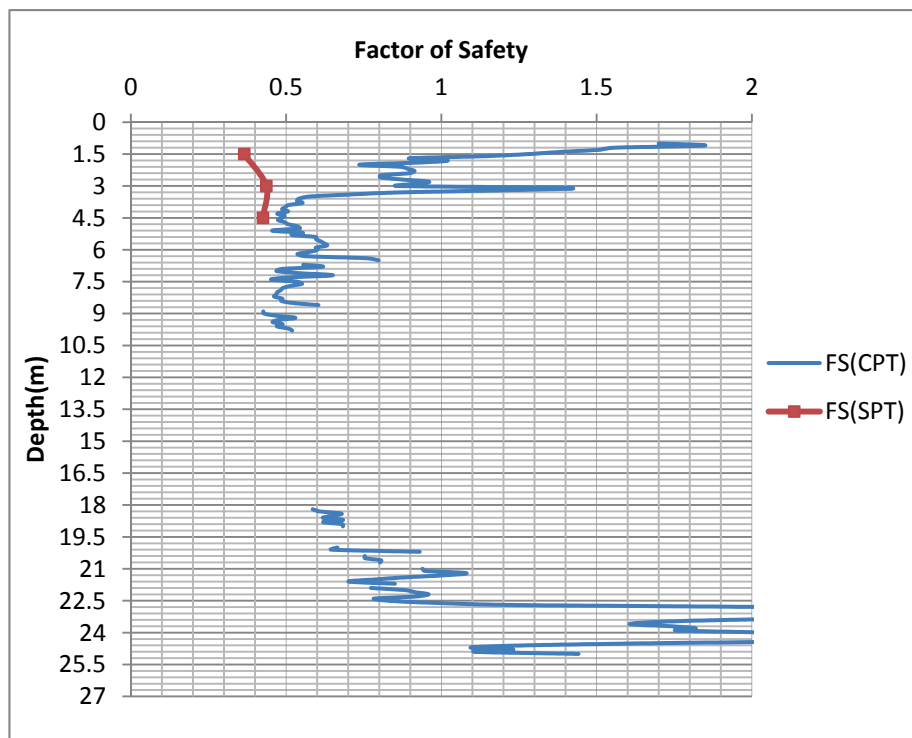


Fig 4.1: Depth(m) vs FS at BRAMANGAON

4.2.2 Liquefaction Potential of ASHIAN CITY

On the basis of soil characteristics of this locations that have been presented in chapter 3. Liquefaction potential based on CPT (Robertson and Wride, 1998) and SPT (Seed et al; 1983) data have been estimated. A typical liquefaction potential analysis has been shown in Fig 4.2. Liquefiable zone is where $F_l < 1$, on the other hand Non liquefiable zone is where $F_l > 1$. The liquefaction analyses results by different procedures have been presented below:

- Liquefaction susceptibility has been estimated based on the method proposed by Seed et al;1983 at different depths. The liquefaction zones vary between 1.5~3 m. (Fig 4.2).
- Liquefaction susceptibility has been estimated based on the method proposed by Robertson and Wride, 1998. From the Fig 4.2, liquefaction zones vary between 1.8~3.9 m and from 12.9~14.4 m.

From the above discussion, it has been seen that liquefaction potential result slightly varies in the two methods. It may be concluded that the soil may liquefy from 1.5~3.9 m and from 12.9~14.4 m depth if an earthquake of sufficient energy occurs. CPT is more reliable than SPT as it is performed at each 0.1m depth.

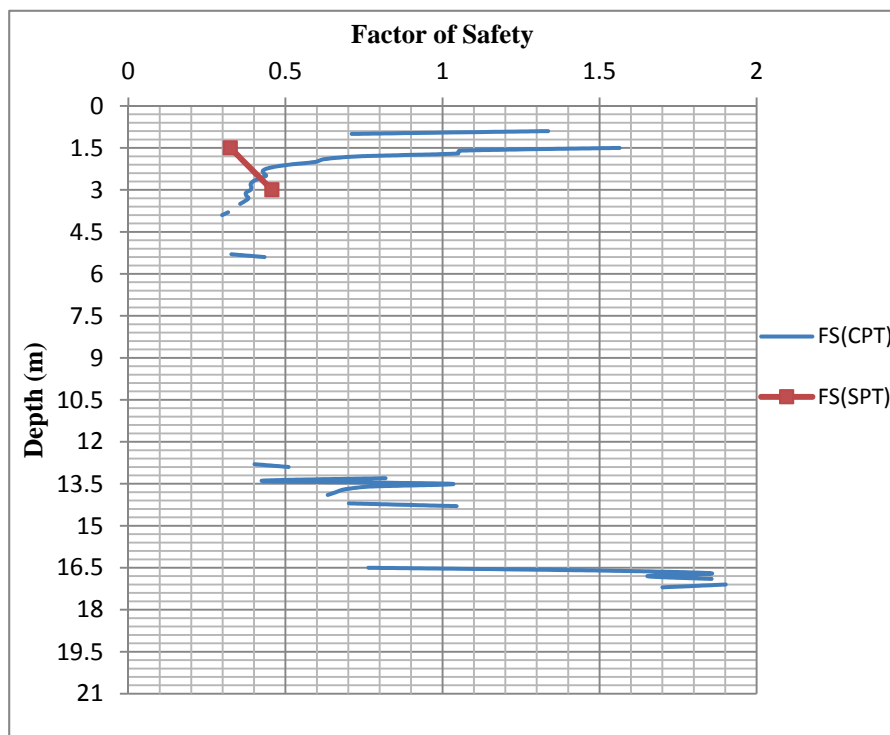


Fig 4.2: Depth(m) vs FS at ASHIAN

Table 4.1: Liquefaction zone of two different method.

Site Name	Liquefaction zone (Seed et al;1983)	Liquefaction Zone (Robertson and Wride, 1998)
BRAMANGAON	1.5~4.5 m	1.5 ~10 m and 18~22.5m
ASHIAN CITY	1.5~3 m	1.8~3.9 m and 12.9~14.4 m
BADDA	1.5~4.5 m	4.5 ~5.5 m and 8~9.5m
BANASREE	1.5~4.5 m	0.7 ~4.8 m and 14.4~15.3 m
GABTOLI	1.5~4.5 m	0.6 ~5.4 m
KAWRAN BAZAR	at 12 m depth	11.4 ~12.3 m
PURBACHAL	1.5~6 m	1.5 ~5.0 m and 15~15.6 m
UNITED CITY	1.5~3 m	3.0~4.5 m. and 10.5~12.0 m
UTTARA	1.5~4.5 m	2.7 ~4.8 m and 8.7~12.3 m
KAMRANGI CHAR	1.5~7.5 m and from 10.5~11.5 m	1.5 ~6 m and 7.5~12 m



PART-XII

BURIED GAS PIPELINE DAMAGE ANALYSIS

**BANGLADESH NETWORK OFFICE FOR
URBAN SAFETY (BNUS), BUET, DHAKA**

Prepared By: Sayeed Hossain

Mehedi Ahmed Ansary

3.0 GENERAL

The damageability of buried gas supply pipelines in seismic Zone can be very serious and it is necessary to take preventive measures that eliminate, or at least decrease, that damageability. Pipelines that are the main source of gas distribution for important cities in seismic zone should be investigated and analyzed in terms vulnerability to earthquakes. Institutions and authorities responsible for the design, Construction and operation of buried pipelines located in seismic zones should demand that the seismic effects are correctly taken into consideration in order to assure the good behavior of such pipelines during their working life.

The damage Produced by breakage or disconnection of pipelines is quite variable and can be related to technical, economical and social aspects. The breakage of gas pipelines, for instance, besides representing a health hazard and fire risk causes leakage and the repairs in the pipeline represent an important cost

The damage algorithm for buried pipe is expressed as a repair rate per unit length of pipe, as a function of ground shaking or ground failure. The development of damage algorithms for buried pipe is primarily based on empirical evidence, tempered with engineering judgment and sometimes by analytical formulations. Empirical evidence means the following: after an earthquake, data is collected about how many miles of buried pipe experienced what levels of shaking and how many pipes were broken or leaking because of that level of shaking.

Repair rate of pipelines due to earthquake is related to either peak ground acceleration (PGA) or peak ground velocity (PGV). There exist a good number empirical relations such as Katayama (1975), O' Rourke (1982), Isoyama & Katayama (1998) and Iosyama (2000) for the Prediction of earthquake-induced pipeline damage analysis which are Presented in chapter two. In case of PGA O'Rourke (1982) and Isoyama (2000) relations are used. In case of PGV O'Rourke (2000) and Isoyama (2001) relations are used to predict the damage rate of pipelines. Finally an estimation of financial loss is presented.

3.1 PIPELINE DATABASE DEVELOPMENT

GIS provides an ideal tool for analyzing relationships amongst spatial datasets. GIS is increasingly used in lifeline engineering for post earthquake investigation of damage and for risk assessment.

The history of gas supply system of Dhaka city is very long. The only known maps available are those created by "TITAS gas T & D Company Ltd" which has been responsible for design, finance and construction of gas Supply System. A copy of maps of gas supply network of 1988 covering the whole Dhaka city at a scale of 1:10000 is collected for this study. This map is scanned at first and then the whole gas pipeline networks are digitized which is illustrated in Figure 3.1.

No distinction is made between different pipe materials or diameters, although it is known from the authority that the network consists of cast iron pipes with diameter 75 mm to 300mm.

Microzonation maps of different intensities are grouped presented in chapter three, and pipeline networks of different diameter are laid in these maps on GIS platform which are shown in Figures 3.2 to 3.3. Finally, the lengths of pipelines are calculated according to intensity from these digitized intensity- pipe maps for analysis which are shown in Table 3.1

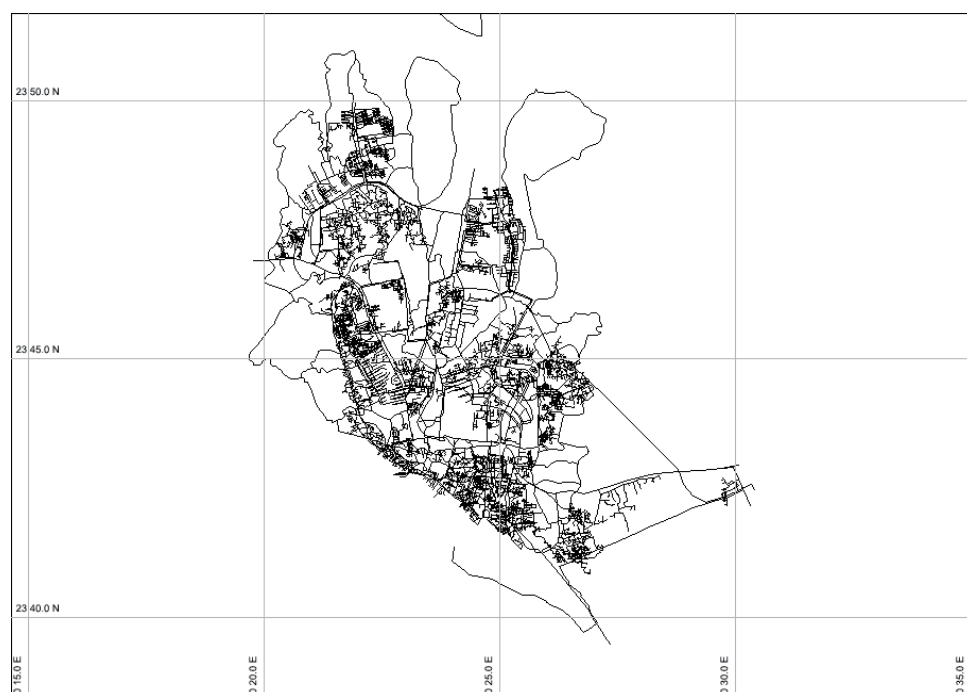


Figure 3.1 Digitized layout of Gas pipe line network of Dhaka City.

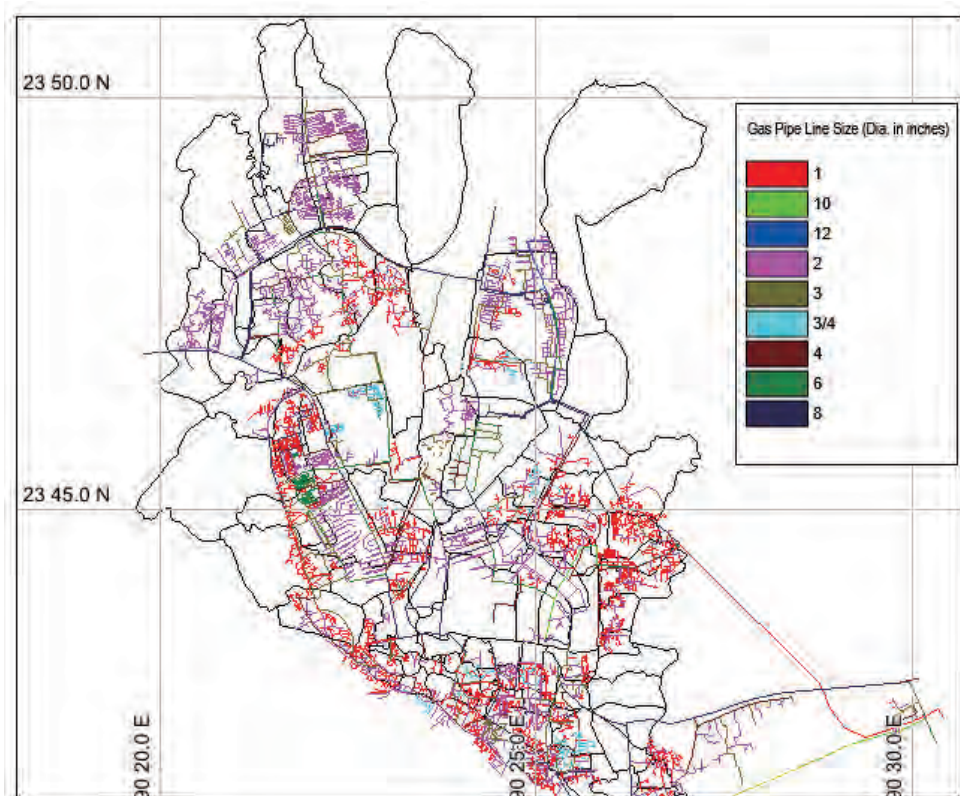


Figure 3.2 Digitized layout of Gas pipe line network of Dhaka City showing diameter of pipe.

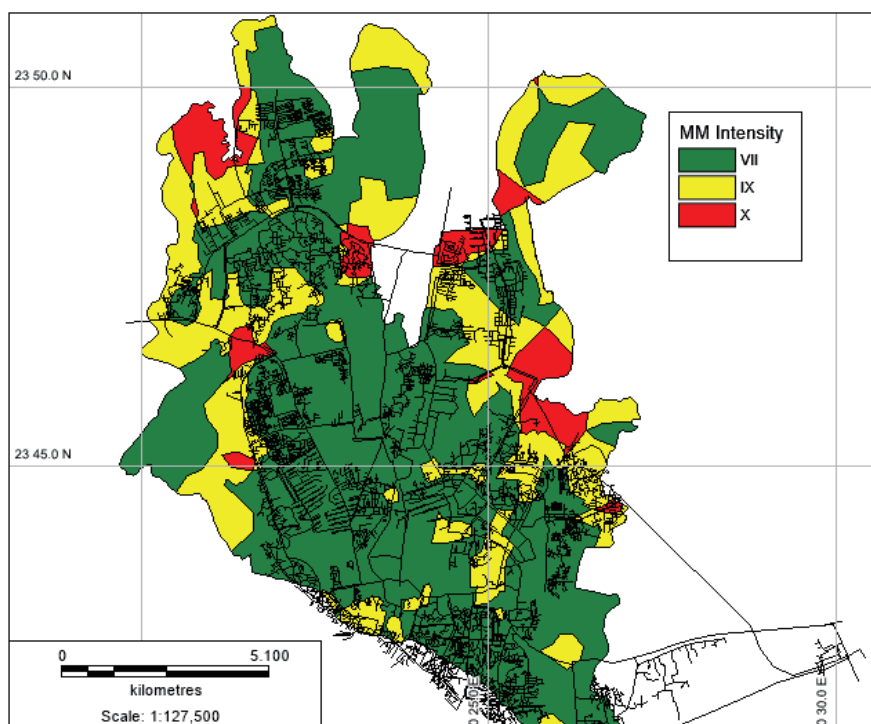


Figure 3.3 Digitized layout of Gas pipe line network superimposed on MM intensity map of Dhaka city.

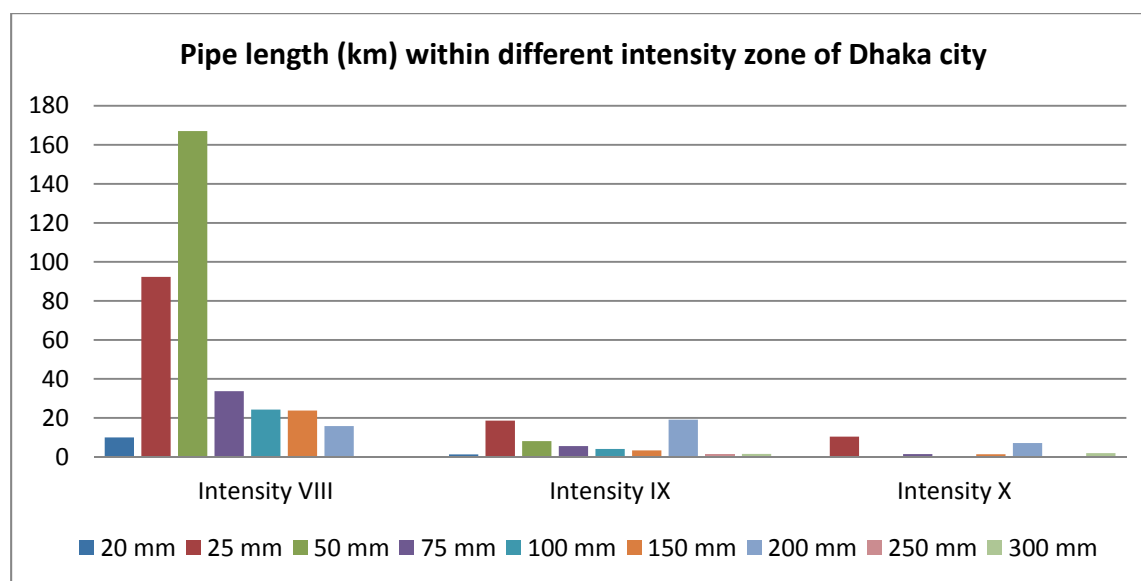


Figure 3.3A Gas Pipe length (km) within different intensity zone of Dhaka city

Table 3.1 Gas pipe line length within different intensity of Dhaka city

Intensity (MMI)	Pipe length (km)										Total Length (km)
	20 mm	25 mm	50 mm	75 mm	100 mm	150 mm	200 mm	250 mm	300 mm	N/A	
8	10.03	92.33	167.02	33.72	24.29	23.79	15.81	0.00	0.00	9.04	376.03
9	1.27	18.58	8.14	5.53	4.06	3.35	19.09	1.50	1.55	4.24	67.31
10	0.00	10.37	0.00	1.43	0.00	1.39	7.09	0.00	1.94	0.00	22.23

3.2 SELECTION OF PEAK GROUND ACCELERATION (PGA) VALUES FROM INTENSITY

In studies related to earthquake damage estimation and earthquake insurance, it has been observed that the Modified Mercalli intensity scale is the easiest and most convenient to work with. Most of the available damage statistics are related to the MM intensity at a site. However, for the recent instrumentally recorded data, the information on ground motion is usually in the form of peak ground motion parameter such as the PGA. Again, many empirical data base relationships are available in the literature to relate the MM intensity with the PGA. Peak ground acceleration is an instrumentally recorded continuous variable whereas modified Mercalli intensity is a subjectively assigned discrete Integer variable. Thus, it should be expected that there will be a range of PGA values corresponding to a given intensity level.

In the past, a number of researchers have developed PGA-MMI relationships. In each of the relationships given below, I is Modified Mercalli intensity and A is peak ground acceleration in cm/sec².

$$\text{Gutenberg and Richter (1942)} \quad \log A = -0.5 + 0.33I \quad 3.1$$

$$\text{Hersberger (1956)} \quad \log A = -0.9 + 0.43I$$

3.2

$$\text{Ambraseys (1974)} \quad \log A = -0.16 + 0.36I$$

3.3

$$\text{Trifunac and Brady (1975)} \quad \log A = 0.014 + 0.3I$$

3.4

All the above relationships are log-linear in format.

Using the above relationships, different PGA values calculated for different MM intensity and show in Table 3.2

Table 3.2 PGA values bashed on different existing empirical relationships for different intensity

Intensity (MMI)	Gutenberg and Richter (1942)	Hershberger (1956)	Ambraseys (1974)	Trifunac and Brady (1975)
5	0.014	0.018	0.045	0.033
6	0.031	0.049	0.102	0.066
7	0.066	0.131	0.234	0.133
8	0.141	0.354	0.535	0.265
9	0.301	0.952	1.226	0.528
10	0.643	2.561	2.809	1.053
11	1.376	6.894	6.434	2.101

MM intensity and PGA values from Table 3.2 have also been plotted in Figure 3.4 for comparison. It can be seen in the graph of Figure 3.4 that for a particular intensity, Ambraseys relation shows higher value and Gutenberg & Richter curve shows lower value. All most all of the remaining curves lie in between these two. The curve from Trifunac & Brady is close to the median value. Henceforth intensity-PGA relationships given by Gutenberg-Richter and Trifunac-Brady are considered for our analysis; values in higher side are ignored.

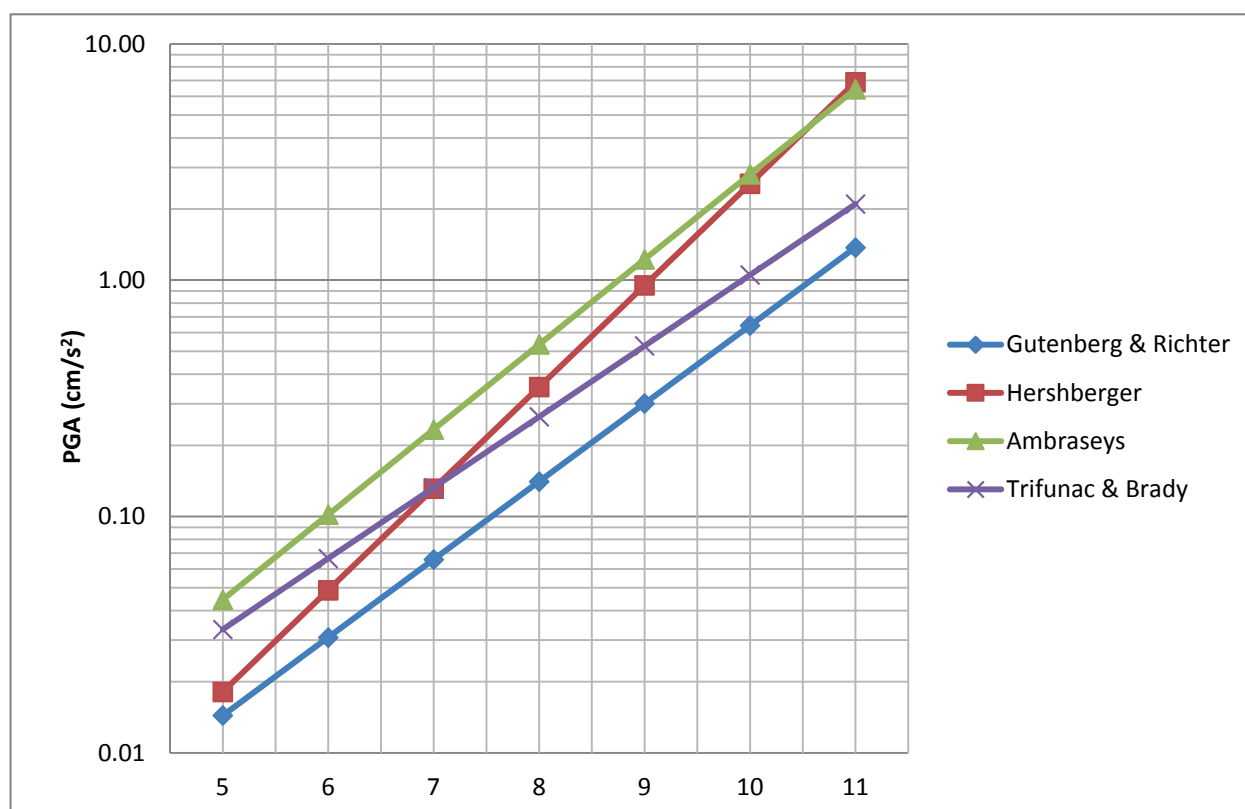


Figure 3.4 Comparison of PGA values derived from different modified Mercalli intensity (PGA-MMI) empirical relationships.

3.3 SELECTION OF PEAK GROUND VELOCITY (PGV) VALUES FROM INTENSITY

A number of researchers have also developed PGV-MMI relationships. In each of the relationships given below, I is Modified Mercalli intensity and V is peak ground velocity in cm/sec. Trifunac and Brady (1975), considered horizontal and vertical components separately.

$$\text{Trifunac and Brady (1975)} \quad \log V_v = -1.10 + 0.28 I \quad 3.5$$

$$\text{Trifunac and Brady (1975)} \quad \log V_H = -0.63 + 0.25 I \quad 3.6$$

$$\text{Wald et al. (1999)} \quad I = 3.47 \log (\text{PGV}) + 2.35 \quad 3.7$$

Using the above relationships (vertical component discarded), different PGV values calculated for different MM intensity and show in Table 3.3

Table 3.3 PGV values bashed on different existing empirical relationships for different intensity

Intensity (MMI)	Trifunac and Brady (1975)	Wald et al (1999)
5	4.169	5.803
6	7.413	11.269
7	13.183	21.881
8	23.442	42.486
9	41.687	82.495
10	74.131	160.181
11	131.826	311.025

MM intensity and PGV values from Table 4.3 have also been plotted in Figure 3.5 for comparison. It can be seen in the graph that Trifunac Brady gives higher value than Wald et. al.

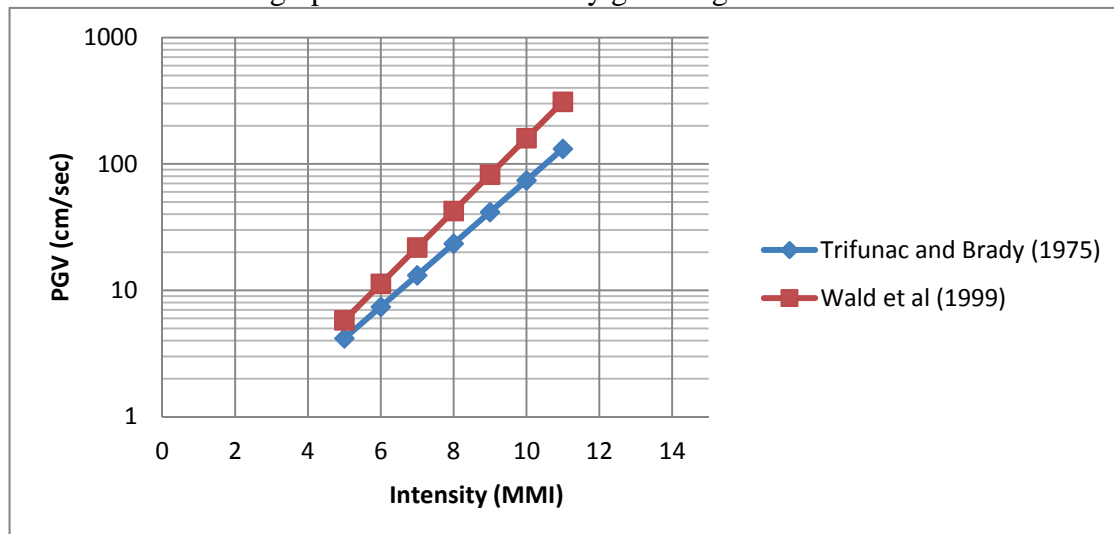


Fig 3.5 Comparison of PGV values derived from different PGV-MMI empirical relationships.

3.3 SELECTION OF DAMAGE ANALYSIS METHODS BASED ON PGA

Different pipeline fragility relation give very different predictions of pipeline damage rate for the same PGA value. The values calculated in Table 3.4 are from katayama et. (1975), Isoyama & Kaiyama (1982), O'Rourke et al. (1998) and Isoyama et al. (2000) fragility relations (Equations 2.9, 2.10, 2.11 and respectively). All these relations assume CI pipe irrespective of diameters.

Table 3.4 pipeline repair rate from different fragility relations for PGA values based on Trifunac and Brady and Gutenberg and Richter relations

Equation Used	Intensity (MMI)	Repair Rate (RR)				
		PGA (cm/S ²)	Katayama et al. (1975)	Isoyama and Katayama (1982)	O'Rourke et. al. (1998)	Isoyama et al. (2000)
Trifunac and Brady	7	130.017	0.011	0.001	0.019	0.002
	8	259.418	0.911	0.072	0.044	0.063
	9	517.607	75.276	4.751	0.105	0.419
	10	1032.761	6218.090	312.448	0.250	2.041
Gutenberg and Richter	7	64.565	0.000	0.000	0.008	0.000
	8	138.038	0.016	0.002	0.020	0.004
	9	295.121	2.077	0.158	0.052	0.094
	10	630.957	266.807	15.774	0.135	0.673

From the selected peak ground acceleration (PGA) values and fragility relations, following four methods are used for damage analysis.

Method 1: In this method PGA and repair rate are based on Trifunac – Brady MMI-PGA relations and O'Rourke damage prediction relation.

Method 2: This method is based on Gutenberg-Richter MMI-PGA relation and O'Rourke damage prediction relation.

Method 3: This method involves Trifunac-Brad MMI-PGA relation and Isoyama damage prediction relation.

Method 4: Where damage analysis is based on Gutenberg-Richter MMI-PGA relation and Isoyama damage prediction relation.

3.4 GAS PIPELINE DAMAGE ANALYSIS BASED ON PGA

Pipeline damage estimation is related to damage prediction relationship. Relative results of different damage prediction relationships are studied in the previous articles. Using the methods outlined in the preceding articles and pipeline lengths calculated from the digitized maps which are shown in Table 3.1. Repair rates and number of repairs are worked out and presented in Table 3.5 to 3.8 and finally a different table, table 3.9 is prepared for comparison of these repair rates which are also presented in graph of Figure 3.7.

Table 3.5 Intensity and number of repairs based on O'Rourke and Trifunac and Brady relation

Intensity (MMI)	PGA (cm/s ²)	Pipe length (km)										Total Length (km)	Repair rate	Repair number
		20 mm	25 mm	50 mm	75 mm	100 mm	150 mm	200 mm	250 mm	300 mm	N/A			
8	259.42	10.03	92.33	167.02	33.72	24.3	23.8	15.8	0.00	0.00	9.04	376.03	0.044	17
9	517.61	1.27	18.58	8.14	5.53	4.06	3.35	19.1	1.50	1.55	4.24	67.31	0.105	7
10	1032.7	0.00	10.37	0.00	1.43	0.00	1.39	7.09	0.00	1.94	0.00	22.23	0.250	6

Table 3.6 Intensity and number of repairs based on O'Rourke and Gutenberg-Richter

Intensity (MMI)	PGA (cm/s ²)	Pipe length (km)										Total Length (km)	Repair rate	Repair number
		20 mm	25 mm	50 mm	75 mm	100 mm	150 mm	200 mm	250 mm	300 mm	N/A			
8	138.04	10.03	92.33	167.02	33.72	24.3	23.8	15.8	0.00	0.00	9.04	376.03	0.02	8
9	295.12	1.27	18.58	8.14	5.53	4.06	3.35	19.1	1.50	1.55	4.24	67.31	0.052	4
10	630.96	0.00	10.37	0.00	1.43	0.00	1.39	7.09	0.00	1.94	0.00	22.23	0.135	3

Table 3.7 Intensity and number of repairs based on Isoyama and Trifunac and Brady relation

Intensity (MMI)	PGA (cm/s ²)	Pipe length (km)										Total Length (km)	Repair rate	Repair number
		20 mm	25 mm	50 mm	75 mm	100 mm	150 mm	200 mm	250 mm	300 mm	N/A			
8	259.42	10.03	92.33	167.02	33.72	24.3	23.8	15.8	0.00	0.00	9.04	376.03	0.063	24
9	517.61	1.27	18.58	8.14	5.53	4.06	3.35	19.1	1.50	1.55	4.24	67.31	0.419	28
10	1032.7	0.00	10.37	0.00	1.43	0.00	1.39	7.09	0.00	1.94	0.00	22.23	2.041	45

Table 3.8 Intensity and number of repairs based on Isoyama and Gutenberg-Richter

Intensity (MMI)	PGA (cm/s ²)	Pipe length (km)										Total Length (km)	Repair rate	Repair number
		20 mm	25 mm	50 mm	75 mm	100 mm	150 mm	200 mm	250 mm	300 mm	N/A			
8	138.04	10.03	92.33	167.02	33.72	24.3	23.8	15.8	0.00	0.00	9.04	376.03	0.004	1

9	295.12	1.27	18.58	8.14	5.53	4.06	3.35	19.1	1.50	1.55	4.24	67.31	0.094	6
10	630.96	0.00	10.37	0.00	1.43	0.00	1.39	7.09	0.00	1.94	0.00	22.23	0.673	15

The result presented in Table 3.5 shows pipeline length, repair rate and number of repairs based on O'Rourke damage prediction relation for different peak ground acceleration (PGA) derived from Trifunac and Brady PGA-MMI relation. The result presented in Table 3.6 shows pipeline length, repair rate and number of repairs based on O'Rourke damage prediction relation for different peak ground acceleration (PGA) derived from Gutenberg and Richter PGA-MMI relation. The result presented in table 3.7 shows pipeline length, repair rate and number of repairs based on Isoyama damage prediction relation for different peak ground acceleration (PGA) derived from Trifunac & Brady PGA-MMI relation. The result presented in Table 3.8 shows pipeline length, repair rate and number of repairs based on Isoyama damage prediction relation for different peak ground acceleration (PGA) derived from Gutenberg and Richter PGA-MMI relation.

Table 3.9 Intensity and number of repairs based on O'Rourke and Trifunac and Brady relation

Intensity (MMI)	Pipeline Repair Rate (RR) based on relations:			
	O'Rourke and Trifunac-Brady (OTB)	O'Rourke and Gutenberg-Richter (OGR)	Isoyama and Trifunac and Brady (ITB)	Isoyama and Gutenberg-Richter (IGR)
8	0.044	0.020	0.063	0.004
9	0.105	0.052	0.419	0.094
10	0.250	0.135	2.041	0.673

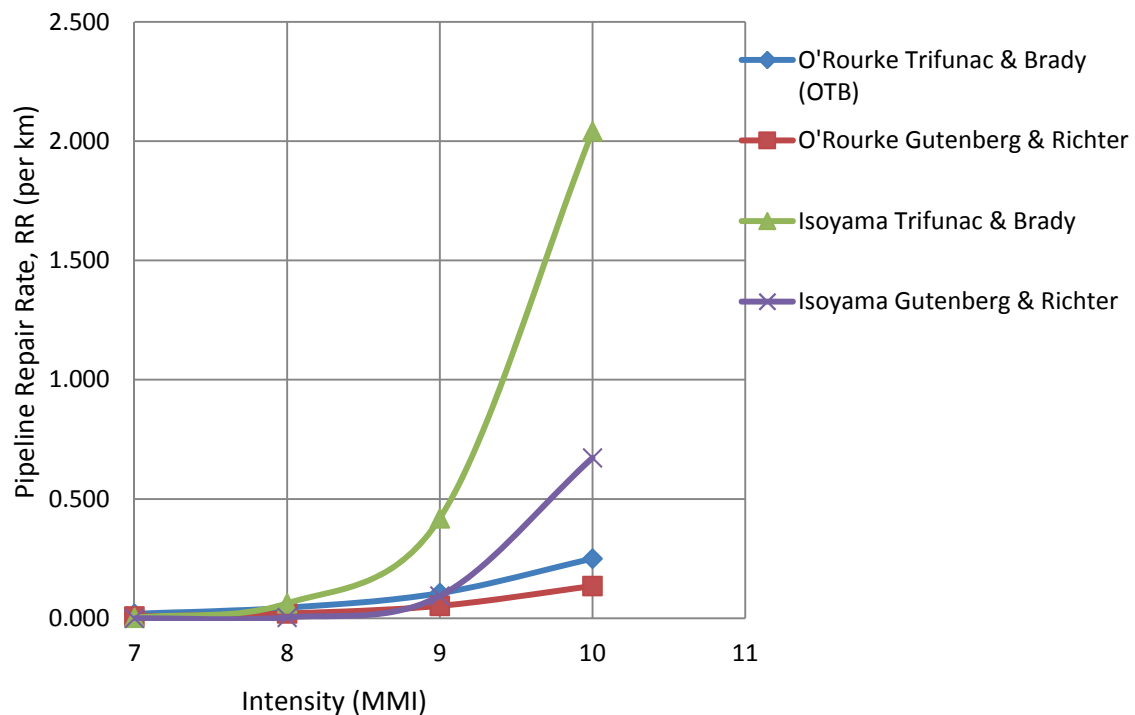


Figure 3.7 Comparison of pipeline repair rate for different Intensity and fragility relation.

From the table 3.9 and Figure 3.7 it is seen that repair rates of O'Rourke and Trifunac and Brady relation are two times higher than those of O'Rourke and Gutenberg and Richter relation for all intensities. On the other hand Isoyama and Trifunac and Brady relation shows 15 times higher repair rate than the repair rate obtained from Isoyama and Gutenberg and Richter relation for intensity 8 while it is 5 times and 3 times higher for intensity 9 and 10 respectively. On the whole it is seen from these relations that repair rates vary from 0.004 to 0.06 for intensity 8, 0.052 to 0.424 for intensity 9 and 0.134 to 2.029 for intensity 10. However due to absence of real repair rate data in Bangladesh, it is advisable to use a range of repair rates instead of a single value in the event of damage analysis of buried water supply pipelines due to earthquake.

3.5 SELECTION OF DAMAGE ANALYSIS METHODS BASED ON PGV

Different pipeline fragility relation give very different predictions of pipeline damage rate for the same PGA value. The values calculated in Table 4.10 are from O'Rourke & Ayala (1993), Endinger et al. (1995, 1998), Isoyama et al. (2000) & O'Rourke et al. (2001).

Table 3.10 Pipe line repair rate form different fragility relations for PGV values based on Trifunac and Brady and Wald et. al. relations.

Equation Used	Intensity (MMI)	Repair Rate (RR)				
		PGV (cm/sec)	O'Rourke & Ayala (1993)	Endinger et al. (1995, 1998)	Isoyama et al. (2000)	O'Rourke et al. (2001)
Trifunac and Brady (1975)	7	13.183	0.033	0.027		
	8	23.442	0.121	0.086	0.050	0.119
	9	41.687	0.442	0.267	0.222	0.287
	10	74.131	1.613	0.836	0.625	0.455
Wald et al (1999)	7	21.881	0.104	0.075	0.038	0.099
	8	42.486	0.461	0.278	0.231	0.293
	9	82.495	2.051	1.033	0.743	0.487
	10	160.181	9.128	3.843	2.010	0.681

From the selected peak ground acceleration (PGV) values and fragility relations, following four methods are used for damage analysis.

Method 1: In this method PGV and repair rate are based on Trifunac – Brady MMI-PGV relations and Isoyama damage prediction relation.

Method 2: This method is based on Wald et al MMI-PGV relation and O'Rourke damage prediction relation.

Method 3: This method involves Trifunac-Brad MMI-PGV relation and Isoyama damage prediction relation.

Method 4: Where damage analysis is based on Wald et al MMI-PGV relation and O'Rourke damage prediction relation.

3.6 GAS PIPELINE DAMAGE ANALYSIS BASED ON PGV

Using the methods outlined in the preceding articles and pipeline lengths calculated from the digitized maps which are shown in Table 3.1. Repair rates and number of repairs are worked out and presented in Table 3.11 to 3.14 and finally a different table, table 3.15 is prepared for comparison of these repair rates which are also presented in graph of Figure 3.8.

Table 3.11 Intensity and number of repairs based on O'Rourke and Trifunac and Brady relation

Intensity (MMI)	PGV (cm/s)	Pipe length (km)										Total Length (km)	Repair rate	Repair number
		20 mm	25 mm	50 mm	75 mm	100 mm	150 mm	200 mm	250 mm	300 mm	N/A			
8	23.44	10.03	92.33	167.02	33.72	24.29	23.79	15.81	0.00	0.00	9.04	376.03	0.119	45
9	41.69	1.27	18.58	8.14	5.53	4.06	3.35	19.09	1.50	1.55	4.24	67.31	0.287	19
10	74.13	0.00	10.37	0.00	1.43	0.00	1.39	7.09	0.00	1.94	0.00	22.23	0.455	10

Table 3.12 Intensity and number of repairs based on O'Rourke and Wald

Intensity (MMI)	PGV (cm/s)	Pipe length (km)										Total Length (km)	Repair rate	Repair number
		20 mm	25 mm	50 mm	75 mm	100 mm	150 mm	200 mm	250 mm	300 mm	N/A			
8	42.49	10.03	92.33	167.02	33.72	24.29	23.79	15.81	0.00	0.00	9.04	376.03	0.293	110
9	82.49	1.27	18.58	8.14	5.53	4.06	3.35	19.09	1.50	1.55	4.24	67.31	0.487	33
10	160.18	0.00	10.37	0.00	1.43	0.00	1.39	7.09	0.00	1.94	0.00	22.23	0.681	15

Table 3.13 Intensity and number of repairs based on Isoyama and Trifunac and Brady relation

Intensity (MMI)	PGV (cm/s)	Pipe length (km)										Total Length (km)	Repair rate	Repair number
		20 mm	25 mm	50 mm	75 mm	100 mm	150 mm	200 mm	250 mm	300 mm	N/A			
8	23.44	10.03	92.33	167.02	33.72	24.29	23.79	15.81	0.00	0.00	9.04	376.03	0.050	19
9	41.69	1.27	18.58	8.14	5.53	4.06	3.35	19.09	1.50	1.55	4.24	67.31	0.222	15
10	74.13	0.00	10.37	0.00	1.43	0.00	1.39	7.09	0.00	1.94	0.00	22.23	0.625	14

Table 3.14 Intensity and number of repairs based on Isoyama and Wald

Intensity (MMI)	PGV (cm/s)	Pipe length (km)										Total Length (km)	Repair rate	Repair number
		20 mm	25 mm	50 mm	75 mm	100 mm	150 mm	200 mm	250 mm	300 mm	N/A			
8	42.49	10.03	92.33	167.02	33.72	24.29	23.79	15.81	0.00	0.00	9.04	376.03	0.231	87
9	82.49	1.27	18.58	8.14	5.53	4.06	3.35	19.09	1.50	1.55	4.24	67.31	0.743	50
10	160.18	0.00	10.37	0.00	1.43	0.00	1.39	7.09	0.00	1.94	0.00	22.23	2.010	45

Table 3.15 Intensity and number of repairs based on various PGV based relation.

Intensity (MMI)	Pipeline Repair Rate (RR) based on relations:			
	Isoyama et al. (2000) & Trifunac Brady	O'Rourke et al. (2001) & Trifunac Brady	Isoyama et al. (2000) & Wald	O'Rourke et al. (2001) & Wald
7	0.000	0.000	0.038	0.099
8	0.050	0.119	0.231	0.293
9	0.222	0.287	0.743	0.487
10	0.625	0.455	2.010	0.681

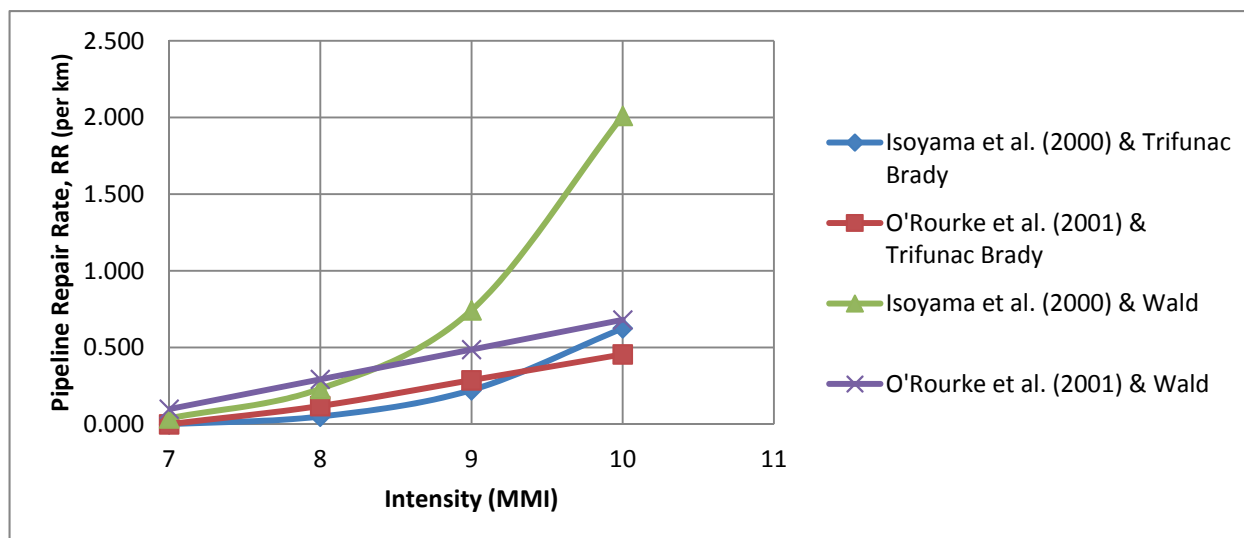


Figure 3.8 Comparison of pipeline repair rate for different Intensity and PGV based fragility relation.

3.7 Comparison of Repair rate

From above analysis a comparison of pipeline repair rate based on PGV and PGA has done and presented in figure 3.9 figure 3.10 & figure 3.11. Although pipe line repair rate of various fragility relations are available but fragility relations based on PGA is more acceptable in context of Bangladesh since all data available are based on PGA. But PGV based fragility relation is more reliable than PGA as discussed in chapter 2.

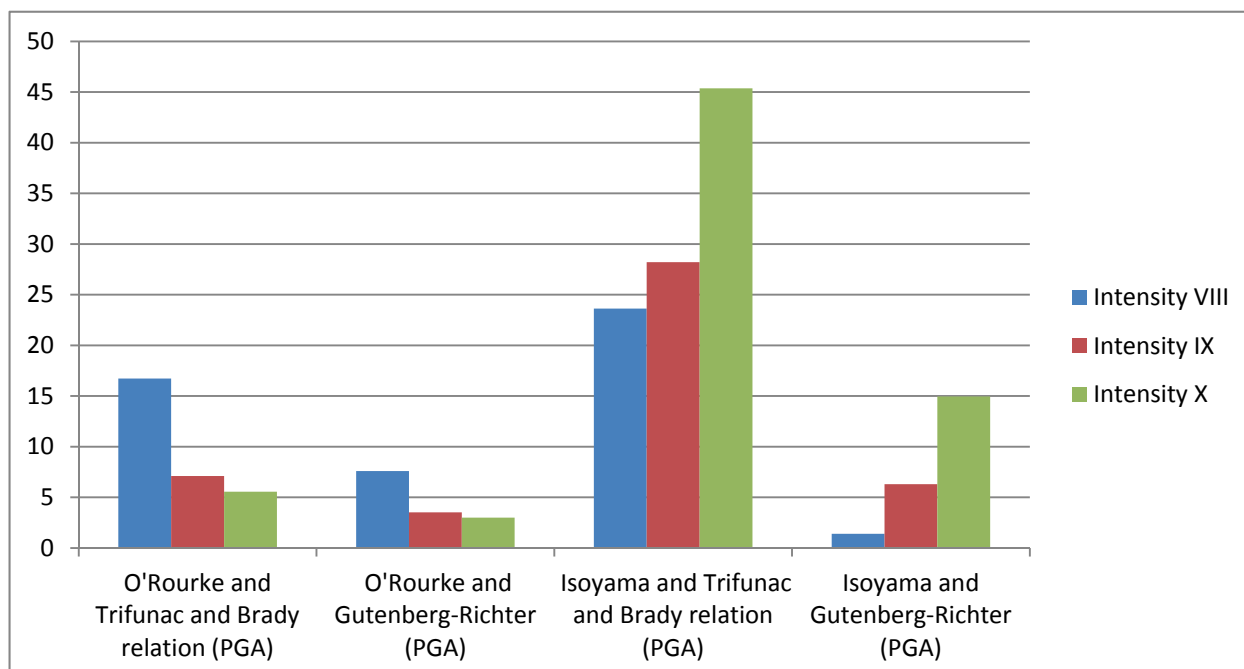


Figure 3.9 Comparison of pipeline repair rate for different Intensity and PGA based fragility relation.

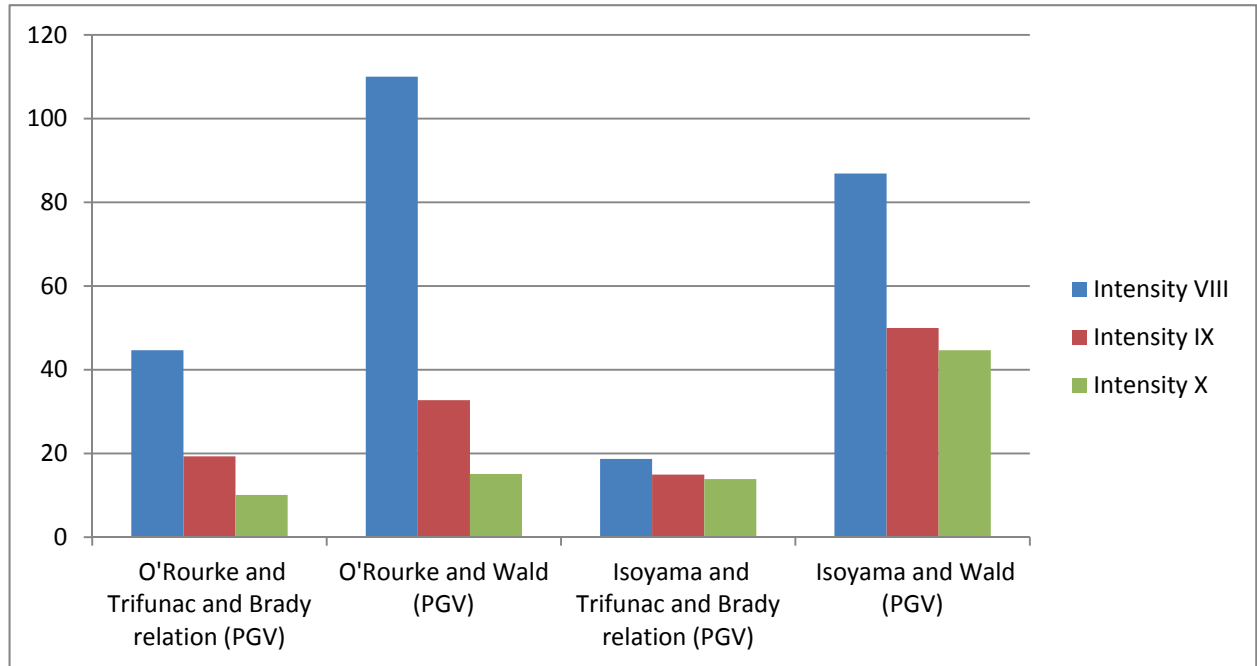


Figure 3.10 Comparison of pipeline repair rate for different Intensity and PGV based fragility relation.

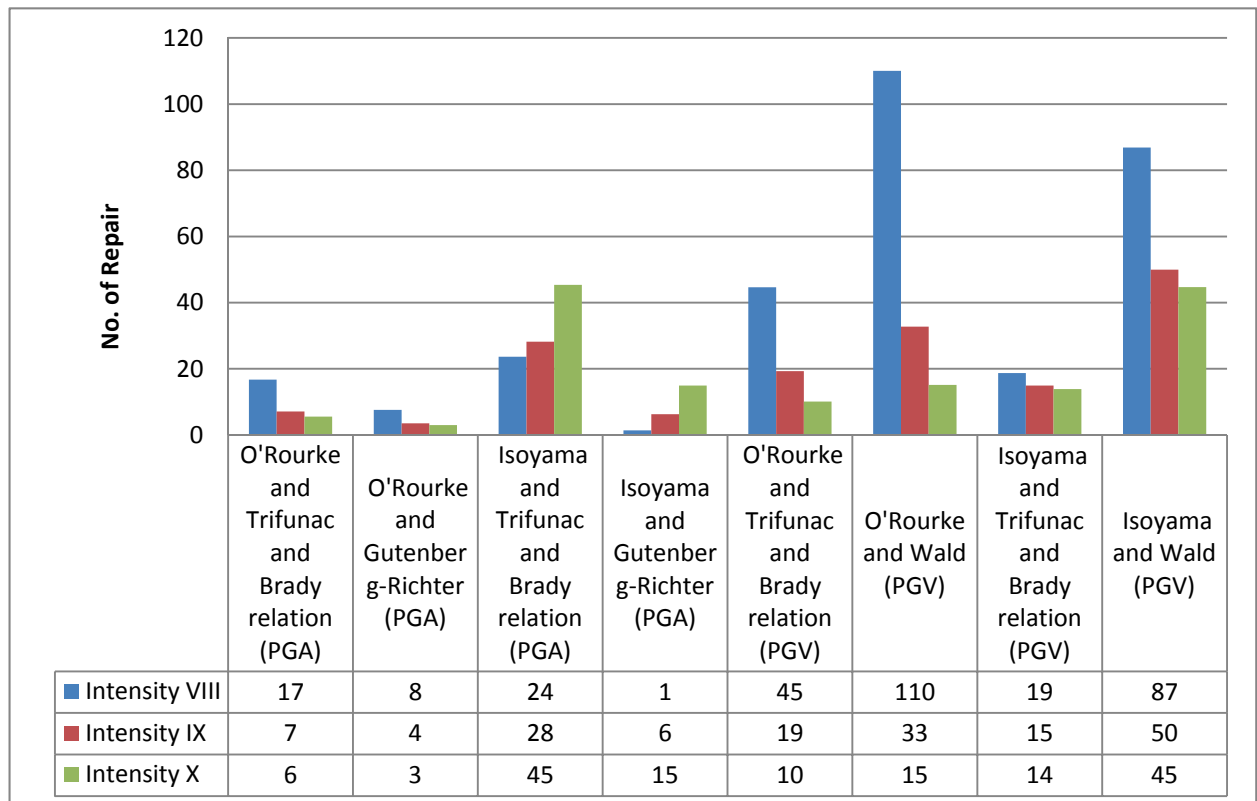


Figure 3.11 Comparison of pipeline repair rate both for PGV & PGA based fragility relation for different Intensity at Dhaka City.

3.8 ESTIMATION OF THE EXPECTED MONETARY LOSSES

In this study only the direct loss is taken into account. The direct loss for the gas pipeline consists of two major parts: (1) The vented gas cost and (2) The repair cost.

3.8.1 THE VENTED GAS COST

Usually repairing the damaged gas pipeline includes welding procedure and grinding for polishing the surface. As the natural gas is explosive, it is necessary to completely vent the pipeline section gas before welding procedure. The isolation and then ventilation tasks are applicable by using Line Break Valve (LBV) among the pipeline in each 20 km. This type of valve has the ability to sense pipeline breaks at the upstream or downstream and shuts off the line immediately in the associated section. In the case of line break or line leak, the closest two LBVs to the damaged joint isolate the pipe section and only the containing gas of this section is vented for the purpose of repairing. Therefore this amount of vented gas is the wasted gas. By assuming the average working pressure of pipeline equal to 55 bars and natural gas as an ideal gas, the wasted gas volume can be calculated as written in Eqn. 4.8

$$V = \frac{\pi D^2}{4} * L * P_{ave}$$

3.8

Where V is the volume of gas with standard pressure (1 bar), D is pipe diameter, L is length of pipe and P_{ave} is average working pressure. Usually pipe having diameter 20 mm to 100 mm is subjected to low pressure as 15 bar (200 psi) and 150 to 200 mm is subjected to relatively high pressure like 55 bars. Considering this the amount of vented gas has been calculated and presented in table 4.10

Table 3.10 Vented gas cost within pipe

Pipe dia (mm)	Length in KM intensity 8	Length in KM intensity 9	Length in KM intensity 10	Volume of gas using equation 4.6 (in cum)
20	10.03	1.27	-	2.34
25	92.33	18.58	10.37	39.23
50	167.02	8.14	-	226.60
75	33.72	5.53	1.43	118.44
100	24.29	4.06	-	146.70
150	23.79	3.35	1.39	1,217.61
200	15.81	19.09	7.09	3,187.39
250	-	1.50	-	177.30
300	-	1.55	1.94	596.00
Total				5,711.59

Cost considering Tk 50/cum is Tk. 2.86 million

3.8.2 THE PIPELINE REPAIR COST

Generally when a pipe is damaged due to ground failure, the type of damage is likely to be a break while when a pipe is damaged due to seismic wave propagation, the type of damage is likely to be leak. In the loss of methodology, it is assumed that damage due to seismic waves will consist of 80% leaks and 20% breaks, while damage due to ground failure will consist of

20% leaks and 80% breaks. As damage due to ground failure is beyond the scope of this work it is assumed that 80% leak and 20% breaks will occur.

Pipeline repair cost is approximately 5 to 7 times more than the construction procedure as a consequence of the mobilization costs, machinery transfer for each repair and lack of time for pressurizing the line after repair to make the line alive. Usually the cost of construction of 300 mm dia pipe is Tk. 12 million/km. This has been found from information of “News watch of National Geographic” and by article published in “Daily Star” analyzing the proposed India Myanmar natural gas pipeline project through Bangladesh. From above rate analysis it is assumed that repair cost for 20mm to 150mm diameter pipe is Tk. 45 million/km and for 200mm to 300 mm diameter pipe Tk.60 million/km. Based on this data pipe line repair cost for both case of PGA and PGV based analysis has been furnished in table 3.11 & 3.12

Table 3.11 Pipe line repair cost from PGA base fragility relations.

Pipe dia (mm)	No of repair	Repair cost / point	Total repair cost (in million of Tk.)
20	2	45,000.00	0.09
25	36	45,000.00	1.62
50	15	45,000.00	0.68
75	9	45,000.00	0.41
100	4	45,000.00	0.18
150	7	45,000.00	0.32
200	24	60,000.00	1.44
250	1	60,000.00	0.06
300	5	60,000.00	0.30
Total			5.09

Total loss is Tk.2.86 million (vented gas) + Tk. 5.09 million (Lline repair) = Tk. 8.00 million for PGA based relation.

Table 3.12 Pipe line repair cost from PGV base fragility relations.

Pipe dia (mm)	No of repair	Repair cost / point	Total repair cost (in million of Tk.)
20	4	45,000.00	0.18
25	57	45,000.00	2.57
50	46	45,000.00	2.07
75	16	45,000.00	0.72
100	10	45,000.00	0.45
150	12	45,000.00	0.54
200	34	60,000.00	2.04
250	2	60,000.00	0.12
300	6	60,000.00	0.36
Total			9.05

Total loss is Tk.2.86 million (vented gas) + Tk. 9.05 million (Lline repair) = Tk. 12.00 million for PGV based relation.

3.9 SUMMARY

The pipeline network is very important for daily life in Dhaka city like elsewhere. It must be kept well maintained, especially to the city. It offers basic need, but it can be greatly damaged by earthquake. In Order to predict the damage of gas pipeline network after earthquake, the fragility curves are very useful means to do so. Different available pipeline fragility relations such as Katayama (1975), O'Rourke (1982), Isoyama and Katayama (1998) and Isoyama (2000) are compared. Finally using two relations namely O'Rourke (1982) and Isoyama (2000) damage rate of pipe lines is determined where PGA/PGV values obtained from Trifunac and Brady, Guutenberg and Richter & Wald MMI-PGA/PGV relations are used.

Pipeline damage rate is expressed in number of repairs per unit length of pipe. No of repairs for both PGA and PGV based fragility relations has been furnished and compared. It has been found that PGV based fragility relation results higher number of repair than PGA.

Any hazard especially earthquake hazard invokes financial involvement. So monetary loss estimation directly related to pipeline damage due to earthquake is a first step to mitigate the risk. This study also presented a picture of monetary loss due to earthquake damage of gas pipeline network for different intensity. Total cost estimated for damage of pipeline is Tk-8.0 million. Though this figure of amount apparently is not large, secondary or indirect loss due to damage of buried gas supply pipelines may be greater, such as interrupted gas supply to business and industrial sectors cause reduction of output. The fire hazard following gas leakage may be tremendous in many cases.



PART-XIII

STRUCTURAL ASSESSMENT OF LIBRARY BUILDING, BUET, DHAKA



BANGLADESH NETWORK OFFICE FOR URBAN SAFETY (BNUS), BUET, DHAKA

Prepared By: Shoeb Ahmed

Mehedi Ahmed Ansary

Structural Assessment of Library Building, BUET, Dhaka

Library building of BUET, Dhaka has been assessed on request of Chief Engineer of BUET with a view to check the recent condition of roof beams as a number of cracks have been seen. This assessment has been carried out by Shoyeeb Ahmed and Mr. Marful Hassan. The cracks are detected by UPV.

According to ACI 224R-90, (Table 4.1) Tolerable crack widths, reinforced concrete:-

Exposure Condition	Tolerable Crack Width (in)	(mm)
Dry air or protective membrane	0.016	0.41
Humidity, moist air, soil	0.012	0.30
Decing chemicals	0.007	0.18
Seawater and sea water spray: wetting and drying	0.006	0.15
Water Retaining Structure	0.004	0.10

***So according to this guideline our tolerable crack width is 0.30 mm

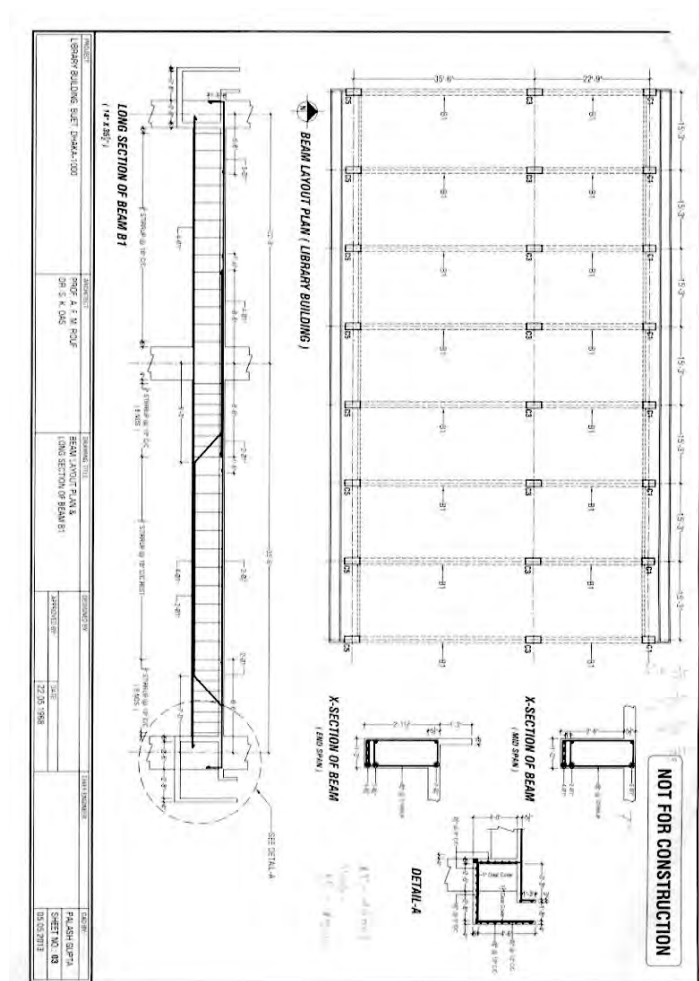


Figure: Structural design of library building (plan)

UPV DATA:-**Beam No. 1:-**

SL.	Beam	Location	X-Section	$t_1(\mu s)$	$t_2(\mu s)$	Depth (mm)	Crack width(mm)	Comments
1	B1	Interior Joint crack	$1'2'' \times 2'$ – $11\frac{1}{2}''$	71.9	140.0	20	0.12	Negligible Crack width

Beam No. 2:-

SL.	Beam	Location	X-Section	$t_1(\mu s)$	$t_2(\mu s)$	Depth (mm)	Crack width(mm)	Comments
2	B2	Shrinkage crack	$1'2'' \times 2'$ – $11\frac{1}{2}''$	89.1	132.9	90	0.12	Negligible Crack width

Beam No. 3:-

SL.	Beam	Location	X-Section	$t_1(\mu s)$	$t_2(\mu s)$	Depth (mm)	Crack width(mm)	Comments
3	B3	At bottom flexural crack	$1'2'' \times 2'$ – $11\frac{1}{2}''$	61.6	97.5	74	0.12	Negligible Crack width

Beam No. 4:-

SL.	Beam	Location	X-Section	$t_1(\mu s)$	$t_2(\mu s)$	Depth (mm)	Crack width (mm)	Comments
4	B4	Shrinkage crack	$1'2'' \times 2'$ – $11\frac{1}{2}''$	124.16	193.9	79	0.12	Negligible Crack width
4		Shrinkage crack		147.7	246.4	61	0.12	Negligible Crack width
4		At bottom flexural crack		76.4	109.8	101	0.12	Negligible Crack width

Beam No. 5:-

SL.	Beam	Location	X-Section	$t_1(\mu s)$	$t_2(\mu s)$	Depth (mm)	Crack width (mm)	Comments
-----	------	----------	-----------	--------------	--------------	------------	------------------	----------

5	B5	At Joint crack	$1'2'' \times 2'$ – $11\frac{1}{2}''$	112.0	169.6	86	0.12	Negligible Crack width
6		Shrinkage crack		148.9	217.8	95	0.22	Moderate Crack width
7		Shrinkage crack		546.9	368.6	91	0.12	Negligible Crack width

Beam No. 6:-

SL.	Beam	Location	X-Section	t_1 (μs)	t_2 (μs)	Depth (mm)	Crack width (mm)	Comments
8	B6	Shrinkage crack	$1'2'' \times 2'$ – $11\frac{1}{2}''$	155.0	269.0	52	0.12	Negligible Crack width
8		Shrinkage crack		98.2	190.6	21	0.12	Negligible Crack width
8		Shrinkage Crack		139.4	196.9	106	0.12	Negligible Crack width
8		Flexural Crack		89.6	147.2	65	0.22	Moderate Crack width

Beam No. 7:-

SL.	Beam	Location	X-Section	t_1 (μs)	t_2 (μs)	Depth (mm)	Crack width (mm)	Comments
9	B7	At Bottom	$1'2'' \times 2'$ – $11\frac{1}{2}''$	82.2	125.3	84	0.12	Negligible Crack width
10		At Joint		80.6	11.7	112	0.12	Negligible Crack width

Beam No. 8:-

SL.	Beam	Location	X-Section	t_1 (μs)	t_2 (μs)	Depth (mm)	Crack width (mm)	Comments
11	B8	Flexural Crack	$1'2'' \times 2'$ – $11\frac{1}{2}''$	99.9	143.9	100	0.12	Negligible Crack width
12		Shrinkage Crack		87.6	164.4	32	0.12	Negligible Crack

								width
--	--	--	--	--	--	--	--	-------

Beam No. 9:-

SL.	Beam	Location	X-Section	t_1 (μs)	t_2 (μs)	Depth (mm)	Crack width (mm)	Comments
13	B9	Flexural Crack	$1'2'' \times 2'$ $- 11\frac{1}{2}''$	67.4	97.5	94	0.12	Negligible Crack width

Beam No. 10:-

SL.	Beam	Location	X-Section	t_1 (μs)	t_2 (μs)	Depth (mm)	Crack width (mm)	Comments
14	B10	Flexural Crack	$1'2'' \times 2'$ $- 11\frac{1}{2}''$	85.5	157.2	38	0.12	Negligible Crack width
14		Shrinkage Crack		83.0	164.4	12	0.12	Negligible Crack width



PART-XIV

NON-DESTRUCTIVE TESTING AT FACTORY BUILDING OF V GARMENTS LIMITED



BANGLADESH NETWORK OFFICE FOR URBAN SAFETY (BNUS), BUET, DHAKA

Prepared By: Pushpendu Biswas

Mehedi Ahmed Ansary

1.0 Introduction

The Deputy General Manager (Admin, HR & Compliance) of Windy Group vide his letter dated 23/12/2013 (Appendix-A) has approached the Director, BRTC, Bangladesh University of Engineering & Technology (BUET), Dhaka for technical assistance and advice of Bureau of Research, Testing and Consultation (BRTC), BUET for undertaking non-destructive testing on their factory site at Ashulia.

It has been agreed that the terms of reference of the work would be limited to collection of concrete cores to determine concrete strength and non-destructive testing of the factory at different levels using Ferro scanning to detect rebars. This report is the outcome of their findings.

2.0 Determination of Concrete Strength by Core Test

Concrete cores have been collected from six locations of the factory building and concrete strength of core has been measured at the BUET Concrete laboratory. The concrete strength of core collected from those locations varies between 2360 and 5120 psi for Brick Aggregates.

Figure 1 shows core cutting locations. The results and location has been included in Appendix-B.

3.0 Rebar Detection for Buildings Using Ferros scanner

Altogether ten locations (columns and roof slabs) have been scanned with ferros scanner machine to check the number and diameter of the steel used in the factory building. Figure 2 shows the position of scanned beams, columns and roof slabs. Figures 3 to 28 show all the results of scanning. At all locations, image scan and line scan have been carried out.

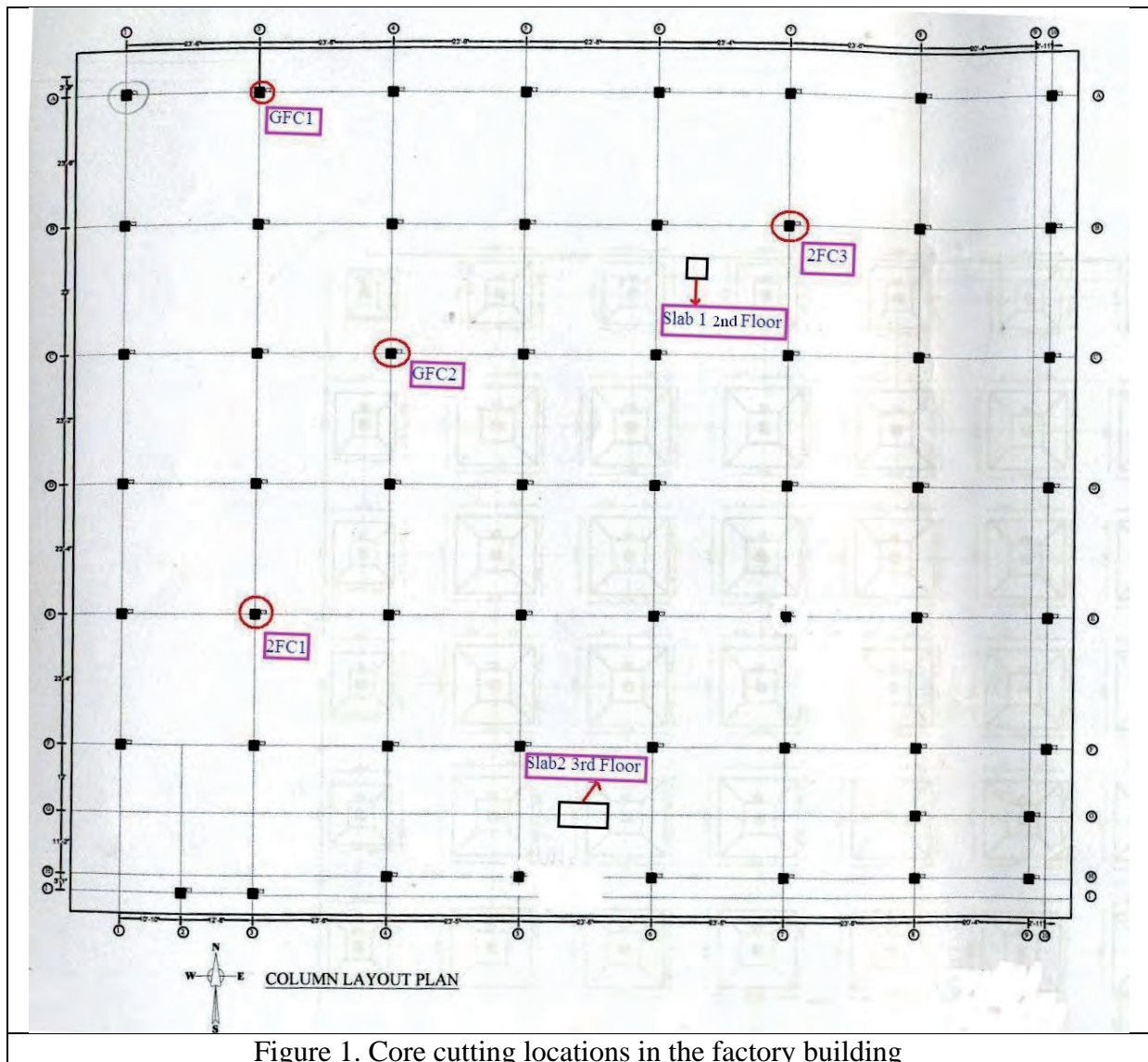


Figure 1. Core cutting locations in the factory building

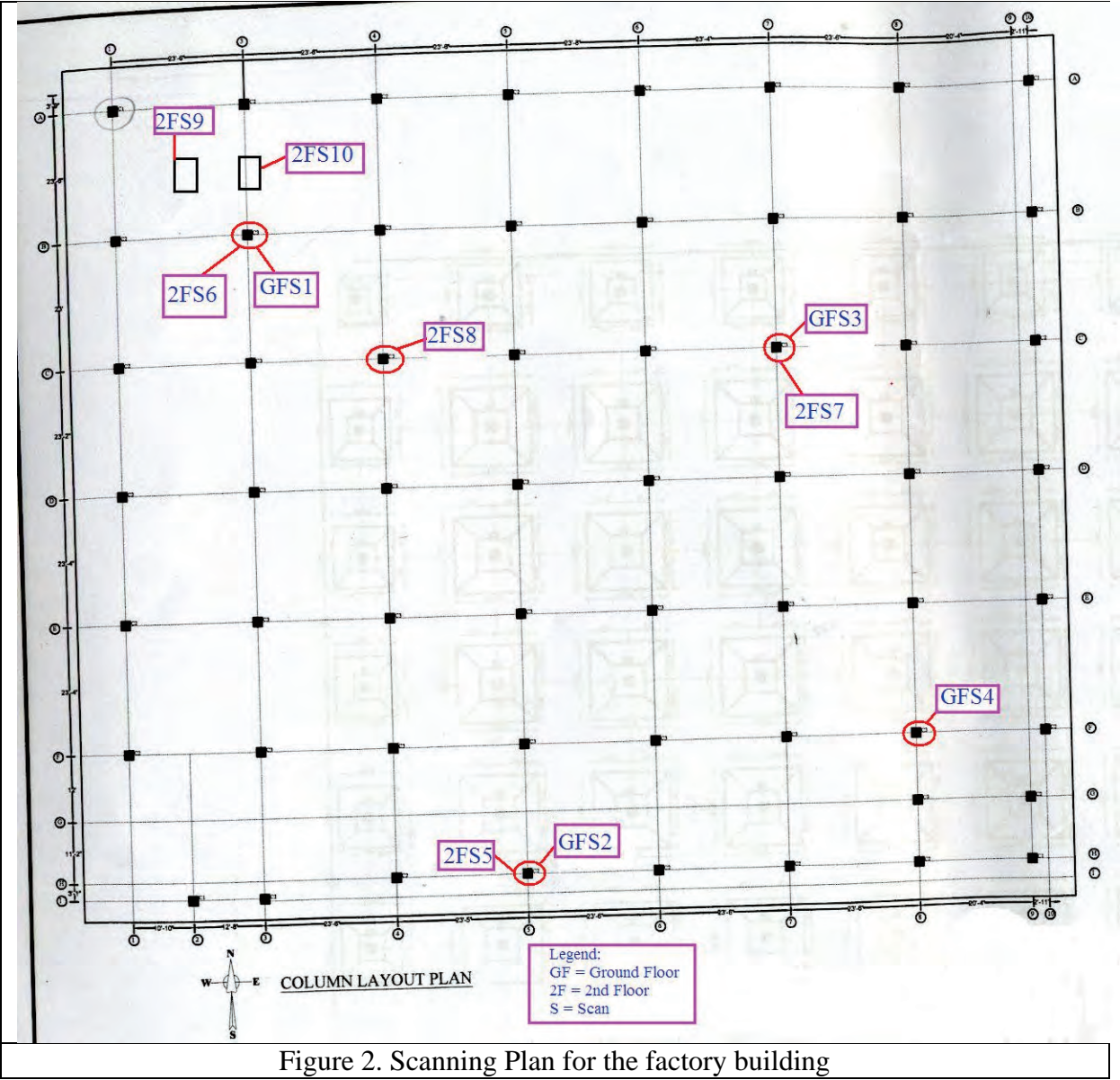


Figure 2. Scanning Plan for the factory building

COLUMNS

Figures 3 and 4 are showing the Image scan result of column GFS-1 (long side and short side respectively) at a height of 4'-2" from the ground. Figure 5 is the cross section of that column.

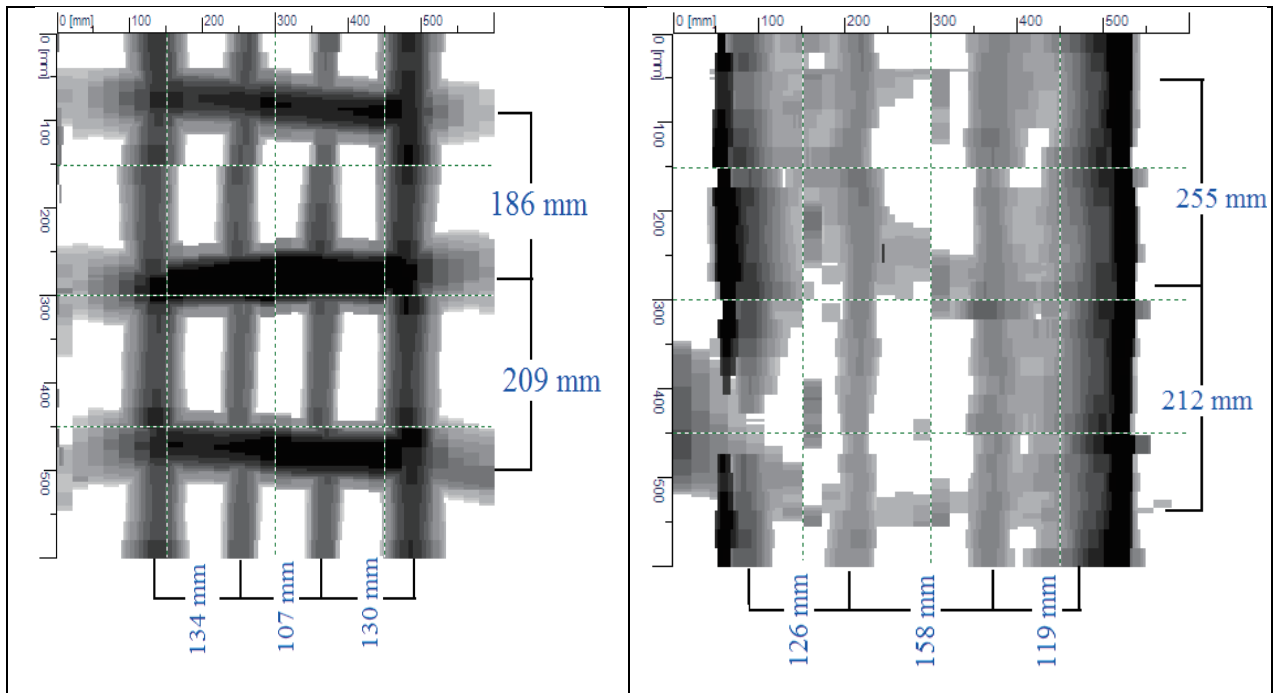


Figure 3 Image scan result of column GFS1 (long side)

Figure 4 Image scan result of column GFS1 (Short side)

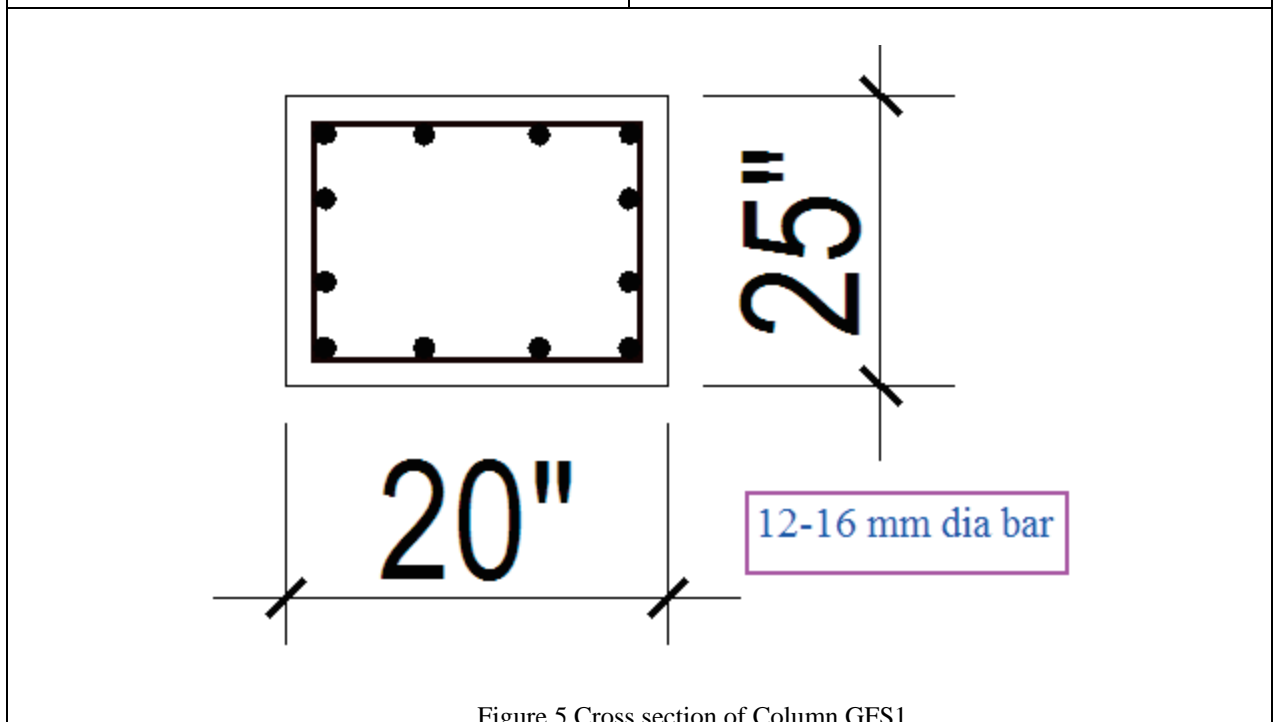


Figure 5 Cross section of Column GFS1

Figures 6 and 7 are showing the Image scan result of column GFS2 (long side and short side respectively) at a height of 1'-10" from the ground. Figure 8 is the cross section of that column.

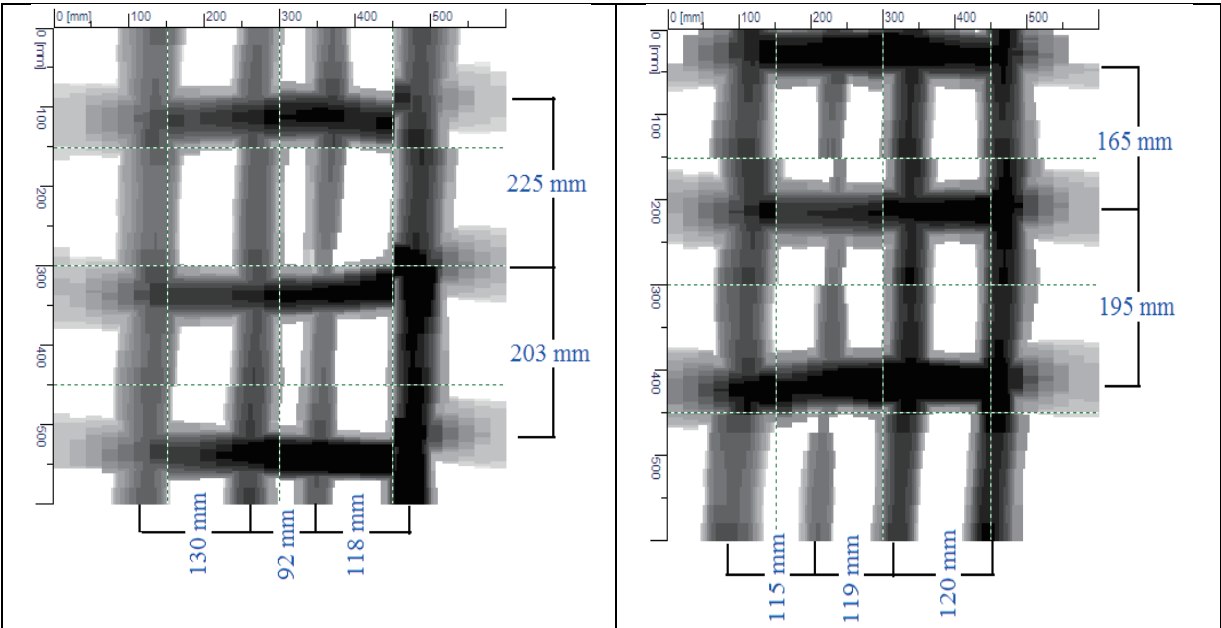


Figure 6 Image scan result of columnGFS2 (long side) Figure 7 Image scan result of columnGFS2 (Short side)

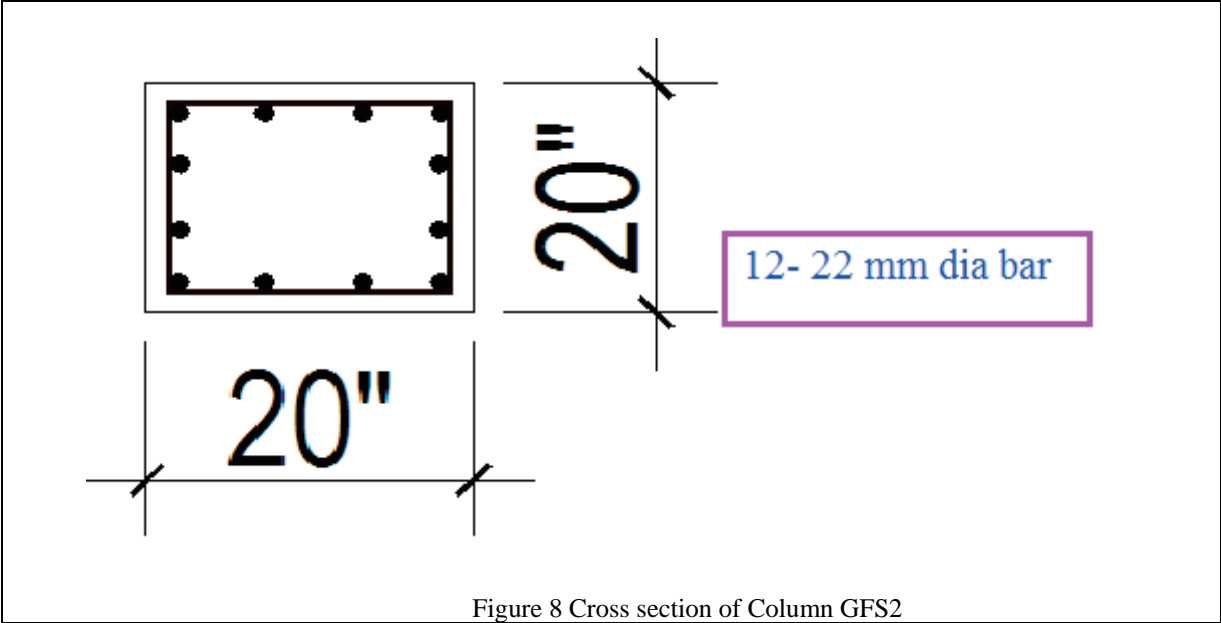


Figure 8 Cross section of Column GFS2

Figures 9 and 10 are showing the Image scan result of column GFS3 (long side and short side respectively) at a height of 3'-0" from the ground. Figure 11 is the cross section of that column.

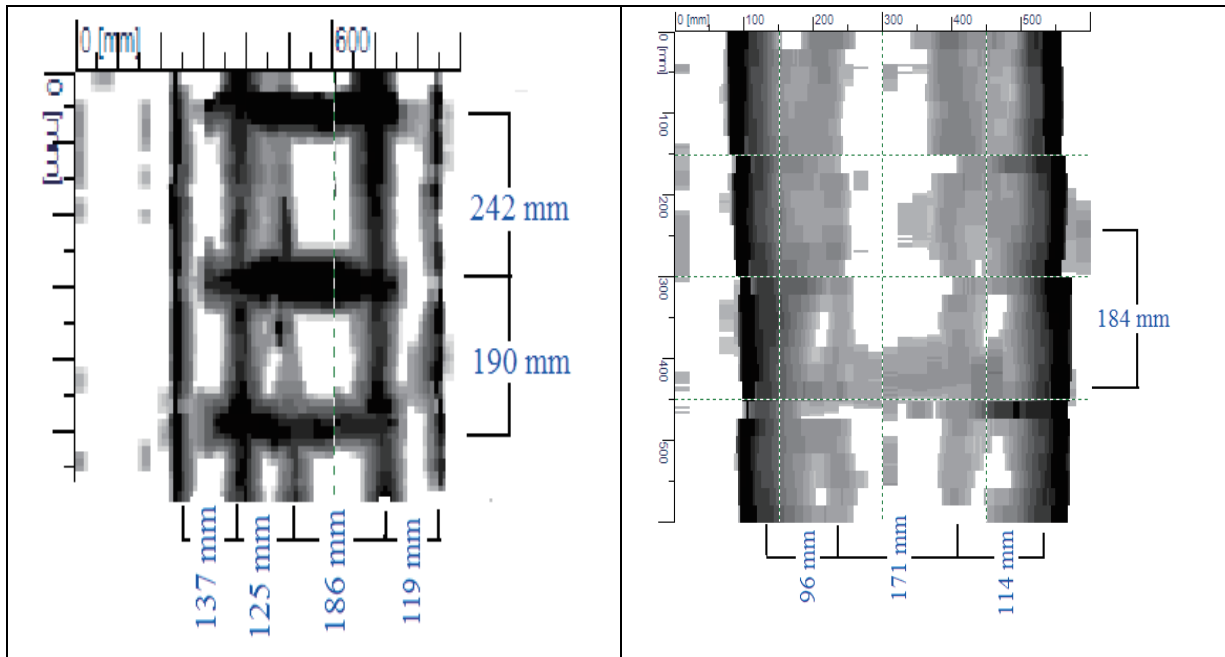


Figure 9 Image scan result of column GFS3 (long side)

Figure 10 Image scan result of column GFS3 (Short side)

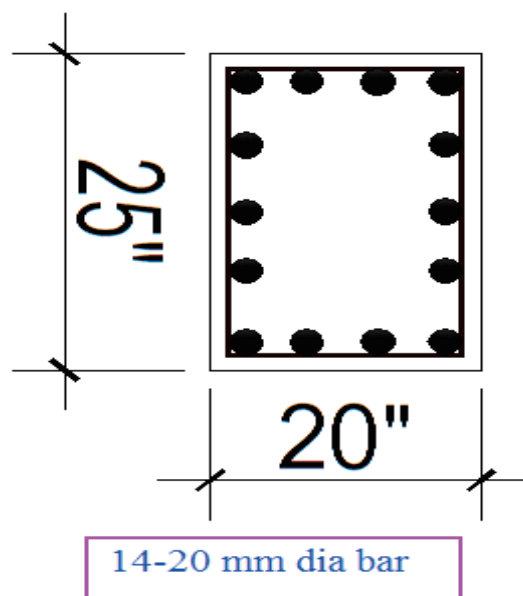


Figure 11 Cross section of Column GFS3

Figures 12 and 13 are showing the Image scan result of column GFS4 (long side and short side respectively) at a height of 3'-0" from the ground. Figure 14 is the cross section of that column.

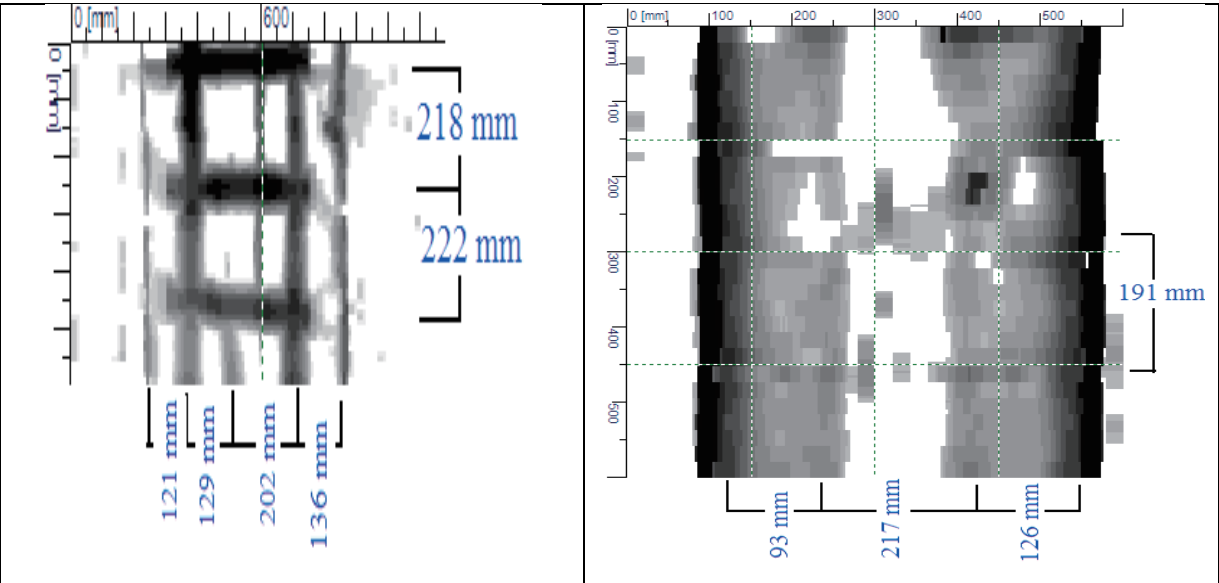


Figure 12 Image scan result of column GFS4 (long side)

Figure 13 Image scan result of column GFS4 (Short side)

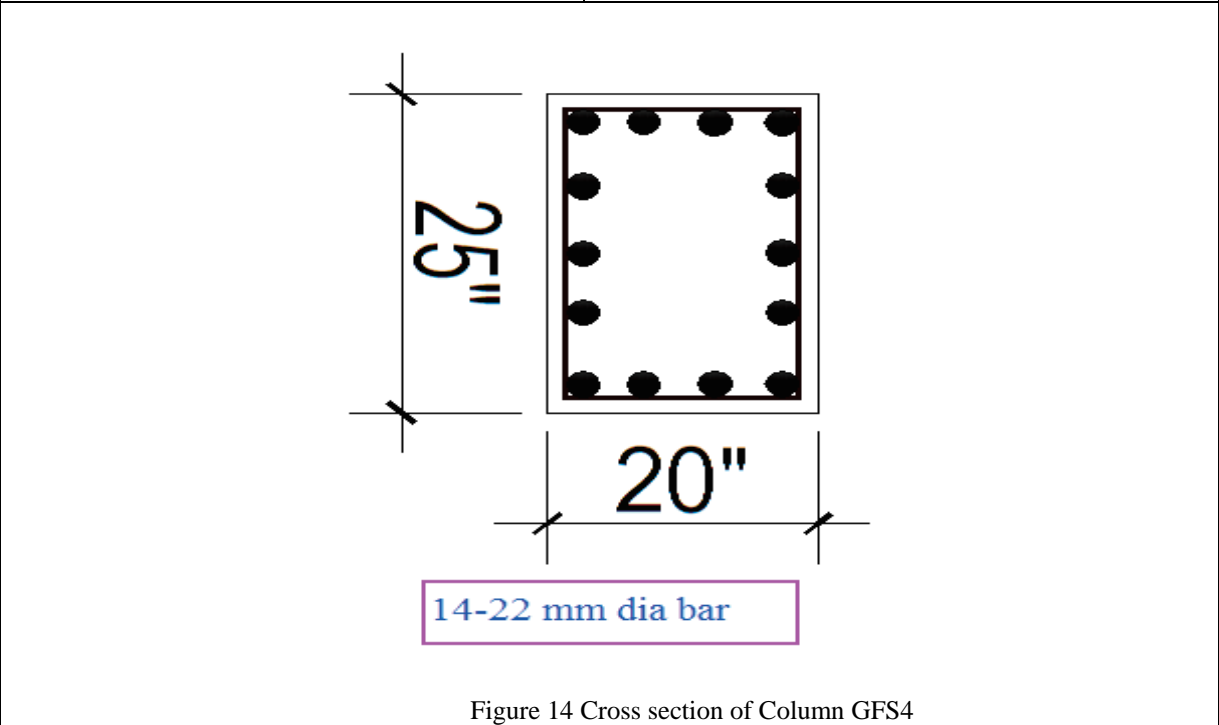
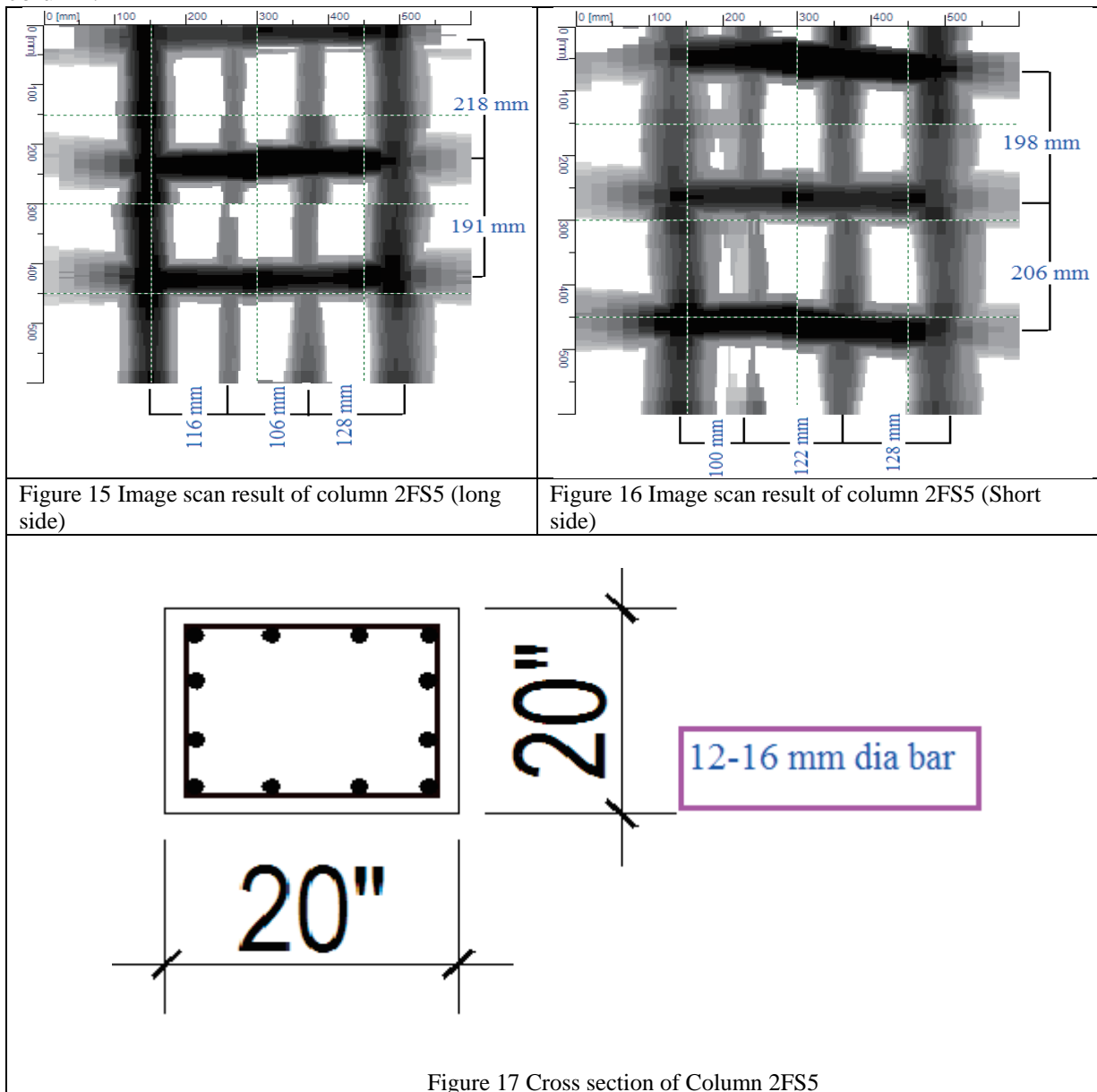


Figure 14 Cross section of Column GFS4

Figures 15 and 16 are showing the Image scan result of column 2FS5 (long side and short side respectively) at a height of 3'-0" from the ground. Figure 17 is the cross section of that column.



Figures 18 and 19 are showing the Image scan result of column 2FS6 (long side and short side respectively) at a height of 3' and 6' respectively from the ground. Figure 20 is the cross section of that column.

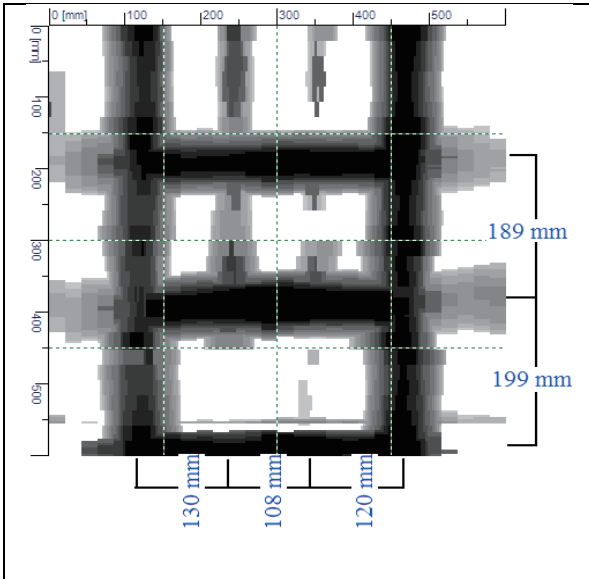


Figure 18 Image scan result of column 2FS6 (long side)

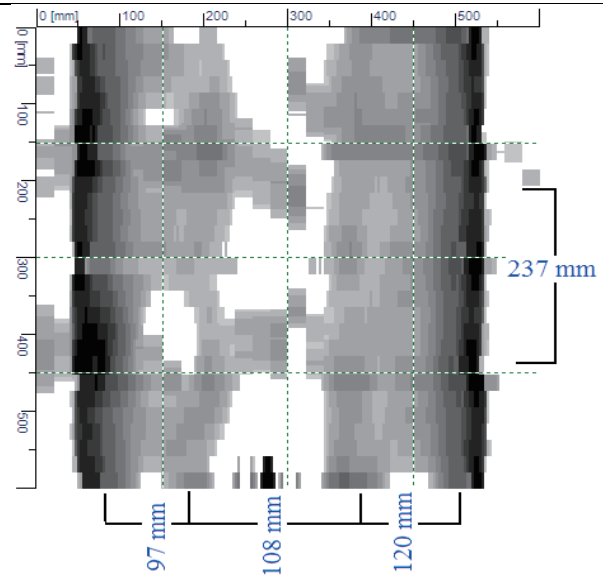


Figure 19 Image scan result of column 2FS6 (Short side)

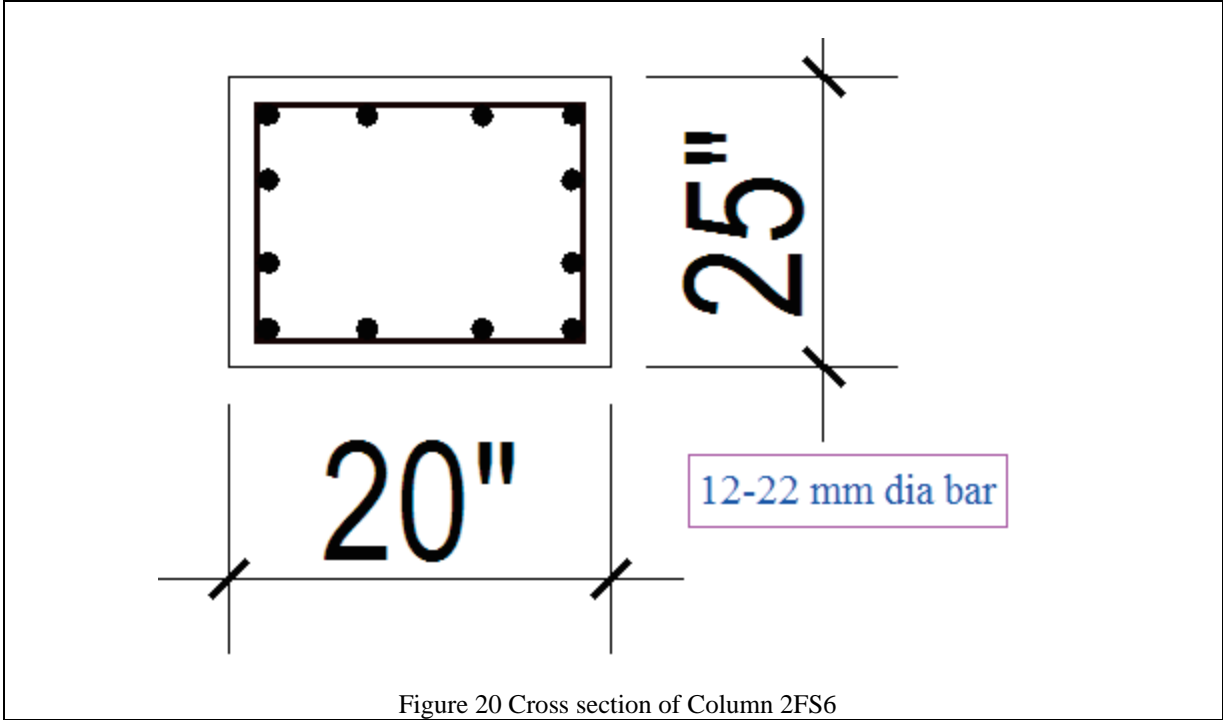


Figure 20 Cross section of Column 2FS6

Figures 21 and 22 are showing the Image scan result of column 2FS7 (long side and short side respectively) at a height of 3' and 6' respectively from the ground. Figure 23 is the cross section of that column.

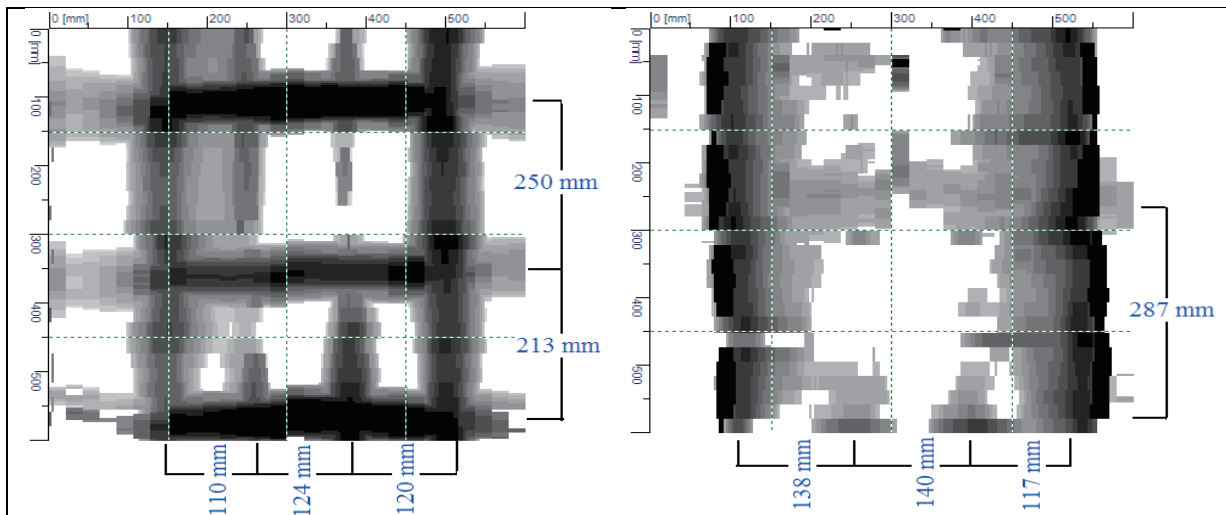


Figure 21 Image scan result of column 2FS7 (long side)

Figure 22 Image scan result of column 2FS7 (Short side)

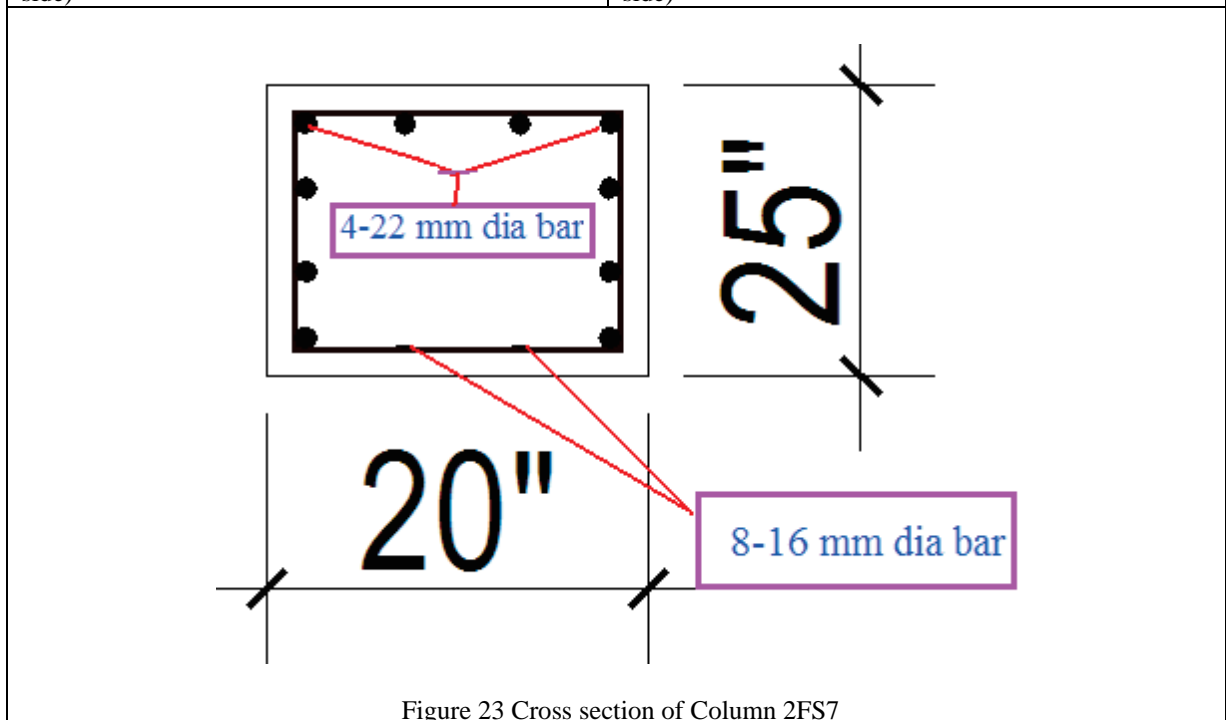
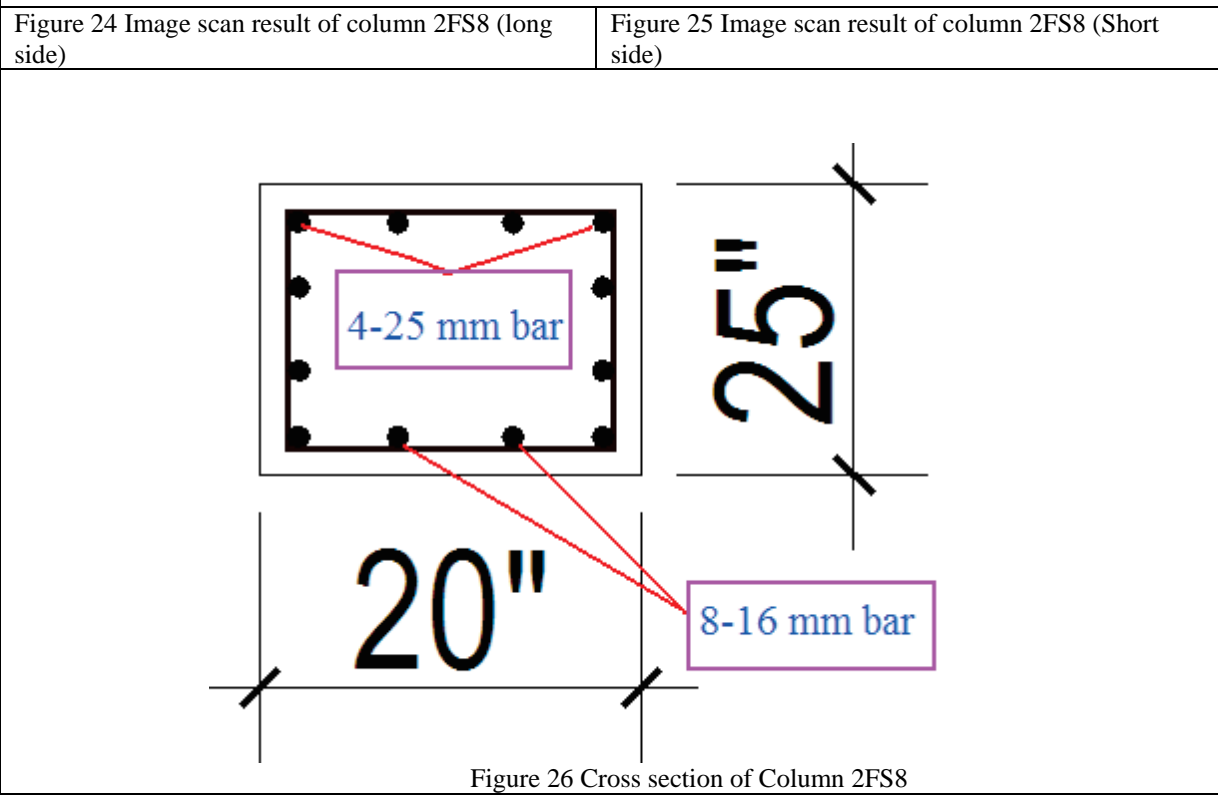
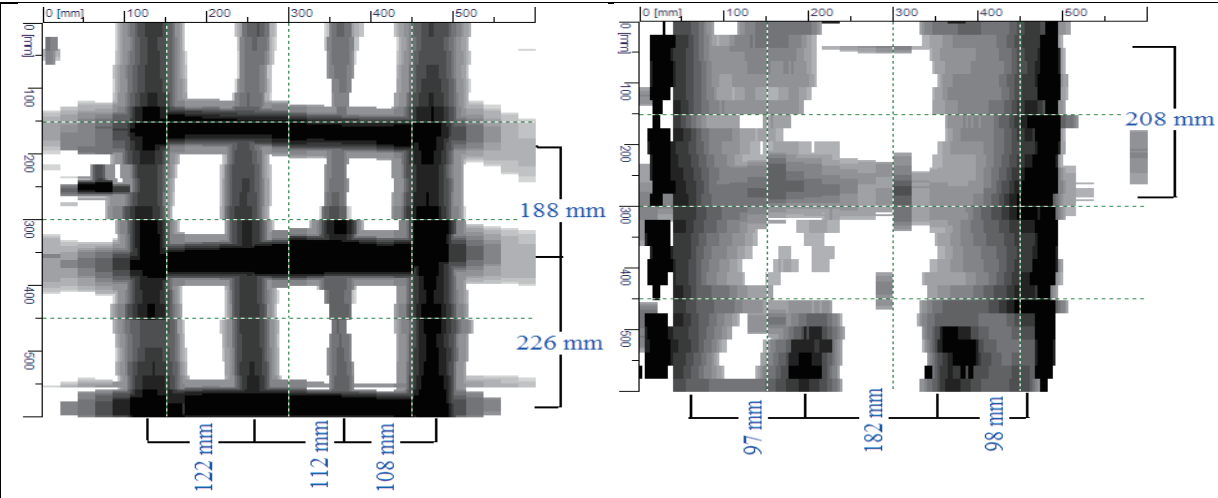


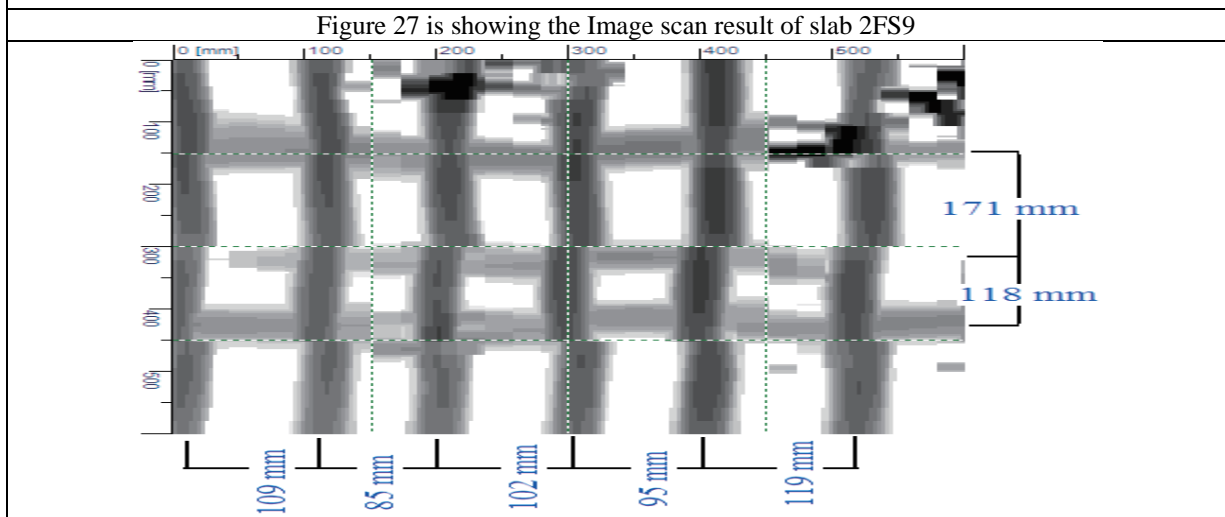
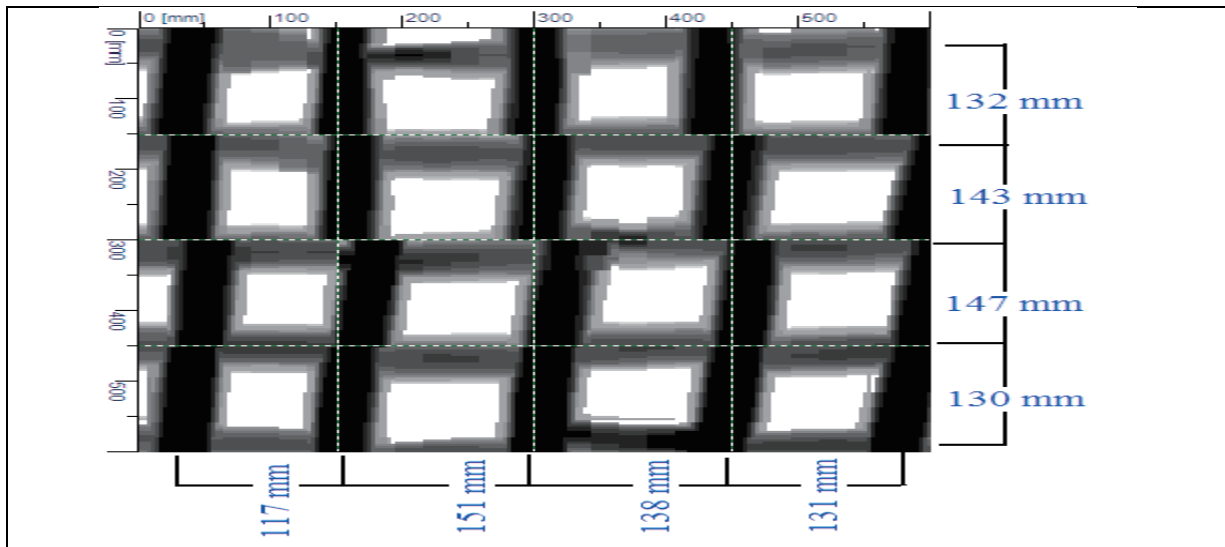
Figure 23 Cross section of Column 2FS7

Figures 24 and 25 are showing the Image scan result of column 2FS8 (long side and short side respectively) at a height of 3’ and 6’ respectively from the ground. Figure 26 is the cross section of that column.



SLABS

Figures 27 and 28 are showing the Image scan result of Slab at locations 1 (2FS9) and 2 (2FS10). The bars in both directions are 10 mm diameter at both slab locations.





PART-XV

MULTIHAZARD VULNERABILITY ASSESSMENT OF WARD 29 IN DHAKA CITY

**BANGLADESH NETWORK OFFICE FOR
URBAN SAFETY (BNUS), BUET, DHAKA**

Prepared By: Naima Rahman

Mehedi Ahmed Ansary

1.INTRODUCTION

Dhaka City is at risk of earthquake and has been experiencing many fire accidents at present and in most cases lack of proper precautionary measures along with the institutional inefficiency, insufficient equipment support and lack of public awareness are making the situation worse. In this study, ward 29, an old part of Dhaka city has been selected for vulnerability assessment of both earthquake and fire. The earthquake vulnerability assessment of buildings has been conducted by two different visual screening methods, i.e. FEMA-RVS and Turkish Simple Survey (Level-I) and fire vulnerability has been conducted by Community Vulnerability Assessment Tool (CVAT). From the opinion of experts weight of factors of vulnerability has been determined by Analytical Hierarchal Process (AHP). Finally vulnerability scores for earthquake and fire have been calculated using Statistical Package for Social Survey (SPSS). From the vulnerability analysis, it has found that about 28.6% buildings are highly vulnerable to earthquake according to RVS (FEMA) and 35.3% are highly vulnerable to earthquake according to RVS (Turkish level I). 78% building are vulnerable to fire.

2.BACKGROUND

According to the World Risk Report prepared by the Geneva-based World Economic Forum (WEF) Bangladesh is the fifth most natural disaster prone country in the world due to lack of adequate mangrove forests and absence of coastal embankment. According to a study conducted by Comprehensive Disaster Management Programme (CDMP) under Ministry of Food and Disaster Management, some 78,323 buildings will be destroyed completely if a 6-magnitude earthquake shakes Dhaka originating from its beneath, causing havoc throughout the densely populated capital city. In case of a 7.5-magnitude earthquake originating from Madhupur Fault, some 72,316 buildings in the city will be damaged totally while 53,166 partially. If an 8.5-magnitude of tremor from the plate boundary of Fault-2 hits the region, some 238,164 buildings will be destroyed completely across the country. CDMP conducted the study from February 2008 to August 2009. There will be an economic loss of about US \$ 1,112 million for only structural damage in case of a 7.5-magnitude earthquake from the Madhupur Fault, it estimates. Economic loss due to damage of structures will be US \$ 650 million and US \$ 1,075 million respectively in case of an 8-magnitude earthquake from the plate boundary-2 and in case of a 6-magnitude earthquake from under Dhaka city. Some 30

million tonnes of debris, equal to 2,880,000 truckloads (25 tonnes for per truck), will be generated if a 6-magnitude earthquake jolts the city from beneath of it. A 7.5-magnitude earthquake from the Madhupur Fault will generate a total of 30 million tonnes of debris, killing some 131,029 people instantly and injuring 32,948 others. According to the study, at least 10 major hospitals, 90 schools in the capital will be destroyed completely and another 241 hospitals and clinics, 30 police stations and four fire stations partially in case of a 7.5 magnitude quake. Bangladesh is situated at a high risk zone for earthquake and an unprecedented human disaster may occur in the city anytime for even a moderate to heavy tremor. A powerful earthquake needs at least 100-150 years to be originated for a particular region and in that sense it is overdue for Bangladesh and parts of Assam, as 112 years have passed by since a heavy tremor from Dawki Fault hit the region. Bangladesh is highly vulnerable to a powerful earthquake. There is need for demolishing old and risky buildings of the city as a first step towards minimizing casualties in such natural disasters. As a number of moderate to heavy earthquakes are overdue for some parts of the country, including the capital, it is important to get ready for the possible disasters by raising safety awareness of people. If a quake of lower magnitude lasts for a minute it may destroy 80-90 percent of the urban concrete structures. Gas leakage management, power supply control, firefighting, alternative power generation, wireless communication system, heavy equipments for removing debris and emergency clinical facilities are the top priority areas for attention. According to a research conducted by Professor Roger Bilham of Colorado State University in the USA, major earthquakes might take place in the sub-Himalayan region, including Bangladesh. Another study of Michigan University has pinpointed that Dhaka is one of the earthquake vulnerable city out of top cities because of its unplanned urbanization. A strong earthquake of 8.6-magnitude occurred in Assam on August 15 in 1950, killing 1,526 people. Another 8.1-magnitude quake hit Assam on June 12 in 1897, killing 1,500 people. The casualties were less because of low density of population and fewer numbers of concrete structures at that time (The daily star, 2010).

The historical seismicity and recent tremors occurred in Bangladesh and adjoining areas indicate that the country is at high seismic risk. Recently, a series of earthquakes has been experienced throughout the country. The existing urban trend and urbanization process of Bangladesh have caused increased vulnerability to natural disasters like earthquake. The risk in urban center is compounded due to unplanned urbanization and development in high risk zones. Dhaka, the capital of Bangladesh is the center of economy, commerce, politics, etc.

and accommodates a large estimated population of 12.8 million in the wider metropolitan area while the population of Dhaka city stands at approximately 7.0 million as of 2008 (BBS, 2009). According to a report published by United Nations IDNDR-RADIUS Initiatives, Dhaka and Tehran are the cities with the highest relative earthquake disaster risk (Rahman, 2004). Although no moderate to large earthquake has struck Dhaka city in historical past, it experiences minor tremors almost all the year round which indicates the region to be seismically active (Khan, 2004).

Dhaka is vulnerable to earthquake due to high population density, vulnerable structures, low preparedness of people etc. Particularly the older part of the city is relatively more vulnerable to earthquake due to its relatively high density of population e.g. the projected density of population in Kotwali Thana, a major part of Old Dhaka is 1,61,198 per square kilometer in 2009 (BBS, 2001). Besides, the densely built fabric consisting of vulnerable, aged, non-reinforced masonry buildings along with narrow local streets make the locality more earthquake disaster prone.

Earthquake is a cataclysmic event that needs to be addressed in a more concerted way. An important aspect of preparedness for an earthquake is evaluating the building stock particularly in terms of structural vulnerability. When the vast majority of properties do not meet the earthquake resistance standards in the design of buildings, it exposes the occupants to the risk of injury or death arising from the building collapse in the event of a major earthquake. Earthquake induced large destruction occurs due to vast majority of properties not meeting the earthquake resistant standards in building design. One of the reasons for the high level of destruction is the poor building quality particularly of residential in nature. As part of earthquake preparedness, it is essential to undertake a structural vulnerability assessment of properties to determine its resistance level in earthquake and advice necessary steps, such as retrofitting, to rectify any deficiencies. These initiatives will benefit the community providing safeguards from earthquakes as well as the preparedness and technology to address other catastrophes.

Table 1: Major historical earthquakes affecting Dhaka

Name of Earthquake	Magnitude	Intensity at Dhaka	Distance between Epicenter and Dhaka (Km)
Cachar Earthquake, 1869	7.5	V	250
Bengal Earthquake, 1885	7.0	VII	170
Great Indian Earthquake, 1897	8.7	VIII+	230
Srimangal Earthquake, 1918	7.6	VI	150
Dhubri Earthquake, 1930	7.1	V+	250

Source: Ansary, 2006

Once a great earthquake occurs, Dhaka may suffer immense loss of life and property due to unplanned city development. This will have severe long term consequences for the entire country. Damaged structures are the main cause of human injury and death. Earthquake vulnerability assessment of an area put a remarkable importance in proposing an effective evacuation plan considering the prevailing local condition and in any disaster mitigation measures such plan is of utmost importance in reducing the loss to a great extent. The evacuation plan can make the locality self-dependent in coping with a disaster to minimize the risk in time. This research will study the present scenario of the study area, assess the earthquake vulnerability and propose an evacuation plan for the community.

Along with earthquake fire hazard has become a major issue of concern as Dhaka City has been experienced a number of notable fires in the recent years. A report of Bangladesh Fire Service and Civil Defense (BFSCD) shows a rising trend in the number of fire incidents in the Dhaka City (table 2). Dhaka the capital of Bangladesh often faces fire hazards due to its dense building concentrations, narrow roads, flammable building materials, aging water supply and electrical wire, chemical factory in residential areas as well as the lack of preparedness and response skills among local people and the fire authority. The annual monetary loss due to fire accidents is very high in Dhaka City compared with the other urban centers in Bangladesh because of its high concentration of economic activities (table 2).

Table 2: Year-wise number of fire incidents and economic loss

Year	Number of Incident	Economic Loss (in Million Dollar)
2003	1861	13.8
2004	2053	26.7
2005	2279	34.1
2006	1220	29.8
2007	1100	21.6
2008	1110	7.1
2009	1775	11.6
2010	2068	13.4

Source: BFSCD report 2010.

Moreover, fire incidents in shops, industrial and commercial buildings cause heavy toll of life and property. In the recent time, there were huge losses of property due to some big fire incidents in the garments factories. The major causes of those incidents were non-compliance of government's fire fighting and extinguishing law 2003. Besides, disasters in many family lives, such fire incidents also tarnished image of the country. Unplanned urbanization and rapid industrialization are the major causes of a huge number of fire related accidents inflicting colossal damage to lives and property in the country every year. According to a report on Role of Fire Services in Mitigating Losses in Fire Related Incidents, the major accidents occur in readymade garment (RMG) factories that have been flourishing in the country since early nineties. Over 350 garment workers have died and some 1,500 been injured in fire-related incidents since 1990 (The Daily Star, 2006).

In 3rd June 2010, a devastating fire broke out in the densely-populated part of Old Dhaka city at Nimtoli. Fire killed at least 117 people and caused injury to a hundred people. Most of the affected peoples were women and children. Initially it was thought that explosion of two transformers at Nimtoli started the fire but later it has been known the fire originated from an oil stove and spread to the chemical warehouses nearby and resulted high casualties and damages.

Two back to back fires occurred in 15th and 16th January 2012 in Islambag and Lalbag areas in Ward 65 in Old Dhaka. The first incident occurred in a plastic warehouse near the Eidgah ground in West Islambag at around 10:45 PM started from a gas stove. The next day again at the same time another fire occurred in Shahid Nagar area at Lalbag around 10:30 PM. In this case fire originated from a tin shed house. Around 100 shanties, five shops and a printing press caught by fire. (BNUS field Survey, 2012).

This is a common situation in Old Dhaka where most of the buildings have small factories like chemical, plastic, rubber etc. and Warehouse and food shops up to second floor of the residential building. In Old Dhaka no house is equipped with fire fighting equipments like extinguisher, hose pipe etc. They don't have sufficient width of staircase let alone the emergency exit. In this respect, assessment of fire hazard vulnerability in Dhaka City especially in the old part is very important. The old part 'Puran Dhaka' is the most vulnerable area in Dhaka City. In this study Ward 29 (Map 2) of Old Dhaka is selected for the vulnerability assessment. This ward is one of most vulnerable to fire hazard than other because

of its traditional land use and population density. Fire incidents are very common phenomenon in this area. It is also one of the oldest areas of Dhaka City. This ward is mainly used as manufacturing industrial area. Besides several land uses like Warehouse, commercial use, chemical shop, clamber storage and processing shops are also prominent. Land use of this area makes it more unique than the other area of Dhaka City. In this study, assessment of fire hazard vulnerability of the community has been conducted to examine the existing risk of fire in the area and prepare the residents to face this sort of disaster.

Fire is considered as the most common secondary hazard of earthquake (Horwich, 2000), so it is important to assess the integrated vulnerability of fire and earthquake because of their close association. A number of researches have been carried out on fire and earthquake in Dhaka City Corporation (DCC). In a study, Old DCC is categorized into different fire hazard zones according to the frequency of fire incidence (Alam, 2004). About 53% buildings of Ward 68 (Old DCC) are vulnerable to earthquake (Jahan, 2011). But none of the studies focused the integrated vulnerability of fire and earthquake hazard. In this research, an integrated vulnerability assessment of Ward No. 29 in Dhaka South City Corporation (DSCC) will be conducted incorporating both fire and earthquake hazard.

3.METHODOLOGY

The research has been conducted with the following methodology:

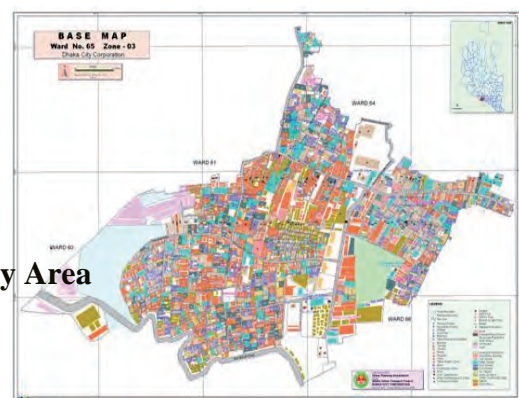
3.1 Selection of the Study Area

Ward No. 29 of DSCC which is selected for the vulnerability assessment of fire and earthquake in this research. This ward is one of the oldest areas in the city with 58233 populations (BBS, 2011) in 0.457 square kilometer area (GIS map). A common scenario of this ward is mixed land use (15.3%) of buildings where most of these have small factories like chemical, plastic, rubber etc., warehouse and small shops up to second floor and residence at upper floors (GIS map). This ward is mainly comprised of manufacturing and processing industries of plastic, warehouses of chemical and unprocessed leather. As a result, fire incident is very common phenomenon in this area (Rahman, 2012). Being the one of the oldest parts of the city, no house is equipped with fire fighting equipments like extinguisher, hose pipe etc. and sufficient accessibility to the adjacent road and staircase for emergency exit of people (Islam, 2008). According to a microzonation map of Dhaka City, the study area

is located in zone 2 with earthquake intensity of IX (Map 1). So a small scale earthquake may cause disaster in this ward.



Map 1: Microzonation Map of Dhaka City considering Earthquake Hazard (Rahman, 2004)



Map 2: Ward 29

3.2 Sampling

The total number of buildings of Ward 65 is 3,210. For these sample size, survey of 343 buildings will be conducted by stratified sampling procedure keeping the confidence level at 95% and confidence interval is 5. Stratification of sample will be chosen according to the percentage of construction type, number of storey and structure use of the study area. Socioeconomic survey will be conducted by random sampling to know social vulnerability of fire and earthquake in the study area. The total number of household in the study area is 13,123. But survey of households living in 343 sample buildings will be conducted to investigate the overall condition of each building.

3.3 Data Collection

Base map of the study area will be collected from Dhaka City Corporation (DCC) in both hard copy and GIS shapefile. Field survey of the buildings will be conducted on the basis of the DCC base map by checklist. Based on field survey GIS map will be edited. Characteristics of building such as construction type, land use, number of storey, floor area, land area, age of building, having fire source, having pounding effect, soft storey, soft column etc will be identified by the building survey. Socio-economic survey will be conducted by questionnaire to know age, gender, income level, education level, awareness of local people and number of disable people etc in the study area. Focus group discussion (FGD) will be conducted to know the view of local people to adopt various risk reduction strategies of fire and earthquake in their locality. The focus group will be community based organization (CBO), local government representatives, NGOs, cooperative societies, and governing bodies of mosque, madrasa and schools etc.

3.4 Data Analysis

The data obtained through field survey would be classified, tabulated and presented in the form of maps, tables and graphs by using MS-Excel and SPSS for processing and analysis of the collected data and to end up with meaningful results. ArcGIS 10 would be used for mapping hazard zones. To assess the community vulnerability of fire hazard of Ward 29 in Old Dhaka, Community Vulnerability Assessment Tool (CVAT) will be used (Flax, 2002). The earthquake vulnerability assessment of buildings will be conducted by two different visual screening methods, i.e. FEMA-RVS (FEMA 154, 2002) and Turkish Simple Survey (Level-I) procedure (Sucuoglu and Yazgan, 2003). The results of fire and earthquake vulnerability assessments will be integrated using opinion of fire and earthquake experts. A panel of at least 10 to 15 experts of fire and earthquake expert will be consulted to determine the combined vulnerability score of fire and earthquake. Weight of factors of vulnerability will be determined by Analytical Hierarchal Process (AHP). Findings of focus group discussion will be compiled to develop risk reduction strategy which is acceptable to the local people and community.

3.4.1 Earthquake vulnerability analysis

The vulnerability assessment of the existing buildings was done following two different visual screening methods, i.e. FEMA-RVS and Turkish Simple Survey (Level-I) procedure that are universally accepted for quick assessment of the buildings. In Bangladesh both of the methods are well accepted considering the physical context of the region. The basic scores of the buildings found in the two methods suggest whether the building should perform well in a seismic event or require further investigation by an experienced seismic design professional. Thus the safest buildings are segregated from those needed more detailed structural analysis. In this study the building vulnerability assessment survey was conducted by the fresh graduated students in civil engineering. So data authentication can be ensured up to a limit. The detailing of the used survey procedures are discussed in the following sections.

3.4.1.1 FEMA- Rapid Visual Screening (RVS) method

The Federal Emergency Management Agency (FEMA) of the United States of America has developed pre-earthquake screening method of potential seismic hazard assessment of buildings based on rapid visual screening method, widely known as RVS method, originated in 1988, with the publication of the FEMA 154 Report, a Handbook. It is generally used for rapid evaluation of seismic vulnerability profiles of existing building stocks. RVS provides a procedure to identify record and rank buildings that are potentially seismically hazardous (FEMA 154, 2002).

RVS method is used to quickly determine if detail evaluation of existing building is required. The rapid visual screening method is designed to be implemented without performing any structural calculations. The objective of these methods is to identify, make inventory and rank all high-risk buildings in a specified region so that a strategy of priority based interventions to buildings can be formed. Although RVS is applicable to tall buildings, its principal purpose is to identify:

- Older buildings designed and constructed before the adoption of adequate seismic design and detailing requirements.
- Buildings on soft or poor soils, or
- Buildings having performance characteristics that negatively influence their seismic response.

This screening methodology is encapsulated in a one page form, which combines a description of a building, its layout and occupancy, and a rapid structural evaluation related to its seismic hazard. This procedure requires only visual inspection and limited data collection. The inspection, data collection and decision-making process typically occurs at the building site. It is a “sidewalk survey” approach that enabled users to classify surveyed buildings into two categories: those acceptable as to risk to life safety or those that may be seismically hazardous and should be evaluated in more detail by a design professional experienced in seismic design. Once identified as potentially hazardous, such buildings should be further evaluated by a design professional experienced in seismic design to determine if, in fact, they are seismically hazardous.

The Data Collection Form of RVS includes space for documenting building identification information, including its use and size, floor area, etc., a photograph of the building, sketches- building plan and elevation and documentation of pertinent data related to seismic performance, including the development of a numerical seismic hazard and vulnerability score. The scores are based on the expected ground shaking levels in the region as well as the seismic design and construction practices for the city or region. The scores use probability concepts and are consistent with the advanced assessment methods. Basic Structural Hazard Scores based on Lateral Force Resisting System for various building types are provided on the form, and the screener circles the appropriate one. The screener modifies the Basic Structural Hazard Score by identifying and circling Score Modifiers related to observed performance attributes, by adding (or subtracting) them a final Structural Score, ‘S’ is obtained.

The score below which a structure is assumed to require further investigation is termed as “cut-off” score. The value of “cut off” score and choice of RVS form depends on the seismic zonation of the area. It is suggested that buildings having an S score less than the “cut-off” score should be investigated by an experienced seismic design professional experienced in seismic design. If the obtained “final score” is greater than the “cut-off” score the building should perform well in a seismic event. According to FEMA 154 a “cut-off” score of 2 is used in this study. According to the experts, considering the existing site condition it can be assumed that such a large number of buildings may not be vulnerable if an earthquake hits and so 1.5 can be considered as a “cut-off” score.

The Rapid Visual Screening (RVS) method is less time consuming respective to the Turkish screening method. The RVS methodology is not intended for structures other than buildings. For important structures such as bridges and lifeline facilities, the use of detailed evaluation methods is recommended. Even in urban areas, some very weak forms of non-engineered buildings are well-known for their low seismic vulnerability and do not require RVS to estimate their vulnerability. These building types are also not included in the RVS procedure.

Use of RVS results

The results from rapid visual screening can be used for a variety of applications that are an integral part of the earthquake disaster risk management program of a city or a region. The main uses of this procedure are:

- To identify if a particular building requires further evaluation for assessment of its seismic vulnerability.
- To rank a city's or community's (or organization's) seismic rehabilitation needs.
- Design seismic risk management program for a city or a community.
- Plan post-earthquake building safety evaluation efforts.
- Develop building-specific seismic vulnerability information for purposes such as regional rating, prioritization for redevelopment etc.
- Identify simplified retrofitting requirements for a particular building (to collapse prevention level) where further evaluations are not feasible.
- Increase awareness among city residents regarding seismic vulnerability of buildings.

Classification of damage to buildings

The likely damage has been categorized in different grades depending on their impact on the seismic strength of the building. The different damage levels that have been recommended by European Macro Seismic Scale (EMS-98) are described in Table 3 Table 4 provides guidance regarding likely performance of the building in the event of design-level earthquake; this information can be used to decide necessity of further evaluation of the building using higher level procedures. It can also be used to identify need for retrofitting and to recommend simple retrofitting techniques for the ordinary buildings where more detailed evaluation is not

feasible. Generally the score $S < 0.7$ indicates high vulnerability requiring further evaluation and retrofitting of the building.

The damage classification based on the European Macro Seismic Scale (EMS-98) define building damage to be in Grade 1 to Grade 5. The damage classification helps in evaluation of earthquake intensity following an earthquake. They are used in RVS to predict potential damage of a building during code level earthquake.

Table 3: Classification of damage to buildings

Classification of damage to masonry buildings	Classification of damage to reinforced concrete buildings
Grade 1: Negligible to slight damage (No structural damage, slight non-structural damage) Hair-line cracks in very few walls. Fall of small pieces of plaster only. Fall of loose stones from upper parts of buildings in very few cases.	Grade 1: Negligible to slight damage (No structural damage, slight non-structural damage) Fine cracks in plaster over frame members or in walls at the base. Fine cracks in partitions and infills.
Grade 2: Moderate damage (Slight structural damage, moderate non-structural damage) Cracks in many walls. Fall of fairly large pieces of plaster. Partial collapse of chimneys and mumpstys.	Grade 2: Moderate damage (Slight structural damage, moderate non-structural damage) Cracks in columns and beams of frames and in structural walls. Cracks in partition and infill walls; fall of brittle cladding and plaster. Falling mortar from the joints of wall panel.
Grade 3: Substantial to heavy damage (Moderate structural damage, heavy non-structural damage) Large and extensive cracks in most walls. Roof tiles detach. Chimneys failure at roof line; failure of individual non-structural elements. (partitions, gable walls etc)	Grade 3: Substantial to heavy damage (Moderate structural damage, heavy non-structural damage) Cracks in columns and beam-column joints of frames at the base and at joints of coupled walls. Spalling of concrete cover, buckling of reinforced bars. Large cracks in partition and infill walls, failure of individual infill panels.
Grade 4: Substantial to heavy damage (Moderate structural damage, heavy non-structural damage) Serious failure of walls. Partial structural failure of roofs and walls.	Grade 4: Substantial to heavy damage (Moderate structural damage, heavy non-structural damage) Large cracks in structural elements with compression failure of concrete and fractures of rebars. Bond failure of bars, tilting of columns. Collapse of a few columns or of a single upper floor.
Grade 5: Destruction (Very heavy structural damage) Total or near total collapse of a building.	Grade 5: Destruction (Very heavy structural damage) Collapse of ground floor parts.(e.g. wings of the building)

Source: FEMA-154, 2002

Table 4: Expected damage level as function of RVS score

RVS score	Damage Potential
$S < 0.3$	High probability of Grade 5 damage; very high probability of Grade 4 damage.
$0.3 < S < 0.7$	High probability of Grade 4 damage; very high probability of Grade 3 damage.
$0.7 < S < 2.0$	High probability of Grade 3 damage; very high probability of Grade 2 damage.
$2.0 < S < 3.0$	High probability of Grade 2 damage; very high probability of Grade 1 damage.
$S > 3.0$	Probability of Grade 1 damage.

Source: FEMA-154, 2002

The probable damage can be estimated based on the RVS score. However, it should be realized that the actual damage will depend on a number of factors that are not included in RVS procedure. As a result, this table should only be used as indicative to determine the necessity of carrying out simplified vulnerability assessment of the buildings. These results can also be used to determine the necessity of retrofitting buildings where more comprehensive vulnerability assessment may not be feasible.

3.4.1.2 Turkish Simple Survey Method: A Two level seismic risk assessment procedures

Another approach of rapid visual screening was employed for assessment of seismic vulnerability of structure in Turkey. The Turkish Simple Survey procedure is a two level seismic risk assessment procedure which has been proposed on the basis of statistical correlations obtained by employing a database of 477 damaged buildings surveyed after the 1999 earthquake in the cities of Kocaeli and Düzce in Turkey. Researchers from various universities were involved in this program supported by the government of Turkey and JICA (Sucuoglu and Yazgan, 2003). The method uses two levels seismic assessment based on several building parameters that can be easily observed or measured during a systematic survey.

In Turkish data collection form, the structural characteristics and site aspects such as potential pounding between buildings, apparent quality is judged. The basic scoring for both the levels are based on the Height of the building (number of stories) and Local Soil Conditions where three intensity zones are specified in terms of associated PGV (Peak Ground Velocity) ranges. This method considers buildings up to 7 stories where the increasing number of stories reduces the performance score by influencing almost all other Vulnerability Parameters negatively. Pounding effects and apparent quality of the building as well as the structural

characteristics, redundancy and stiffness index, act as weighted vulnerability parameters in the scoring system of Turkish screening.

Once the vulnerability parameters of a building are obtained from two-level surveys and its location is determined, the seismic performance and vulnerability scores are calculated as defined in Figure 2.3. A “cut-off” performance score of 50 has been suggested for both survey levels. In this study, the Turkish Level-I & Level-II method, a more detail evaluation of buildings has used to assess the vulnerability of the structures to be proposed as evacuation places.

Level- I Survey

Level-1 survey is a street side survey procedure based on simple structural and geotechnical parameters that can be observed easily from the sidewalk. The first level incorporates recording of building parameters regarding a structural form and the ground condition

The trained observers collect data through walk-down visits. The parameters that are selected in Level-1 survey for representing building vulnerability are the following:

- a. The number of stories above ground
- b. Presence of a soft story (Yes / No)
- c. Presence of a short column (Yes / No)
- d. Presence of heavy overhangs such as balconies with concrete parapets (Yes/No)
- e. Apparent building quality (Good, Moderate or Poor)
- f. Pounding between adjacent buildings (Yes / No)
- g. Local soil conditions (Stiff/ Soft)
- h. Topographic effects (Yes / No)

All of the above parameters are found to have a negative feature on the building system under earthquake excitations on a variable scale.

3.4.2 Fire hazard vulnerability analysis

To assess fire hazard vulnerability of Ward 29 in Old Dhaka, Community Vulnerability Assessment Tool (CVAT) is used to find out the existing scenario of the area. This tool has 7 steps including:

- Hazard identification

- Hazard analysis
- Critical facilities analysis
- Social analysis
- Economic analysis
- Environmental analysis
- Mitigation opportunities analysis

In this report only critical facilities analysis, social vulnerability analysis, economic vulnerability analysis and in addition structural vulnerability analysis has been done to assess the vulnerability of the community. The tools and methodologies used in this analysis consist of GIS and spatial mapping analysis.

Hazard analysis

Fire score of each building will be calculated from the following equation:

Score for building = weight for accessibility \times (1 for No access or 0 for Access) + Weight for transformer and power line \times (0 for Not Vulnerable or 1 for Vulnerable for electricity pole or 2 for Vulnerable for Transformer) + Weight for floor area ratio \times (0 for Very Low floor area ratio or 1 for Moderately Low floor area ratio.....) + Weight for building material type \times (1 for Pucca or 2 for Semi-kutchha or 3 for Kutchha) + Weight for availability of fire source \times (1 for Available of fire sources and 0 for No available of fire source)

Each building was given a score on the basis of five attributes where weight of each attribute was selected by using the Analytical Hierarchy Process (AHP). AHP is a multi-attribute modeling methodology. AHP is a systematic method for comparing a list of objectives or alternatives or attributes. The process of obtaining the weight of factors is given below:

The five attributes are road accessibility (A1), transformer and electrical wiring system (A2), floor area ratio (A3), building material type (A4) and availability of fire source (A5). A normalized set of weights was established to be used when comparing alternatives using these attributes. A pair wise comparison matrix M was formed where the number in the i th row and j th column gives the relative importance of A_i as compared with A_j . 1-5 Scale was selected from the eight expert's opinion. $a_{ij} = 1$ if the two objectives are equal in importance and $a_{ij} = 2$ if A_i is more important than A_j .

Matrix M which was made by expert opinion is given in the following:

$$M = \begin{bmatrix} 1 & 3 & 2 & 2 & \frac{1}{2} \\ \frac{1}{3} & 1 & \frac{1}{2} & 2 & \frac{1}{3} \\ \frac{1}{2} & 2 & 1 & \frac{1}{2} & \frac{1}{2} \\ \frac{1}{2} & \frac{1}{2} & 2 & 1 & \frac{1}{3} \\ 2 & 3 & 2 & 3 & 1 \end{bmatrix}$$

To normalize the weights, the sums of each column were computed and then each column was divided by the corresponding sum. Thus N was used to denote normalization.

$$N = \begin{bmatrix} 0.231 & 0.316 & 0.267 & 0.235 & 0.188 \\ 0.077 & 0.105 & 0.067 & 0.235 & 0.125 \\ 0.115 & 0.211 & 0.133 & 0.059 & 0.188 \\ 0.115 & 0.053 & 0.267 & 0.118 & 0.125 \\ 0.462 & 0.316 & 0.267 & 0.353 & 0.375 \end{bmatrix}$$

The next step was to compute the average values of each row and used these as the weights in the attribute Hierarchy.

$$W = \begin{bmatrix} 0.247 \\ 0.122 \\ 0.141 \\ 0.135 \\ 0.354 \end{bmatrix}$$

The weights are shown in the map.

Table 5: weight of the attributes

Accessibility	0.247
Transformer and power line	0.122
Floor Area Ratio (FAR)	0.141
Building material type	0.135
Availability of fire source	0.354

Consistency of the comparison matrix

It is unusual for the entire comparison matrix to be consistent. Indeed, given that human judgment is the basis for the construction of this matrix, some degree of inconsistency is expected and should be tolerated provided that it is not unreasonable.

To determine whether or not a level of consistency is reasonable a quantifiable measure for comparison matrix M was developed. To determine the consistency of the comparative matrix consistency ratio was computed by the following equation.

$$CR = \frac{CI}{RI}$$

Where, CI= Consistency Index of M

RI= Random Consistency of M

$$CI = \frac{n_{\max} - n}{n - 1},$$

Where,

n = Number of Attributes

$n_{\max} = M * W$ (Weighted Matrix)

$$RI = \frac{1.98(n - 2)}{n}$$

In that case,

$$n_{\max} = M * W = 5.383$$

$$n = 5$$

Consistency Index of M,

$$CI = \frac{n_{\max} - n}{n - 1}$$

$$= 0.096$$

Random Index,

$$RI = \frac{1.98(n - 2)}{n}$$

$$= 1.118$$

Consistency Ratio

$$CR = \frac{CI}{RI}$$
$$= 0.081$$

The Consistency Ratio (CR) is acceptable if CR is less or equal to 0.1. As the calculated CR comes below 0.01, consistency of comparison matrix is acceptable.

Hazard score for each building was calculated by the above equation using the derived weight. On the basis of this hazard score all the buildings were classified and it is shown in the Fire Vulnerability Map 5.8. The map was classified into five classes: low, moderately low, moderate, moderately high and high.

Critical facilities analysis

This analysis focuses on determining the vulnerabilities of key individual facilities, lifelines, or resources within the community. Critical facilities include emergency shelters, schools, hospitals, nursing homes, public buildings, and facilities for fire and rescue, police, utilities, communications, transportation, etc., or those identified as critical by the risk and vulnerability assessment working group. It is important to protect critical facilities (e.g., through relocation, elevation, or retrofit: backup of essential records; and backup of power supplies) to ensure that service interruption is reduced or eliminated, because these facilities play a central role in disaster response and recovery. Because it is not usually feasible to conduct a structural and operational analysis for every structure in a community, this step helps to prioritize which facilities are most vulnerable, so that individual assessments may be performed later. A structural analysis is used to examine the structural integrity of the building and its ability to withstand potential hazard damage; whereas, an operational analysis helps determine how daily activities will be affected if the building is damaged or if utility services are interrupted. The critical facilities vulnerability analysis has four components:

- First, critical facilities are identified by type and location to determine facilities that provide essential services to the community on a regular basis and are integral to disaster response and recovery operations.
- Second, a critical facilities inventory must be established by collecting general information on facility types and locations. The type and amount of information collected depends on the intended use of the database. Most local emergency management offices collect and maintain

information on certain categories of critical facilities, which may provide a starting point for the critical facilities inventory. It is imperative to collect accurate information because these data will be essential for completing the individual facility assessments in the last step of this analysis.

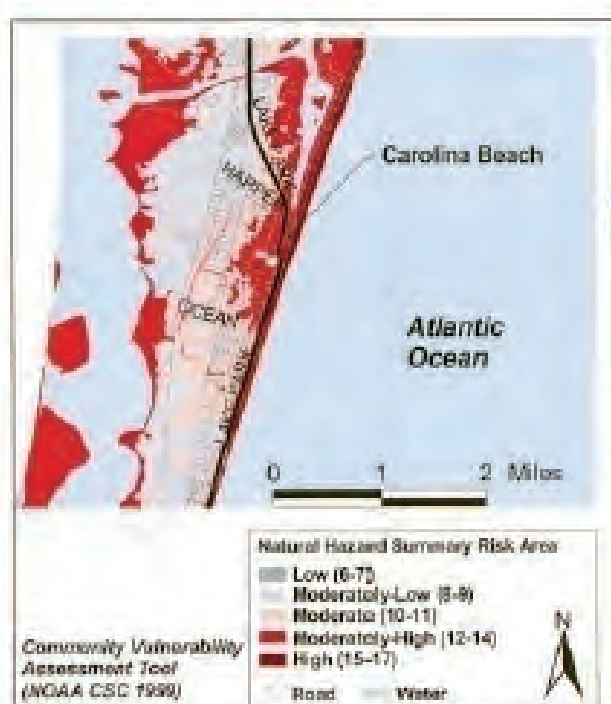
- Third, critical facilities that are in and within close proximity to high-risk areas are identified by overlaying the critical facility locations over the map of hazard-risk areas.
- Next, critical facilities that will require further structural and operational assessments are identified by completing a critical facilities inventory, which should include but is not limited to construction type and quality, location, age, size, occupancy rates, monetary value, insurance coverage, auxiliary-power capability, backup capacity and process for electronic files, and protection and storage procedures for hard-copy documents. Assessment questions should be designed to meet the needs of the audience or investigators. Some questions may require professionally trained inspectors or engineers, while others may rely on subjective evaluations from managers or property owners.

Social analysis

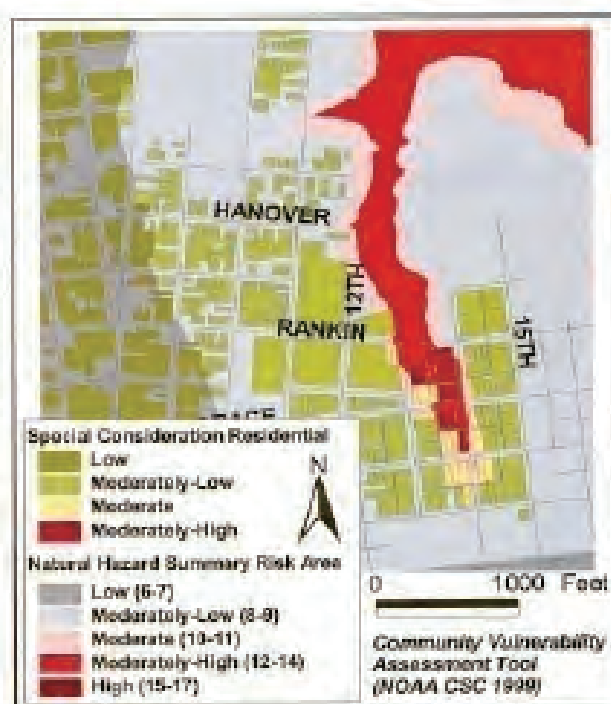
This analysis focuses on societal vulnerability by analyzing special consideration areas (preferably at the neighborhood level), where individual resources for loss prevention and disaster recovery tend to be minimal. Individuals that reside in special consideration areas are more likely to be uninsured or underinsured for hazard damages and have limited financial resources for pursuing individual hazard mitigation options. The population in these areas would be most dependent on public resources (e.g., disaster relief and recovery grants, unemployment assistance, subsidized health care and child care, social services, public transportation, etc.) after a disaster and therefore could indicate good investment areas for hazard mitigation activities. Special consideration areas can be identified by utilizing existing low-to-moderate income designations for community development grants or by analyzing key census data categories. Demographic characteristics can be selected to help identify special considerations such as mobility, literacy, or language, which can significantly hinder disaster recovery efforts. A societal vulnerability analysis is accomplished as follows:

- First, special consideration areas (e.g., areas with high concentrations of poverty, elderly, minorities, single-parent households, rental dwellings, no high school diplomas, public assistance recipients, non-English speaking populations, no vehicle available, etc.) are identified by type and location to determine which populations may require special care or may have more difficulty with disaster response and recovery.

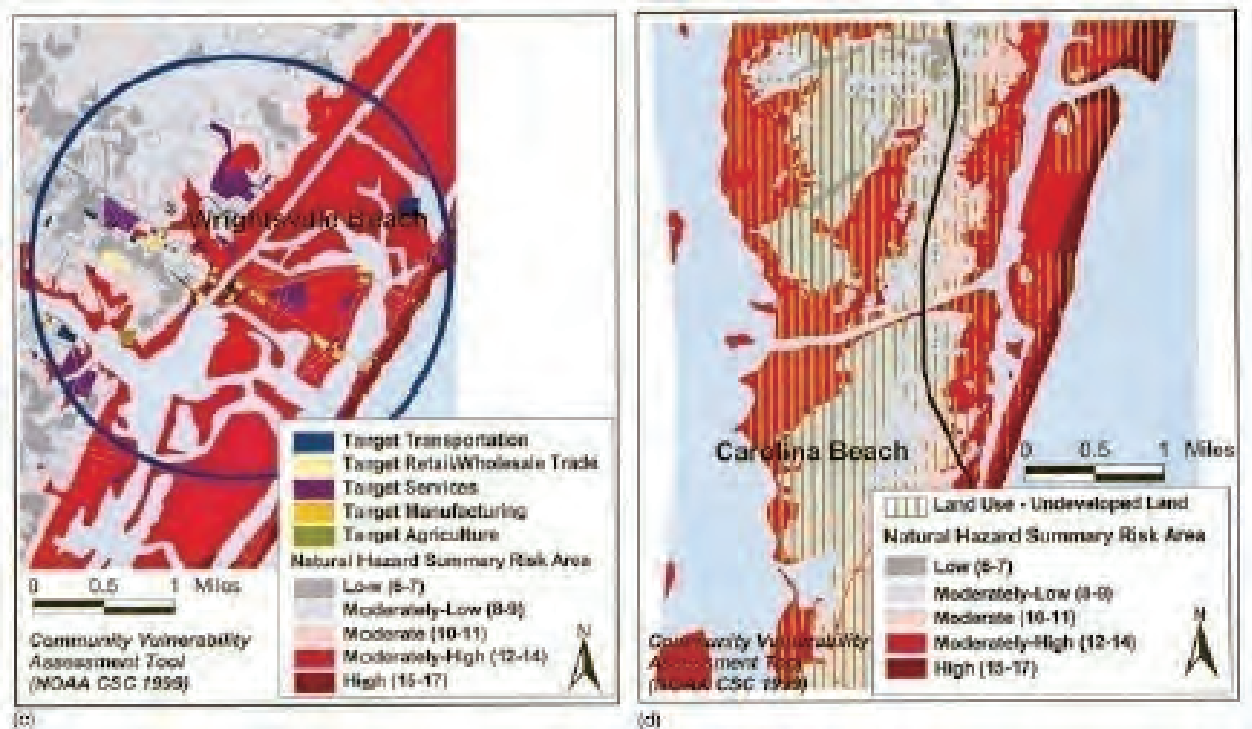
- Second, special consideration areas that are in high-risk areas are identified by overlaying the special consideration neighborhoods onto the risk areas.
- Next, a general inventory is completed of special consideration areas that are located in high-risk areas. There are several ways to complete this type of inventory. A community might elect to conduct a windshield survey to determine the number and type of vulnerable facilities in high-risk areas, unless these data are readily available from the local tax assessor's office. New Hanover County used a parcel-based land use inventory in a GIS format to distinguish the number and type of residential structures located in each census block group that was identified as a special consideration area.



(a)



(b)



Map 3: (Color) Examples of GIS maps used for the Community Vulnerability Assessment Tool process in New Hanover County, North Carolina: (a) Natural hazard summary risk areas (Step 2-Hazard analysis); (b) Special consideration residential areas with high risk areas (Step 4-Societal vulnerability analysis); (c) Economic sectors in high-risk areas (Step 5-Economic vulnerability analysis); (d) Tracts of undeveloped land in high-risk areas (Step 7-Mitigation opportunities analysis)

Economic analysis

This analysis focuses on economic vulnerabilities to hazard impacts by identifying major economic sectors and mapping primary centers of activities in those sectors. Economic centers are areas where hazard impacts could have adverse effects on the local economy and would therefore be ideal locations for targeting certain hazard mitigation strategies. Some of the most devastating disaster costs to a community include the loss of income associated with business interruptions and the loss of jobs associated with business closures. A progressive community will actively pursue business continuity plans and hazard mitigation options to prevent or minimize such losses. It is important to begin this step by conducting a general overview of the local economy to provide a basis for targeting business sector partners in community-wide hazard mitigation efforts. The identification process will rely on local expertise such as the chamber of commerce or economic development council. Economic information can also be derived from widely available data sources such as the county

business patterns located on the U.S. Census Bureau Web site (<http://www.census.gov/>). Land use or zoning data can often help in mapping business and industrial centers. Steps to accomplish an economic vulnerability analysis are as follows:

- First, the primary economic sectors and their geographic locations must be identified (i.e., economic centers) to determine which businesses are most important to the community (e.g., products and services, employment, tax revenue, disaster response and recovery capabilities, etc.).
- Second, primary economic centers that are located in high-risk areas are identified by overlaying the economic center locations over the risk areas.
- Third, a general inventory of high-risk economic centers is conducted. A community may choose to conduct a windshield survey to determine the number and type of vulnerable facilities in high-risk areas if this information is not readily available. A table (e.g., GIS attribute table or spreadsheet) can be used to summarize the type of industries, the number of facilities within each industry, the number of employees, the percentage of employees per industry and/or facility, and the annual payroll to help narrow the focus for facilities to be targeted for hazard mitigation.
- Fourth, large employers that are located in high-risk areas are identified to help prioritize the facilities on which to perform further analyses. Economic census data can help identify employment levels by economic sector and determine the size threshold.
- Next, a structural and operational vulnerability analysis is conducted. While this step is largely up to the private sector, it is recommended that vulnerability assessments for large employers be addressed in a manner similar to critical facilities. FEMA endorses engaging with key private sector establishments in hazard mitigation partnerships and asking them to assess their structural and operational vulnerability to hazards.

Environmental Vulnerability Analysis

This analysis focuses on identifying locations where secondary environmental impacts caused by natural hazards (primary impacts) may occur. Before embarking on this step, it is necessary to explain the terms “secondary impacts” and “secondary risk sites.” Secondary impacts occur when natural hazards (e.g., flood) trigger additional hazards such as toxic releases or hazardous spills. Therefore, a solid-waste facility or a building that stored hazardous materials would be characterized as “secondary risk sites” if they are in close proximity to areas of environmental concern (e.g., wetland). Although CVAT uses the term “secondary risk sites,” these are often called “hazardous facilities.” Environmental impacts

are important to consider, as they not only jeopardize habitats and species, but can also threaten public health (e.g., water quality), various economic sectors (e.g., tourism and fishing), and quality of life (e.g., access to natural landscapes and recreational activities). For example, flooding (a primary hazard) can result in contamination (a secondary hazard) whereby raw sewage, animal carcasses, chemicals, pesticides, hazardous materials, etc. are transported through sensitive habitats, neighborhoods, and businesses. These circumstances can result in major cleanup and remediation activities, as well as natural resource degradation. Data can be obtained from state and local emergency management offices, local planning commissions, and environmental and natural resource management agencies to locate natural resources and secondary risk sites. Steps to accomplish an environmental vulnerability analysis are as follows.

- First, secondary risk sites (e.g., hazardous materials, toxic release sites, solid-waste facilities, nuclear power plants, underground storage tanks, oil facilities, ports, marinas, discharge sites, etc.) and key natural resource sites (e.g., wetlands, sensitive/endangered species and habitats, fisheries, wildlife refuges, aquaculture sites, shellfish harvest areas, groundwater recharge areas, etc.) are identified.
- Next, secondary risk sites and environmentally sensitive areas are overlaid onto the risk areas to determine the types of hazardous materials and locations of potential releases into environmentally sensitive areas. (Lisa et al, 2002)

3.5 Preparation of Final Report

All information and finding are gathered and presented by tables, graphs and maps to prepare the final report. Some recommendations based on the findings are provided to improve the overall conditions of Ward 29 in the report.

4.EXISTING SCENERIO OF STUDY AREA

Ward 29 is situated at the old part of Dhaka City also named as 'Puran Dhaka' beside the river Buriganga. Total 343 building which cover 16.76% of existing buildings in the study area were surveyed including mosques, schools, college, community centers and clubs etc to assess earthquake and fire hazard vulnerability of buildings.

4.1 Age of Building

As the study area is one of the oldest parts of Dhaka city, there are some buildings aged above 50 years. In contrast, newly constructed buildings which were constructed up to 10 years before dominate with about 49% share. 29% buildings are constructed 11 to 20 years before and 15% buildings are constructed 21 to 30 years before. Figure 1 shows distribution of age of buildings in the study area.

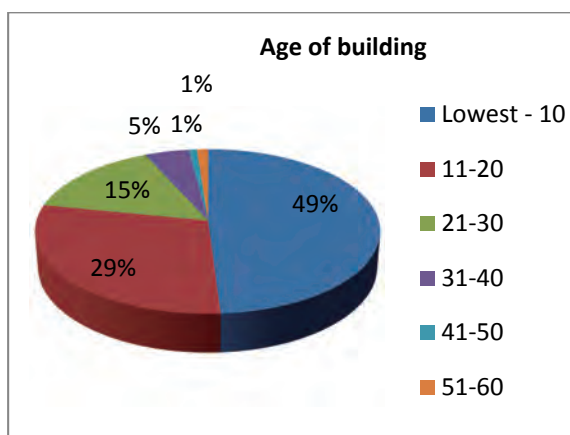


Figure 1: Distribution of age of building



Figure 2: Old buildings

4.2 Building Type

Among 343 surveyed buildings 228 buildings are pucca, 114 are semipucca and only one is katcha (figure 3). Among pucca only 2 buildings are C2 (Concrete shear wall buildings) type building. C3 (Moment resisting frame) type building dominates with 74.1% occupancy. URM (Unreinforced masonry buildings) buildings which are mostly semipucca buildings are 25.4% in the study area (figure 4).

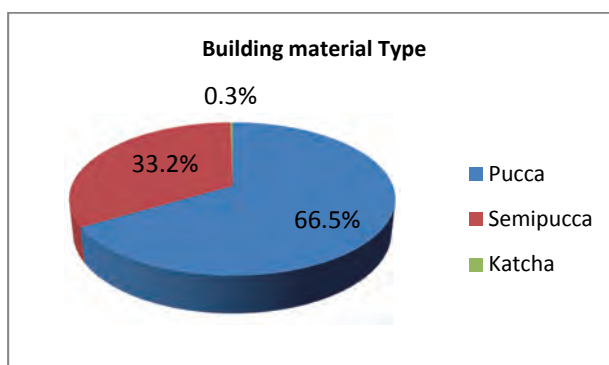


Figure 3: Distribution of building material type

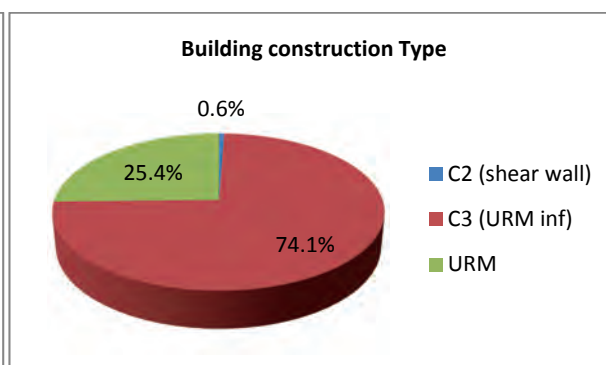


Figure 4: Distribution of building construction type

4.3 Number of Storey

The area mainly comprises of one to six storey buildings where two storey buildings are the highest with 22.7% occupancy. Buildings above 6 storey are very limited (3%). The tallest building in the study area is a 9 storey building. One storey building is 12.8%. 4 storey and 5 storey buildings dominate with 18.7 % and 18.1 % share respectively. The following table shows the frequency and percentage of buildings with different number of floor.

Table 6: Distribution of different number of storey

Number of Storey	Frequency	Percent
1	44	12.8
2	78	22.7
3	50	14.6
4	64	18.7
5	62	18.1
6	34	9.9
7	9	2.6
8	1	0.3
9	1	0.3
Total	343	100



Figure 5: High-rise building

4.4 Floor Area of building

Owners of the buildings of the study area do not follow the building construction regulation of RAJUK. So Floor Area Ratio (FAR) of buildings is equal to the number of floor for this ward. Building floor area covers the total land area of the plot. Floor area varies from 120 square feet to 8000 square feet. Most of the buildings (28.3%) have 501-1000 square feet floor area. Buildings with 120-500 square feet which are mostly commercial shops and shanty are 19.2% (figure 6).

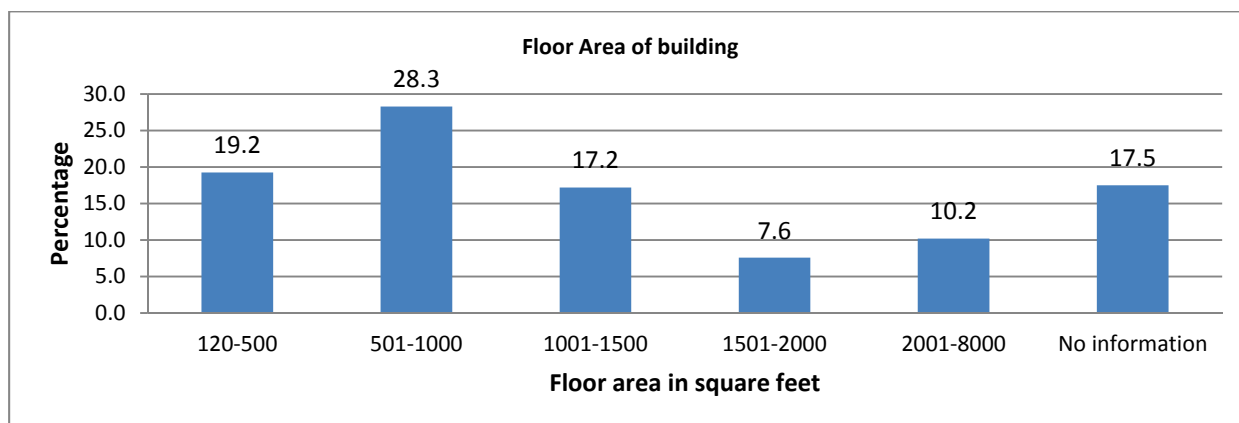


Figure 6: Distribution of floor area in the study area

4.5 Use of Buildings

From the field survey, it has been found that about 60% buildings are used as mixed use activity such as shops and industry at ground floor and residence at upper floor. This is a common scenario of Old Dhaka. 20% buildings are of pure residential use. Commercial and industrial uses are 10% and 7% respectively. Community services and service facility are 2% and 1% respectively (figure 7).

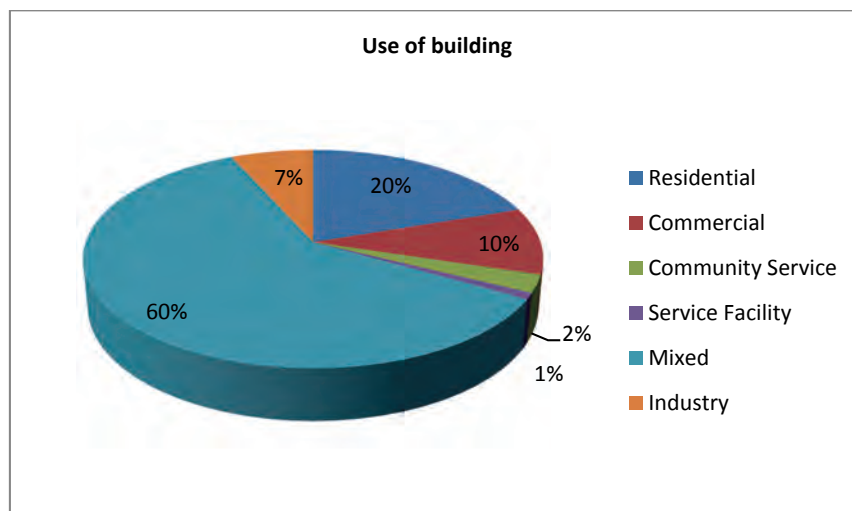


Figure 7: Distribution of use of building in the study area



Figure 8: Different uses of building

5. EARTHQUAKE VULNERABILITY ANALYSIS

5.1 Apparent Quality, Pounding Effect, Soft Storey, Short Column and Heavy Overhang

Among 343 surveyed buildings, 185 buildings (54%) are good quality structures; 29% are moderate and 17% are poor in apparent quality. Most of the buildings (91.84%) have no

space in between the adjacent buildings. About 8% buildings have soft storey while 4% have short column.

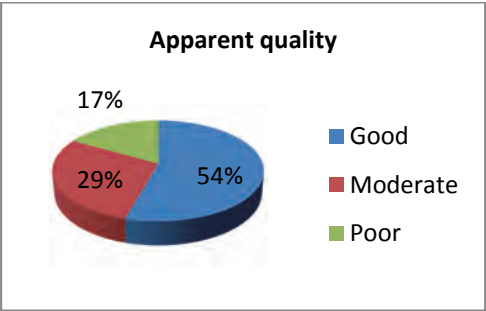


Figure 9: Apparent quality of building

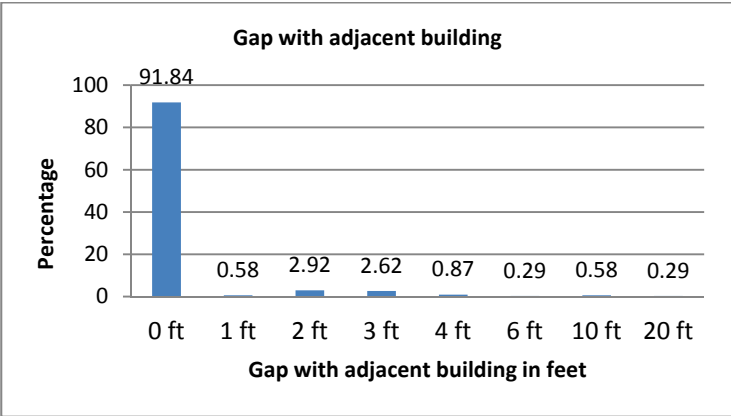


Figure 10: Gap with adjacent building



Figure 11: Poor quality building



Figure 12: Heavy overhang of building

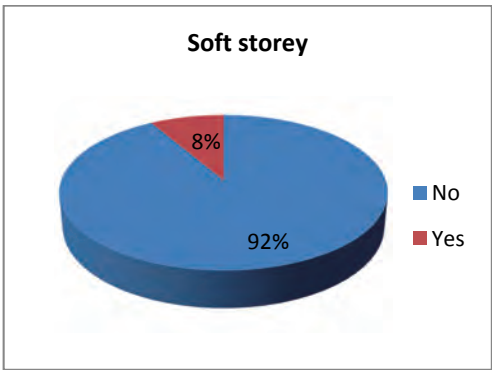


Figure 13: Soft storey

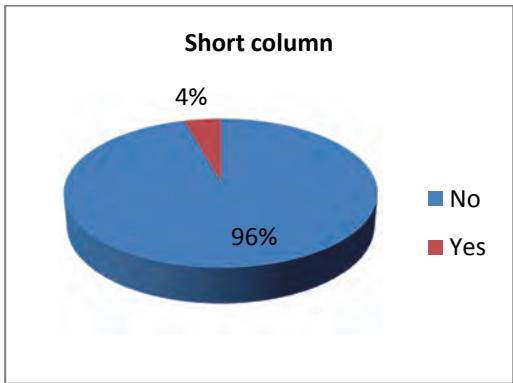


Figure 14: Short column

22% buildings in the study area have heavy overhang which lead to earthquake vulnerability of building. Width of overhang varies from 0.5 feet to 5 feet. Most of the buildings have overhang with 2 feet (8.75%), 1 foot (5.54%) and 3 feet (5.25%).

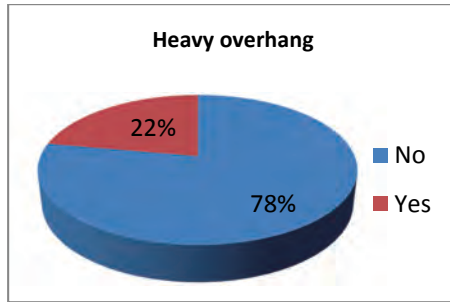


Figure 15: Heavy overhang

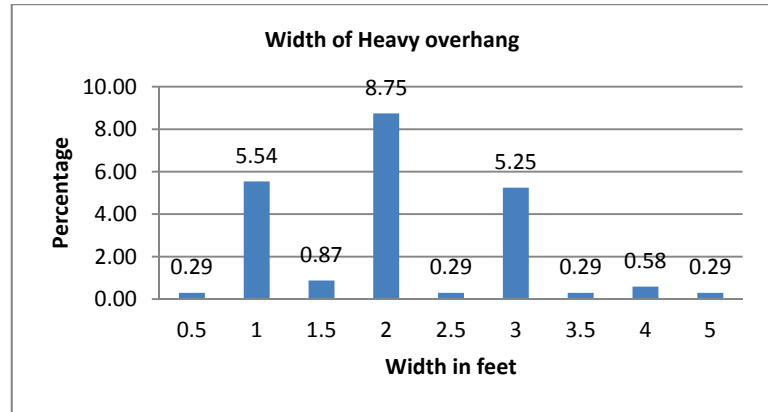


Figure 16: Width of heavy overhang

5.2 Vertical Irregularity and Plan Irregularity

Buildings with irregular shape with respect to both plan and elevation shape tend to be more vulnerable to earthquake. 25.7 % buildings are vertically irregular and 74.3% buildings are regular in their elevation shape. It has also found from field survey that 91% buildings of the study area have rectangular or square plan i.e. the shape of the plan are regular and rest 9% buildings have irregularity in their plan.

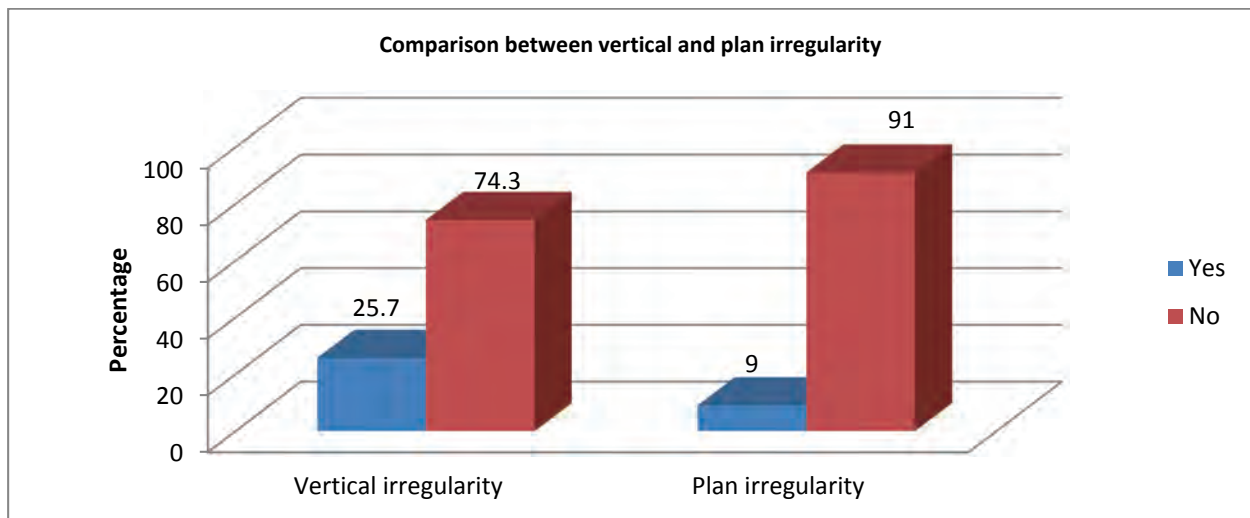


Figure 17: Comparison between vertical irregularity and plan irregularity

5.3 Rapid Visual Screening

Among 373 surveyed buildings, 20 buildings (5.83%) scored less than 1 according to RVS (FEMA). 70.75% buildings scored 3 to 3.4 value which means most of the building are structurally safe according to RVS (FEMA). According to RVS (Turkish level I), about 56.56% buildings scored above 110. Buildings having scores less than 50 are only 2.62%. The following charts show category of buildings according to RVS score in the study area.

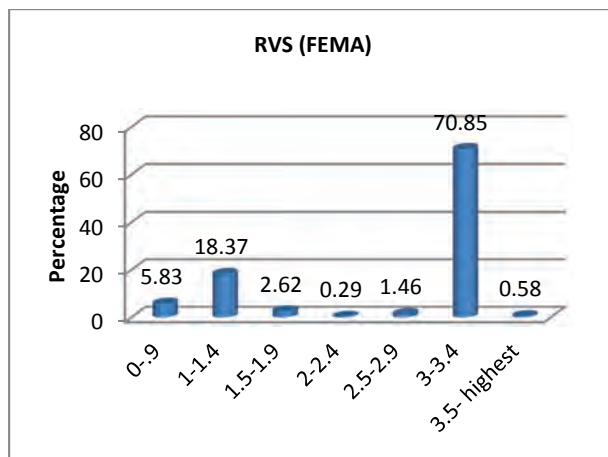


Figure 18: RVS (FEMA)

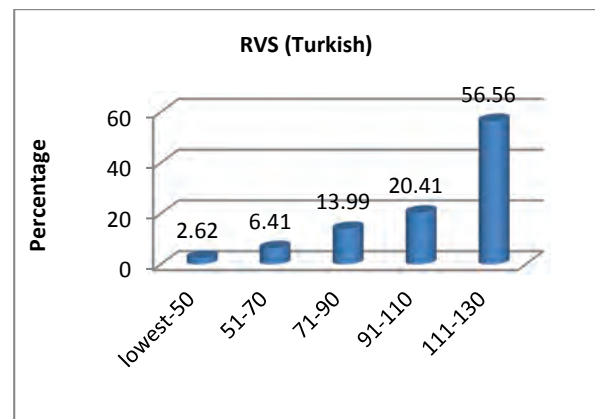


Figure 19: RVS (Turkish level I)

6. FIRE HAZARD VULNERABILITY ANALYSIS

6.1 Existence of Fire Source

As a traditional old part of Dhaka City, Ward 29 contains different types of economic activities such as plastic manufacturing industries, warehouse of flammable material like chemicals and plastic etc that can trigger a fire or can be vulnerable to fire accidents. That is why these sort of economic and other uses that can generate a fire disaster in the locality are identified and classified into some broader categories.

They are given below:

1. Chemical
2. Plastic
3. Leather
4. Generator
5. Gas stove

Buildings where fire sources and flammable materials are available in the study area were located during the field survey. Around 9% buildings are found with no fire sources. 38% buildings have plastic, 9% have chemicals, 6% have leather and 1% have generator. Rest 37% buildings which are mainly residential have gas stove as a source of fire (Fig. 5.3).

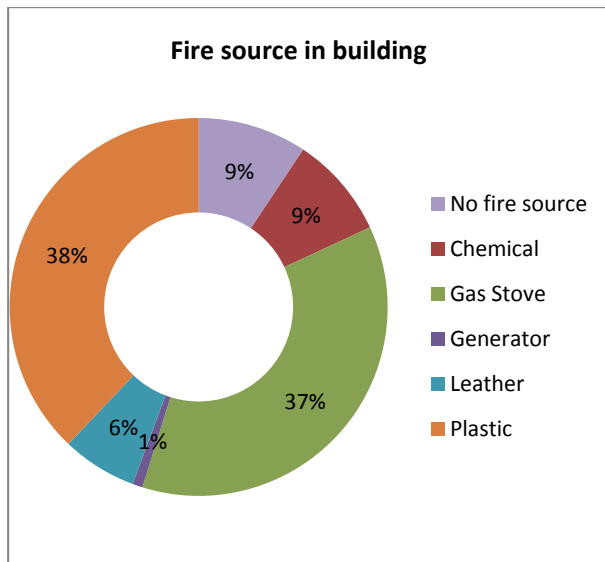


Figure 20: Fire source in building

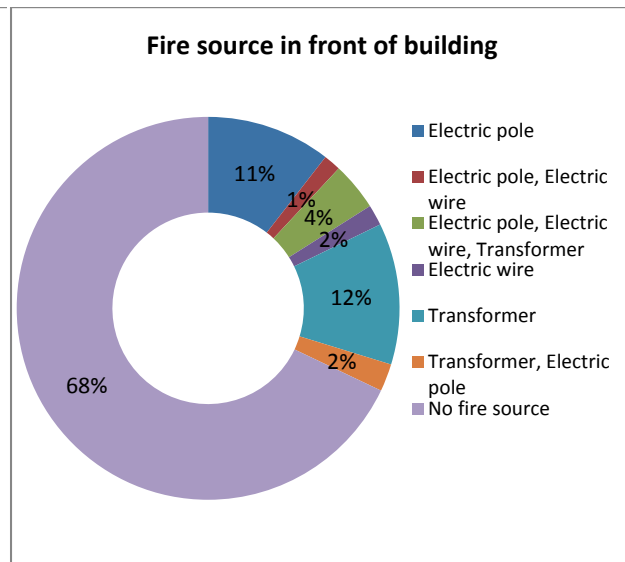


Figure 21: Fire source around building

Electricity poles are distributed throughout the study area. One or more than one transformer has been found in every neighborhood. It has been found that in some places two transformers are located so near to each other that they can create a hazardous situation if any one explodes. The study reveals that around 11% buildings adjacent to electricity poles are vulnerable to fire where as 12% buildings adjacent to transformers are vulnerable. 2% houses have electric wire, 2% have both electric pole and transformer, 1% has both electric wire and electric pole, and 4% have electric wire, electric pole and transformer. The rest 68% have no fire source around. It is shown in figure-5.2.



Figure 22: Fire source in front of building

6.2 Accessibility of fire truck

Accessibility is one of the important attributes for making fire vulnerability map. Fire affected plots are supposed to be served by fire engines coming from fire stations which carry

water, ladder and various fire fighting equipments. If the roads leading to the affected plot are not accessible to fire engines, the plot cannot be served effectively by fire fighters and it become vulnerable to fire. In our country, fire engines can go through roads at minimum 10 feet width. This information was taken from a fire fighting expert. Besides, traffic jam is another factor affecting the accessibility by road. From the field survey, it was found that the number of the buildings that get access is 46%. Rest of the buildings (around 54%) is not accessible to fire engines (Figure 24)



Figure 23: Narrow road inaccessible for fire truck

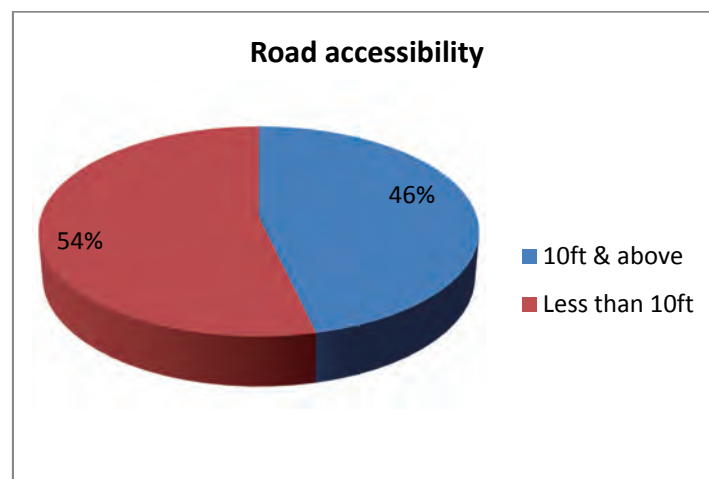


Figure 24: Distribution of road accessibility

6.3 Staircase width

From the field survey it was found that widths of the staircase of building in the study area vary from 1 foot to 8 feet. Most of the buildings (16.3%) have 3 feet wide staircase, 14.6% have 4 feet staircase and 10.2% have 6 feet staircase (table 7)

Table 7: Distribution of width of staircase

Width in feet	Frequency	Percent
1	1	0.3
2	24	7
3	56	16.3
4	50	14.6
5	17	5
6	35	10.2
7	2	0.6
8	14	4.1
No information	144	42
Total	343	100

6.4 Fire Vulnerability Score

Percentages of buildings having different categories of fire score are shown in figure 25. The vulnerability score of buildings of the study area range from 0.41 to 1.88. Lower value indicates less vulnerability whereas higher value indicates high vulnerability. Most of the buildings (78.5%) have fire score more than 1 which indicates most of the buildings in the study area are vulnerable to fire. Buildings having fire score less than 0.5 are only 0.9%, having score 0.51- 0.75 are 5.5% and having 0.76 – 1.00 are 15.2%.

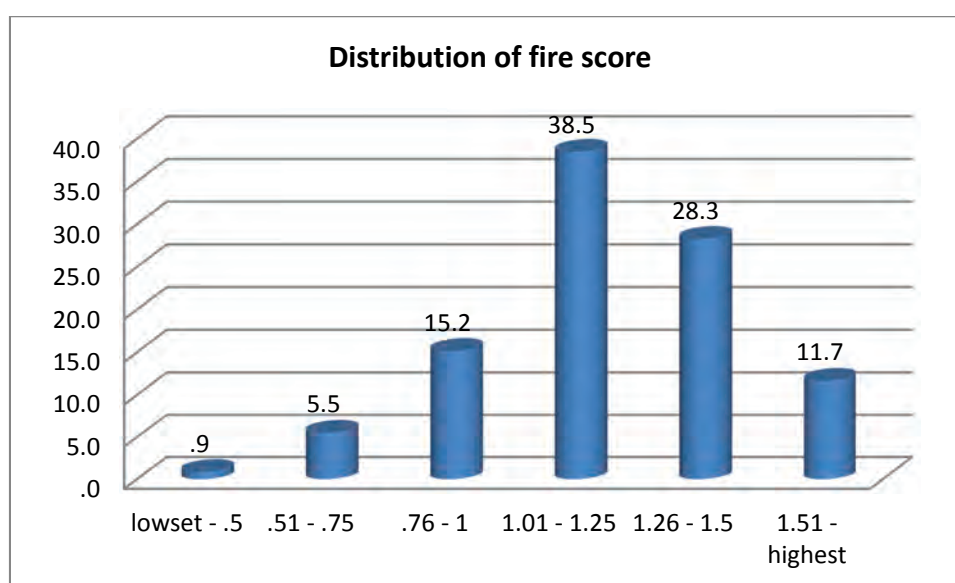


Figure 25: Distribution of fire score

7. MAJOR FINDINGS

Ward 29 is at risk of earthquake and some fire incidents have already occurred. From the fire vulnerability analysis it has been found that maximum numbers of buildings of the study area

are highly vulnerable (78.5%) to fire. Most of the highly fire vulnerable buildings are located in Islambag Road. Buildings of Water works Road and Lalbag area are less vulnerable because of being residential areas with mixed commercial use. The surveyed buildings cover 16.76% of existing structures in the study area.

The study area comprises both old buildings and newly constructed buildings where buildings constructed up to 10 years before dominate with about 49% share.

Pucca buildings dominate with about 50% occupancy among which about 74.1% are C3 (moment resisting frame) type building. Unreinforced masonry buildings which are mostly semipucca are 25.4% in the study area.

Two storey buildings are the highest with 22.7% occupancy where as buildings above 6 storey are very limited (3%). The tallest building in the study area is a 9 storey building. Most of the buildings (28.3%) have 501-1000 square feet floor area.

About 60% buildings are used as mixed use activity such as shops and industry at ground floor and residence at upper floor.

Most of the buildings (54%) are of good apparent quality and most of the buildings (91.84%) have no space in between the adjacent buildings. About 8% buildings have soft storey while 4% have short column and 22% buildings have heavy overhang which lead to earthquake vulnerability. 25.7 % buildings are vertically irregular and 9% buildings have irregularity in their plan.

5.83% scored less than 1 according to RVS (FEMA). 70.75% buildings scored 3 to 3.4 values which mean most of the buildings are structurally safe according to RVS (FEMA). According to RVS (Turkish), about 56.56% buildings scored above 110. Buildings having scores less than 50 are only 2.62%.

Around 9% buildings are found with no fire sources in building whereas 68% have no fire source around. 54% buildings have no access for fire truck.

Most of the buildings (78.5%) have fire score more than 1 which indicates most of the buildings in the study area are vulnerable to fire.

8.CONCLUSIONS

The research assessed the vulnerability of old part of Dhaka city to earthquake and fire hazard. In many studies, Dhaka is considered as one of the most vulnerable city to earthquake. Recently the city also followed a number of notable fire accident which means the city is also at risk of fire. Old part of Dhaka is more vulnerable to any hazard due to high population density, mixed uses of land and violation of building construction regulation. The study area was found to more vulnerable to fire but less vulnerable to earthquake. But due to narrow road, lack of critical facilities and lack of preparedness among local people may lead to a great disaster if a small scale earthquake occurs.

REFERENCES

- http://www.daily-sun.com/details_yes_08-10-2011_Fire-hazard-vulnerability:-A-case-study-in-Dhaka-city_366_2_28_1_0.html.
- Islam, M.M. and Adri, N., Fire Hazard Management of Dhaka City: Addressing Issues Relating to Institutional Capacity and Public Perception. Jahangirnagar Planning Review, Vol. 6, pp. 57-67, 2008.
- Rahman, M.M. and Talukder, M.R.A. “Mapping Earthquake Management in Dhaka City: A Scoping Study.” Bangladesh Research Publications Journal, ISSN: 1998-2003, Volume: 6, Issue: 4, Page: 462-466, 2011.
- Khan, A.A. “Earthquake hazard: Dhaka city perspective”, The Daily Star, Vol. 5 No. 40, 2004.
- The Daily Star, Dhaka city at risk of massive destruction, 2010, accessed from <http://archive.thedailystar.net/newDesign/news-details.php?nid=123247>.
- Horwich, G., “Economic Lessons of the Kobe Earthquake.”Economic Development and Cultural Change, volume 48, page 521–42, 2000.
- Alam, M.J.B and Baroi, G.N., Fire hazard categorization and risk assessment for Dhaka city in GIS framework, Journal of Civil Engineering (IEB), Volume 32 (1), Page 35-45, 2004.
- Jahan I, Ansary M, Ara S, Islam I., Assessing social vulnerability to Earthquake Hazard in Old Dhaka, Bangladesh; Asian Journal of Environment and Disaster Management (AJEDM), 3(3):285–300, 2011.
- http://www.dhakasouthcity.gov.bd/Documents/New%20DCC_South_Ward%20Report_22.12.2011.doc

- http://www.bbs.gov.bd/WebTestApplication/userfiles/Image/Census2011/Dhaka/Dhaka/Dhaka_C01.pdf
- http://www.dhakasouthcity.gov.bd/Page/About/Link/2/List_id/220/Ward_no_&Area
- GIS database of Detailed Area Plan (DAP) of Dhaka City, 2006.
- Rahman N., Ansary, M.A. Community under Fire Threat: An Assessment of Fire Hazard Vulnerability of Ward 65 in Dhaka City, presented in 11th International Symposium on New Technologies for Urban Safety of Mega Cities in Asia, Mongolia, 2012.
- BNUS Annual Report, 2011.
- Rahman, M. G. F. “Seismic Damage Scenario for Dhaka City”, M.Sc. Engg. Project thesis, Department of Civil Engineering, BUET, Dhaka, 2004.
- Flax, L. K., Jackson, R. W. and Stein, D. N. “Community Vulnerability Assessment Tool Methodology” Natural Hazards Review Vol. 3 (ISSN 1527-6988), 162-176, 2002.
- F.E.M.A. Federal Emergency Management Agency 154, 2002.
- Sucuoglu, H. And Yazgan, U., Simple Survey Procedures for Seismic Risk Assessment in Urban Building Stocks. Seismic Assessment and Rehabilitation of Existing Buildings, 97-118, NATO Science Series, IV/29, Editors: S.T. Wasti and G. Ozcebe, Kluwer, 2003.

APPENDIX-A

1. Checklist of field survey 2013

SL No.	Parameter	Value
1	Adjacent road width	
2	Building material type	
3	Number of storey	
4	Building floor area	
5	Plot land area	
6	Present land use	
7	Adjacent land use	

8	Total population living in the building	
9	Condition of staircase	
10	Staircase width	
11	Existence of fire source in building	
12	Existence of fire source in front of building	
13	Apparent quality of building	
14	Gap with adjacent building (Pounding effect)	
15	Soft storey (only column at ground floor)	
16	Short column (only column at any other floor)	
17	Heavy overhang	
18	Width of heavy overhang	

2. FEMA 154 data collection form

Rapid Visual Screening of Buildings for Potential Seismic Hazards
FEMA-154 Data Collection Form

HIGH Seismicity

Address: _____ Zip: _____

Other Identifiers: _____

No. Stories: _____ Year Built: _____

Screened: _____ Date: _____

Total Floor Area (sq. ft.): _____

Building Name: _____

Use: _____

PHOTOGRAPH

Scale: _____

OCCUPANCY			SOIL		TYPE								FALLING HAZARDS				
Assembly	Govt.	Other	Number of Persons (0-10, 11-100, 101-1000, 1000+)	S1 (pt)	S2 (pt)	S3 (pt)	S4 (pt)	S5 (pt)	C1 (pt)	C2 (pt)	C3 (pt)	PC1 (pt)	PC2 (pt)	RM1 (pt)	RM2 (pt)	URM (pt)	
Commercial	Industrial	Residential															Rock
Assembly	Govt.	Other															
Commercial	Industrial	Residential															
Emer. Services		School															

BASIC SCORE, MODIFIERS, AND FINAL SCORE, S

BUILDING TYPE	W1	W2	S1	S2	S3	S4	S5	C1	C2	C3	PC1	PC2	RM1	RM2	URM
Basic Score	4.4	3.8	2.8	3.0	3.2	2.8	2.8	2.5	2.8	1.6	2.6	2.4	2.8	2.8	1.8
Mid Rise (4 to 7 stories)	N/A	N/A	+0.2	+0.4	N/A	+0.1	+0.4	+0.4	+0.4	+0.2	N/A	+0.2	+0.4	+0.4	0.0
High Rise (> 7 stories)	N/A	N/A	+0.6	+0.8	N/A	+0.3	+0.6	+0.6	+0.6	+0.3	N/A	+0.4	+0.8	+0.8	N/A
Vertical irregularities	-0.8	-0.4	-0.6	-1.0	N/A	-1.0	-1.0	-1.5	-1.0	-1.0	N/A	-1.0	-1.0	-1.0	-1.0
Plan irregularities	-0.5	-0.5	-0.5	-0.5	-0.5	-0.5	-0.5	-0.5	-0.5	-0.5	-0.5	-0.5	-0.5	-0.5	-0.5
Pro-Cost	0.0	-1.0	-1.0	-0.8	-0.6	-0.8	-0.2	-1.2	-1.0	-0.2	-0.8	-0.8	-1.0	-0.8	-0.2
Post-Benchmark	+2.4	+2.4	+1.4	+1.4	N/A	+1.5	N/A	+1.4	+2.4	N/A	+2.4	N/A	+2.8	+2.8	N/A
Soil Type C	0.0	-0.4	-0.4	-0.4	-0.4	-0.4	-0.4	-0.4	-0.4	-0.4	-0.4	-0.4	-0.4	-0.4	-0.4
Soil Type D	0.0	-0.8	-0.8	-0.8	-0.8	-0.8	-0.8	-0.8	-0.8	-0.8	-0.8	-0.8	-0.8	-0.8	-0.8
Soil Type E	0.0	-0.8	-1.2	-1.2	-1.0	-1.2	-0.8	-1.2	-0.8	-0.8	-0.4	-1.2	-0.4	-0.8	-0.8

FINAL SCORE, S

COMMENTS

Detailed
Evaluation
Required

YES NO

* = Estimated, unpermitted, or unknown data
URM = Do Not Know

RR = Braced frame
FD = Flexible diaphragm
LM = Light metal

MSF = Moment-resisting frame
RC = Reinforced concrete
RD = Rigid diaphragm

SW = Shear wall
TU = Tilt up
URM (NF) = Unreinforced masonry (NF)



PART-XVI

STANDARD GARMENTS FIRE: AN INTRIGUE AGAINST RMG SECTOR OF BANGLADESH

**BANGLADESH NETWORK OFFICE FOR
URBAN SAFETY (BNUS), BUET, DHAKA**

Prepared By: Naima Rahman

Mehedi Ahmed Ansary

On 28th November 2013 two 6-storied and a ten-storied building of Standard Group in Konabari of Gazipurwereset fire by hundreds of Ready Made Garment (RMG) workers. Bangladesh Garment Manufacturers and Exporters Association (BGMEA) termed the fire incident as “sabotage” as the blaze had been said to be set upon by workers who were angered over rumours of two colleagues dying in police firing.

Direct witnesses said that some people announced through the horn speakers of a nearby mosque that police had killed two workers in the Standard Group factory for demanding a separate pay structure for the employees in the group’s jumper factory. Hearing the announcement, at least 200 workers of Standard Group along with some non-workers stormed and torched the company’s two multi-storied buildings, brushing aside the policemen on duty at the gates. Firefighters around 1:30pm of 29th November were able to douse the flames.



Figure 1: Burning front section of Standard garments factory building in Gazipur



Figure 2: Burning clothes in standard garments

There have been no reports of any life loss or casualty but the ten storied building was totally damaged due to fire. The workers also torched 31 vehicles inside the compound of which, 18 covered vans were fully loaded with goods. The loss will exceed Tk. 900 crores as demanded

from the garment owner side. Standard Group was considered as one of the most compliant factories in Bangladesh by BGMEA and BKMEA for its good reputation.



Figure 3: Police routed aggressive RMG workers



Figure 4: Fire Fighters working in the building



Figure 5: Fire on the third floor around 1:00pm



Figure 6: Covered vans loaded with cloths burnt



Figure 7: Cleaning process after fire-control



Figure 8: Prime-ministers press conference



PART-XVII

GROUND PENETRATING RADAR TESTING AT THE PROPOSED UNDERGROUND LPG STORAGE TANK AT SOUTHERN AUTOGAS STATION, TEJGAON

**BANGLADESH NETWORK OFFICE FOR
URBAN SAFETY (BNUS), BUET, DHAKA**

Prepared By: Mominul Haque

Mehedi Ahmed Ansary

1.0 Introduction

The GPR tests at the autogas station have been carried out on February 13 and 21, 2014. This report is the outcome of the measurements through GPR. Figure 1 shows the test site.



Figure 1 Investigated site

2.0 Ground Penetrating RADAR (GPR) Test Program

Ground Penetrating Radar (GPR) is a near-surface geophysical technique that can provide high resolution scan of the dielectric properties of the earth. GPR works by sending a tiny pulse of energy (Electromagnetic Energy) into a material and recording the strength and the time required for the return of any reflected signal. A series of pulses over a single area make up what is called a scan. Reflections are produced whenever the energy pulse enters into a material with different electrical conduction properties or dielectric permittivity from the material it left. The strength, or amplitude, of the reflection is determined by the contrast in the dielectric constants and conductivities of the two materials. GPR is a rapid and useful technique for nondestructive assessment of subsoil, locating underground pipelines and reinforcement in buildings, foundation and bridges etc.

Scope of this project included subsurface layer investigation and identification of utility location.

GPR data were collected using 100 MHz and 200 MHz antenna for subsurface layer investigation and 400 MHz antenna for identification of utility location with a GSSI SIR-3000 control unit. All data were collected in simple line scan format. The direction of arrow in site plan and data collection grids indicates the starting and ending point GPR scan.

The collected data sets were processed by specialized software program RADAN. Three basic kind of processing tools were used in order to calculate accurate depth, to remove noise and to improve display for documentation purpose.

Time-Zero Correction: A corrected Time-Zero provides a more accurate depth calculation because it sets the top of the scan to a close approximation of the ground surface. Time-zero correction also remove the section of data that occurs before direct wave.

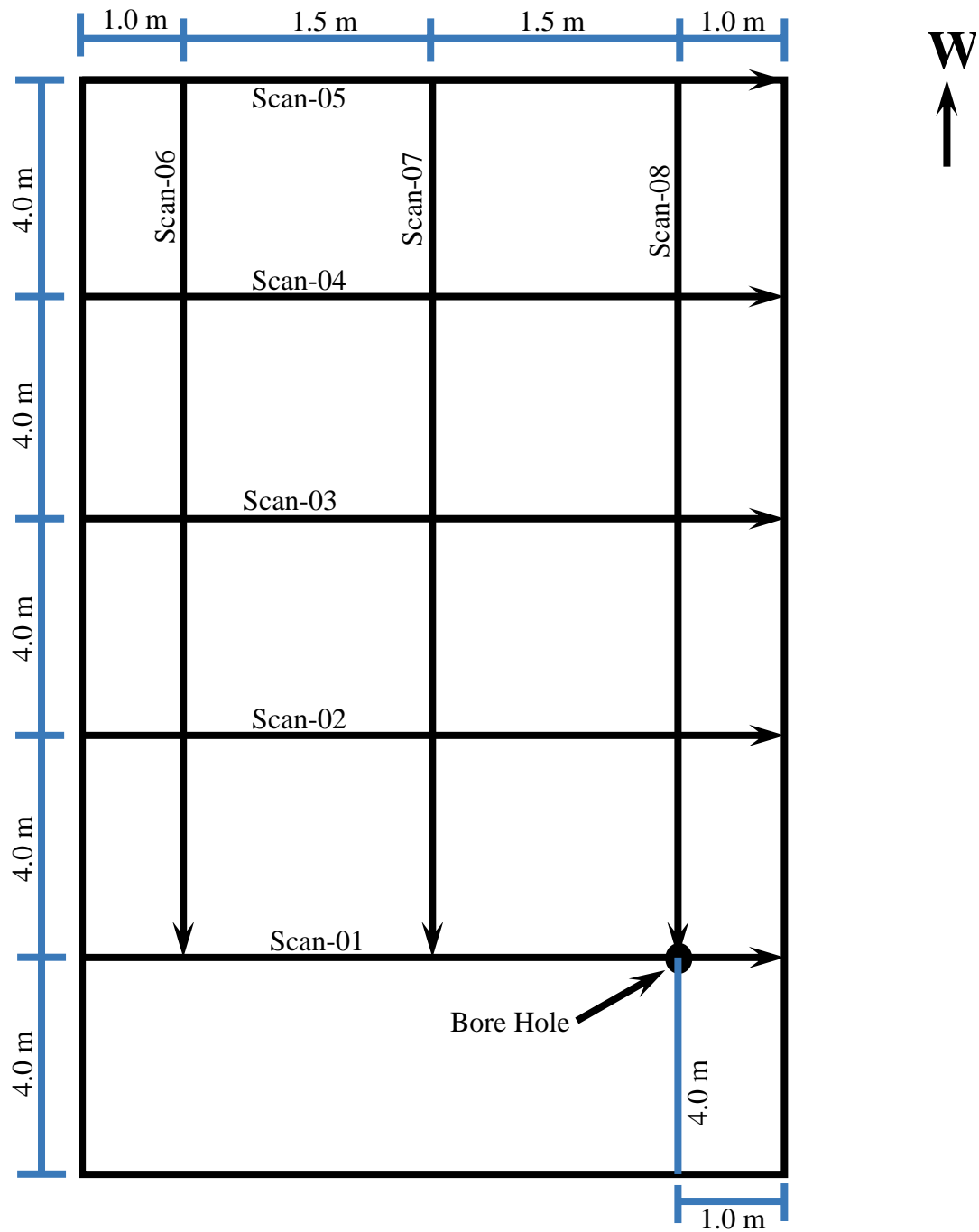
Infinite Impulse Response (IIR): Often used to remove noise.

Finite Impulse Response (FIR): Background noise, often seen as horizontal banding, may be removed using the FIR Filter.

3.0 Results of Ground Penetrating RADAR (GPR):

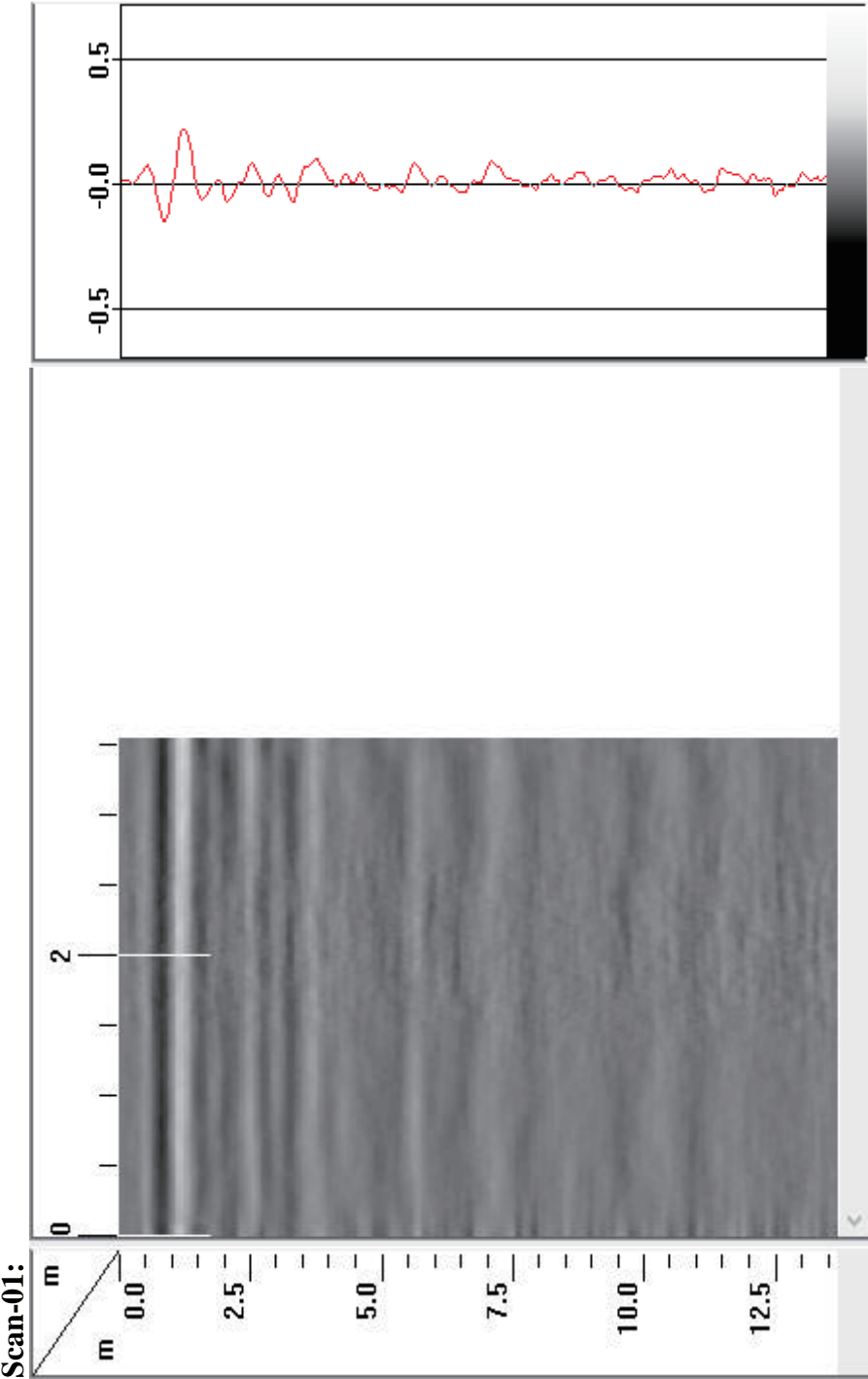
The results of 100 MHz GPR data are presented in Appendix-B. These data don't show any clear contrast of soil layers. The results of 200 MHz GPR data are presented in Appendix-C. These data show two clear soil layers, one up to a depth of 22 ft (6.5 m) and another below it. The results of 400 MHz GPR data are presented in Appendix-D. These data show rebar locations at the top of the soil layer (confirmed by the top concrete slab), a clear soil layer up to a depth of 6 ft (2.05 m) and probable locations of pipe line at 2 ft and 4 ft locations.

GPR_ 100MHz
Site Plan & Data Collection Grids:



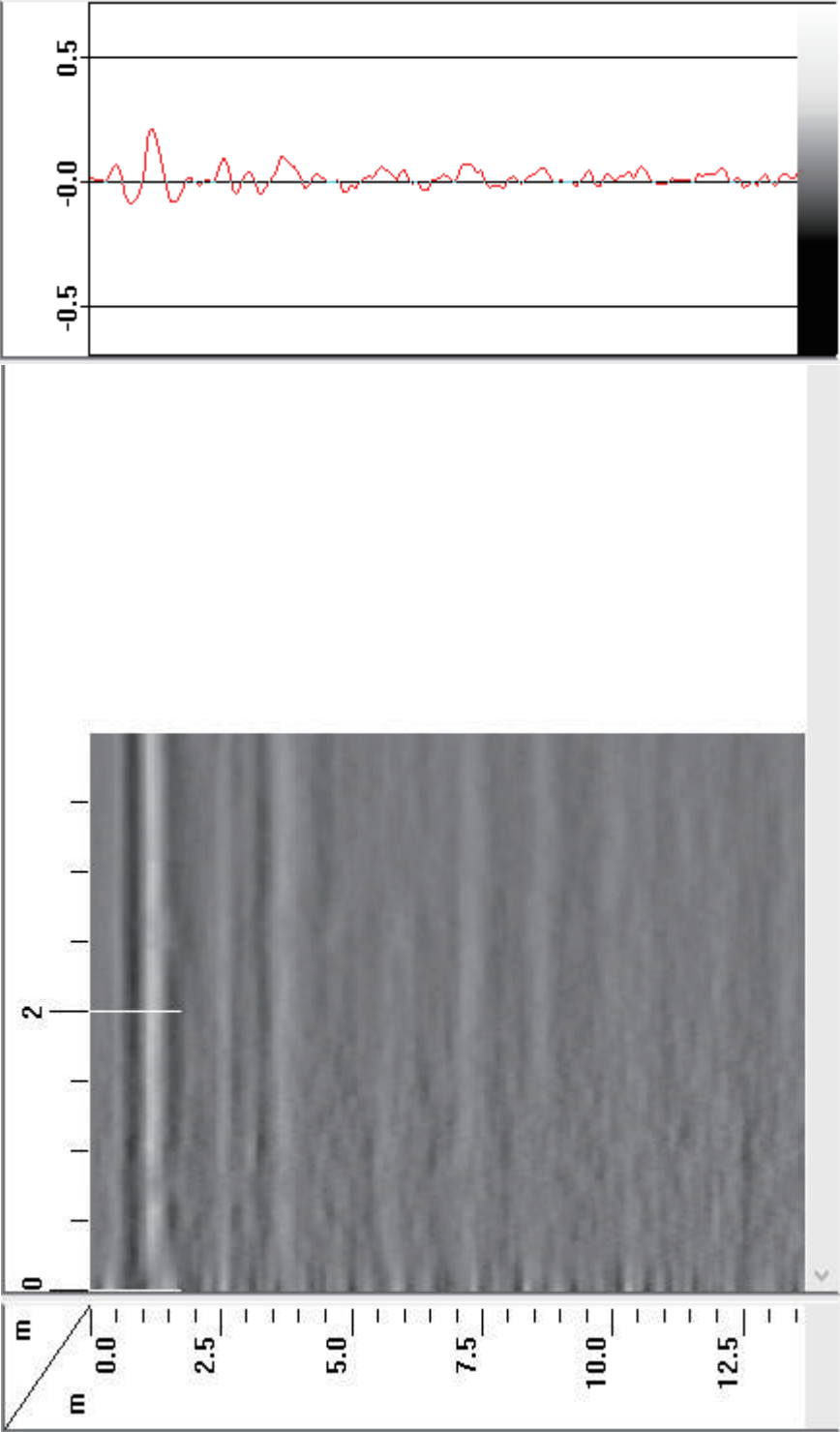
Data Processing

Display gain -03
Display mode- True gray
Corrections: (Time-zero correction)
Filters: FIR&IIR

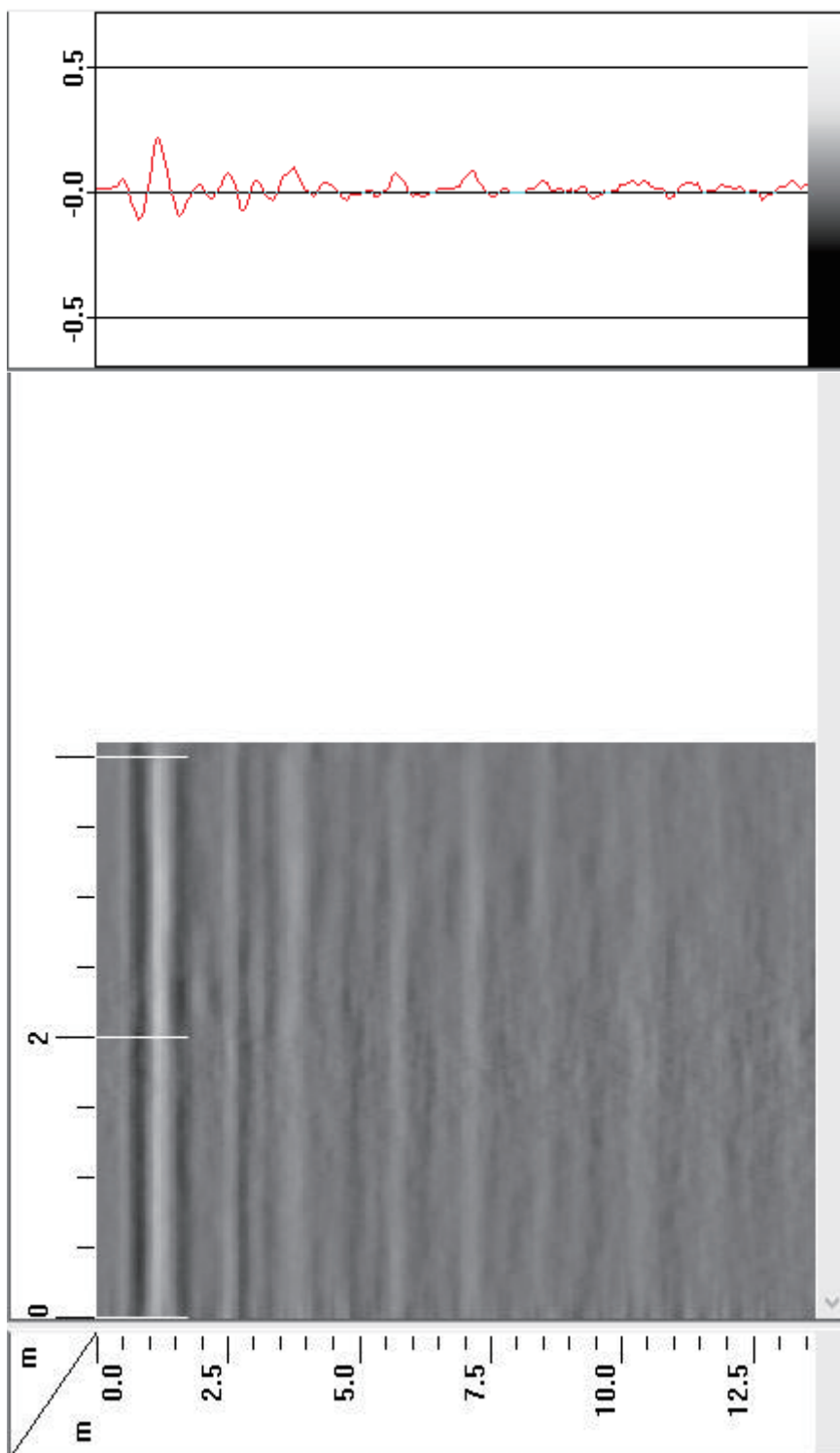


Scan-01:

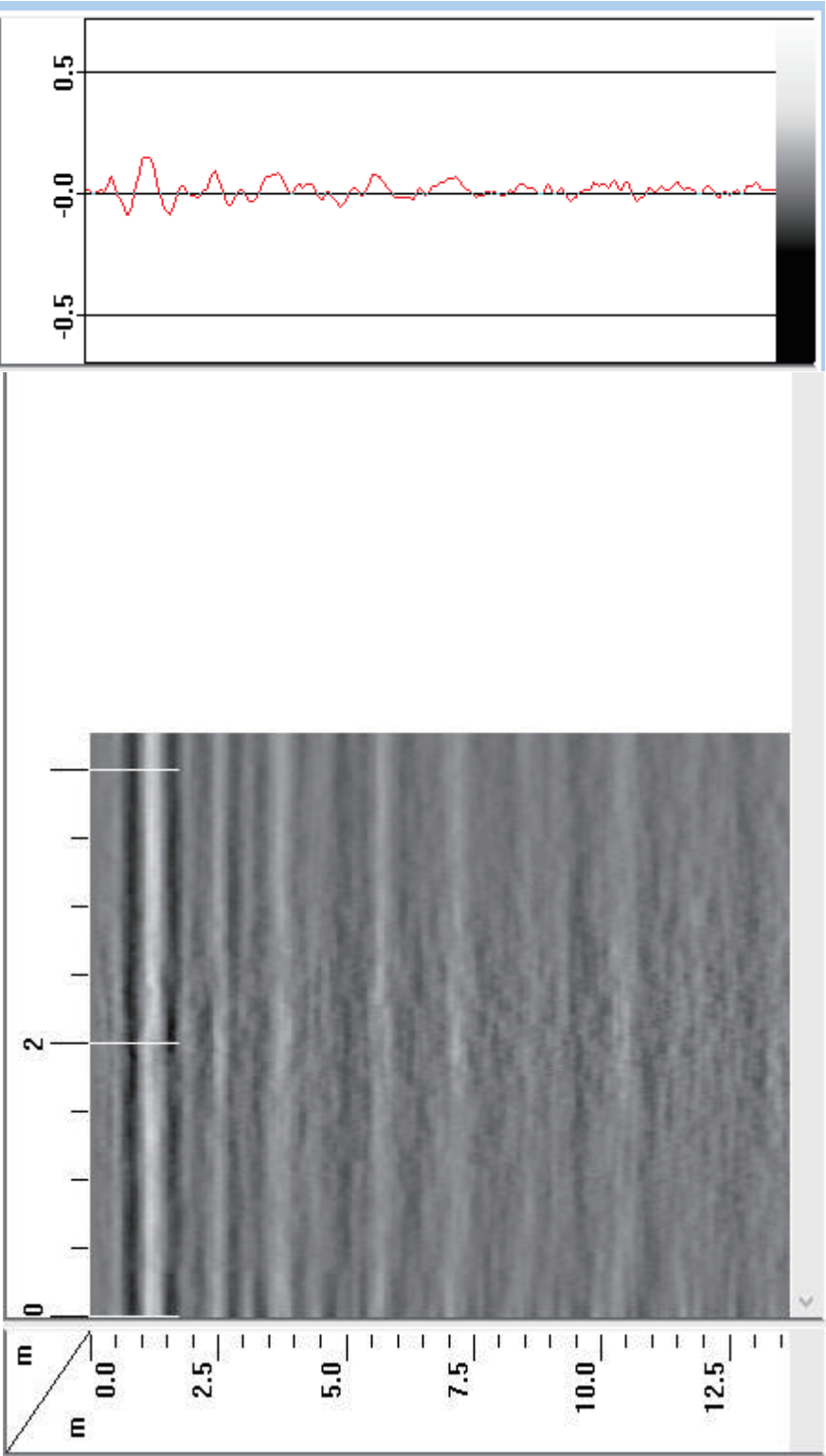
Scan-02:



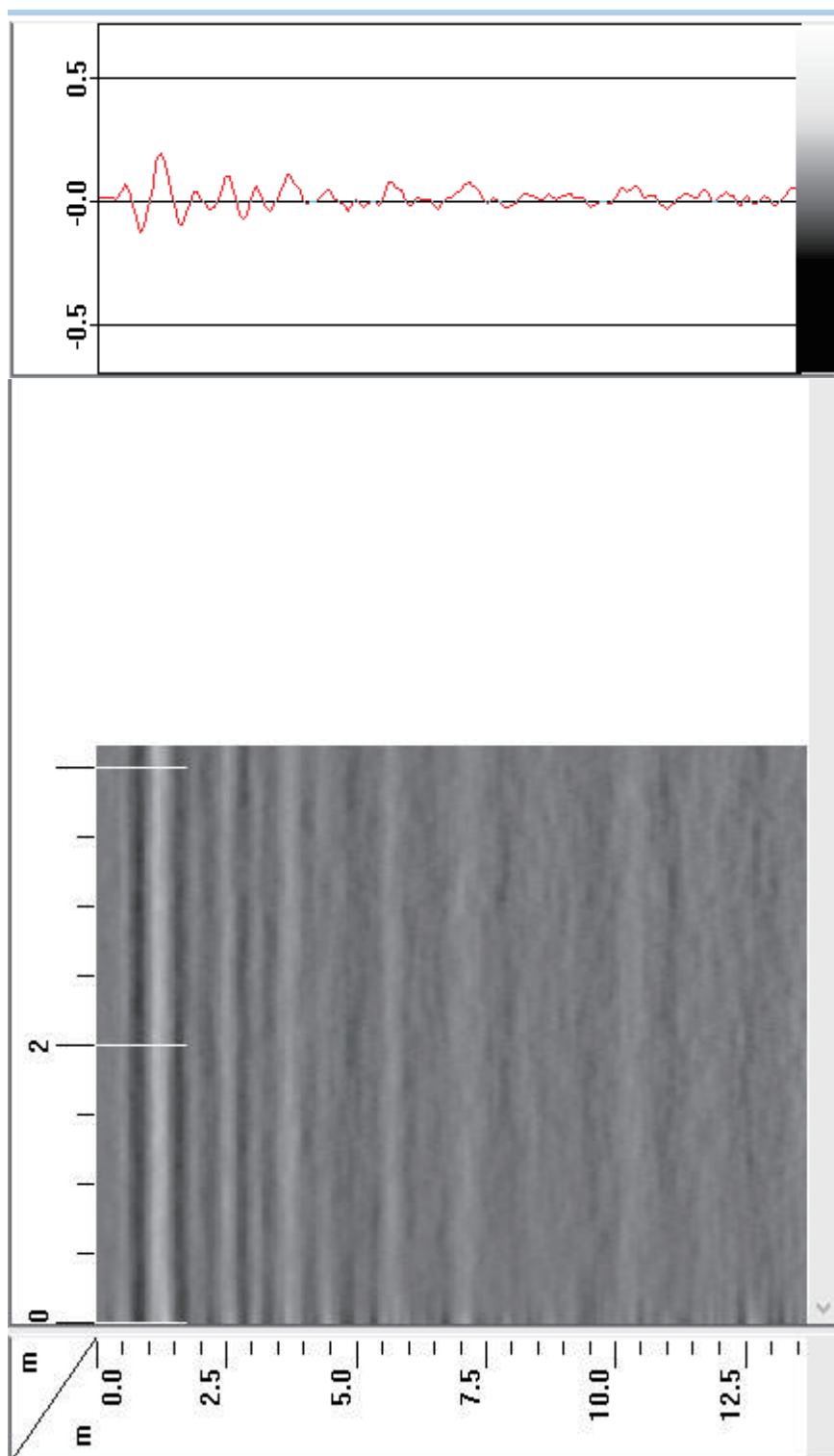
Scan-03:



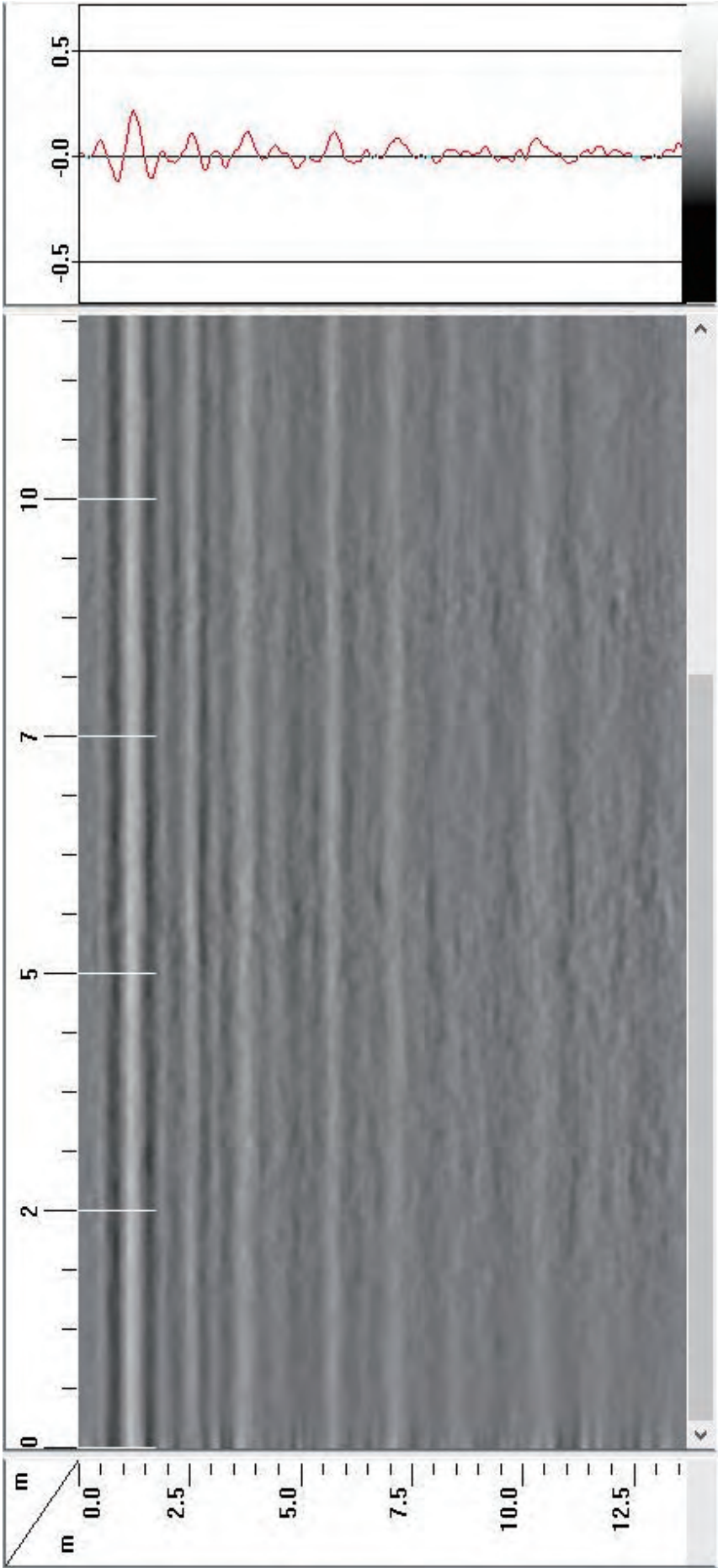
Scan-04:



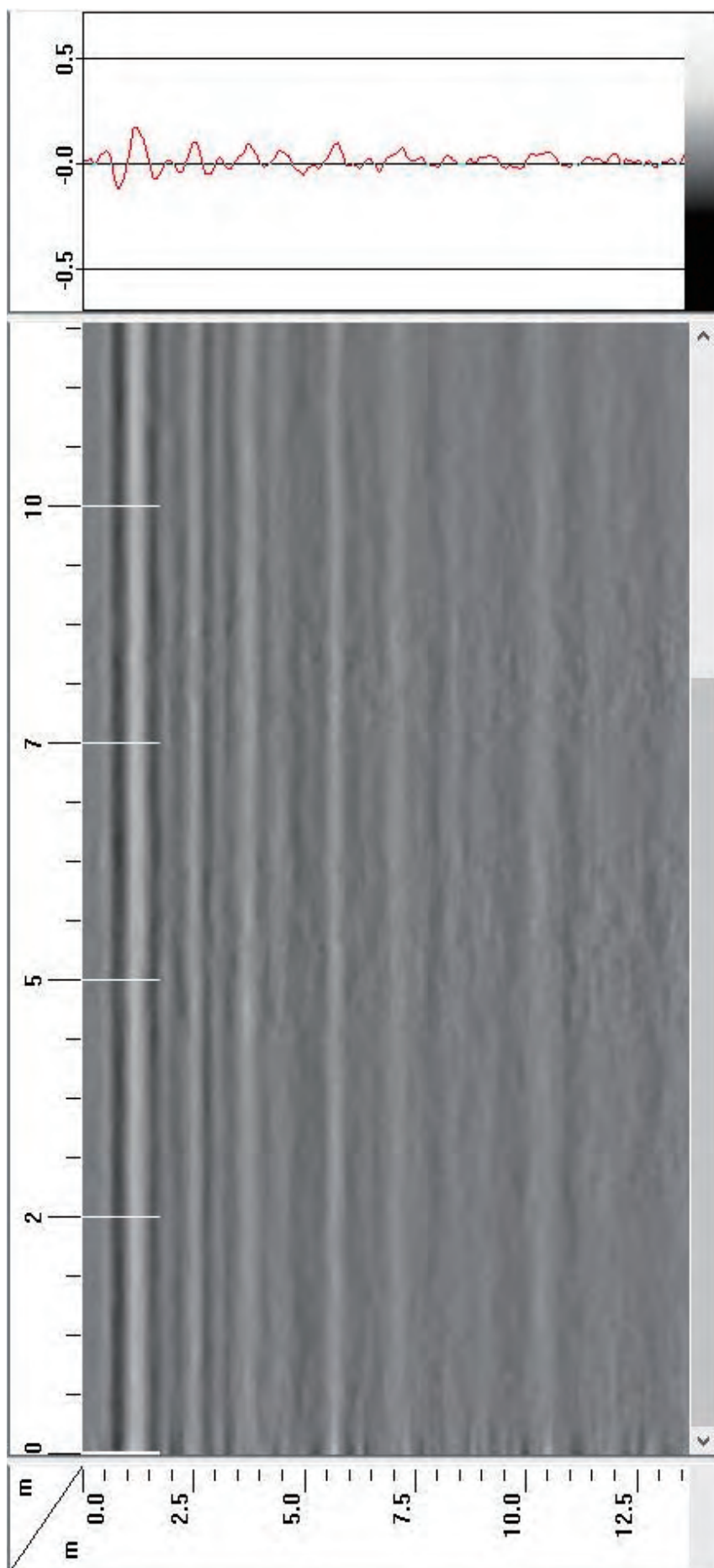
Scan-05:



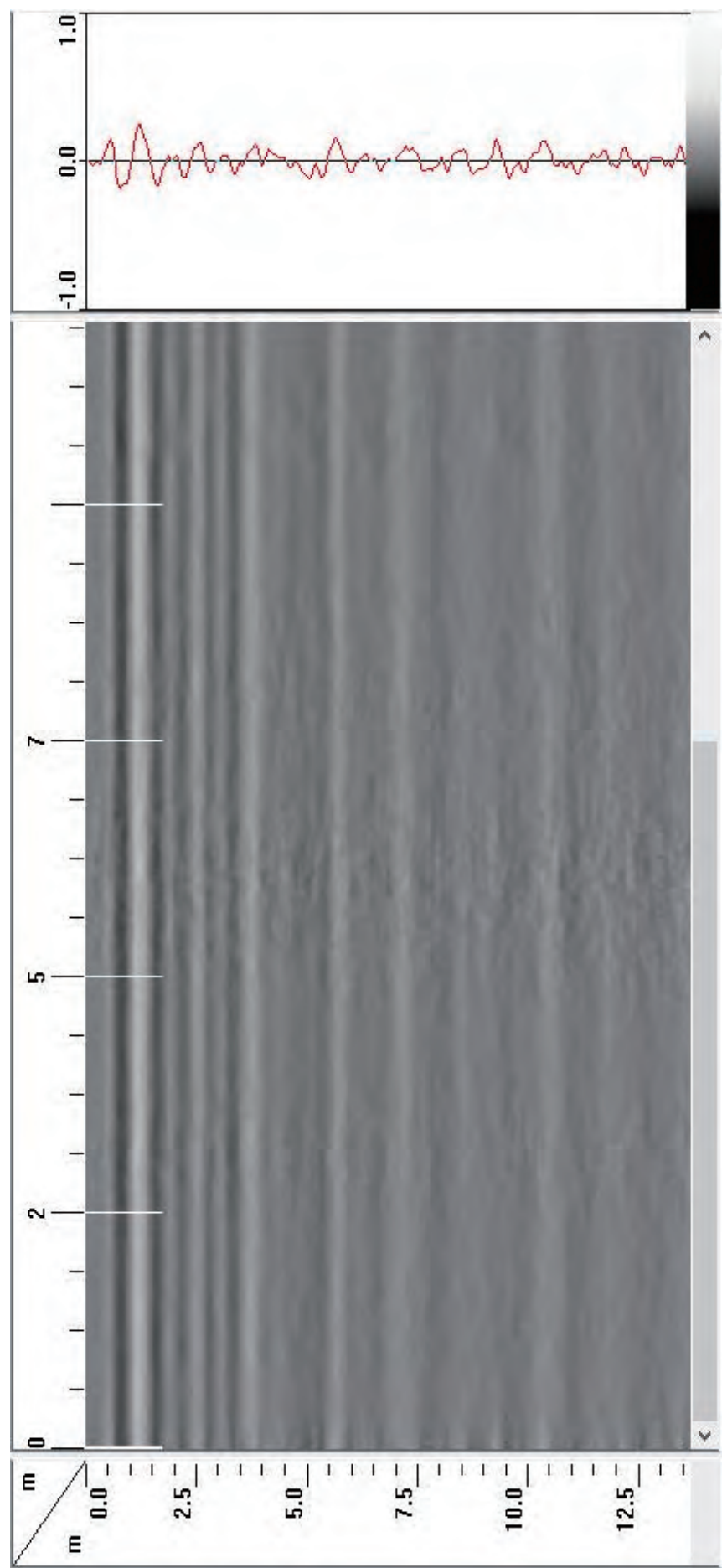
Scan-06:



Scan-07:

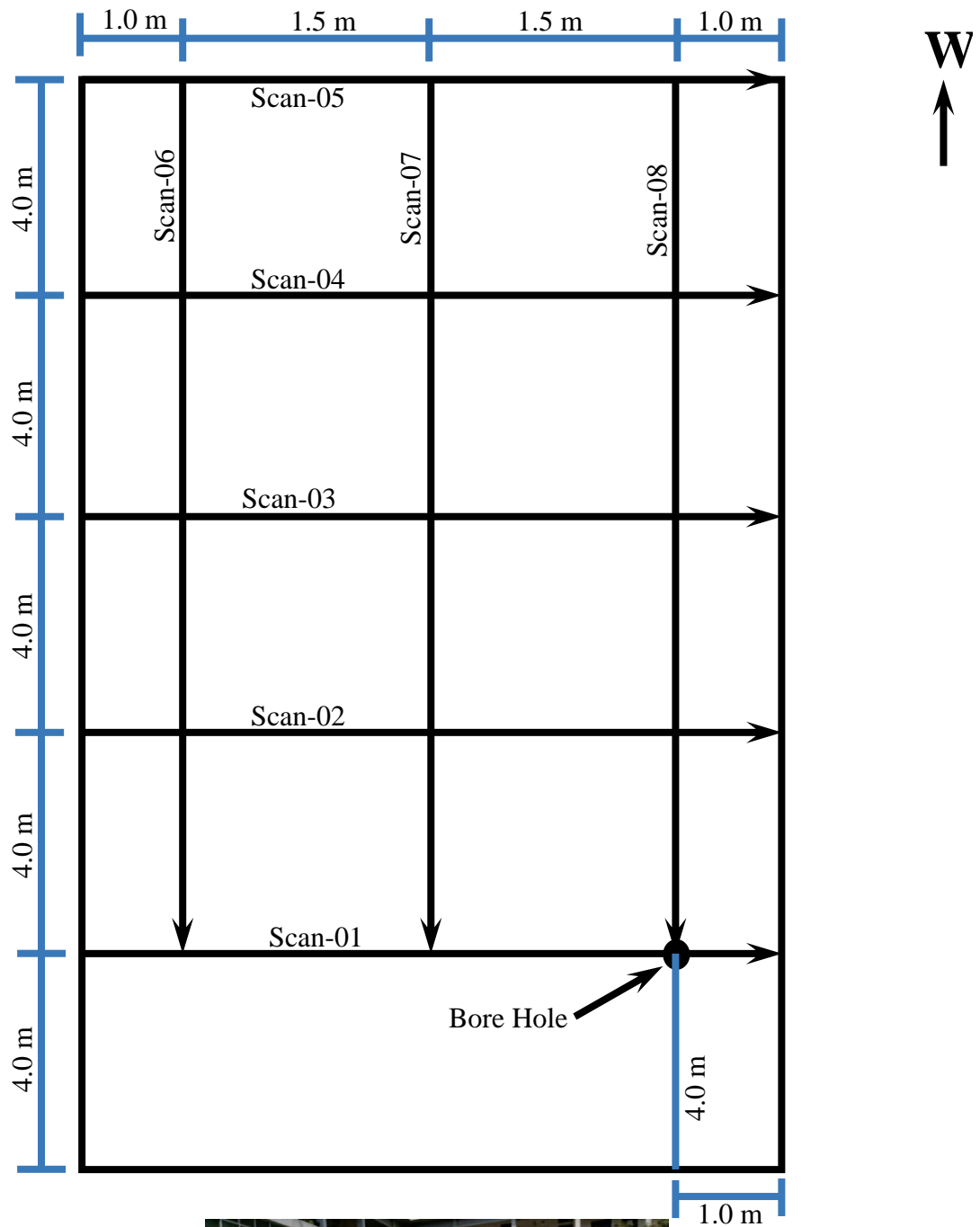


Scan-08:



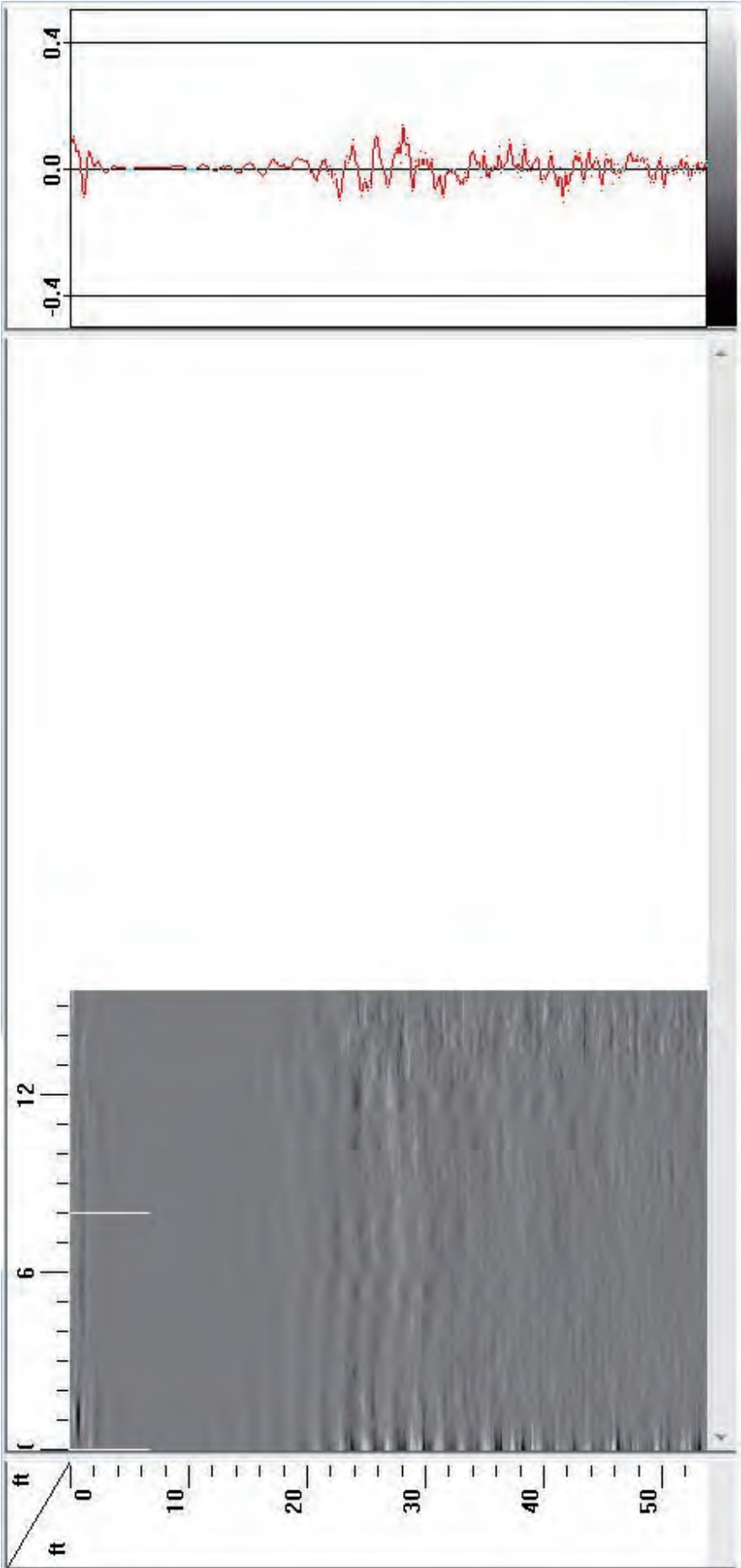
GPR_ 200MHz

Site Plan & Data Collection Grids:

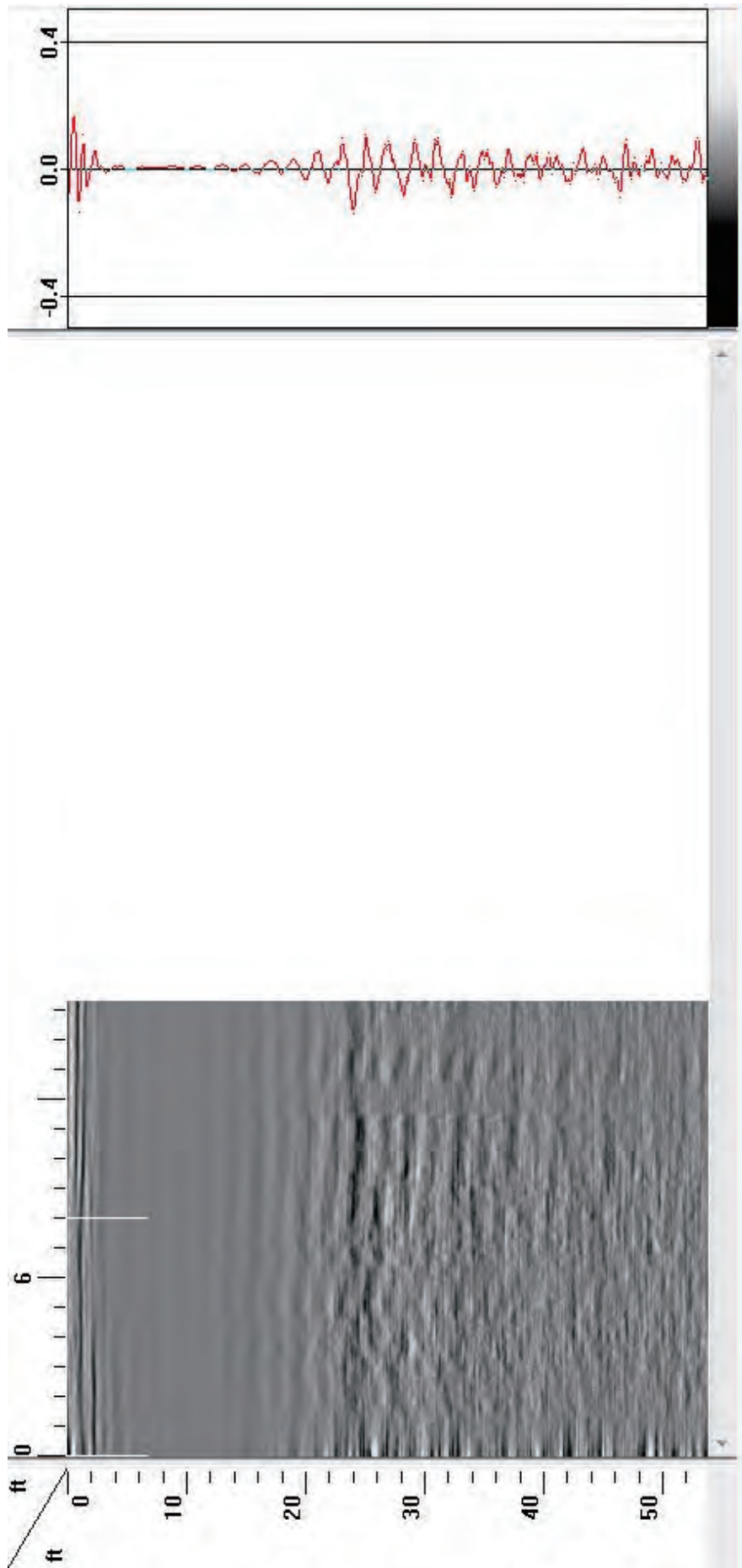


Data Processing

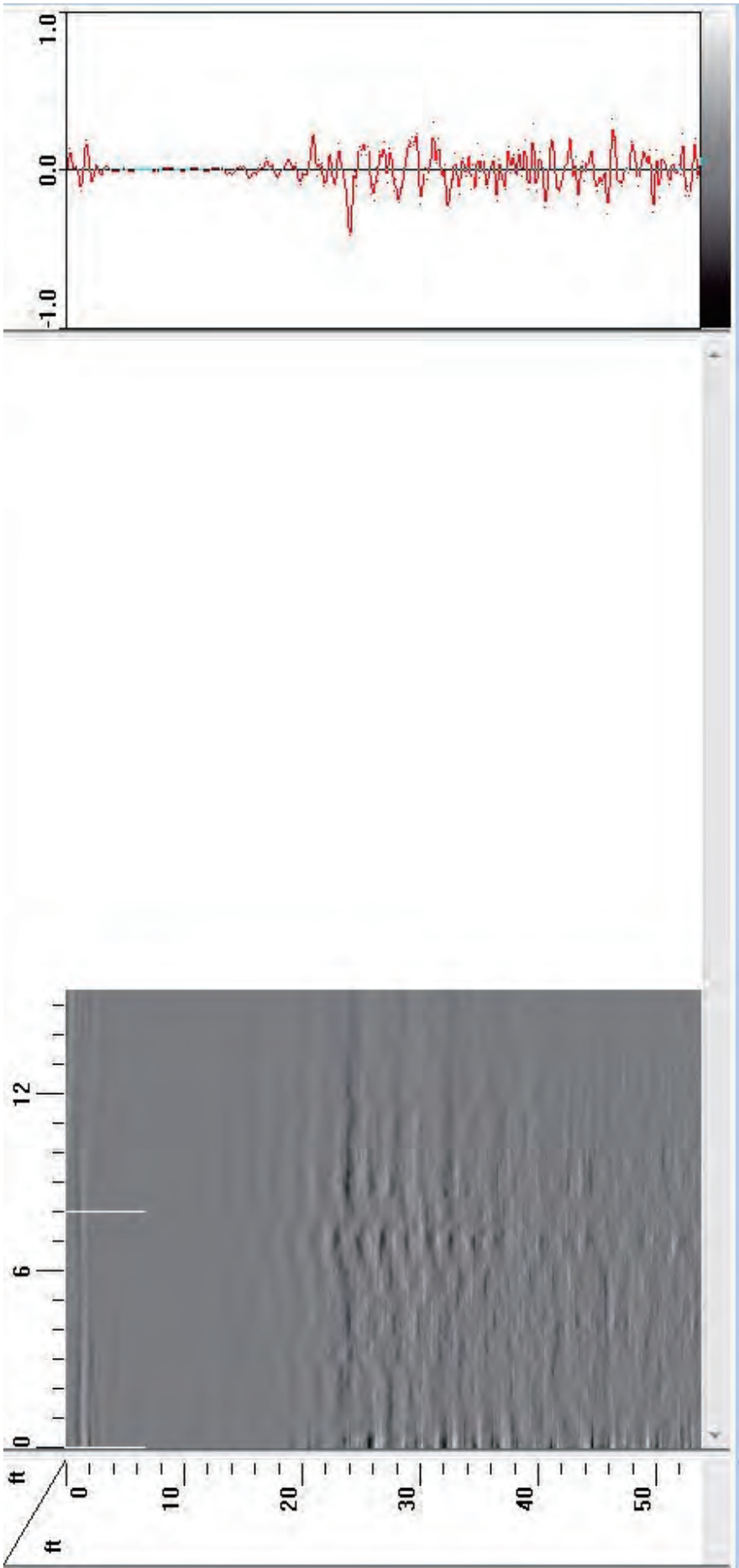
Scan-01:



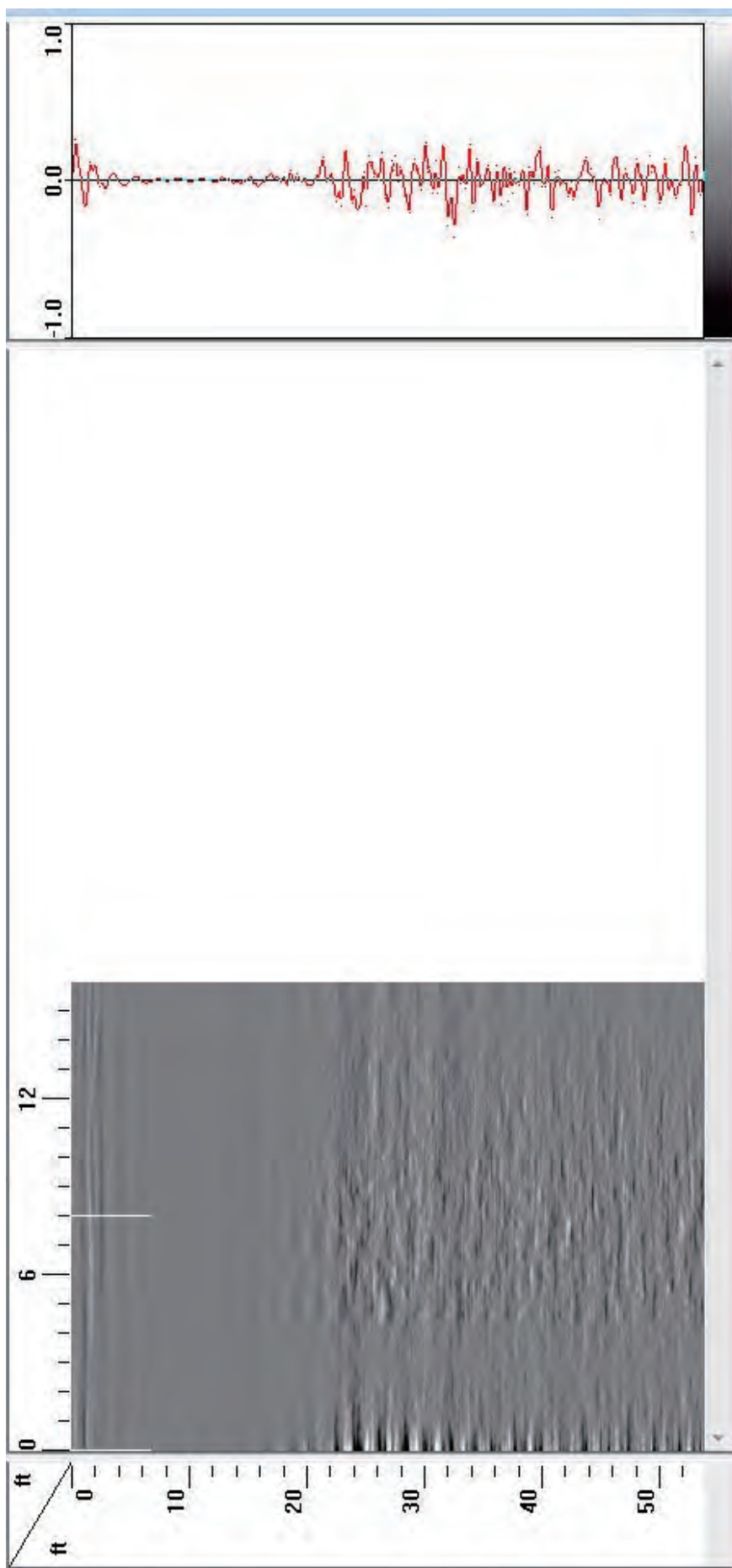
Scan-02:



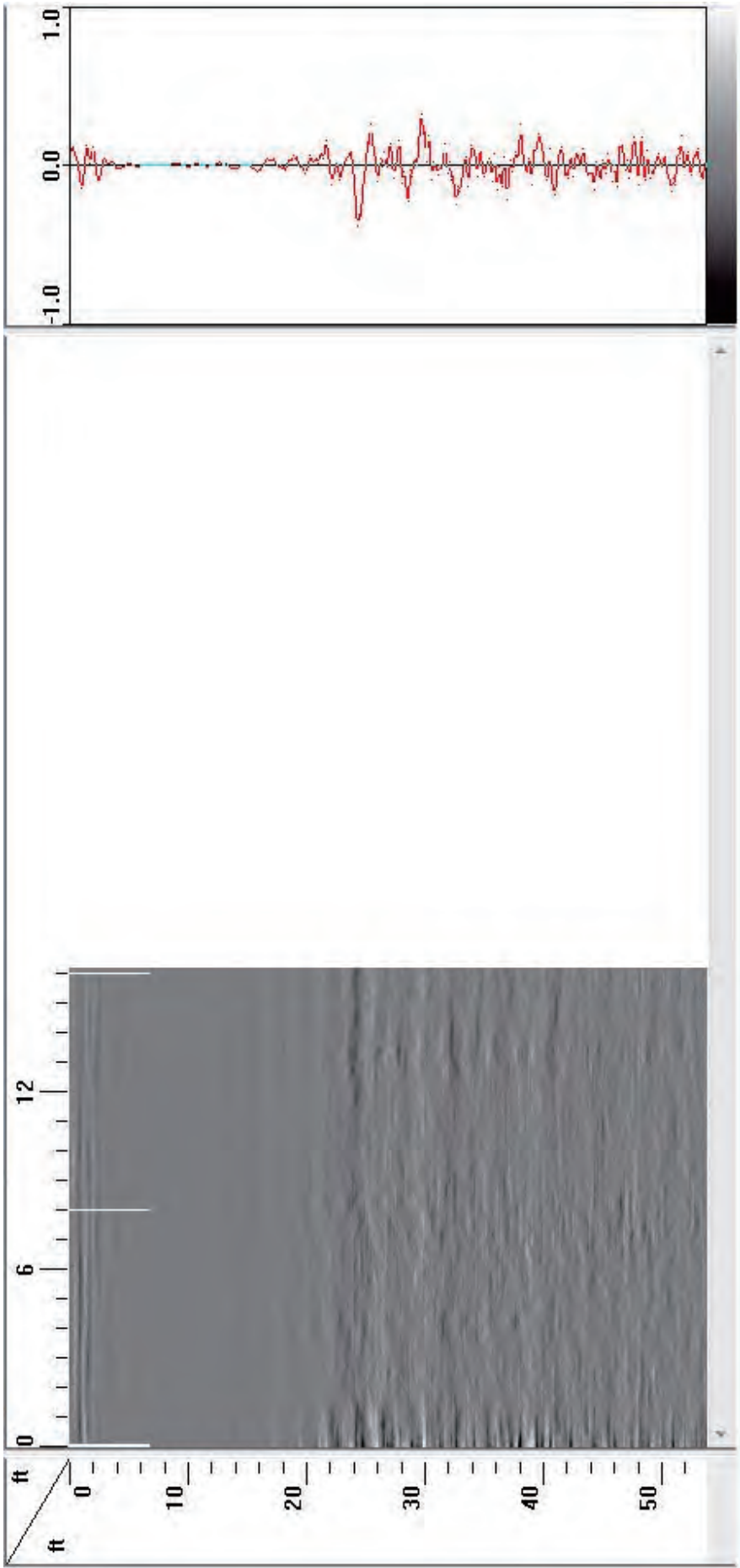
Scan-03:



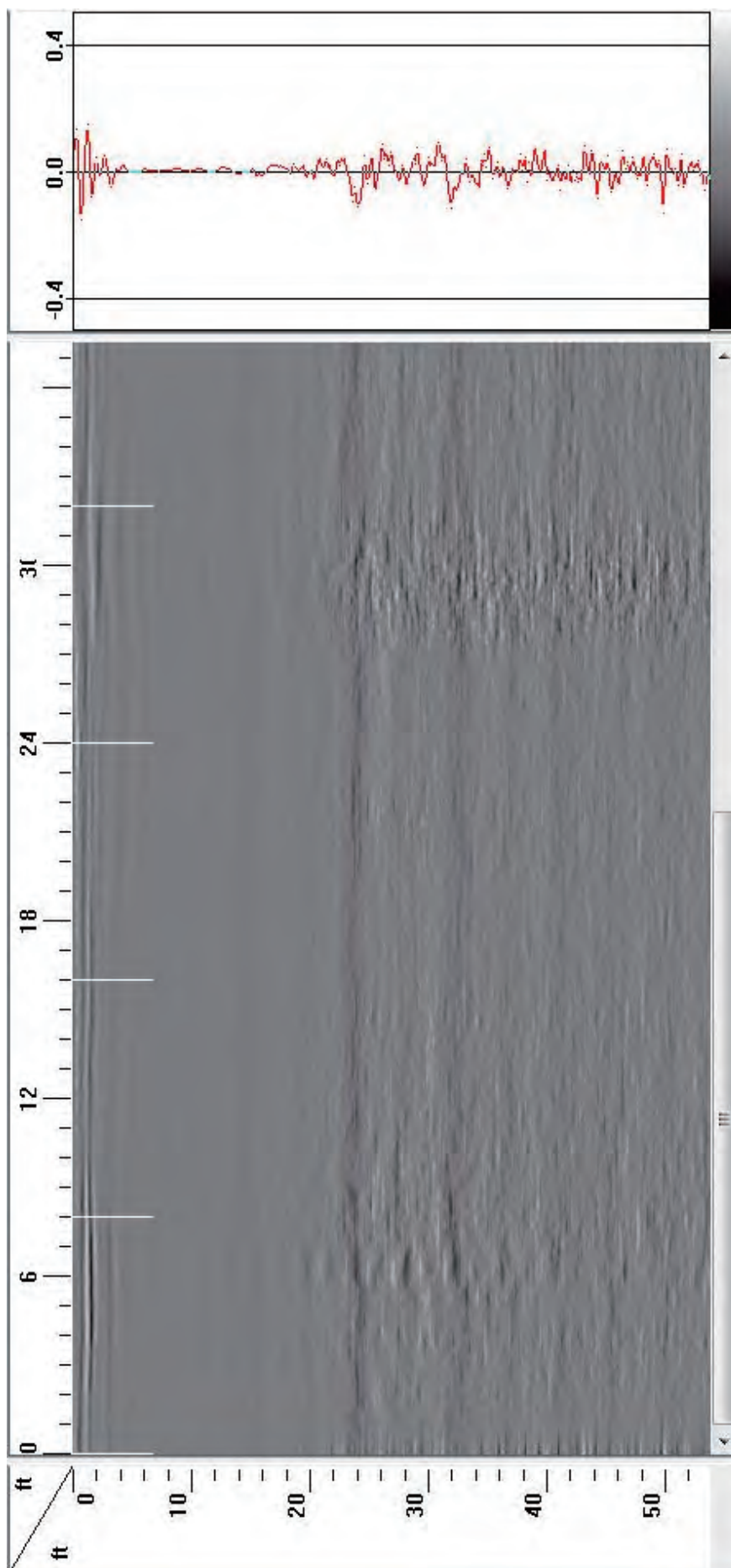
Scan-04:



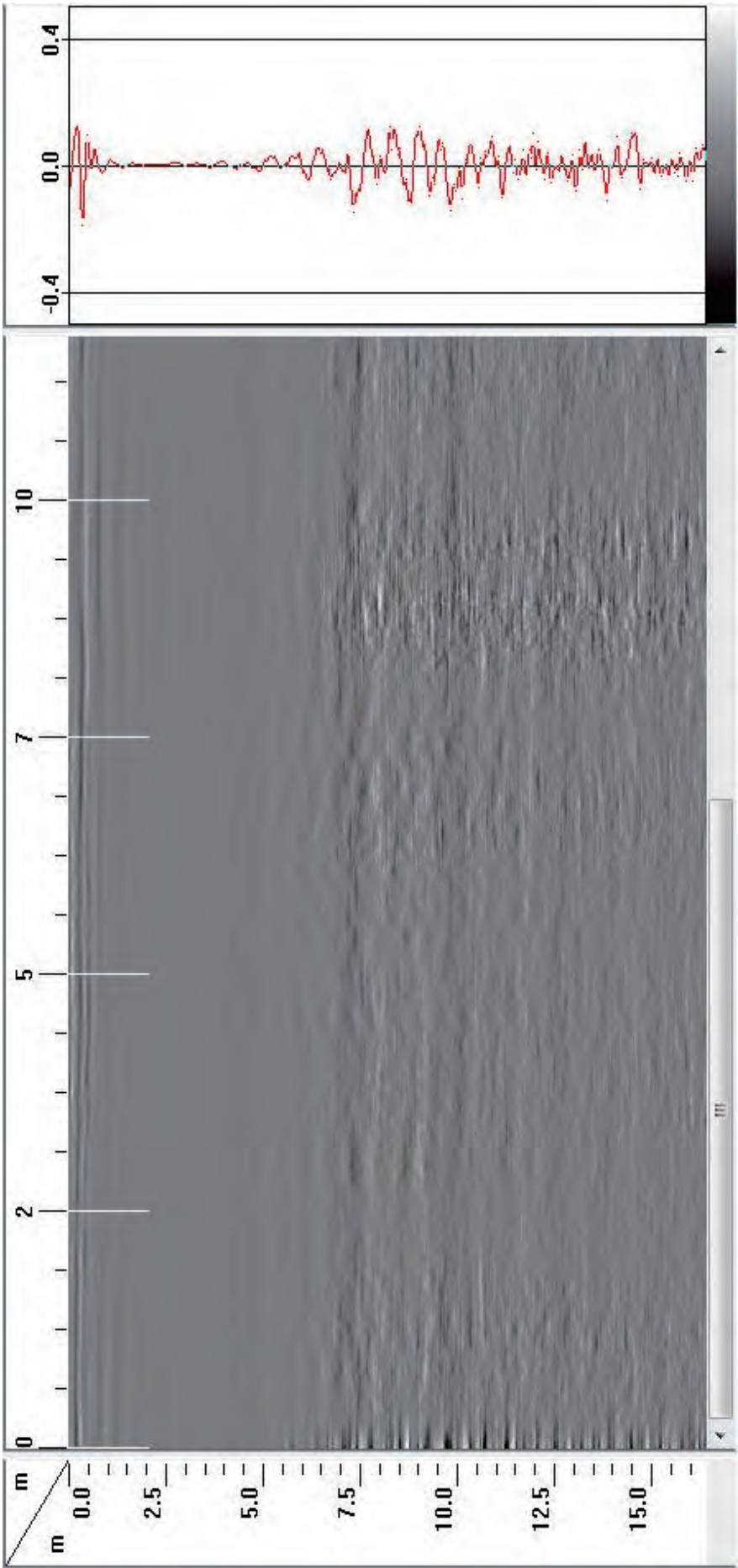
Scan-05:



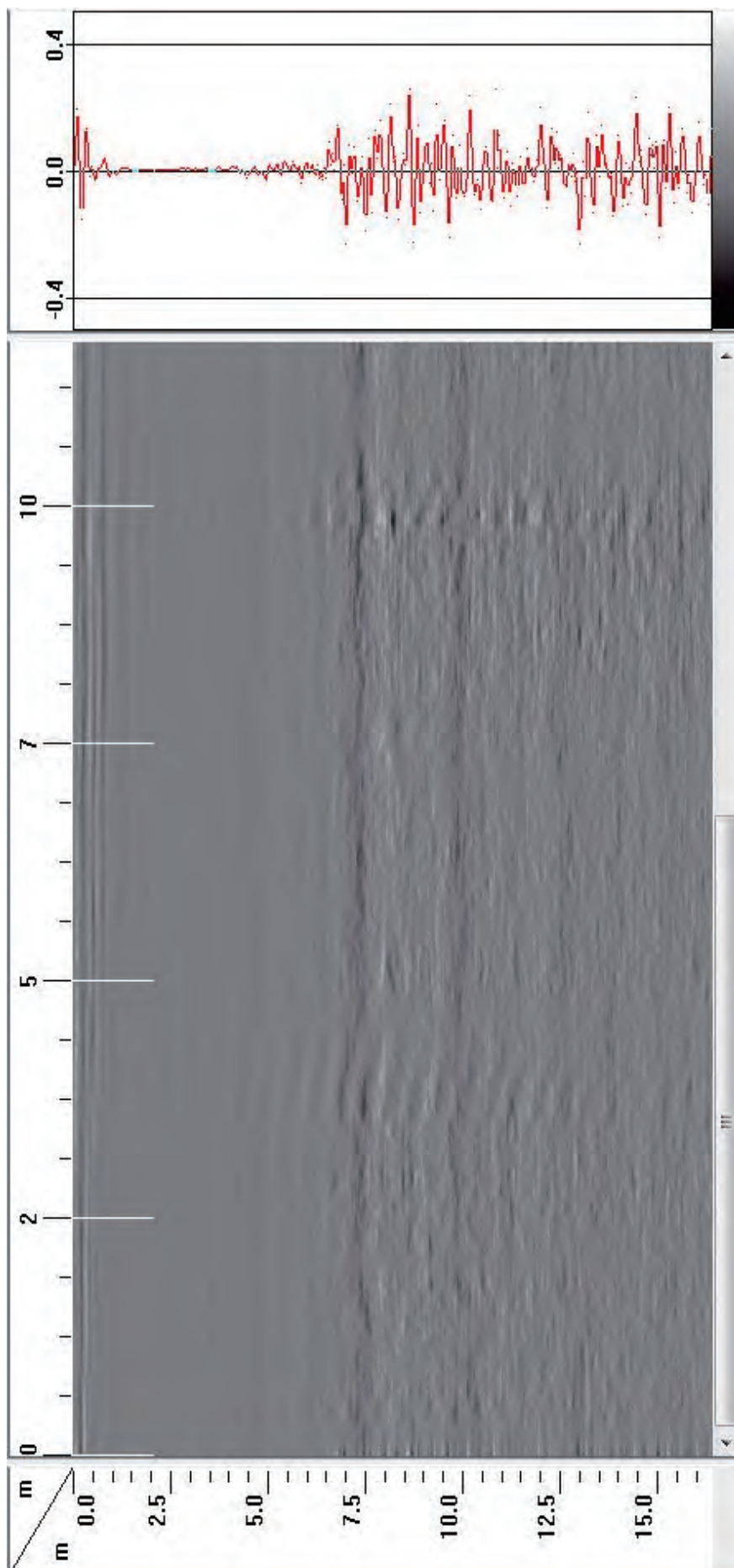
Scan-06:

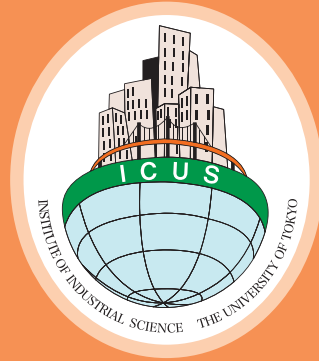


Scan-07:



Scan-08:





International Center for Urban Safety Engineering
Institute of Industrial Science, The University of Tokyo

4-6-1 Komaba, Meguro-ku,

Tokyo 153-8505, Japan

Tel: +81-3-5452-6472

Fax: +81-3-5452-6476

<http://icus.iis.u-tokyo.ac.jp>

E-mail: icus@iis.u-tokyo.ac.jp

ISBN4-903661-69-5

